LONDON'S GLOBAL UNIVERSITY

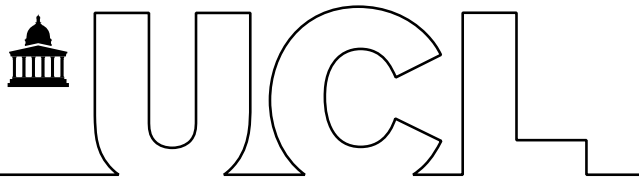

Analysis of the novel Lipid transfer protein Anchored at Membrane contact sites (LAM) family

A thesis submitted to the

University College London

in the fulfilment of the requirements for the degree of

Doctor of Philosophy

Supervisor: Dr Tim Levine

Department of Cell Biology,

Faculty of Brain Science, Institute of Ophthalmology

2017

Declaration

I, Louise Wong, confirm that the work presented in this thesis is my own. Where information has been derived from other sources, I confirm that this has been indicated.

June 2017

Abstract

Membrane contact sites are dynamic structures where two organelles come into close proximity to regulate and facilitate the flow of material and information between them. One type of inter-organelle communication is lipid exchange, which is essential for membrane maintenance and in response to environmental and cellular stimuli. We recently discovered a new family of Lipid transfer proteins Anchored at Membrane contact sites (LAMs) that is present in all eukaryotes. LAM proteins are integral Endoplasmic Reticulum (ER) proteins containing at least one domain that is structurally similar to the StARkin domain superfamily, a specialised fold that can bind amphipathic ligands such as lipids. The budding yeast, *Saccharomyces cerevisiae,* has six such proteins: Lam1p-6p. Lam1p-4p are located at contacts between the ER and the plasma membrane (PM), and Lam1p-3p are implicated in retrograde sterol traffic between the ER and PM. The PM contains a high concentration of sterol where it increases rigidity by altering the packing characteristics of the phospholipids in the bilayer. Sterol is also important in the ER, where its levels are low but it is both synthesised and sensed. However, the mechanism by which sterol traffics between the ER and the PM is unknown. This investigation characterises the phenotype of yeast delete LAM strains on Amphotericin B, a sterol sequestering antifungal agent and shows that the conserved StARkin domain of LAM proteins is responsible for resistance against Amphotericin B. *Aspergillus fumigatus,* a filamentous fungus, has two LAM proteins and the removal of *Af*LamA causes a severe growth phenotype. Also, *in vitro* studies indicate that LAM StARkin domains have a clear sterol transfer activity and a mutation that can diminish the function *in vivo* and *in vitro* has been identified. These findings present a new candidate protein family for intracellular sterol trafficking.

Dedication

To my beloved brother, Howard Wong, 1985-2012

I dedicate this thesis to:

my brother, you are dearly missed and always remembered

and to my mother, for your encouragement and infinite support.

Acknowledgements

I would like to thank my supervisor, Dr Tim Levine, for the guidance and inspiration through what has been an exciting and at times, a challenging project. Your expertise, creativity and passion have helped me become the scientist that I am and aspire to be for the rest of my career. I could not have learnt or achieved as much as I did without your supervision and influence and most significantly your tremendous enthusiasm for all things science! I am extremely thankful that you gave me the chance to work on such an original project and more importantly as part of your lab.

The members of the Levine group have contributed immensely to my work and to my time in the lab: first and foremost, Alberto: thanks for being there from the start. It was my pleasure to have worked together on this project and also undertaking the PhD journey with you. I have no doubts that sharing lab and office space with me was not always easy with my 'organised' mess, so thanks for putting up with me! Sarah: your infectious energy inspired me when I needed motivation. Rachel: thanks for showing the way to becoming a fully-fledged PhD student.

My time at the Institute of Ophthalmology has been made easier by many staff members who maintain equipment and support all of us here, thank you for your help. I am also deeply indebted for the expert discussions, advice and resources to all the brilliant scientists from all around the world whom I have met over the course of my PhD. I gratefully acknowledge the funding from the MRC that made my PhD possible. I also extend my gratitude to the Cockcroft lab for the lipid transfer expertise, Cordeiro lab (UCL) and Ben who has helped made many experiments possible and also the F2G Ltd lab (Manchester) who supported both my PhD funding and a significant part of this project especially Nicola.

To all fellow lab/office members, past and present, I thank you for being there through the ups and downs of experiments and life, providing support and most importantly friendship (and also so much conversation that I thought I would never get any work done!). I am especially grateful to Ingrid and Tom for being late night office buddies – I'm sure I would have been more motivated to finish my work quicker if it were not for your excellent company. To all friends and family, I thank you for being part of my life. Now this thesis is done and I am no longer a student, I definitely do not have any excuse for not sharing the responsibility at the pub.

To my family, a huge thanks for all their love and encouragement. To my parents, I am so grateful that you gave me the opportunities to study that you did not

have for yourselves and for your extraordinary support you have always offered. I hope that I have made you proud. To my brothers, you have been there throughout my life and, you influenced so much of who I am, thus I could not have started this journey without you.

Finally, my dearest Thomas, you have been by my side throughout as my unwavering rock through the toughest and the best of times giving me unconditional support, care and friendship. The completion of my PhD has been a long journey and life did not stand still during this time. It is only due to your extraordinary patience, kindness and love that I am able to be here. You encouraged me from afar when I first started this PhD and then you gave me strength when my brother passed away. We have begun our life together in London, and I can never be happier than coming home to you (and our cats!). When life was the difficult during my diagnosis, surgery and recovery and also the long time before that when I was not quite right, you never left me alone. You supported me mentally, emotionally and physically and we prevailed because of you. Writing is not my forte, but you have tolerated my complaints and whining during the completion of this thesis. There are no words that can express my gratitude and appreciation for all that you have done and been for me. This achievement is as much yours as mine. I thank you with all my heart and soul for being you.

Contents

List of Figures

List of Tables

List of Abbreviations

aa	amino acid
ACAT	Acyl-CoA cholesterol acyltransferase
ABC	ATP-binding cassette
AEBSF	4-(2-aminoethyl) benzene sulfonyl fluoride hydrochloride
Af	*Aspergillus fumigatus*
AmB	Amphotericin B
AU	arbitrary units
BAG	Bcl-2-associated athanogene
BAR	Bin-Amphiphysin-Rvs domain
BLAST	Basic Local Alignment Search Tool
BMP	bis(monoacylglycero)phosphate
bp	base pair
BSA	bovine serum albumin
Ca^{2+}	calcium ions
cAMP	cyclic adenosine monophosphate
CETP	cholesteryl ester transfer protein
Cer	ceramide
CERT	ceramide transfer protein
Chol	cholesterol
CL	cardiolipin
CLANS	Cluster Analysis of Sequences
Cn	*Cryptococcus neoformans*
D	aspartic acid
DAG	diacylglycerol
Dansyl	5-dimethylaminonapthalene-1-sulfonyl
DHE	dehydroergosterol
DNA	deoxyribonucleic acid
DOPC	dioleoyl phosphatidylcholine
DOPE	dioleoyl phosphatidylethanolamine
DPPC	dipalmitoyl phosphatidylcholine
DUF	domain of unknown function
E	glutamic acid
E-syt	extended synaptotagmin
Ec	*Escherichia coli*
EDTA	ethylenediaminetetraacetic acid
EMC	ER-membrane protein complex
ER	endoplasmic reticulum
ERK	extracellular signal–regulated kinase
ERMES	ER–mitochondria encounter structure
eTULIP	extracellular TULIP
FA	fatty acyl chain
FFAT	two phenylalanines (FF) in an acidic tract
Fo	*Fusarium oxysporum*
FRET	Förster resonance energy transfer
GalCer	galactosylceramide
GFP	green fluorescent protein
GPL	glycerophospholipid
GRAM	glucosyltransferases, Rab-like GTPase activators and

	myotubularin
GSL	complex glycosphingolipids
GRP75	glucose-regulated protein 75
HOPS	homotypic fusion and vacuole protein sorting
Hs	*Homo sapiens*
IMM	inner mitochondrial membrane
INSIG	insulin-induced gene
ISL	yeast inositol sphingolipid
iTULIP	intracellular TULIP
K	lysine
KO	knock out strain
L	cell lysate
LA	cell lysate after incubation with Ni^{2+} beads
LAM	lipid transfer protein anchored at a membrane contact site
LTC	lipid transfer at contact sites
LTP	lipid transfer protein
MCS	membrane contact site
MENTAL	MLN64 N-terminal
Mfn	mitofusin
MIC	minimal inhibitory concentration
mins	minutes
MLN64	metastatic lymph node 64 protein
MORN	membrane occupation & recognition nexis
MSP	major sperm protein
MW	molecular weight
MβCD	methyl-β-cyclodextrin
NBD	7-nitrobenz-2-oxa-1,3-diazol-4-yl
NE	nuclear envelope
NVJ	nucleus–vacuole junction
OMM	outer mitochondrial membrane
ORD	OSBP-related ligand-binding domain
ORF	open reading frame
ORP	OSBP related protein
OSBP	oxysterol-binding protein
OSH	yeast oxysterol-binding homology proteins
PA	phosphatidic acid
PC	phosphatidylcholine
PCR	polymerase chain reaction
PCTP	phosphatidylcholine transfer protein
PE	phosphatidylethanolamine
PH	pleckstrin homology
PI	phosphatidylinositol
PI(3,4)P_2	phosphatidylinositol 3,4-bisphosphate
PI(3,4,5)P_3	phosphatidylinositol 3,4,5-trisphosphate
PI(4,5)P_2	phosphatidylinositol 4,5-bisphosphate
PI3P	phosphatidylinositol 3-phosphate
PI4P	phosphatidylinositol 4-phosphate
PIP_2	phosphatidylinositol-biphosphate
PITP	PI transfer protein
PL	phospholipid
PLTP	phospholipid transfer protein

PM	plasma membrane
pmaER	PM associating ER
PO_4	phosphate group
POPC	palmitoyl-oleoyl-phosphatidylcholine
PP	purified protein
PS	phosphatidylserine
PSI-BLAST	position-specific iterated BLAST
R	arginine
RFP	red fluorescent protein
RT	room temperature
S1P	sphingosine-1-phosphate
SAB	Sabourand
Sc	*Saccharomyces cerevisiae*
SCAP	SREBP cleavage-activating protein
SM	sphingomyelin
SMP	synaptotagmin-like, mitochondrial and lipid-binding proteins
Sp	*Schizosaccharomyces pombe*
Sph	sphingosine
SREBP	sterol regulatory element-binding protein
SRPBCC	StART/RHOαC/PITP/Bet v 1/CoxG/CalC
StART	StAR-related lipid-transfer protein
STI	Soybean trypsin inhibitor
TAG/TG	triacylglyceride
TGN	trans Golgi network
TLC	thin layer chromatography
TM	transmembrane
TOR	target of rapamycin
TORC2	TOR complex 2
TULIP	tubular lipid binding protein
VancE	vacuolar non-NVJ cytoplasmic ER
VAP	VAMP associating protein
VASt	VAD1 analog of StAR-related lipid transfer
vCLAMP	vacuolar and mitochondrial patch
VDAC	voltage-dependent anion channel
WT	wild type
Ysp	yeast suicide protein

Introduction

CHAPTER 1

Introduction

1.1 General Introduction

Intracellular lipid traffic is essential in cells with more than one membrane environment, i.e., two or more membrane-bound organelles. The function of a membrane bound cell or organelle is dependent on the maintenance of membranes in response to environmental and cellular stimuli. Thus inter-organellar lipid exchange is crucial for cell survival. Lipid transfer proteins (LTPs) facilitate the movement of lipids across the cytosol from one membrane to another. As lipids are essentially insoluble in water, spontaneous lipid transfer would not occur without such a catalyst. The defining feature of a lipid transfer domain is an internal cavity lined with hydrophobic residues that can solubilise a lipid and thus enable its transfer across the aqueous cytosol. In this introduction, I will discuss the general overview of intracellular lipid transfer and more specifically sterol transport.

1.2 Lipids and cellular membranes

1.2.1 Lipid bilayers

Lipids are hydrophobic or amphipathic biomolecules made up of hydrocarbon chains (Fahy *et al.*, 2008). These molecules are essential dynamic regulators of various cellular processes, including growth, replication, signalling, survival and membrane trafficking, as well as an important cellular storage of energy. However, the most important property of lipids is the ability to form a barrier enclosing cellular compartments [Figure 1.1]. The amphipathic nature of lipids is critical to the structure of a membrane bilayer, which arises due to the energetically unfavourable interaction of the hydrophobic lipid tails with water; the polar head groups preferentially face out to the aqueous cytosol, and the tails are protected by forming a hydrophobic core. This membrane is impermeable to polar molecules, such as salts, sugars and water and thus can function as a barrier between different compartments, for example between the organelles and the cytosol, or the cell and its surroundings.

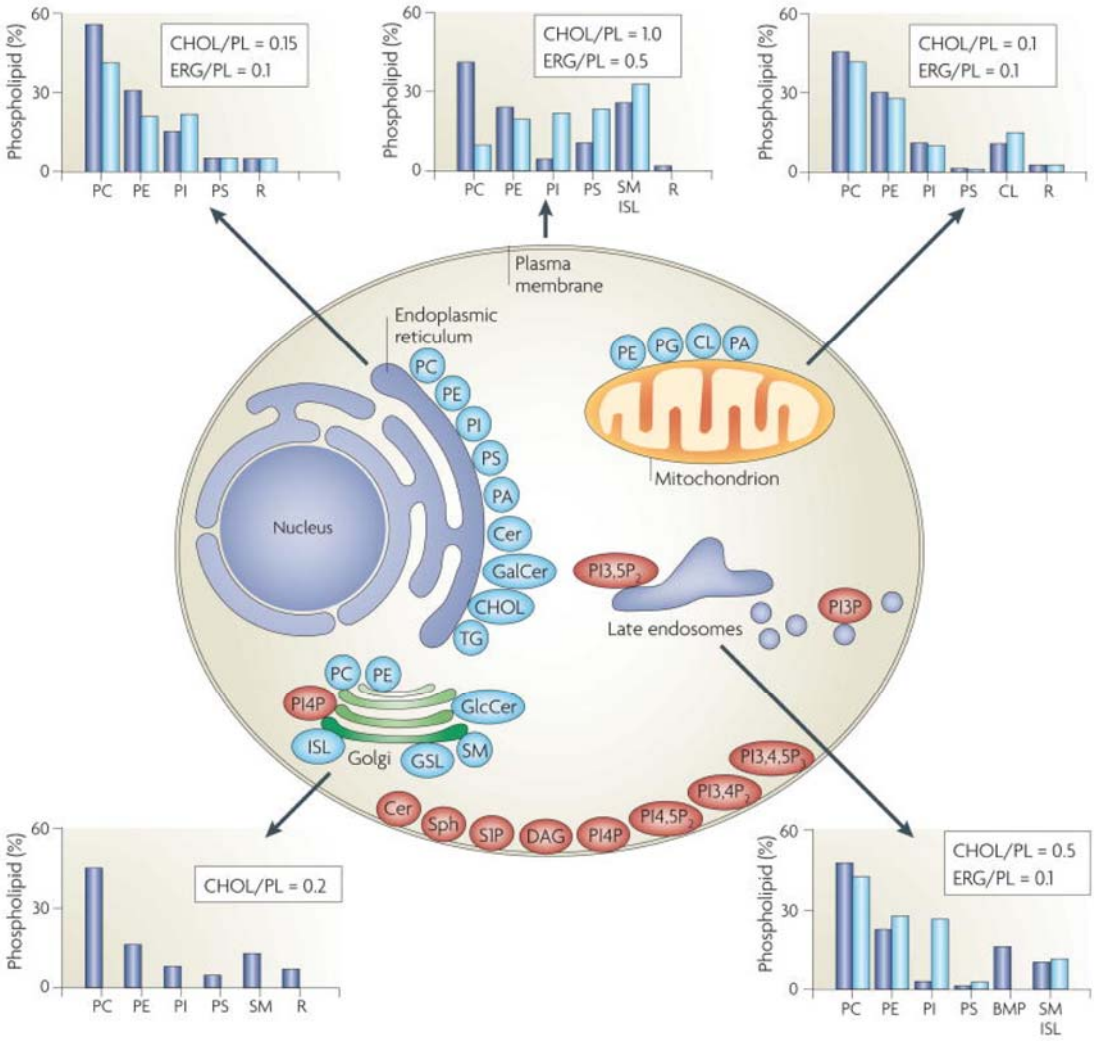

Figure 1.1 **Lipid composition of cellular membranes**
Lipid composition of membranes in the cell varies between organelles. The main figure shows sites of lipid biosynthesis. Major lipids are shown in blue ovals and lipids involved in signalling and organelle recognition are shown in red ovals. Signalling and recognition lipids make up less than 1% of total PL except for ceramide. 45% of mitochondria lipids are synthesised on site. Lipid composition data shown in graphs is given as a percentage of total PLs. Light blue indicates lipid levels for yeast and dark blue indicates lipid levels for mammalian cells. The molar ratio per organelle of mammalian cholesterol and yeast ergosterol to PL is also included. Figure from (van Meer, Voelker and Feigenson, 2008). Abbreviations: PL, phospholipid; PC, phosphatidylcholine; PE, phosphatidylethanolamine; PS, Phosphatidylserine; PI, phosphatidylinositol; PA, phosphatidic acid; Cer, ceramide; GalCer, galactosylceramide; TG, triglyceride; PI4P, phosphatidylinositol 4-phosphate; PI3P, phosphatidylinositol 3-phosphate; PI(4,5)P_2, phosphatidylinositol 4,5-bisphosphate; PI(3,4)P_2, phosphatidylinositol 3,4-bisphosphate; PI(3,4,5)P_3, phosphatidylinositol 3,4,5-trisphosphate; S1P, sphingosine-1-phosphate; DAG, diacylglycerol; GSL, complex glycosphingolipids; ISL, yeast inositol sphingolipid; BMP, bis(monoacylglycero)phosphate; SM, sphingomyelin; Sph, sphingosine; CHOL, cholesterol; ERG, ergosterol; CL, cardiolipin.

Membrane-bound organelles are only found in eukaryotes and allow specific functions in different, separated compartments within the cell. Each organelle membrane has a unique/distinct protein and lipid composition tailored to its function, creating organelle identity [Figure 1.1]. Proteins are often localised to their organelle destination by specific peptide motifs or domains to target them to the correct membrane. However, lipids do not contain such domains yet still have specific distribution. The majority of cellular lipids are synthesised in the ER, and thus precise intracellular lipid traffic is needed from where lipids are created to their destination in specific membrane compartments.

There are three major categories of membrane lipids – glycerolipids, sphingolipids and sterol lipids [Figure 1.2]. Glycerolipids and sphingolipids are fatty acid based; the fatty acyl structure is composed of a long hydrocarbon chain (usually 16 or 19 carbons) that can be saturated where there are no double bonds or unsaturated where there are one or more double bonds. Glycerolipids are defined by their glycerol backbone, which can be linked to one, two or three fatty acid chains. The most abundant structural lipids in a eukaryotic membrane are glycerophospholipids, a subdivision of glycerolipids. For example phosphatidylcholine (PC), contains a phosphate with a choline head group, a glycerol backbone (glycerol-3-phosphate) and two fatty acid acyl chains [Figure 1.3A]. Ether glycerolipids have one fatty acid acyl chains but have an ether group attached to the glycerol backbone.

The backbone of sphingolipids is an unsaturated mono alcohol sphingosine instead of a glycerol group as is the case for glycerolipids. Sphingophospholipids, one type of sphingolipid, contain a phosphate group and together with glycerophospholipids and ether glycerolipids, are labelled as phospholipids (PLs). Sphingomyelin is the most common sphingolipid and is very similar in structure to phosphatidylcholine (PC), a glycerophospholipid [Figure 1.3B]. Glycolipids contain a mono or oligosaccharide rather than a phosphate group, and being involved in cell recognition and intracellular communication amongst other less well defined functions, they are found exclusively on the external face of the cell membrane.

The third major class of membrane lipids are sterols, which include cholesterol, ergosterol (yeast) and stigmasterol (phytosterol, i.e. in plants) discussed in more detail below.

1.2.2 Function of sterol in a membrane

A major lipid component of eukaryotic plasma membranes (PM) is sterol, which is important for regulating the rigidity of the cell membrane via interactions with

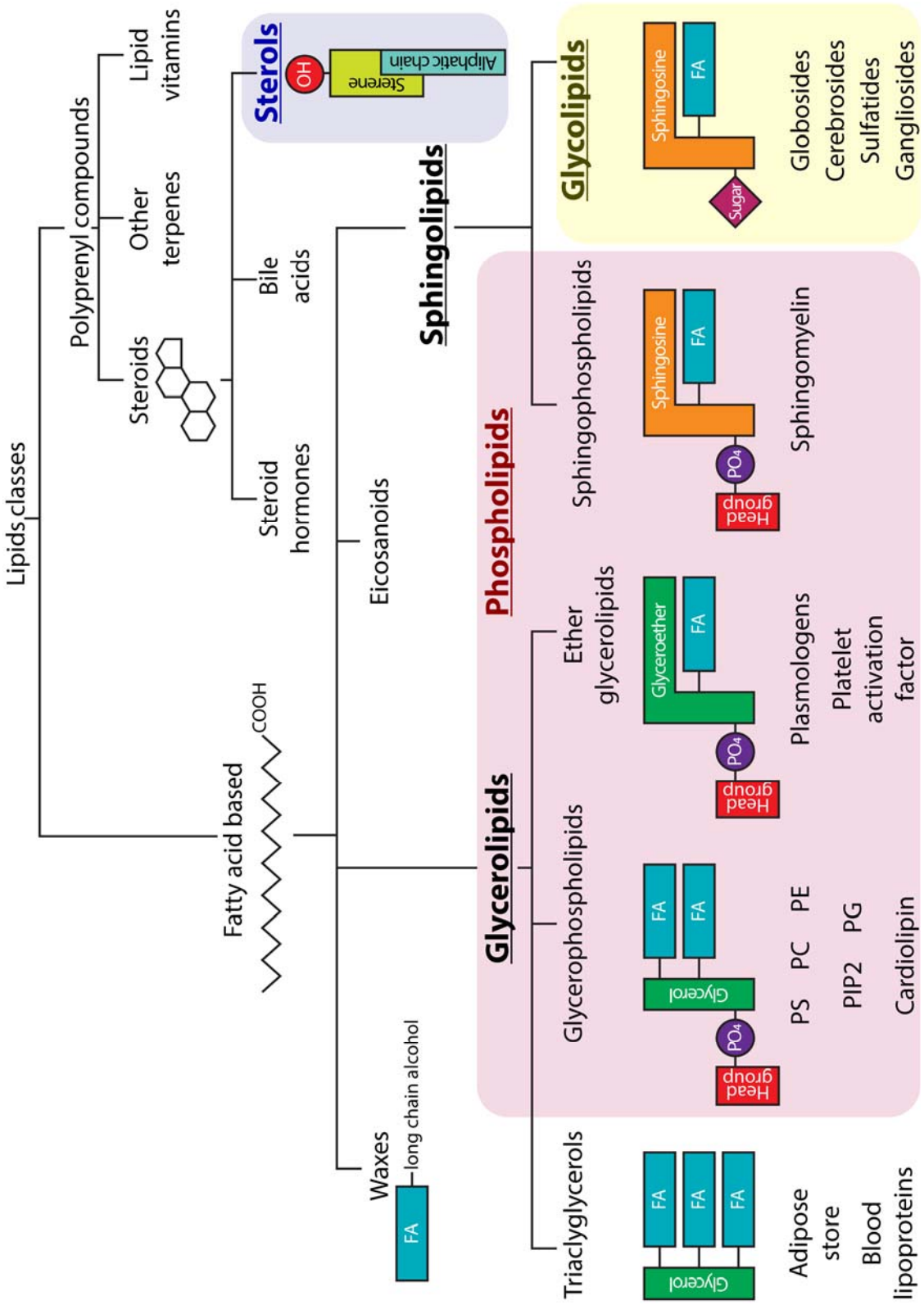

Figure 1.2 **Common types of lipids and their structure architectures**
Sterols (light blue), which include yeast ergosterol and mammalian cholesterol, have a steroidal tetracyclic ring structure. Triaclyglycerols and waxes are neutral storage lipids. Glycerolipids and sphingolipids have either a glycerol or sphingosine as a backbone, to which one or more long chain alkyl group are attached. Fatty acid acyl chains vary in length and saturation. The phospholipid group (pink) is composed of both glycerolipids and sphingolipids with a phosphate group. Common polar head groups include choline, serine and inositol. Glycolipids (yellow) are found on the outer leaflet of the plasma membrane. Abbreviations: PC, phosphatidylcholine; PE, phosphatidylethanolamine; PS, Phosphatidylserine; PIP_2, phosphatidylinositol-bisphosphate; PG, phosphatidylglycerol; FA, fatty acyl chain; PO_4, phosphate group.

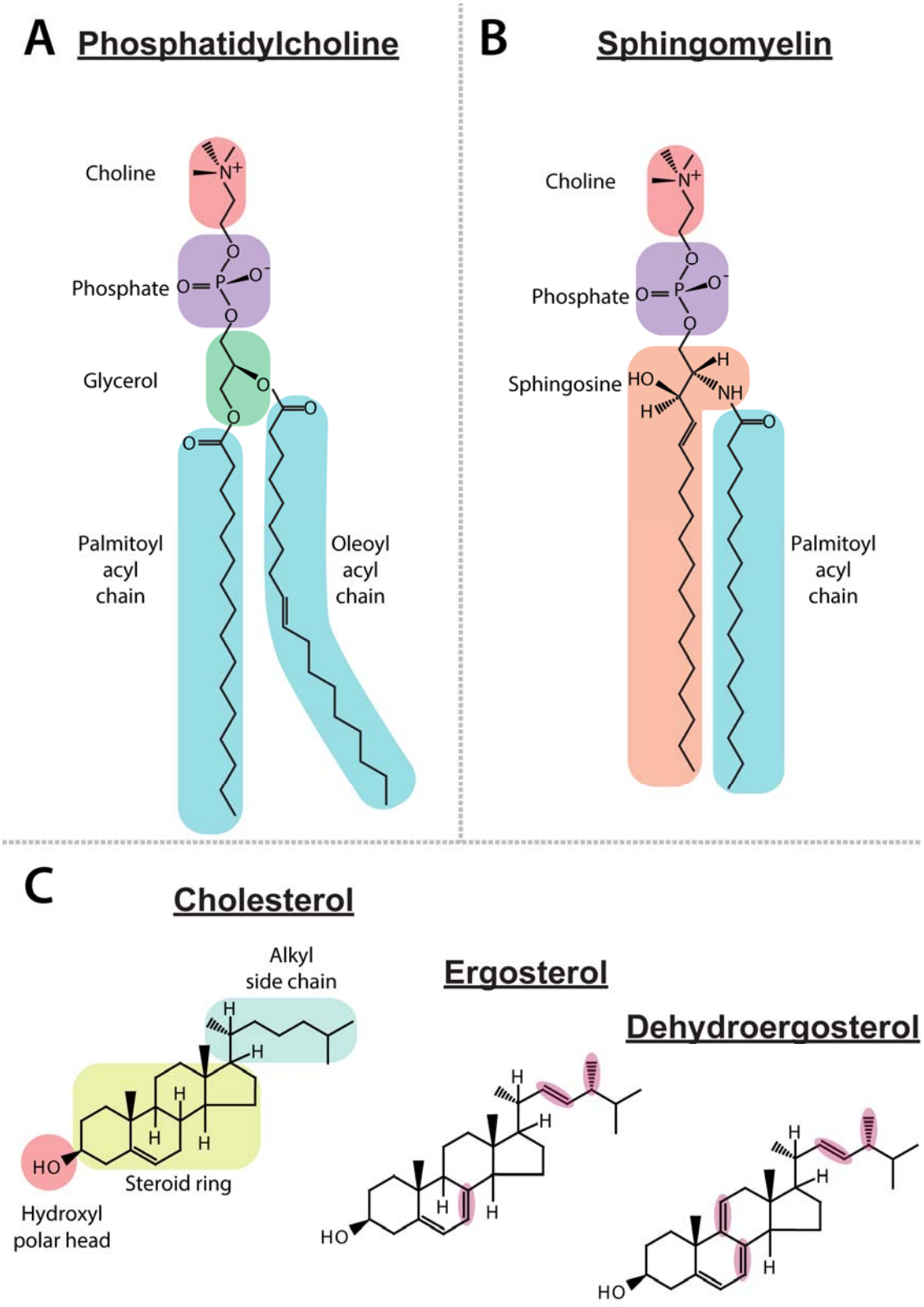

Figure 1.3 **Chemical structure of common membrane lipids**
A) Palmitoyl-oleoyl-phosphatidylcholine structure and components. The palmitoyl acyl chain is saturated whereas the oleoyl acyl chain is monounsaturated. **B**) Palmitoylsphingomyelin structure and components. The sphingosine backbone replaces the glycerol and acyl chain of phosphatidylcholine but the choline and phosphate head group remains the same. **C**) Structures of mammalian cholesterol, yeast ergosterol and dehydroergosterol. Components of sterols are indicated with cholesterol. Structural differences of ergosterol and dehydroergosterol to cholesterol are highlighted.

saturated membrane lipids. In a bilayer, acyl chains of PLs and glycolipids pack in parallel, perpendicular to the surface of the bilayer. When unsaturated, one or more double carbon-carbon bonds cause a kink in the chain thus decreasing the packing of the bilayer [Figure 1.3A]. However, single carbon-carbon bonds can freely rotate leading to the flexibility of the acyl chains.

Sterol molecules are not formed of a conventional large polar head group and long hydrophobic tail combination as is the case for PLs [Figure 1.3]. Instead, they are composed of a small polar hydroxyl group, a rigid steroid ring and a short non-polar hydrocarbon side chain [Figure 1.3C]. In a membrane, the hydroxyl group of the sterol is positioned beneath the polar heads of PLs between acyl chains and the planar hydrophobic steroid ring aligns parallel to the saturated acyl chains allowing Van der Waal bonds to form between the two [Figure 1.4A]. This arrangement between the planar rings of sterol and otherwise flexible acyl chains of PLs generates tighter packing and increased order (Stockton and C.P. Smith, 1976). Interactions between sterol and saturated acyl chains not only serve to increase rigidity, but they also increase fluidity characterised as a 'liquid ordered' phase. In a liposome, 'liquid ordered', 'liquid disordered' and 'solid' phase is determined by the ratio of saturated membrane lipids: unsaturated membrane lipids:sterol (Feigenson, 2006). By positioning themselves between the PLs, the sterols prevent the lipids from packing too much and crystallising, thereby avoiding phase transitions and encouraging fluidity at low temperatures.

Sterols in membranes also influence extra- and intra-cellular signalling, regulating gene transcription, protein sorting, protein degradation, enzyme activity, vacuole fusion, endocytosis, and membrane trafficking (Schulz and Prinz, 2007). Specialised cells in higher eukaryotes also use sterol as precursors to steroid hormones, oxysterols and bile acids (Ikonen, 2006). Steroidogenesis, a process converting cholesterol to steroids is carried out by P450scc/CYP11A1 enzyme that resides in the inner mitochondrial membrane. Bile acids are produced via two pathways; the classic (neutral) pathway requires CYP7A1 in the ER, and the alternative (acidic) pathway involves the 27-Hydroxylase (CYP27A1) which converts the most abundant oxysterol, 27-hydroxycholesterol from cholesterol in the mitochondria (Ferdinandusse and Houten, 2006).

1.2.3 Regulation of cholesterol synthesis

The *de novo* synthesis of sterol occurs via the mevalonate pathway, although sterols can also be released from internal storage of esterified cholesterol. Almost all stages of the mevalonate pathway, including the final step, are catalysed in the ER

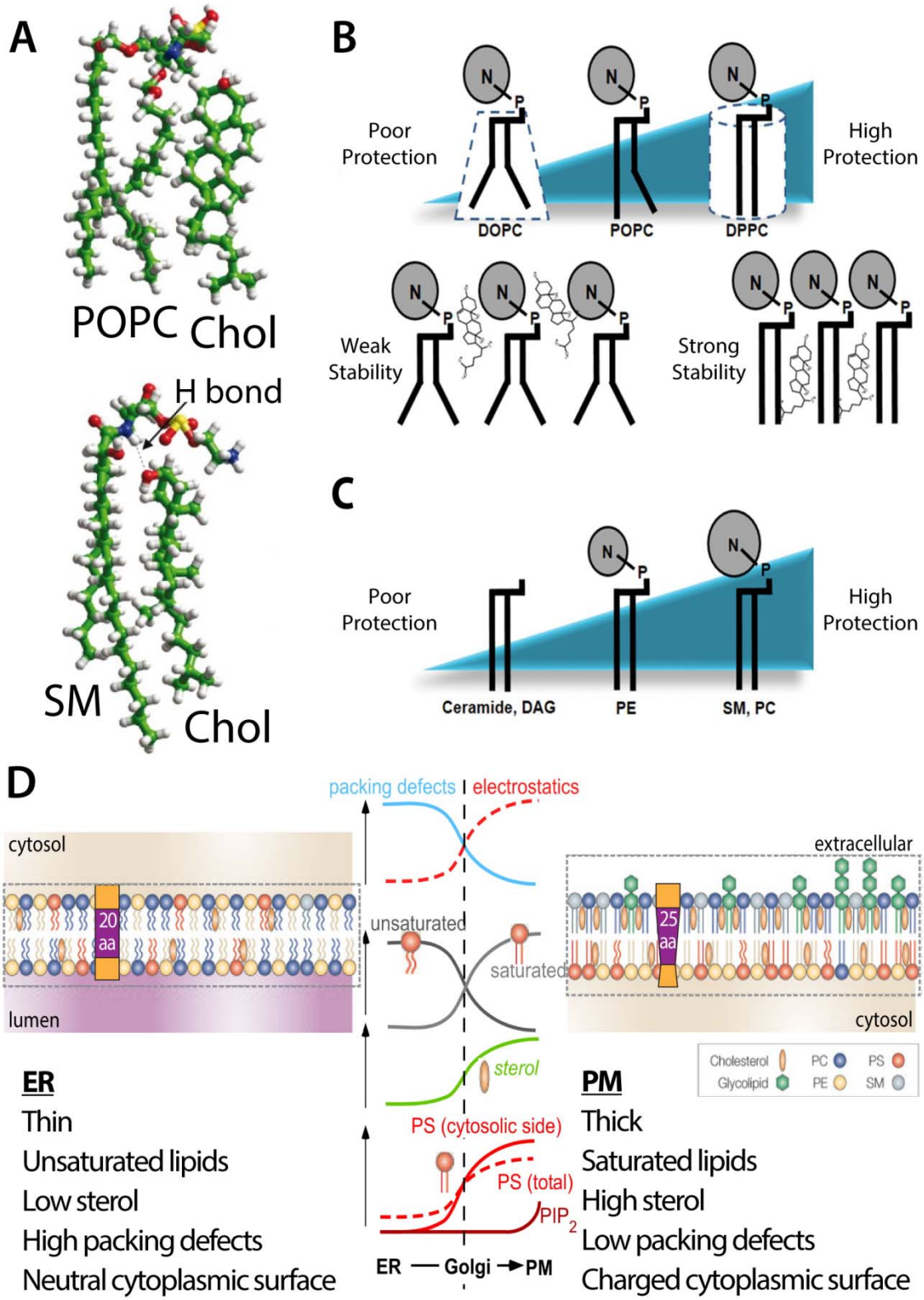

Figure 1.4 **Sterol interactions with membrane lipids**
A) In a membrane, cholesterol (Chol) can interact with glycerophospholipids (i.e. palmitoyl-oleoyl-phosphatidylcholine (POPC)) or sphingolipids (i.e. sphingomyelin (SM)). Figure from (Fantini and Barrantes, 2013). **B)** Acyl chain saturation increases sterol stability in the membrane; sterol is more stable in membranes with dipalmitoyl phosphatidylcholine (DPPC) than with dioleoyl phosphatidylcholine (DOPC). **C**) Sterol is protected by membrane lipids with larger head groups. Figures from (Iaea and Maxfield, 2015). **D**) The ER contains a high proportion of unsaturated phospholipids and a low percentage of sterols thus the bilayer is flexible. The PM is rich in saturated phospholipids and sterols. This is reflected in the high rigidity and impermeability. Adapted from (Holthuis and Levine, 2005; Bigay and Antonny, 2012).

(Goldstein and Brown, 1990). Mammalian cells can also take up external cholesterol via receptor-mediated endocytosis of lipoproteins whereas yeast cells carry out uptake of free cholesterol via PM-localised ABC (ATP-binding cassette) transporters in yeast[1]. These new supplies of sterol require redistribution across all cellular membranes calling for a highly specific and regulated transport system to link the origins and destinations of cholesterol (see 1.2.4 below for more details on sterol distribution). Furthermore, a malfunctioning sterol transport system can cause disease. Most obviously, Niemann-Pick Type C is a fatal neurodegenerative disease characterised by the accumulation of cholesterol in late endosomes and lysosomes reducing availability of sterol for use in membranes and steroid synthesis including neurosteroids (Mukherjee and Maxfield, 2004). This lysosomal storage disease is caused by mutations of NPC1 and NPC2, a pair of sterol transfer proteins and although there is no known cure, cyclodextrin has been proposed as a potential therapeutic treatment (Liu, 2012).

A homeostatic mechanism involving transcription factor SREBP-2 (sterol regulatory element-binding protein 2) controls total cellular levels. SREBP-2 is usually bound to SCAP (SREBP cleavage-activating protein) in the ER and INSIG1 (Insulin-induced gene 1) as a complex to sense fluctuating ER cholesterol levels. When ER cholesterol drops below a threshold of ~5% mol:mol[2], SREBP-2 is activated. This requires SCAP to escort SREBP-2 to the Golgi where SREBP-2 is cleaved, freeing the N-terminal fragment of SREBP-2. The cleaved NH_2 fragment containing bHLH-Zip is now able to migrate to the nucleus and binds to sterol regulatory elements, thus activating the transcription of the required sterol synthesis and uptake genes. When ER cholesterol rises above the 5% mol:mol threshold, the SCAP-SREBP-2 complex binds to the chaperone protein INSIG1 anchored on the ER, preventing the transport to the Golgi (Iaea and Maxfield, 2015). Therefore, there is down-regulation of sterol acquisition genes.

1.2.4 Intracellular distribution of sterol

Cellular membranes have distinct lipid compositions and therefore also distinct sterol compositions. Sterol is the most abundant lipid species in the cellular lipidome, accounting for 30-40% of total cellular lipid and is unevenly distributed throughout the various cellular membranes [Figure 1.1]. It is found at its highest concentration at the PM (~40% mol:mol of total PM lipids). Its ability to increase rigidity ensures impermeability of the plasma membrane to polar solutes in the outside environment

[1] Where the term 'yeast' is used, the species referred to is *Saccharomyces cerevisiae.*
[2] % mol:mol describes the percentage of a component out of the total moles.

(Corvera *et al.*, 1992; Wüstner, 2009). The PM sterol levels account for most (60-90%) of the total cellular cholesterol, in contrast to the site of sterol synthesis, the ER which harbours only <12.5% of total cellular sterol (Lange *et al.*, 1999; Nilsson *et al.*, 2001), where it accounts for ~5% mol:mol of total ER lipid content (Lange and Steck, 1997; Radhakrishnan *et al.*, 2008). It is still unknown how the gradient is exactly regulated (see Section 1.5.1 Creation of lipid gradients).

1.2.5 Sterol affinity in membranes

Sterol retention of a membrane and the movement of the sterol in and out of the membrane are thought to depend on the affinity of the sterol to the lipids already within that membrane, though this may or may not be the only factor. PLs made with long or saturated chains found in the PM enhance Van der Waal interactions with sterol molecules [Figure 1.4B] (McConnell and Radhakrishnan, 2003). Unsaturated acyl chains of phospholipids such as dioleoyl phosphatidylcholine (DOPC) and to a lesser extent, palmitoyl-oleoyl-phosphatidylcholine (POPC) increase the chemical activity coefficient of cholesterol due to the double carbon-carbon bond creating a bend in the tail. DOPC has double carbon-carbon bonds in both acyl chain tails whereas POPC has a double bond in only one. The bent acyl chains provide more room between the phospholipids, thereby decreasing protection to the sterol. PLs with saturated chains such as dipalmitoyl phosphatidylcholine (DPPC) have straight acyl chains and therefore permit stronger Van der Waal bonds (Chong, 1994). The stronger affinity between sterol and the saturated hydrocarbon chains provides higher protection to the cholesterol, with sterol desorbing slower from membranes containing more saturated lipids compared to unsaturated lipids (Ramstedt and Slotte, 2002). Highly protected sterol cannot readily leave the membrane, hence has lower chemical activity compared to sterol that is associated to unsaturated PLs. The high level of saturated lipids in the PM compared to the ER reflects this protective function of the PM for sterols.

Sterol protection is also provided by and is dependent on the head group of the PLs [Figure 1.4C] (Huang and Feigenson, 1999). The PL head group acts as an ‘umbrella’, protecting the cholesterol in the membrane. PLs with large head groups such as PC provide protection to the buried sterol molecule in the membrane to cytoplasmic sterol-binding proteins. Conversely, PLs with small head groups such as phosphatidylethanolamine (PE) provide less protection. Diacylglycerol (DAG) and ceramide provide no protection as they lack head groups (Mesmin and Maxfield, 2009).

1.2.6 Sterol pools

The PM is enriched in lipids that have high affinity to sterols such as saturated species of glycerophospholipids and more notably sphingomyelin [Figure 1.4D] (Ohvo and Slotte, 1996; Schneiter *et al.*, 1999). Sphingomyelin contains a saturated acyl chain and a 4,5-trans unsaturated sphingoid long chain backbone allowing more Van der Waal interactions with sterol (Fantini and Barrantes, 2013). It has been shown that decreasing levels of sphingomyelin allows a fraction of sterol from the PM to move to the ER implying that at least some of the sterol in the PM is retained by its association to sphingomyelin (Slotte and Bierman, 1988; Scheek, Brown and Goldstein, 1997; Das *et al.*, 2014).

It is using this ability of sphingomyelin to sequester sterol that the plasma membranes were found to harbour more than one pool of sterol. Sterol retention by sequestering lipids was first described as a 'J-shaped curve' when it was discovered that small variations in PM sterol content above a threshold resulted in substantial changes in the ER sterol pool (Lange *et al.*, 1999). It was thought that this sphingomyelin-sequestered sterol formed one of two pools. However, a later study showed that there were, in fact, at least three pools (Das *et al.*, 2014). Using a sterol probe, ^{125}I-labelled mutant version of bacterial toxin, Perfringolysin O, Das *et al.* revealed that the first pool of cholesterol was accessible without any alteration to the sphingomyelin in the PM suggesting that this particular pool is independent from sphingomyelin. This pool was found to fluctuate depending on levels of sterol in the cell and is only present when there is >35% mol:mol of sterol in PM. The second pool of sterol was only accessible after treatment of the PM with sphingomyelinase, reinforcing the previous theory of sphingomyelin-sequestered sterol. Even after depletion of sphingomyelin, a portion of cholesterol was still retained which upon removal, caused disintegration of the PM integrity indicating the importance of a minimal amount of sterol in the plasma membrane (Das *et al.*, 2014). The release of sphingomyelin-sequestered sterol by sphingomyelinase can only account for one type of complex as there are many variations of saturated lipids in the PM with which sterol may interact. Hence, the remaining cholesterol may be formed of multiple pools yet to be characterised.

1.3 Intracellular lipid transfer

1.3.1 Three classes of intracellular lipid movement

The growth and survival of cells that have more than one membrane compartment is thought to require precise intracellular lipid traffic. In eukaryotes, lipid

synthesis and modifying enzymes are predominantly targeted to a specific organelle, the ER. Thus the lipids themselves must traffic to other membranes.

There are three categories of intracellular lipid movement, the first being lateral movement which refers to the diffusion of a lipid laterally within each leaflet of the membrane. This type of movement occurs quickly and spontaneously; in a representative fluid dynamic cellular membrane a typical lipid molecule exchanges places with its neighbours about 10^7 times per second allowing a movement of several micrometres (or a length of a large bacteria) per second at 37°C (Fahey *et al.*, 1977). In other words, lipids move 10-100 times faster than transmembrane proteins in a membrane. The second mode of intracellular lipid movement is the transverse exchange between two leaflets of a bilayer, also known as flip-flopping (Holthuis and Levine, 2005). The speed and efficiency of this movement are dependent on the nature of the lipid that is moving. For DAG or sterol, lipids with little or no polar headgroup, trans-bilayer exchange is relatively quick and does not need catalysing proteins. For lipids such as PLs or glycolipids, the lipid movement must be catalysed by flippases that shield the polar head groups from the hydrophobic core of the membrane as the energetic barrier would otherwise be too high (Bretscher, 1973). The final form of lipid transfer is the movement of lipid between membranes, which occurs via vesicular and non-vesicular transport.

1.3.2 Transport of cellular sterol between membranes

The homoeostasis of the cellular sterol levels must deal with the constant biosynthesis of sterol in the ER and the acquisition of sterol from external sources. Cholesterol cannot be fully metabolised in mammalian cells. However, it can be converted to oxysterols/steroids for other use and esterified to cholesterol esters with long chain fatty acids for storage in lipid droplets or release as lipoproteins. In yeast, sterol esterification is carried out by two ACATs (Acyl-CoA cholesterol acyltransferases) which are localised in the ER. The proximity of sterol synthesis and sterol esterification components suggests that newly synthesised sterol could be esterified immediately. However, only a small percentage of the new sterol is converted to sterol esters (Lange, Strebel and Steck, 1993). In addition, excess accumulation of sterol in the ER is toxic (Feng *et al.*, 2003). Hence, if newly synthesised sterol is not esterified, it must be efficiently transported out from the ER, suggesting a highly regulated and efficient sterol transport system acting along the forward sterol transport path in the cell.

Most of the time, the internal synthesis of sterol is sufficient for the survival of the cell. Nonetheless, some mammalian cells require internalisation of external cholesterol from low-density lipoproteins for normal growth. This necessity for additional cholesterol is the case for neurones in the central nervous system which can produce enough endogenous cholesterol to survive, differentiate and form immature synapses but require glia-derived lipoproteins to form a sufficient number of synaptic contacts (Mauch *et al.*, 2001). Endocytosis internalises lipoproteins with a cholesterol ester core in mammalian cells where they are hydrolysed in late endosomes and lysosomes and then released for cellular use.

All cell types can also take up external free cholesterol. For budding yeast, this occurs only under anaerobic conditions where the lack of oxygen necessary for sterol synthesis triggers them to be conditional sterol auxotrophs (Jacquier and Schneiter, 2012). In this situation, the synthesis of ergosterol stalls and the yeast cells become sterol auxotrophs. ABC transporters in the class G subfamily (ABCG), Aus1p and Pdr11p in the plasma membrane are synthesised to take up sterols from the growth medium. Without these two ABCG transporters, yeast cannot grow under anaerobic conditions (Wilcox *et al.*, 2002). The mechanism of sterol uptake by the transporters is still unknown. Additionally, after the uptake into the PM, it is still not fully understood how sterol is distributed throughout the cell (Li and Prinz, 2004), though internalised sterol can reach the ER to be esterified and stored in lipid droplets.

Mammalian ABC transporters also mediate sterol levels (Velamakanni *et al.*, 2007). Specifically, human ABCG5/ABCG8 heterodimers mediate sterol efflux, and a recent structural study proposes observed two symmetrical vestibules on opposing faces of the transmembrane domains to be entryways for sterols to access the core of the dimer (Lee *et al.*, 2016). The proposed sterol-binding surface of the vestibules possesses several residues conserved across eukaryotic evolution. One of these conserved residues was mutated in an *in vivo* functional reconstitution assay, which showed that a mutation in the putative cholesterol-binding site prevented the restoration of cholesterol transport (Lee *et al.*, 2016). ABCG5 and ABCG8 are the first ABCG transporters to have been crystallised, further structural studies on both human and yeast will find the conserved characteristics of all ABCG transporters and their links to sterol and steroid binding.

1.3.3 Complications of unravelling intracellular sterol transport

Specifics of both the forward and backward transport of sterol through the cell are still unidentified as there are many challenges surrounding lipid transport; most lipids are unevenly distributed in multiple membranes, and whilst almost all lipids are

produced in the ER, a handful of lipids are synthesised in other compartments. Lipids by their nature must be incorporated and therefore targeted to membranes. In addition, most lipids are not exclusive to one membrane, for instance, all membranes have sterols at varying levels, and thus a specific signalling sequence to target to one membrane would not be suitable for lipids. Unlike protein transport, lipid transport is not limited to the vesicular pathway; mitochondria (and also chloroplasts) are not connected to the secretory pathway, yet mitochondrial membranes contain many ER synthesised lipids including a low level of cholesterol, and a small number of lipids are produced in the mitochondria, which are then transported to other cellular membranes. Mammalian cells also synthesis sterol based hormones and bile acids with mitochondria localised enzymes (see section 1.2.2 for details). Evidence of an essential link between the ER and the mitochondria was demonstrated when the cell was observed to compensate for the reduction of ER-mitochondria contacts by expanding vacuolar-mitochondria contacts allowing a diversion of communication (see section 1.4.7 for more details on these contact sites) (Elbaz-Alon *et al.*, 2014; Hönscher *et al.*, 2014). The multiplicity of lipid trafficking pathways may explain the general failure of genetics to identify lipid transport genes.

1.3.4 Vesicular pathway is not responsible for bulk sterol transport

Molecular transfer between different organelles can be vesicular or non-vesicular. The first model for sterol transport was based on the vesicular pathway. However, it is now accepted that this cannot be the process of bulk lipid transport. There are five significant pieces of evidence to support non-vesicular transport of sterol. The first is that treatment of Brefeldin A, a drug that disrupts the Golgi and the secretory pathway by inhibiting vesicle formation, had little effect on lipid transport including sterol transport (Urbani and Simoni, 1990; Vance, Aasman and Szarka, 1991; Heino *et al.*, 2000). The second showed that the cytoskeletal network, which is essential for efficient vesicular traffic could also be pharmaceutically disrupted with no effect on sterol transport (Kaplan and Simoni, 1985b). The third piece of evidence involved genetically disrupting the secretory pathway in budding yeast mutants where SEC18, a gene required for ER-PM vesicular traffic was mutated. These strains show little blocking of sterol traffic (Baumann *et al.*, 2005). The fourth point is that the speed of cholesterol transfer from the ER to the PM ($t_{½}$ = five minutes) is much faster than vesicular protein traffic (and also for phospholipids PC, PS and PE with $t_{½}$ as two, two and 20 minutes respectively) (Sleight and Pagano, 1983; Kaplan and Simoni, 1985a; Urbani and Simoni, 1990; von Filseck, Čopič, *et al.*, 2015). Finally, mitochondria and

also chloroplasts are not connected to the secretory pathway, and they acquire many of their lipids from the ER including sterol, which is found at low levels in all cells. In yeast, the concentration of ergosterol measured in the mitochondria was 11% mol:mol in the inner mitochondrial membrane and 4% mol:mol in the outer mitochondrial membrane (Bottema and Parks, 1980). Thus, sterol transport must be occurring via a non-vesicular pathway if sterol is present in mitochondria. Consequently, it has been suggested that the bulk of sterol transfer between membranes is via a non-vesicular manner.

1.3.5 Spontaneous diffusion is not sufficient

One suggested method of non-vesicular transport is diffusion; this passive, spontaneous sterol transport has been reported to occur between membranes *in vitro* where sterol molecules can 'jump' across two closely apposed membranes (McLean and Phillips, 1984; Dawidowicz, 1987). For this to transpire, sterol must first desorb from the donor membrane to be solubilised in the aqueous phase, diffuse across the distance required to reach the acceptor membrane and then be absorbed by the acceptor membrane. However, the desorption/solubilisation of the hydrophobic sterol molecule is an energetically unfavourable and rate limiting step (Phillips *et al.*, 1980; McLean and Phillips, 1984). Cholesterol is essentially insoluble; the critical micellar concentration of cholesterol in water is ~25-40 nM (Haberland and Reynolds, 1973). Therefore, it would reason that a high amount of energy would be needed to remove the sterol molecule from its preferred environment in a membrane to a single molecule state in an aqueous environment. This high-energy requirement is consistent with the experimental evidence, which supports desorption as a slow, rate-limiting step. In contrast, the absorption of sterol from an aqueous environment to a hydrophobic membrane environment is fast (McLean and Phillips, 1984).

Considering the slow *in vitro* lipid transfer speeds ($t_{½}$ for cholesterol is ~2 hours and for PC up to 83 hours), the diffusion-based mechanism, despite potentially having a small role in cellular sterol transport, is insufficient and unlikely to be responsible for the main transport of sterol (McLean and Phillips, 1984).

Lipid transfer proteins (LTPs) or domains broadly refer to soluble proteins with a hydrophobic pocket that have an ability to transfer lipids *in vitro* (D'Angelo, Vicinanza and De Matteis, 2008). These proteins are structured to solubilise and shield hydrophobic ligands from a membrane into an aqueous environment. Thereby the concept of lipid transfer proteins can significantly decrease the energy required to

overcome the obstacle of desorption and solubilisation of a lipid, a problem unsolved by spontaneous diffusion.

1.3.6 Lipid transfer by proteins at contact sites

A simplified model of lipid transfer by LTPs would be the ER around the nucleus being the origin and the PM being the destination. Assuming that the nucleus takes up 7% of a yeast cell volume (Jorgensen *et al.*, 2007) and a normal yeast cell being 2-3 μm in radius (*r*), a lipid inside a lipid transfer domain must cross a distance of 1.5-2.2 μm [Equation 1].

Equation 1 Diffusion distances of LTPs in yeast

$$volume\ of\ cell = \frac{4\pi r^3}{3}$$

$$r_{nucleus} = 0.26\, r_{cell}$$

The diffusion constant (*D*) of a small protein with a size similar to that of a lipid transfer domain is 30 $\mu m^2 s^{-1}$ through the cytoplasm (Baum *et al.*, 2014). The equation describing the time (*t*) for three-dimensional Brownian diffusion across a distance (*x*) is:

Equation 2 Diffusion time of LTPs in the cytosol

$$t = \frac{x^2}{6D}$$

This formula generates the time of one cycle to be 50-100 milliseconds. Assuming an efficient unidirectional lipid transfer domain, a maximum of 10-20 molecules of lipids can be transported per second. However, the proposed *in vivo* rate of sterol transport between the ER and the PM is 10^5 sterol molecules per second suggesting that approximately perfectly efficient 10^4 transfer proteins are needed (Sullivan *et al.*, 2006). By considering membrane contact sites (MCSs) between the ER and other organelles (see section 1.4 for more details on MCSs) as being the sites of bulk lipid transfer, the number of sterol transfer proteins can be reduced. Supporting this theory is the high enrichment of proteins linked to lipid biosynthesis and more significantly LTPs and putative LTPs in the regions of ER that form contacts with other membrane-bound organelles. However, the restriction of diffusion distance to 30 nm (the separation between MCS and PM) reduces the time per transfer dramatically to 10 microseconds thus reducing the number of perfect sterol transport proteins required for

the observed rate to one. Accordingly, for the observed rate to hold true with higher numbers of LTPs present, there must be some complexities yet to be determined that LTPs acting at contacts can overcome such as transfer against a gradient. A recent review modelling the rate limiting factor as diffusion distance versus sterol desorption has suggested that contact sites have no role in the speed of transfer but to facilitate specific transport of lipids in restricted local membrane compartments (Dittman and Menon, 2016). It should also be noted that the rate of 10^5 sterol molecules per second used for the calculations above and the modelling by Dittman and Menon may be an underestimation (Dittman and Menon, 2016). The original study which proposed this speed measured the equilibrium of newly made radiolabelled ergosterol at the PM that is extractable by MβCD (Sullivan *et al.*, 2006). Theoretically, this would only measure 'free' ergosterol, which is approximately 8% of cellular sterol compared to the 60% of cell sterol available in the PM. Still, the authors were only able to extract ~0.3-0.4% of total ergosterol content thus the measured speed could be limited by the rate of ergosterol moving to the MβCD extractable pool on the PM, which is only ~0.5% of PM sterol. Further studies suggest that there is indeed a delay between sterol moving from the ER to the PM and sterol moving to the MβCD accessible PM sterol pool (Georgiev *et al.*, 2011).A significantly higher rate would in turn require more LTPs to maintain this, even in the short distances calculated above. Thus further studies in revealing the true *in vivo* sterol transfer rate will be required to make conclusive numerical analysis, though rough estimates for comparisons can be tentatively made.

1.4 Membrane Contact Sites

1.4.1 ER membrane contact sites

The ER network spans the entirety of the cell by branching out from the nuclear envelope, thus coming into close proximity with most types of organelles [Figure 1.5A]. Developments in understanding contacts between ER and other cellular compartments have suggested that lipid transfer can occur at membrane contact sites (MCSs) (Holthuis and Levine, 2005). When two membrane-bound organelles are in close proximity (~30nm), they can exchange materials through the MCSs such as during signalling events, regulating Ca^{2+} homoeostasis, lipid synthesis and trafficking between organelles (Carrasco and Meyer, 2011; Stefan *et al.*, 2011; Stefan, Manford and Emr, 2013). Also, MCS are also essential for cell physiology such as organelle positioning and movement including during cell division and organelle fission/division (Friedman *et al.*, 2011; Rowland *et al.*, 2014; Phillips and Voeltz, 2015). For example, maturing endosomes

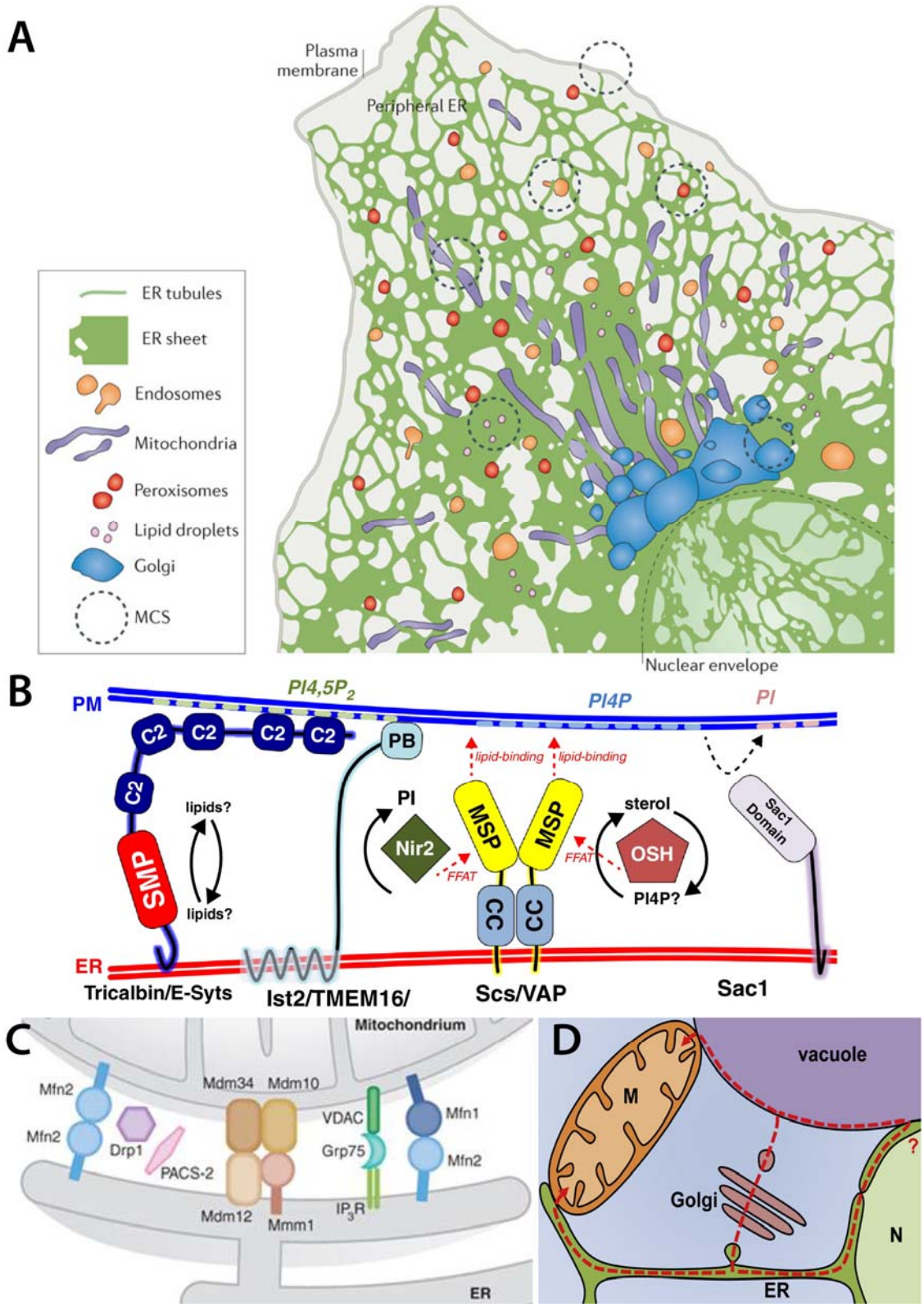

Figure 1.5 **Membrane contact sites and proposed tethers**
A) The ER (green) makes contacts (dashed circles) with the PM mitochondria, endosomes, peroxisomes, lipid droplets and the Golgi. Figure from (Phillips and Voeltz, 2015). Proteins that play a role in (**B**) ER-PM (Figure from (Henne *et al.*, 2015)) and (**C**) ER-mitochondria tethering (Figure from (de Brito and Scorrano, 2008)). Note that not all proposed tethers are illustrated. **D**) Routes for lipid transfer (red dotted lines) from the ER to the Mitochondria via ERMES or vCLAMP. Figure from (Klecker and Westermann, 2014).

make contact with the ER during trafficking from the PM to the lysosome (53% of early endosomes compared to 99% of late endosomes), and the ER has been suggested to facilitate constriction during mitochondrial fission (Friedman *et al.*, 2013; Murley *et al.*, 2013).

Electron microscopy was first used to detect the MCSs, including ER-PM and the ER and the mitochondria contacts (Benhard and and Rouiller, 1956). MCSs can be stable and durable, for example, between the PM and the ER and between the ER and the mitochondria, where the contacts appear stable throughout the cell cycle (Nguyen *et al.*, 2012). However, some contacts show very dynamic characteristics, for instance, the NVJ (nucleus-vacuolar junction), which expands upon entry to stationary phase (Millen *et al.*, 2009). These appositions are established and maintained by tethering structures that keep the two membranes close but not physically joined thus precluding membrane fusion. The dependency of tethering proteins for contact sites is reflected by the upregulation of Nvj1p transcription, which expands the NVJ during periods of reduced growth (Millen *et al.*, 2009).

1.4.2 MCS targeting proteins

A tethering protein by definition must be capable of localising at membrane contact sites and so must be able to target specifically to the membranes of both sides of the contact. The most recognisable membrane targeting domain is a transmembrane (TM) domain that can embed the protein into the membrane, which is the case for many proteins such as Mmm1p/Mdm10p/Mdm34p from the ER-mitochondria encounter structure ERMES, an ER and mitochondria tethering complex (Kornmann and Walter, 2010) (see section 1.4.4 for details on ER-mitochondria contacts). Although more than one TM domain generates a multipass protein, TM domains alone can only target a protein to a single membrane. To be able to target two membranes simultaneously, a membrane protein must also have another type of membrane targeting element.

A contact site tether or localising protein may form protein complexes to target both membranes at the same time using protein-protein interactions. To give an example, Mdm12p is a member of the ERMES complex, but unlike Mmm1p/Mdm10p/Mdm34p, it does not have a transmembrane helix but uses protein-protein interactions with the other members to join the complex. Specific motifs and domains may regulate protein-protein interaction. One of the most known interactions is between FFAT (two phenylalanines in an acidic tract) or FFAT-like motifs and VAMP-associated proteins (VAPs) that are localised on the ER membrane (Loewen, Roy and Levine, 2003; Mikitova and Levine, 2012; Murphy and Levine, 2016). Some oxysterol-

binding protein (OSBP)–related proteins (ORPs) have FFAT motifs to target them to ER-residing VAP.

OSBP has both a FFAT motif to target it to ER membranes via VAP and a PH domain that targets it to the Golgi (Kawano *et al.*, 2006; Peretti *et al.*, 2008). A PH domain is a common structurally conserved domain of approximately 120 residues consisting of two perpendicular anti-parallel β-sheets and a C-terminal amphipathic helix. Although the PH domain is best known for binding to phosphorylated phosphoinositols (Harlan *et al.*, 1994), there is increasing evidence that protein-protein interaction is also an important characteristic of the domain (Lemmon, 2007; Scheffzek and Welti, 2012). For example, a PH domain can simultaneously bind a protein ligand and phosphoinositides (Lodowski *et al.*, 2003). OSBP is associated to the Golgi membranes by its PH domain. This interface is altered by reductions in PI4P in the Golgi and Golgi GTPase Arf1p mutations (Levine and Munro, 2002) which suggest requirements of both protein-lipid and protein-protein interactions. In contrast, the PH domain of Num1p is suggested to solely bind to $PI(4,5)P_2$ (Yu *et al.*, 2004).

Lipid interaction modules, including polybasic regions and C2 domains, are common ways of targeting to membranes. Examples of polybasic regions are the lysine-rich part of STIM1 at the C-terminal predicted to bind $PI(4,5)P_2$ and $PI(3,4,5)P_3$ at the PM that facilitates its localisation to ER-PM junctions (Carrasco and Meyer, 2011). A C2 domain is an all β-strands structure of approximately 140 residues and can have a range of interactions with PLs including $PI(4,5)P_2$, often but not always in a calcium ion-dependent manner, for example, E-Syts (see section 1.5.3) (Giordano *et al.*, 2013; Corbalan-Garcia and Gómez-Fernández, 2014). C2 domains bind two or three Ca^{2+} via aspartic/asparagine residues on binding loops and bind PLs via a lysine-rich polybasic region in a β-groove, although C2 domains can have both, only one or neither binding features.

1.4.3 ER-PM contacts

The yeast ER has distinct domains, the nuclear envelope (NE), cytoplasmic ER, and PM associated ER (pmaER) (West *et al.*, 2011). The pmaER exists along the perimeter of the cell and covers approximately 40% of the plasma membrane. The cytoplasmic ER which includes the central cisternal ER and tubular ER is located in-between the NE and the pmaER joins them together to form a large continuous membrane-bound organelle spanning the entire cell (West *et al.*, 2011). This expansive network throughout the cell allows contacts with most other membrane-bound organelles such as the mitochondria where the ERMES complex is found (Levine,

2004). The ER is the principal source of lipid synthesis, and it would be reasonable to hypothesise that the cell uses these ER contact sites with other membrane-bound organelles to carry out essential lipid transport. The compositions of proteins at these membrane contact sites are distinct from the rest of the ER, most obviously containing 'tethering' proteins to constrain the two membranes in close proximity in addition to an enrichment of lipid synthesising enzymes. Significant to the bulk traffic of sterol from the ER to the PM, six integral ER proteins are proposed to tether almost all of ER-PM contact sites that are present along 40% of the PM (Manford *et al.*, 2012). Scs2p and Scs22p are yeast VAPs, Tcb1-3p are tricalbins that are homologous to mammalian extended-synaptotagmins (E-Syt), and Ist2p is related to human TMEM16 [Figure 1.5B].

VAP proteins contain a C-terminal TM region that anchors the protein to the ER. In addition, it has an N-terminal MSP (major sperm protein) domain. The PM is enriched in PI4P and PS to which the MSP binds with high affinity (Kagiwada and Hashimoto, 2007). VAPs are able to bind to a range of FFAT-motif-containing proteins such as OSBP but also Opi1p, a regulator of glycerophospholipid synthesis and Nir2, a PITP (PI transfer protein) (Loewen, Roy and Levine, 2003; Chang *et al.*, 2017). E-Syts have been shown to transfer lipids via their SMP (synaptotagmin-like mitochondrial lipid binding protein) domain in addition to their proposed tethering function (see section 1.5.3 Tubular Lipid binding protein). These proteins contain an N-terminal hairpin that anchors the protein onto the ER but does not span the full bilayer and multiple C2 domains that can bind to $PI(4,5)P_2$ which is enriched at the PM (Manford *et al.*, 2012). TMEM16/Ist2 is a multi-pass transmembrane ER protein. There is a C-terminal polybasic region thought to bind PM lipids which is connected to the TM helices by a long flexible region (Manford *et al.*, 2012). It should be noted that the deletion of Scs2p causes the highest effect of ~50% reduction in pmaER, however, the removal of Tcb1-3p shows no effect unless in conjunction with Scs2p (Manford *et al.*, 2012). In mammalian cells, junctophilins have also been found to be a protein family that contributes to ER-PM contacts (Takeshima *et al.*, 2000). Junctophilins have a C-terminal TM domain that anchors them to the ER/sarcoplasmic reticulum and an N-terminus membrane occupation and recognition nexus (MORN) domain. The MORN domain has been shown to bind phosphatidylserine (PS) and $PI(3,4,5)P_3$ (Bennett *et al.*, 2013). A regulated tether complex of stromal interacting molecule 1(STIM1) and Orai1 has also been shown in mammalian cells, which is dependent on Ca^{2+} signalling and high levels of $PI(4,5)P_2$ (Carrasco and Meyer, 2011; Maléth *et al.*, 2014). Upon Ca^{2+}

release from the ER, STIM1 oligomerises and promotes the formation of ER-PM contacts by interacting with PI(4,5)P_2 on the PM with PM-localised Orai1 (Liou *et al.*, 2005; Zhou *et al.*, 2010; Carrasco and Meyer, 2011).

In support of MCS being hubs for lipid transfer, the purification and analysis of the pmaER shows an enrichment of lipid biosynthesis enzymes such as Erg9p and Erg1p involved in sterol synthesis and Pss1p involved in phosphatidylserine synthesis (Pichler *et al.*, 2001).

1.4.4 ER-mitochondria contacts

Mitochondria are one of the few organelles not connected to the secretory pathway, and they can only synthesise a small portion of lipids required for their growth. They are also the site of PS decarboxylation, an essential step for PE and PC synthesis as PS is the precursor for both lipids. Lipid traffic between the ER and the mitochondria occurs purely by non-vesicular methods which suggest that ER-mitochondria contacts have a significant role in intermembrane lipid transport between these two organelles. Similarly to the pmaER, mitochondria-associated ER membranes are enriched in lipid biosynthesis enzymes (Stone and Vance, 2000). In yeast, the proteins, Mdm12p, Mdm10p, Mdm34p and Mmm1p, form a complex called the ER-Mitochondria Encounter Structure (ERMES) which is thought to play a role in tethering the ER and the mitochondria. However, human homologs have yet to be identified [Figure 1.5C] (Kornmann *et al.*, 2009; Murley *et al.*, 2013). Mmm1p, Mdm12p and Mdm24p have been shown to contain SMP domains suggested to be lipid transfer domains (see section 1.5.3 for details on SMP domain-containing proteins). Gem1p, a mitochondrial GTPase, co-localises to ERMES and can regulate the size of the contacts. ERMES was found to be necessary for mitochondria division involving the ER, where a strand of tubular ER can be seen to constrict the site of fission (Murley *et al.*, 2013). A recent study has found another large complex called the ER-membrane protein complex (EMC) consisting of six proteins, Emc1-6p which interacts with Tom5p in the mitochondria (Lahiri *et al.*, 2014). The removal of both the EMC and ERMES causes fatality indicating that ER-mitochondria contacts are essential for the cell and that EMC and ERMES work independently.

In humans, Mfn2 (Mitofusin 2) is considered to be an ER-mitochondria tether. ER residing Mfn2 can interact *in trans* with Mfn1 or Mfn2 on the mitochondrial membrane [Figure 1.5C] (de Brito and Scorrano, 2008; Naon *et al.*, 2016). In Mfn2 deficient cells, ER-mitochondria contacts are reduced but are still present, suggesting additional tethering proteins or complexes. Another suggested tether is the VDAC1

(voltage-dependent anion channel) that binds to GRP75 (glucose-regulated protein 75) to ER-residing Ca^{2+} release channel, IP_3R [Figure 1.5C] (Szabadkai *et al.*, 2006). The removal of IP_3R, like Mfn2 still shows the presence of ER-mitochondrial contacts. It is possible that ER-mitochondria contacts are tethered by different proteins and complexes that respond to different stimuli to allow the dynamic regulation of ER-mitochondrial contacts (see section 1.4.7 for ERMES involved regulation).

1.4.5 NVJ and VancE

In yeast, the NVJ is a region of the vacuole (yeast equivalent to lysosomes) that forms contact with the NE, which is continuous with the ER and the inner nuclear membrane. The NVJ is important for microautophagy of the nucleus and is upregulated during starvation (Millen *et al.*, 2009). Nvj1p (nucleus-vacuole junction 1), an NE integral protein, tethers this contact site via its cytosolic domain that associates with Vac8p. In turn, Vac8p associates with the vacuolar membrane by its N-terminal myristoylation and palmitoylation thus causing the membranes to be situated near each other. The deletion of either Nvj1p or Vac8p abolishes almost all NVJ contacts (Pan *et al.*, 2000). Additionally, Vac8p is suggested to be in newly identified vacuolar non-NVJ cytoplasmic ER (VancE) contacts (Gatta *et al.*, 2015; Wong and Levine, 2016). Other proteins thought to be localised to VancE contacts include Mdm1p and Nvj3p (Henne *et al.*, 2015). In mammalian cells, there have been extensive studies of ER contacts with endosomes/lysosomes which play key roles in endosome maturation after endocytosis (Friedman *et al.*, 2013).

1.4.6 Vacuolar and mitochondrial patch contacts (vCLAMP)

Vps39p, Rab7p and Vps13p are markers of vacuolar and mitochondrial patch (vCLAMP) contacts. vCLAMP was discovered as a putative alternative route for ER synthesised lipids to be transported to the mitochondria bypassing the ER-mitochondria contacts (see section 1.4.7). Vps39p, a protein of the HOmotypic fusion and vacuole Protein Sorting (HOPS) tethering machinery and Rab GTPase Ypt7p were found to be necessary for vCLAMP formation (Elbaz-Alon *et al.*, 2014; Hönscher *et al.*, 2014). In addition, the formation of vCLAMP is regulated by Vps39p phosphorylation, which is altered depending on the carbon source; vCLAMP contacts are detected when yeast is grown in glucose but disassemble upon growth on non-fermentable carbon sources (Hönscher *et al.*, 2014).

1.4.7 Dynamic interface of ERMES and vCLAMP

Intriguing further investigations by Elbaz-Alon *et al.*, one of the two groups who discovered vCLAMP, found that the contact sites between mitochondria and the ER,

and between mitochondria and the vacuole, were co-regulated [Figure 1.5D] (Elbaz-Alon *et al.*, 2014). Mitochondria are not connected to the secretory pathway, and so all lipids must be trafficked by non-vesicular transport most likely via contact sites. The loss of ERMES complex removes a substantial number of ER-mitochondria contacts, which causes a significant expansion of the vCLAMP interface to almost the entire circumference of each mitochondrion. Vice versa, the loss of vCLAMP induces an increase in ERMES contact sites. This regulation of the two contact sites is essential for normal phospholipid transport, allowing a direct transport path from ER to mitochondria or a diverted journey via vacuoles and vCLAMPs. The deletion of both contact sites results in lethality, reinforcing the role of contact sites in lipid transfer and identifying contact site redundancies that may obscure the identification of proteins involved in lipid transfer at MCS (Elbaz-Alon *et al.*, 2014; Hönscher *et al.*, 2014; Lang *et al.*, 2015). In support of a dynamic balance between different MCS, further studies have revealed that Vps13p localises to not only vCLAMP, but also the NVJ and endosome-mitochondria contacts (Lang *et al.*, 2015; Park *et al.*, 2016). Thus proteins which can localise to multiple contacts may have important roles in rerouting lipid transfer or indeed other functions that depend on MCS.

1.5 Lipid transfer proteins

1.5.1 Creation of lipid gradients

Lipid transfer proteins are hypothesised to transport lipids down a lipid gradient. Lipid synthesis and hydrolysing enzymes can be used to supply a gradient to generate lipid transfer. For example, lipid synthesis can be concentrated to the sites of LTP activity to create a favourable local lipid concentration to reverse the overall gradient between donor and acceptor membranes (Pichler *et al.*, 2001; Maeda *et al.*, 2013). On the other hand lipid metabolism of newly transported lipids can create a lipid gradient, for instance, ceramide is metabolised into sphingomyelin in the Golgi after transportation by ceramide transfer protein (CERT) thereby metabolically trapping the lipid (Hanada *et al.*, 2003). However, normal cellular lipid gradients may prevent the use of such mechanism. Sterol is quite clearly present at a very high level in the PM yet at a very low concentration at the site of synthesis, the ER. It is still not clearly defined how sterol is transported continually from the ER against a the gradient of increasing sterol levels along the secretory pathway.

To regulate sterol gradients, different sterol pools are hypothesised to have a role in lipid gradient maintenance. Sterol has lower chemical activity when surrounded by

sphingolipids and saturated glycerophospholipids compared to 'free' sterol in a membrane, which has higher chemical activity, therefore, higher extractability (see section 1.2.5 and Figure 1.4). It is suggested that sterol LTPs transfer sterols between the high chemical activity portions of two membranes, which would go down a gradient towards the late membranes such as from the ER to the PM. The low chemical activity sterol pool that is caused by the protection of PM lipids consequently traps the newly transported sterol at the PM, thereby maintaining the sterol gradient of highly extractable sterol and promoting sterol accumulation in the PM (Sullivan *et al.*, 2006; Georgiev *et al.*, 2011; Beh *et al.*, 2012; Mesmin, Antonny and Drin, 2013).

An alternative hypothesis is that one molecule's transport is coupled with another in a counter exchange model. This pair would require supply and elimination of the second ligand to drive the transfer of the first lipid ligand against its gradient. For example by the specific lipid synthesis in conjunction with lipid consumption which is the case with Osh4p, an LTP which transfers sterol, and PI4P which is synthesised by Pik1p and hydrolysed by Sac1p (see section 1.5.2 OSBP related proteins for further explanation). Both hypotheses may be valid as the protection given to sterol by membranes containing saturated PLs and sphingolipids favours sterol accumulation by Osh4p, in contrast to membranes with unsaturated PLs (von Filseck, Vanni, *et al.*, 2015).

1.5.2 OSBP related proteins

ORPs (OSBP related proteins) form a protein family shared between yeast and humans which are argued to be sterol transfer proteins. The ORP homologue family defined by the presence of an ORP-related domain (ORD) has been implicated in intracellular traffic of sterol, and it exists in all eukaryotes [Figure 1.6A + B]. An ORD is a ~350 aa domain with a highly conserved motif (EQVSHHPP) which is found in the C-terminal of all human ORPs. In addition to the ORD, many ORPs also contain membrane or membrane protein interacting domains such as PH domains and FFAT motifs.

Yeast oxysterol-binding homology proteins

There are seven oxysterol-binding homology (OSH) proteins found in yeast, and three members are extended well beyond the ORD to include two membrane binding elements (PH domain and FFAT motif) allowing them to be situated between the ER and another organelle (Schulz *et al.*, 2009). All seven members have an ORD that has high sequence similarity to human ORDs. A single deletion of one OSH member does

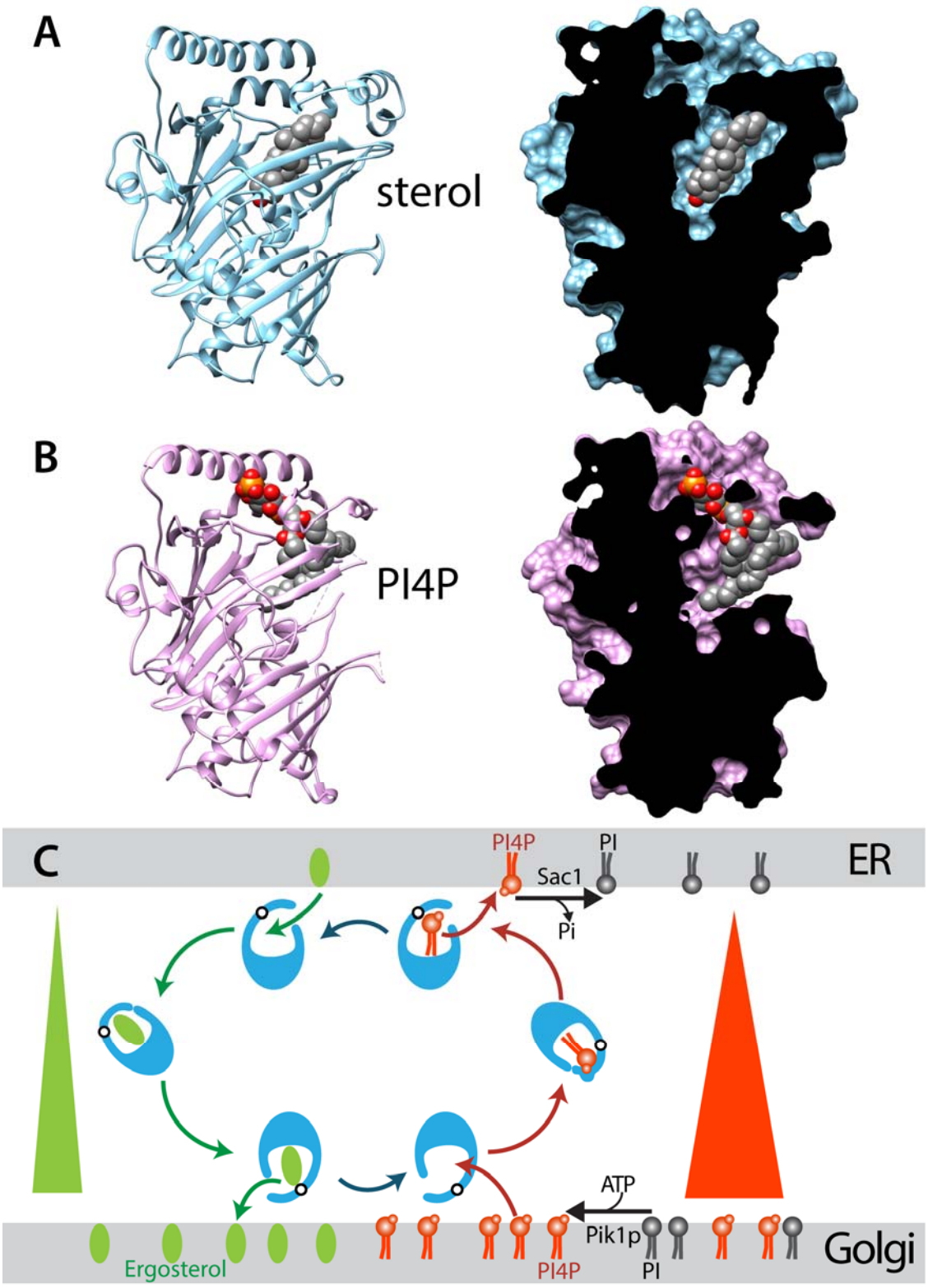

Figure 1.6 **Osh4p countertransport of ergosterol and PI4P**
Crystal structure of Osh4p bound to **A**) cholesterol (PDB: 1ZHY) and **B**) PI4P (PDB: 3SPW). Both ligands bind in the same cavity shown in the cross section of the protein shown on the right. **C**) Osh4p carries out counter transport of ergosterol and PI4P between the ER and the Golgi. Sac1 on the ER converts PI4P (red) to PI (grey) and Pik1p generates PI4P at the Golgi. Osh4p (blue) transports PI4P down a high gradient to the ER where PI4P is hydrolysed thus it picks up ergosterol (green) and carries out secondary active transport up a shallower concentration gradient. The concentration gradient is indicated by triangles.

not show apparent phenotypes under normal growth conditions. However, the abolition of all seven OSH genes is lethal, with the expression of one of the OSH members (except Osh1p) restoring viability indicating the seven members of the family share a common function (Beh *et al.*, 2001). OSH proteins have been proposed to transfer sterol in both directions from the ER to the PM and PM to the ER as sterol levels in the PM were shown to change in delete strains while total cellular sterol stayed the same (Jiang *et al.*, 1994; Raychaudhuri *et al.*, 2006; Sullivan *et al.*, 2006; Beh *et al.*, 2009). The lack of effect on overall cellular sterol suggests a defect in the transport of sterol towards the PM that results in an accumulation of sterol inside the cell. In addition, functional OSH proteins were found to be required for efficient sterol transport from the PM to the ER where sterol becomes esterified (Sullivan *et al.*, 2006).

However, there is some disagreement with the sterol transport theory as a study by the Menon group where the deletion of all seven OSH genes showed only a reduction of ~50% sterol traffic in yeast (Sullivan *et al.*, 2006; Georgiev *et al.*, 2011). Instead, it has been suggested that the OSBP homologs in yeast regulate the organisation of sterols at the PM by affecting sterol sequestering rather than an active role in transporting sterol as the inactivation of the OSH proteins indicated an alteration of the distribution of sterol in the external leaflet of the PM (Georgiev *et al.*, 2011). In addition, instead of sterol, PS is the lipid ligand of choice for Osh6/7p and ORP5/8, transporting it between the ER and the PM (Maeda *et al.*, 2013; Chung *et al.*, 2015; von Filseck, Čopič, *et al.*, 2015; von Filseck, Vanni, *et al.*, 2015).

Osh4p binds sterol

Osh4p, also known as Kes1p, is the most abundant yeast ORP homolog and has been extensively studied *in vitro* for its sterol transfer ability. Osh4p is very similar to Osh5p, having >80% similarity in sequence. Both OSH proteins have no other domain other than the ORD domain, thus are small proteins consisting of the ~350 aa ORD with small extensions. Deletion of both Osh4p and Osh5p causes a resistant to nystatin, a drug that affects ergosterol. The phenotype suggests that the PM levels of sterols are affected, but as total cellular sterol levels are shown to be unaffected, it indicates a role of ergosterol transport to, or the organisation of ergosterol, at the PM. Osh4p binds to sterols at a 1:1 stoichiometry [Figure 1.6A] (Im *et al.*, 2005). A flexible N-terminal lid of 29 residues shuts the sterol into the hydrophobic cavity, though intriguingly a lidless Osh4p had the same binding affinity to sterol (K_d ~0.3 μM) (Im *et al.*, 2005).

Osh4p transfers sterol in a countercurrent with PI4P

Recent studies of Osh4p have found it to bind and transport PI4P via its sterol binding hydrophobic cavity [Figure 1.6B]. Previous to this, it was shown to bind sterol, but anomalies were observed that were linked to effects of PI4P and $PI(4,5)P_2$. Localisation of Osh4p is mainly cytosolic, but it also localises to the Golgi membrane (Fairn *et al.*, 2007; LeBlanc and McMaster, 2010). Alteration of PI4P levels by Sac1 affected the targeting of Osh4p to the Golgi contacts (Li *et al.*, 2002; Fairn *et al.*, 2007). Also, overexpression of Osh4p reduced cellular levels of PI4P. During *in vitro* lipid transfer assays with artificial membranes, charged PLs such as PS and $PI(4,5)P_2$ accelerated sterol transfer by Osh4p which was otherwise carried out at a slow rate (Raychaudhuri *et al.*, 2006). Sterol extract and transfer were also $PI(4.5)P_2$ dependent in *in vivo* assays (Raychaudhuri *et al.*, 2006).

Assays using dehydroergosterol (DHE), a fluorescent derivative of ergosterol, and measuring real-time transfer showed that PI4P inhibited sterol transport by Osh4p. The reason for this was then proved to be that Osh4p can also transfer PI4P and therefore there is competition between the two lipid ligands for the protein. It has now been proven that Osh4p is able to transport sterol and exchange it for PI4P thus moving the two lipids in opposite directions [Figure 1.6C] (de Saint-Jean *et al.*, 2011). The structure of Osh4p binding with PI4P was solved showing that the competition is due to one PI4P acyl chain occupying the same pocket that sterol is positioned when bound to Osh4p [Figure 1.6A + B]. Intriguingly, the lid of Osh4p shows a different conformation when the protein is bound to PI4P compared to when it is bound to sterol. This conformation change was used to explain how Osh4p exchanges sterol for PI4P in a countercurrent model between two distinct membranes (de Saint-Jean *et al.*, 2011). It is suggested that when bound to PI4P, the lid of Osh4p remains flexible so that it is more prone to transfer PI4P to ER-like neutral unsaturated membranes whereas when bound to sterol, Osh4p has a tightly closed lid and is favoured to be transported towards a better packed Golgi membrane containing PI4P (von Filseck, Vanni, *et al.*, 2015). In fact, the PI4P countercurrent allowed Osh4p to create and increase the sterol gradient in *in vitro* transfer assays. When without PI4P, Osh4p would only carry out a slow transfer, following the gradient (von Filseck, Vanni, *et al.*, 2015). This novel model of Osh4p proposes that Osh4p uses the PI4P gradient between the ER and the Golgi to transfer sterol to the Golgi [Figure 1.6C]. The PI4P is ATP-dependently synthesised by Pik1p on the Golgi and is hydrolysed by Sac1p when it arrives on the ER membrane. Osh4p can then pick up sterol and transfer it to the Golgi where it encounters the

generated PI4P promoting the release of the sterol into the Golgi membrane thereby restarting the cycle.

The secretory pathway, particularly the exocytic vesicular budding of the Golgi is likely to depend on sterol build-up; >20% of lipids in these vesicles are sterol molecules compared to ~10% in the trans Golgi network (TGN) (Klemm *et al.*, 2009). Pik1p synthesises PI4P in the Golgi membrane and during quiescence or starvation Pik1p dissociates from the punctate Golgi regions and Sac1, responsible for PI4P hydrolysis usually in the ER, accumulates in the Golgi (Faulhammer *et al.*, 2007; Blagoveshchenskaya *et al.*, 2008). The movement of these proteins depletes Golgi PI4P thus decreasing anterograde trafficking. Another piece of evidence for the effect of Osh4p on secretion is that the deletion of Osh4p prevents protein transport to the plasma membrane (Proszynski *et al.*, 2005). One intriguing investigation suggests that Osh4p has a role in decreasing PI4P from exocytotic vesicles as they leave for the PM (Ling, Hayano and Novick, 2014). It is feasible that a function of Osh4p is to remove remaining PI4P from budding vesicles as it delivers sterol required for secretion.

Human OSBP

OSBP is the founding member of the ORP family and was, as the name suggests, initially found as an oxysterol binding protein (Dawson *et al.*, 1989). However, it was later shown to preferentially bind cholesterol (Wang *et al.*, 2008; Wang, 2009). In addition to its ORD, OSBP contains a FFAT motif that can interact with VAP-A in the ER and a PH domain which can target to PI4P containing membranes (Levine and Munro, 2001). Though the vesicular pathway links the ER and the TGN, contacts are observed between these two organelles where several LTPs localise such as phosphatidylinositol transfer protein (PITP/Nir2), OSBP and CERT (Hanada *et al.*, 2003; Litvak *et al.*, 2005; Perry and Ridgway, 2006). As with the yeast homologue Osh4p, it was shown that OSBP works in a countercurrent model with PI4P exchange *in vitro* (Mesmin *et al.*, 2013). In addition, it has been suggested that OSBP, when soluble in the cytoplasm, can act as a sensor for sterol and oxysterol by changing conformation depending on its ligand and producing downstream effects (Perry and Ridgway, 2006; Wang, 2009). When bound to cholesterol but not localised at membranes, OSBP, via a structural shift in the PH domain, associates with protein phosphatases (serine/threonine phosphatase, PP2A and tyrosine phosphatase, HePTP) forming a complex and allowing dephosphorylation of extracellular signal–regulated kinase (ERK). It is thought that there is a sterol-binding region of alanine/glycine-rich residues at the N-terminal of the ORD domain which controls binding to cholesterol but

not 25-hydroxycholesterol (Wang *et al.*, 2008). Depletion of cholesterol, or the addition of 25-hydroxysterol causes dissociation of the phosphatase complex and therefore prevents dephosphorylation of ERK1/2. There have not been further studies that consolidate all findings on transfer by OSBP transfer with sensing functionality.

A transfer function and a sensor function are not incompatible with each other as it is feasible that a lipid transfer protein can also be a lipid sensor. It is likely that an LTP in a bound and unbound state or bound state with different lipids would have slight structural variations and this change could trigger downstream effects. One could envisage that OSBP binds and dissociates from the ER-Golgi contacts by its own negative feedback loop - once it has depleted PI4P in the Golgi, it can return to the cytosol (Mesmin *et al.*, 2013).

During quiescence or starvation, cells down-regulate anterograde trafficking by depleting Golgi PI4P. A reduction of PI4P at the Golgi would cause mass OSBP dissociation from the Golgi and decrease countercurrent transfer, decreasing cholesterol traffic to the Golgi perhaps due to requiring less secretion. More OSBP would theoretically be free in the cytoplasm to carry out scaffolding functions with ERK phosphatases regulated by cellular cholesterol levels.

25-hydroxysterol is emerging as an important regulator of immune function and has been found to be more efficient at inhibiting sterol biosynthesis which contributes to the protection of the cell (Cyster *et al.*, 2014). One hypothesis could be an increase in 25-hydroxysterol coinciding with a decrease in cholesterol levels would prevent cholesterol and PI4P counter transfer by OSBP thus override the association of the phosphatase complex, releasing the enzymes to prevent inactivation of ERK.

Osh6p/7p transfer PS in a countercurrent with PI4P

PS, like sterol, is found at a higher concentration at the PM than its site of synthesis, the ER. Osh6p/Osh7p and ORP5/ORP8 bind PS rather than sterol, and the PS-specific binding residues are highly conserved between yeast and humans (Maeda *et al.*, 2013). In both yeast and mammalian cells, these proteins are localised to ER-PM contact sites. ORP5/ORP8 are ER integral proteins and required their PH domains to bind to PI4P on the PM (Chung *et al.*, 2015). Increasing PI4P synthesis at the PM recruits ORP5/ORP8 to ER-PM contacts, and pharmaceutical inhibition of the PI4P kinase causes dissociation from the PM observed as diffusion along the ER. An artificial lipid transfer assay with the purified ORD showed the ability to act as a PS and PI4P counter exchanger. Similarly, yeast Osh6/7p were demonstrated as counter exchangers of PS with PI4P. Therefore it is suggested that they can drive PS transport

by the generation of PI4P at the acceptor membrane (equivalent to PM or TGN) (von Filseck, Čopič, *et al.*, 2015). ER-localised Sac1 acting *in cis* would dephosphorylate the newly transferred PI4P in the ER, which conceals the PI from pick up by the now empty ORD. The lipid transfer domain can now bind only PS and transfers it to the acceptor membrane.

In light of the recent discovery that Osh4p/Osh6p/Osh7p binds PI4P and with sterol binding not being a universal feature for all ORP/OSH proteins (Maeda *et al.*, 2013; Tong *et al.*, 2013; Chung *et al.*, 2015; von Filseck, Čopič, *et al.*, 2015), it could be that the unifying characteristic is the recognition of PI4P. There is already evidence that Osh3p localises to ER-PM contacts in response to PM PI4P levels and also, modulates PI4P in the PM (Stefan *et al.*, 2011). In addition, the countercurrent model [Figure 1.6C] reveals the importance of secondary lipid ligands that may have lower binding affinities than the primary lipid ligand of the protein.

1.5.3 Tubular Lipid binding protein

The tubular lipid binding protein (TULIP) superfamily is characterised by an elongated αβ protein with a hydrophobic tunnel and includes extracellular (eTULIPs) and intracellular (iTULIPs) forms of the proteins. In some cases, this hydrophobic cavity is shaped like a groove so that the lipid acyl chains are positioned inside, but the headgroup is exposed (Schauder *et al.*, 2014). iTULIPs are a recent addition to the TULIP family, which previously had been thought to contain only extracellular proteins (Zilversmit, Hughes and Balmer, 1975). eTULIPs have long been established to transport various lipids, for example, Human CETP (cholesteryl ester transfer protein) transports cholesteryl esters while PLTP (phospholipid transfer protein) transports PLs (Tollefson, Ravnik and Albers, 1988; Qiu *et al.*, 2007). Most TULIPs have been shown to work as a dimer (Beamer, Carroll and Eisenberg, 1997).

The discovery of iTULIPs was brought about by the development of bioinformatics tools that could detect remote homology (see section 1.5.6 on Bioinformatics and lipid transfer proteins). The breakthrough study was purely computation and found that synaptotagmin-like, mitochondrial and lipid-binding protein (SMP) domains of previously unknown function were intracellular homologues of eTULIPs (Kopec, Alva and Lupas, 2010). The SMP domains are approximately 200 residues composed of four β-strands and two α-helices either side [Figure 1.7A].

Synaptotagmin-like proteins

As the name suggests, this subgroup of SMPs is related to the synaptotagmins. They possess multiple C-terminal Ca^{2+}- depending lipid binding C2 domains as their

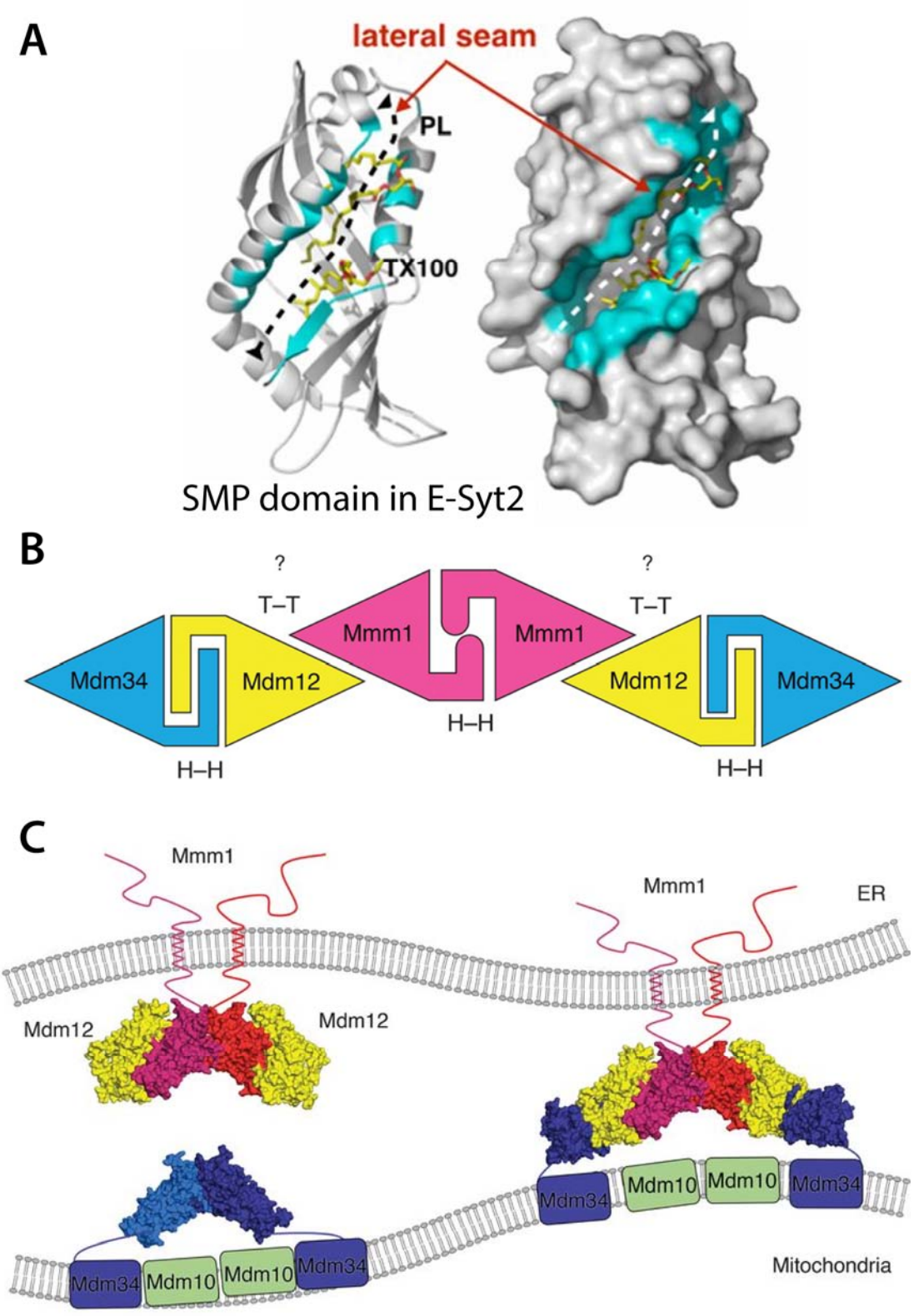

Figure 1.7 **SMP domains of E-Syt2 and ERMES members**
A) Structure of E-Syt2 SMP domain bound to a phospholipid and Triton X-100 detergent showing a cavity with an open along the length of the SMP domain. Figure from (AhYoung *et al.*, 2015). **B**) Diagram illustrating a model of a hexamer containing the SMP domains of Mmm1p (pink), Mdm12p (yellow) and Mdm34p (blue). 'H-H' indicates a head-to-head interaction whereas 'T-T' shows tail-to-tail contacts between the SMP domains. **C**) Representation of the proposed organisation of Mmm1p, Mdm12p and Mdm34p associations within ERMES complexes. Mdm12p-Mmm1p-Mmm1p-Mdm12p form a tetramer which is anchored to the ER by Mmm1p. Mdm34 is anchored to the OMM and its SMP domain is thought to cap each end of the Mdm12p-Mmm1p tetramer to for a heterohexamer. Figures from (Jeong, Park and Lee, 2016).

namesake synaptotagmin, allowing binding to Ca^{2+} ions and phosphoinositides such as $PI(4,5)P_2$ [Figure 1.5B] (Schulz *et al.*, 2009). The difference is the presence of an SMP domain in both the human forms, called extended-synaptotagmins E-Syt1/2/3 and their yeast homologs called tricalbins Tcb1/2/3p (Manford *et al.*, 2012; Giordano *et al.*, 2013). The yeast tricalbins are suggested to be tethers between the ER and the PM that form pmaER contacts, though effects on the ER-PM contacts when Tcb1/2/3p are removed can only be observed when Scs2p is also removed (Manford *et al.*, 2012). Tricalbins are integral ER proteins that associate with the PM. They consist of either three or five C2 domains and the SMP domain (Manford *et al.*, 2012). The SMP domain is necessary for contact site localisation of the tricalbin, indicating an important targeting role of the domain (Toulmay and Prinz, 2012). Human E-Syts differ from tricalbins by their hairpin motif that is inserted in the ER rather than a complete transmembrane helix (Giordano *et al.*, 2013).

E-Syts have been shown to regulate the dynamic tethering of the ER and the PM-induced by Ca^{2+} and $PI(4,5)P_2$ (Giordano *et al.*, 2013). A rise in cytosolic Ca^{2+} induces an expansion of areas of apposition between the ER and the PM by recruiting E-Syts tethers. Deletion of the human E-Syts in a triple knockout cell line also shows loss of Ca^{2+} enhanced ER-PM contact sites, suggesting a shared function to the yeast tricalbins as potential tethers (Saheki *et al.*, 2016). However, ER-PM contacts in normal conditions and triple knockout animal models were found to be unchanged suggesting other players in mammalian ER-PM tethers (Saheki *et al.*, 2016).

E-Syt1 is localised at the ER and unlike E-Syt2/3, is triggered by a Ca^{2+} increase to localise to ER-PM contacts by an extra Ca^{2+} regulated C2 domain (third C2 domain in a series of five) (Giordano *et al.*, 2013). Thus E-Syt1 could mediate ER-PM tethering dependent on Ca^{2+}. On the other hand, E-Syt2/3 are constitutively bound to PM even in resting Ca^{2+} levels via interactions of the fifth C2 domain with $PI(4,5)P_2$ in the PM (Min, Chang and Sudhof, 2007; Giordano *et al.*, 2013).

In addition to their potential tethering functions, E-Syts have been shown to bind and transfer lipids. Also, C2 domains in yeast Tcb2p/3p bind phosphatidylinositol phosphates, sphingolipids precursors, phytoceramide and phosphorylated long chain base (Gallego *et al.*, 2010). The crystallisation study which confirmed the bioinformatics discovery of SMP and TULIP structural homology was carried out with human E-Syt2 which revealed its tubular structure formed as a dimer occupied by glycerophospholipids with a stoichiometry of 2:1 (lipid to monomer) (Schauder *et al.*, 2014). There seems to be no particular preference for the headgroup, which would fit

with the properties of the TULIP structure where the lipids' hydrophobic tails are nested in the hydrophobic groove whereas the head groups are exposed to the solvent. *In vitro* transfer assays also showed that E-Syts could shuttle lipids between ER and PM-like liposomes dependent on the integrity of the SMP domain, including DAG, a metabolite of $PI(4,5)P_2$ which was found to accumulate in triple E-Syt knockout cells (Saheki *et al.*, 2016). In this study, Saheki *et al.* purified the cytosolic portion of E-Syt1 and used the histidine tag to anchor the protein to nickel-conjugated lipids in the donor liposome. The acceptor liposome contained high levels of $PI(4,5)P_2$ with which the C2 domains interact. phosphatidylethanolamine (PE) transfer between the liposomes occurred only when the SMP domain was intact and was sped up rapidly upon addition of 0.1-0.2 mM Ca^{2+}. The Ca^{2+} activation of membrane tethering by E-Syt1 for lipid transfer in *in vitro* assays, suggests that the lipid transfer function of E-Syt1 only occurs when a cytosolic Ca^{2+} increase recruits it to ER-PM contacts (Saheki *et al.*, 2016).

SMP mitochondrial proteins

Another subgroup is the mitochondrial proteins; three yeast proteins, Mmm1p, Mdm12p and Mdm34p, have been identified as potential ER to mitochondria tethers as three of four permanent components in the complex ERMES [Figure 1.5C]. The SMP domains of all three proteins are predicted to reside in the gap between the ER membrane and the mitochondrial membrane. Although the role of these SMP domains has not been confirmed, the SMP domains have been linked to lipid transfer and tethering. The SMP domain of Mmm1p is essential for the localisation to ER-mitochondria contacts (Toulmay and Prinz, 2012).

Mdm12p does not have a transmembrane domain to localise it to membranes. Instead, the localisation of Mdm12p to the ER-mitochondria contact sites relies on protein-protein interaction with the other members of the complex. Structural studies on Mdm12p show that the SMP domain has an unexpected extra dimerisation site and the authors, Jeong *et al.*, suggest that the SMP domain of Mdm12p interacts through the two ends of its SMP domain with Mdm34p (head-to-head interaction) and Mmm1p (tail-to-tail interaction) [Figure 1.7B + C] (Jeong, Park and Lee, 2016). SMP domains in Mdm12p and Mmm1p form a 2:2 stoichiometry heterotetramer elongated tubular shaped channel and can bind PLs (AhYoung *et al.*, 2015). PC, PE and phosphatidylglycerol (PG) were shown to bind to the purified SMP complex with Mmm12p and Mmm1p, but PC was found to be the preferred lipid ligand in competition assays. The SMP domain of Mdm34p was also found to associate with the Mmm1p/Mdm12p heterotetramer via Mdm12p [Figure 1.7B + C]. This interaction has

been proposed to be via the N-terminus β strand of Mdm34p and Mdm12p to form a heterohexamer (Jeong, Park and Lee, 2016). However, this interaction was weak, which could point to a transient handoff situation between Mmm1p/12p at the ER and Mdm34p at the outer mitochondrial membrane.

There are conflicting data on whether ERMES has a lipid transfer function. In favour, the deletion of any of the ERMES subunits slows PC synthesis via the Lands pathway that involved PS decarboxylation to form PE by Psd1p in mitochondria (Kornmann *et al.*, 2009). In addition, *in vitro* assays show involvement in PS transfer but not PE (Kojima, Endo and Tamura, 2016). However, an artificial construct that has only tethering activity showed partial rescue of the phenotype in delete ERMES cells and in another study the deletion of ERMES did not affect the mitochondrial PS decarboxylation (Kornmann *et al.*, 2009; Nguyen *et al.*, 2012). In spite of contradicting evidence, the role of ERMES in lipid transfer cannot be disproved due to the proven circularity of lipid transfer between the ER, mitochondria and the vacuole (see section 1.4.7 for more details on this regulation) where the vCLAMP compensates for the loss of ERMES and vice versa (Elbaz-Alon *et al.*, 2014). Further investigation must be carried out to find whether the SMP complex has a role in lipid transfer and to determine the specificity of binding to lipids if any.

SMP containing Nvj2p

The final member of known yeast SMP proteins is Nvj2p which contains a TM domain, and also a PH domain suggested to bind PIPs and sterol (Gallego *et al.*, 2010; Toulmay and Prinz, 2012). Though it is found to localise in the ER, Nvj2p is particularly enriched at the NVJ, which is dependent on the presence of NVJ tethers Nvj1p and Vac8p (Huh *et al.*, 2003; Toulmay and Prinz, 2012). Human HT008, a homologue of Nvj2p also was enriched at the NVJ when expressed in yeast cells. The deletion of SMP removed the enrichment of Nvj2p at NVJ contacts. However, a recent study suggests that upon ER stress or the elevation of ceramide, Nvj2p induces contacts between the ER and the Golgi thus acting as a tether (Liu *et al.*, 2016). Nvj2p lacking the N-terminal TM domains was able to partially rescue ceramide transfer in cells defective in vesicular ceramide transport, though targeting to other membranes prevented this activity. This activity required the SMP domains. Therefore, it is possible that the SMP domain of Nvj2p is responsible for ceramide transfer.

1.5.4 StAR-related lipid transfer proteins

In addition to ORPs, another lipid transfer domain implicated in cholesterol transport is the StART (StAR-related lipid transfer) fold. StAR (StARD1), a 30 kDa

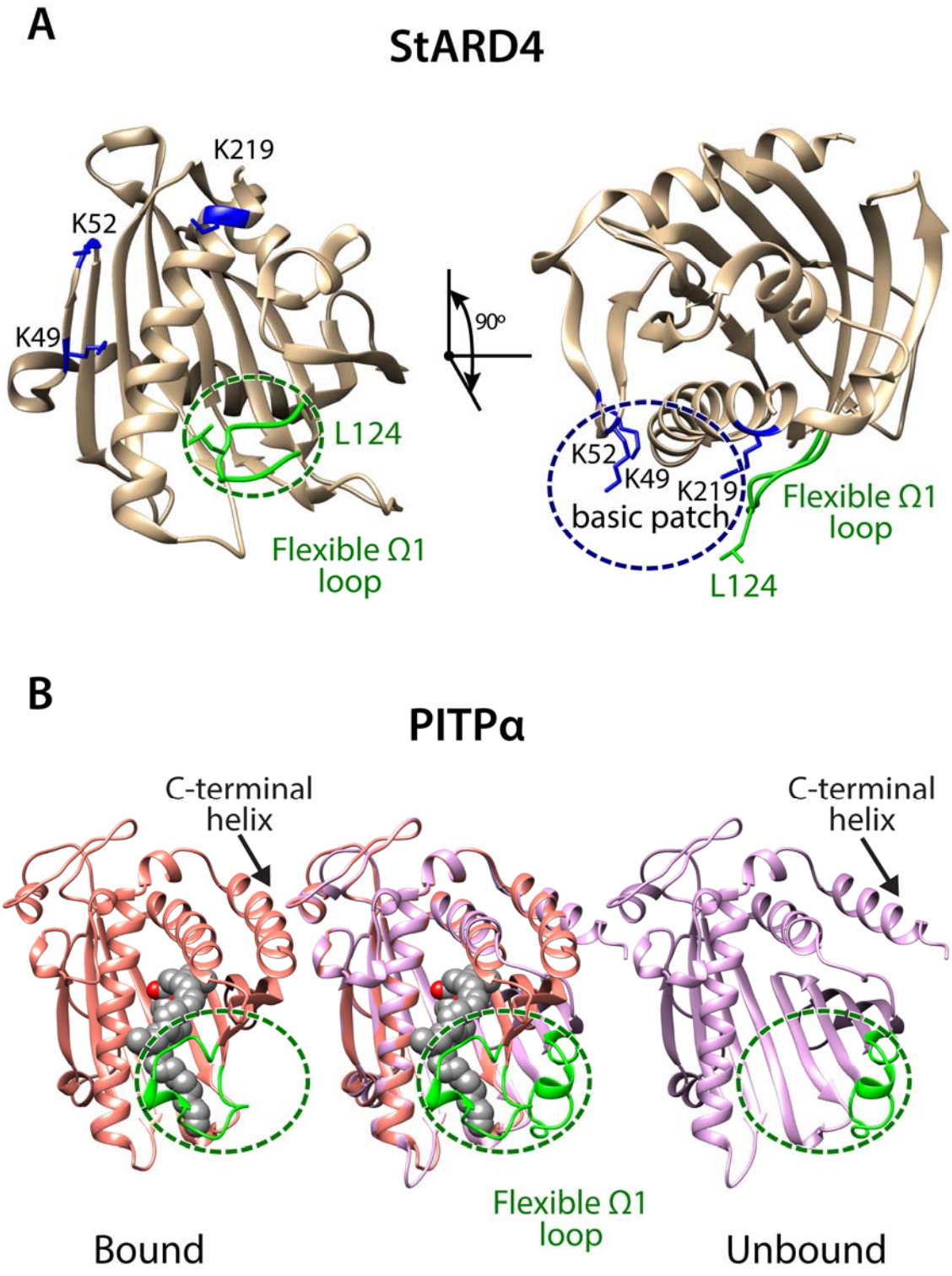

Figure 1.8 **StARD4 and PITP structures**
A) Structure of StARD4 (PDB: 1JSS) showing residues forming the basic patch in blue and the flexible Ω1 loop in green. Alanine^{124} is important for the flexibility of the loop which is thought to act as a lid into the cavity. **B**) Structure of PITP with no ligand (PDB: 1KCM) and bound with PC (PDB:1T27). The flexible Ω1 loop is highlighted in green and can be seen to undergo large movements between bound and unbound states. A C-terminal helix is also shown to move, capping the entrance to the cavity when bound with PC.

protein that is required for the acute regulation of steroidogenesis, is the founding member of the StART family (Alpy and Tomasetto, 2005). The StART fold is a ~210 aa domain formed of 9 β-stranded sheet surrounding two α helices to create a grip-like fold enclosing an internal hydrophobic cavity that provides a site for ligand binding [Figure 1.8A]. It was originally proposed that the C-terminal α helix is a 'lid' to the binding site that required a conformational change when lipids access the binding pocket (Baker, Yaworsky and Miller, 2005; Miller, 2007). Later the Ω-1 loop that is between strands β5 and β6 was suggested as the lid, and most recently, work by Iaea and Maxfield shows that sterol binding and release require movement of the Ω-1 loop and insertion of the C-terminal α helix into the membrane (Mesmin, Antonny and Drin, 2013; Iaea et al., 2015). From this domain, a family of StART domains was defined which can bind a range of different lipids (Alpy and Tomasetto, 2005). There is no StART domain in yeast. However, it is well documented that there are 15 StART proteins in mammals which are divided into six subfamilies (Alpy and Tomasetto, 2005; Clark, 2012).

StARD1, StARD3 (MLN64), StARD4, StARD5 and StARD6 are StART proteins that bind cholesterol and oxysterol. StARD2 (PCTP), StARD7 and StARD10 bind glycerophospholipids such as PC or PE. StARD11, also known as ceramide transfer protein (CERT), binds and transports ceramide and contains a PH domain and FFAT motif to associate with membranes. StARD8/12/13 are Rho-GTPase signalling proteins, StARD14/15 are
thioesterases, and the function of StARD9 is unknown (Clark, 2012; Alpy and Tomasetto, 2014).

StARD1

StARD1 has an N-terminal mitochondrial targeting sequence that is cleaved upon import into the mitochondrion (Stocco and Clark, 1996). StARD1 is implicated in cholesterol transport between the mitochondrial outer and inner membrane in mammalian cells to initiate synthesis of steroid hormones at the site of the cytochrome P450. It has been suggested that there is a pH-dependent insertion of the C-terminal helix into the OMM (outer mitochondrial membrane) to anchor the protein (Baker, Yaworsky and Miller, 2005; Yaworsky *et al.*, 2005). Mutations in StARD1 causes congenital lipoid adrenal hyperplasia due to the defect in steroid hormone production by the adrenal gland (Bose *et al.*, 1996). However, the exact mechanism of cholesterol transfer is unclear. One study has shown that the StART domain of StARD1 is capable of binding a broad range of lipid ligands including glycerophospholipids in a mass

spectrometry study of bound metabolites, which may hint at a counter exchange model involving secondary lipid ligands similar to that shown by ORPs (Schrick *et al.*, 2004).

MLN64/StARD3

StARD3 (also known as MLN64 - metastatic lymph node 64) was found to contain a domain that shares the same structure with StARD1 (Moog-Lutz *et al.*, 1997; Watari *et al.*, 1997). MLN64 shares 37% sequence identity with StARD1 (Reitz *et al.*, 2008). MLN64 is a late endosome integral protein that binds cholesterol at late endosomes. The MENTAL (MLN64 N-terminal) domain is composed of four transmembrane helices and anchors the protein to endosomal membranes (M. Zhang *et al.*, 2002) whereas StART domain at the C-terminal is predicted to face the cytoplasm (Tsujishita and Hurley, 2000). MLN64 also has a FFAT motif that has been shown to bind VAPs in the ER thereby allowing MLN64 to be situated at both ER and endosomal membranes at contact sites. Overexpression of MLN64 increases steroidogenesis, which is suggested to be due to the mobilisation of lysosomal cholesterol (M. Zhang *et al.*, 2002).

StARD4

StARD4 can extract sterol in vitro, binding with 1:1 stoichiometry. *In vivo*, StARD4 rapidly equilibrates cholesterol levels between the endosomal recycling compartment and the PM and also with the ER, however, its exact mechanism of function has not been pinpointed (Soccio *et al.*, 2005; Rodriguez-Agudo *et al.*, 2011). Interestingly StARD4 is the only known sterol carrier for which gene transcription is regulated by SREBP-2. StARD4 is a short protein composed of only the StART domain which has no membrane-targeting modules and therefore is a cytosolic protein. However, under certain circumstances StARD4 can associate with the ER, though this targeting is not well understood (Soccio *et al.*, 2005; Rodriguez-Agudo *et al.*, 2011). Recent work by Iaea *et al.* has shown that there is a surface patch of basic residues which is able to interact with positively charged lipids such as PS [Figure 1.8A] (Iaea *et al.*, 2015). Replacing these basic residues with uncharged amino acids diminished sterol transfer activity of StARD4. Therefore it is possible that the polybasic region can regulate the recruitment of StARD4 to various organelles. In addition, this study showed that along with membrane association by the polybasic region, the flexible Ω1 loop, predicted to be the lid is required to facilitate the insertion of the C-terminal α-helix into the membrane [Figure 1.8A]. Upon binding with cholesterol, it is suggested that movement of the C-terminal or Ω1 loop allows undocking from the membrane (Murcia *et al.*, 2006; Roostaee *et al.*, 2009; Iaea *et al.*, 2015).

CERT

CERT is composed of a FFAT motif and two distinct domains, the StART domain, which binds and transports ceramide and a PH domain, which associates with PI4P. The TGN surface is particularly high in levels of PI4P allowing the N-terminus PH domain of CERT to bind to the TGN membrane. The middle region between the PH domain and the StART domain of CERT contains a FFAT motif (two phenylalanines in an acidic tract) which mediates binding to VAP-A (Lev *et al.*, 2008). These two associations with the Golgi and the ER via VAP-A allows CERT to be situated at the contact site carrying out ceramide transport from the ER to the Golgi. Upon entry to the Golgi, ceramide is converted to sphingomyelin or glucosylceramide preventing reverse transportation back to the ER. It is suggested that phosphorylation of CERT induces auto-inhibition of its transfer activity and its targeting to ER-Golgi contacts (Fugmann *et al.*, 2007; Kumagai *et al.*, 2007; Saito *et al.*, 2008; Tomishige *et al.*, 2009; Kumagai, Kawano-Kawada and Hanada, 2014). This negative feedback loop is thought to control sphingomyelin synthesis due to ceramide and PC conversion to sphingomyelin and DAG at the TGN. DAG activates a phosphorylation chain resulting in hyperphosphorylation of CERT thereby decreasing its affinity to PI4P, inhibiting the ceramide transfer activity, and reducing sphingomyelin synthesis. At the ER, loss of sphingomyelin causes dephosphorylation of CERT by ER integral phosphatase, returning the ability to associate with the Golgi and activation of ceramide transfer (Kumagai *et al.*, 2007).

Class I PITP

There are two classes of PITPs (phosphatidylinositol transfer proteins), Class I PITPs include PITPα and PITPβ and Class II PITPs include RdgBα and RdgBβ (Allen-Baume, Ségui and Cockcroft, 2002). Class I PITP binds and transfers PI and PC [Figure 1.8B]. Crystallisation studies found that PITP shares the same structural elements as members of the StART family (Yoder *et al.*, 2001). Similarly to StART domains, PITPs have a hydrophobic cavity able to bind lipids and a flexible Ω1 loop which undergoes significant movement upon lipid binding [Figure 1.8B] (Yoder *et al.*, 2001; Schouten *et al.*, 2002). The C-terminal helix has been shown to be essential for lipid transfer activity of PITPα though not for lipid binding(Tremblay *et al.*, 1998). Lipid transfer requires the ability to associate and dissociate with donor and acceptor membranes. When the C-terminus is removed, PITPα shows higher affinity for membranes, and it is suggested that due to this increase in membrane association, PITPα is immobilised to one membrane (Tremblay *et al.*, 1998; Allen-Baume, Ségui and Cockcroft, 2002). Without

the ability to dissociate from a membrane, the protein is unable to participate in transfer. It is proposed that when PITPα is empty, the open conformation of the C-terminus helix exposes a hydrophobic surface that promotes membrane association (Allen-Baume, Ségui and Cockcroft, 2002). Upon binding with a ligand, this C-terminal helix closes, allowing the protein to dissociate with the membrane, thus facilitating transfer.

RdgB/Class II PITP

The subfamily of PITPs that are related to Retinal degeneration type B in flies (RdgB or Nir in humans) might utilise a counter-exchange mechanism similar to that of the OSH/ORP family described in section 1.5.2. RdgBα and its human homologue Nir2 are class II PITPs and accordingly are best known for their ability to transfer PI which is shared with other PITPs through conserved residues in the binding pocket (Tilley *et al.*, 2004; Cockcroft *et al.*, 2016). However, they can also transfer PC and PA. In addition to the conserved PITP domain, RdgBα also has an LNS2 domain, found to bind PA at the PM, a DDHD domain and a FFAT motif, which is thought to play a part in its recruitment to ER-PM contact sites via interaction with VAPs (Kim *et al.*, 2013). Nir2 in human cells has been found to localise on the Golgi. In addition, it translocates to the PM following PIP_2 hydrolysis by phosphoinositide phospholipase C activated by growth factors (Kim *et al.*, 2013). In the PM, PA is produced from $PI(4,5)P_2$-derived DAG. PITP could transfer this PA to the ER where it is synthesised to PI which is then transferred to the PM to supply PI for $PI(4,5)P_2$ synthesis. It is suggested that the function of this complex exchange system can control the homoeostasis of $PI(4,5)P_2$ and that RdgBα/Nir type PITPs are responsible for the transfer of both PA to the ER and PI to the PM in a countercurrent (Cockcroft *et al.*, 2016).

1.5.5 SRPBCC

The StART and PITP protein families belong to a superfamily called SRPBCC (StART/RHOαC/PITP/Bet v 1/CoxG/CalC), also known as the StAR-kin superfamily (as all members have structural relation (kin) to StAR, the term StARkin is used from here on) and Bet v I superfamily (Iyer, Koonin and Aravind, 2001; Khafif *et al.*, 2014; Wong and Levine, 2016). The StARkin fold is an αβ fold where a curved 7-stranded β-sheet is combined with two α helices to form a large hydrophobic cavity (as described above in StART). Though all members of this family are defined as having a StARkin fold, the superfamily was composed by aligning 3D structures rather than by sequence homology. Before this study, yeast has only been identified to possess two of the StARkin subfamilies, AHA1 and CoQ10, which are universal proteins, distinct from the StART family.

1.5.6 Bioinformatics and lipid transfer proteins

BLAST (Basic Local Alignment Search Tool) compares a sequence of interest with a database of sequences to identify sequences that resemble the query based on sequence similarity. This tool is useful for identifying homologues of a protein across species and locating domains in a query sequence. Position-Specific Iterated BLAST (PSI-BLAST) is more sensitive than BLAST, using multiple alignments of high scoring sequences for additional iterations. However, StART-like or StARkin lipid binding domains were not found in yeast using PSI-BLAST. Hence there was an assumption that yeast did not have StARkin lipid transfer proteins (Alpy and Tomasetto, 2005; Clark, 2012).

HHpred is a protein sequence alignment tool that is made more sensitive than PSI-BLAST by using predicted secondary structure and hidden Markov models to represent the sequences both query and database of possible targets (Söding, Biegert and Lupas, 2005; Kopec, Alva and Lupas, 2010; Schauder *et al.*, 2014). A lipid-binding domain must fit the criteria of having a hydrophobic pocket in a globular protein that can protect a lipid ligand from the aqueous phase of the cytoplasm, thereby allowing the lipid to travel a distance to another membrane. As such, the structure of a lipid binding protein is as important as the specific residues. This formula has been proven with the discovery of the TULIP fold in the SMPs by structural bioinformatics, using multiple tools including HHpred which was confirmed with crystallography (see section 1.5.3 for more details on TULIPs) (Kopec, Alva and Lupas, 2010; Schauder *et al.*, 2014). Using HHpred allows the predicted structure to play a part in finding StARkin domain containing proteins which have a specific and distinctive αβ fold and so decreases the reliance on the specific search sequence.

Using this program, two new families of eukaryotic StARkin lipid transfer proteins were discovered which were not previously defined using conventional sequence specific bioinformatics software (Gatta *et al.*, 2015). One was the PRELI/Ups family (Connerth *et al.*, 2012), and the other was the family that is the subject of this investigation, here called the Lipid transfer proteins anchored at membrane contact sites (LAMs) (see section 1.5.8) (Khafif *et al.*, 2014; Gatta *et al.*, 2015; Murley *et al.*, 2015). The bioinformatics predicts the StARkin domains fold similarly to conventional StART domains with an αβ grip fold encompassing a hydrophobic pocket to bind lipid ligands (Gatta *et al.*, 2015).

1.5.7 Ups/PRELI

The Ups yeast protein family, also known as PRELI in humans, has been identified as StART related transfer proteins (Connerth *et al.*, 2012; Watanabe *et al.*, 2015). Ups1/2p is intrinsically unstable but is prevented from degradation when it complexes with Mdm35p (TRIAP1 in humans) (Tamura, Iijima and Sesaki, 2010). Mdm35p is composed of three α helices and is shown to wrap around the StARkin structure of Ups1p (Watanabe *et al.*, 2015). The Ups-Mdm35 complexes have been shown to move PLs from the OMM to the IMM (inner mitochondrial membrane); Ups1p specifically moved PA for cardiolipin synthesis whereas Ups2p moves PS for PE production (Connerth *et al.*, 2012; Watanabe *et al.*, 2015; Aaltonen *et al.*, 2016; Miyata *et al.*, 2016). As such, the loss of Ups1p causes a decrease of cardiolipin levels in the mitochondria and accumulation of PA, whereas the removal of Ups2 reduces PE levels in the mitochondria (Tamura *et al.*, 2009; Connerth *et al.*, 2012). The activity of Ups2p-Mdm35p is dependent on growth conditions, for example, during anaerobic growth, the production of PE is upregulated in the mitochondria and coincides with an increase in Ups2p (Miyata *et al.*, 2016). As with some StART proteins, perturbing the Ω1 loop in Ups2p, predicted to form a lid, affects the PS transfer activity. Interestingly, the defective cardiolipin synthesis that occurs with the loss of Ups1p, is partially rescued by the removal of Ups2p but in contrast, the removal of Ups1p in Δ*ups2* does not rescue the defective PE production (Osman *et al.*, 2009; Tamura *et al.*, 2009; Miyata *et al.*, 2016) Furthermore, overexpression of Ups2p causes a decrease of cardiolipin (Tamura *et al.*, 2009). To explain this phenomenon, it has been suggested that Ups2-Mdm35 not only transports PS but also exchanges PS for PA and thus transports PA in the opposite direction. As the OSH protein family and StART-like RdgBα/Nir PITPs have been recently identified as having a countercurrent activity, it is possible that this model could be applicable to other LTPs such as Ups/PRELI.

1.5.8 LAM protein family

Lipid transfer proteins Anchored at Membrane contact sites (LAMs) is a family of six proteins in yeast and was renamed by our lab from its uninformative classification of DUF4782 (Domain of Unknown Function 4782) (Gatta *et al.*, 2015). An alternative name has also been proposed for four out of the six proteins to be Lipid Transfer at Contact sites (LTC) from a different group who also discovered the fold using a structure prediction software (Elbaz-Alon *et al.*, 2015; Murley *et al.*, 2015).

In addition to the StARkin domain, most members of the LAM family contain at least one PH domain related to the GRAM subfamily, and almost all contain one or

more transmembrane domain. PH domains are a common structurally conserved fold of approximately 100-120 amino acids. It has been found that many proteins containing PH domains are involved in membrane-associated processes (Jiang, Ramamoorthy and Ramachandran, 2008). A key element of the LAM family is a transmembrane domain, which indicates that the location will be embedded in a membrane where lipid transfer will be likely to occur. In yeast, there are three pairs of paralogs due to a whole genome duplication, which occurred over millions of years in the past (Kellis, Birren and Lander, 2004). The LAM family of proteins are paired as Lam1p/3p, Lam2p/4p and Lam5p/6p.

Lam1p/Lam3p

Lam1p was initially known as Ysp1p, Yeast suicide protein 1 and was shown to be required for mitochondrial fragmentation in response to stress-induced programmed cell death (Pozniakovsky *et al.*, 2005). Both Lam1p and Lam2p (see below) were found in genetic screens for proteins involved in cell death induced by pheromone or amiodarone (Pozniakovsky *et al.*, 2005; Sokolov *et al.*, 2006). Amiodarone and pheromones target the Ca^{2+} channel, increasing cytosolic Ca^{2+} levels to induce apoptosis via reactive oxygen species. No further investigations into Lam1p have been conducted on its relationship with programmed cell death.

Lam1p and Lam3p have two PH domains, one is the standard PH domain and the second is GRAM-like. The first PH domain of Lam1p interacts with phosphatidylinositol phosphates, PLs, cardiolipin and sphingosine 1 phosphate in a high-throughput TAP protein study (Gallego *et al.*, 2010). The paralog protein, Lam3p (also known as Sip3p) was identified as interacting with the Snf1 protein kinase using its C-terminus; Snf1 is a serine-threonine protein kinase that regulates energy homoeostasis and is suggested to play a role in ergosterol biosynthesis (Lesage, Yang and Carlson, 1994; Zhang, Olsson and Nielsen, 2010). Like Lam1p, the first PH domain of Lam3p was suggested to bind PIs and phosphorylated sphingoid long-chain bases (Vonkova *et al.*, 2015). Aside from the initial study finding Lam3p to be an interactor of Snf1, no further analysis has been conducted on Lam3p and its relation to the Snf1 complex.

High-throughput growth assays show that the most sensitive delete strains to Amphotericin B (AmB) include Δ*lam1*, Δ*lam2* and Δ*lam3* (Hillenmeyer *et al.*, 2008). The high throughput data from Hillenmeyer quantified growth defects of the whole delete collection of nearly 5000 homozygous strains where each strain is deleted for one gene in both alleles. Δ*lam1*, Δ*lam2* and Δ*lam3* were found to be in the 25 most sensitive

strains to Amphotericin B of the whole collection. A fundamental difference between Lam1p/Lam3p and Lam2p is the presence of a C-terminal BAR domain. BAR domains are banana shaped α-helical modules that bind to curved membranes. They themselves can also promote further membrane deformation by oligomerising and generate local lipid composition due to the electrostatic interaction between the polymerised BAR domain (Frost, Unger and De Camilli, 2009; Zhao *et al.*, 2013; Gatta *et al.*, 2015). However, the BAR domains of Lam1p/3p have not been studied in detail. Interestingly, the original Lam3p identifying investigation found that expression of a truncated protein containing only the BAR and PH domain decreased growth on glucose but not on raffinose. No growth phenotype was detected with the full delete strain (Lesage, Yang and Carlson, 1994).

Lam2p/Lam4p

The Lam2p/Lam4p pair of proteins is predicted to have two StARkin domains along with a GRAM-like PH domain and a transmembrane domain. The duplication of the StARkin domains occurred before the whole genome duplication to obtain two paralogs Lam2p/4p; bioinformatics calculates the sequence identity of the two StARkin domains in each protein is ~40% compared to the sequence identity of the StARkin domain between each paralog which is ~55% (Gatta *et al.*, 2015). Initially, Lam2p was named Yeast Suicide Protein 2 (Ysp2p) as it was found to be involved with programmed cell death like Lam1p, also known as Ysp1p. Lam4p was implicated in sterol transport as one of 23 genes found in a screen for proteins involved in sterol import (Sullivan, Georgiev and Menon, 2009). This screen was carried out with tritium sterol (^{3}H cholesterol) to find mutants defective in internalising sterol and therefore able to survive by keeping the toxic radiolabelled sterol outside of the cell (Sullivan, Georgiev and Menon, 2009). However, Δ*lam4* has no AmB sensitivity, so it does not match Δ*lam2*, which is sensitive, similarly to Δ*lam1* and Δ*lam3*.

TORs (target of rapamycin) are Ser/Thr kinases that serve as a central regulator of a complex signalling network underlying growth, proliferation and survival in response to cellular stress. Cells undergo essential lipid regulation in response to stress affecting the membranes such as environment stresses. One complex involved in regulating this pathway is TOR Complex 2 (TORC2), a multiprotein complex involving Tor2p. Whilst TORC1 (which can involve Tor1p or Tor2p) is inhibited by rapamycin, TORC2 is rapamycin insensitive and has been suggested to detect membrane tension to regulated the sphingolipid biosynthetic pathway (Berchtold *et al.*, 2012). TORC2 localises to puncta on the PM that are adjacent to eisosomes, membrane invaginated

nanodomains. Slm1/2p binds to PI(4,5)P_2 on the PM by its PH domain and is usually localised in the eisosomes (Gallego *et al.*, 2010). However, upon membrane stress or inhibitions of sphingolipid synthesis, Slm1/2p relocates to the TORC2 complex on the PM, which in turn activates downstream kinase, Ypk1p, an AGC-type kinase. Slm1p was found associated with Lam2p in a yeast two-hybrid high throughput screening (Uetz *et al.*, 2000), suggesting that there may be an association between LAM proteins and TORC2 signalling. Ypk1p is a kinase that has a role in maintaining lipid levels and distribution in membranes in response to stress by phosphorylating downstream substrates which potentially includes Lam2p and Lam4p, which could point to another way that the TOR signalling pathway is linked to Lam2/4p (Muir *et al.*, 2014). Other substrates of Ypk1p include a ceramide synthase, which results in increased sphingolipids in the PM in response to stress, so it is feasible that Ypk1p also phosphorylates other lipid affecting proteins.

Lam5p/Lam6p

Before this study and the work by the Nunnari and Schuldiner labs, Lam5p/6p were only known as 'GRAM – containing protein' as the GRAM-like PH domain was the only identified domain. No investigations had been carried out on these proteins.

Human LAMa/b/c

The novel LTP family has three human homologues, *Hs*LAMa/b/c (previously known as GramD1a/b/c) and similarly to yeast proteins, are not well characterised with only the PH domain being identified. *Hs*LAMa/b/c have a domain architecture similar to Lam5/6p with a GRAM-like PH domain, a predicted StARkin domain and a TM domain. Expression of *Hs*LAMa in liver tissues was found to be linked with survival of patients suffering from hepatocellular carcinoma, a common liver cancer. Overexpression of *Hs*LAMa was found to promote chemoresistance and tumour growth of hepatocellular carcinoma as well as the self-renewal of hepatocellular carcinoma stem cells by regulating STAT5, a transcription factor that promotes proliferation (Fu *et al.*, 2016). In high-throughput data sets, *Hs*LAMb has been linked to solid and haematological cancer. Genome-wide association studies identified the *Hs*LAMb locus in chronic lymphocytic leukaemia and follicular lymphoma (Di Bernardo *et al.*, 2008; Conde *et al.*, 2010). *Hs*LAMb has also been shown to affect chemoresistance in ovarian cancer cells with the silencing of *Hs*LAMb causing reduced tumour size and was beneficial to the survival of mouse models (Wu *et al.*, 2014).

Plant LAMs

VAD1 in plants was found to contain a StARkin domain in a separate investigation in Arabidopsis (Khafif *et al.*, 2014), where the authors named this domain as VASt (VAD1 Analog of StAR-related lipid transfer). VAD1 is a protein similar to *Hs*LAMa/b/c and Lam5p/6p, containing a PH domain, a StARkin domain and a single TM domain. The mutant *Arabidopsis thaliana vad1* is a lesion mimic mutant showing spontaneous necrotic lesions which usually occurs when controlled program cell death is induced as part of a defence mechanism.

There are addition LAM proteins that are present in plant genomes that are composed of domain structures different to that of fungal and mammalian LAMs. One such additional domain is the C2 domain that is present in a subgroup of LAM proteins found in plants. BAGP1 is a member of this subfamily (Li *et al.*, 2016) and was named for being a BAG (Bcl-2-associated athanogene)-associated GRAM containing protein. The locus was found to be induced in response to fungal infection, and further studies found that BAGP1 was essential for the basal resistance of Arabidopsis to *B. cinerea,* an infectious fungal strain (Jiang, Ramamoorthy and Ramachandran, 2008; Li *et al.*, 2016). In this study, it was also found that BAGP1 interacted with APCB1 and BAG6 in a complex.

Aims of Work

CHAPTER 2

Aims of work

Thus far, the LAM family of proteins has not been characterised, but various data implicates them to be involved with ergosterol in the yeast cell. The presence of a conserved StARkin domain, sensitivity to ergosterol-affecting drugs and an occurrence in a tritium labelled sterol uptake assay links them to sterol binding, sensing or transport. Thus the purpose of this study is to investigate the predicted StARkin domain and to identify any connection between this potential ligand binding domain and the phenotypes identified in high throughput assays. LAM proteins also contain multiple membrane targeting domains and identifying their localisation would yield clues to the function of these proteins. The role of LAM proteins in filamentous fungi will also be investigated to find whether the role of LAM proteins for resistance to Amphotericin B is retained across the fungi kingdom.

The aims of my work will be to:

1. Create and analyse the phenotype of knockout strains of the LAM family of proteins in budding yeast. The manufacturing of these strains will be shown in CHAPTER 4: Analysis of the Yeast LAM family and will be used for further analysis.
2. Clone and study the localisation of members of the LAM family in budding yeast. The localisation of Lam3p will be investigated in depth in CHAPTER 4: Analysis of the Yeast LAM family.
3. Investigate the activity of domains of LAM proteins in budding yeast. Lam2p domains and the second StARkin of Lam4p will be analysed for their activity for AmB basal resistance in CHAPTER 4: Analysis of the Yeast LAM family.
4. Explore the functionality of LAM proteins in filamentous fungi. The LAM homologs in *Aspergillus fumigatus* (*Af*) will be compared to those in

Saccharomyces cerevisiae (*Sc*) LAMs and delete *Af*LAM strains will be created. This work is shown in CHAPTER 5: Fungal LAM characterisation.

5. Investigate function of the predicted LAM StARkin domain. The activity of the predicted StARkin domain of budding yeast and filamentous fungi will be investigated. In addition, *in vitro* characterisation of these domains will be carried out. All chapters will feature aspects of LAM StARkin activity.
6. Clone and purify functional StARkin domains. *In vitro* characterisation of LAM StARkin domain requires successful purification of LAM StARkin constructs which will be demonstrated in CHAPTER 6: *In vitro* studies of sterol binding and transfer by LAM StARkin domains.
7. Probe the *in vitro* lipid binding and transfer properties of the StARkin domains. The detailed examination of LAM StARkin domains will converge on its proposed involvement in cellular sterol transport. These experiments will be presented in CHAPTER 6: *In vitro* studies of sterol binding and transfer by LAM StARkin domains.

Materials & Methods

CHAPTER 3

Materials & Methods

Unless otherwise stated, all methods are carried out at room temperature (RT) (21°C), and the ddH_2O used is Millipore water.

3.1 Chemicals

Yeast mediums were purchased from ForMedium. Lipids were purchased from Sigma, Avanti Lipids or Lipid Products. Unless otherwise stated, all other chemicals were purchased from Sigma-Aldrich.

3.2 DNA

3.2.1 Plasmids

The plasmids used or created in this study are listed in Table 3-1. Bacterial expression vectors were based on pTrcHis$_6$. Yeast expression vectors were based on the pRS4XX vector series composed of a yeast centromere shuttle plasmid with a T7 promoter (Sikorski and Hieter, 1989).

Table 3-1 List of plasmids

Plasmid name	Description
His-Lam2S1	MGGSHHHHHHGMASHHHHHARAPVMT Lam2 829-1027 + R
His-Lam2S2	MGGSHHHHHHGMASHHHHHARAPVMT Lam2 1027-1244 + R
His-Lam4S1	MGGSHHHHHHGMASHHHHHARAM Lam4 731-938 + DV
His-Lam4S2	MGGSHHHHHHGMASHHHHHARAM Lam4 946-1155 + DV
His-GFP-Lam2S1S2	MGGSHHHHHHGMAS GFP Lam2 829-1244
His-Lam2S1S2	MGGSHHHHHHGMASHHHHHARA Lam2 829-1244
His-GFP	MGGSHHHHHHGMASHHHHHARA GFP
His-Lam4S2GR	MGGSHHHHHHGMASHHHHHARA Lam4 946-1155 G1119>R
Lam4S2 linker-His	Lam4 950-1201 HHHHHHHHH

Lam4linker-His	Lam4 1148-1201 HHHHHHHHH
PHO5>GFP-Lam3p	416 PHO5 promoter GFP Lam3
LAM2>GFP-Lam2ΔN	416 LAM2 promoter GFP Lam2 611-1438
LAM2>GFP-Lam2ΔPH	416 LAM2 promoter GFP Lam2 1-610 + 829-1438
LAM2>GFP-Lam2ΔS1	416 LAM2 promoter GFP Lam2 1-828 + 1028-1438
LAM2>GFP-Lam2ΔS2	416 LAM2 promoter GFP Lam2 1-1027 + 1245-1438
LAM2>GFP-Lam2ΔCT	416 LAM2 promoter GFP Lam2 1-1246
PHO5>GFP-GFP	416 PHO5 promoter GFPx2
PHO5>GFP-Lam3StART	416 PHO5 promoter GFP Lam3 771-976
LAM2>GFP-Lam2p	416 LAM2 promoter GFP Lam2
LAM1>GFP-Lam1p	416 LAM1 promoter GFP Lam1
LAM3>GFP-Lam3p	416 LAM3 promoter GFP Lam3
LAM4>GFP-Lam4p	416 LAM4 promoter GFP Lam4
LAM5>GFP-Lam5p	416 LAM5 promoter GFP Lam5
LAM6>GFP-Lam6p	416 LAM6 promoter GFP Lam6
PHO5>GFP-Lam1p	416 PHO5 promoter GFP Lam1
PHO5>GFP-Lam2p	416 PHO5 promoter GFP Lam2
PHO5>GFP-Lam3p	416 PHO5 promoter GFP Lam3
PHO5>GFP-Lam4p	416 PHO5 promoter GFP Lam4
PHO5>GFP-Lam5p	416 PHO5 promoter GFP Lam5
PHO5>GFP-Lam6p	416 PHO5 promoter GFP Lam6
PHO5>GFP-CnLamStART	416 PHO5 promoter GFP *Cn*Lam(XP_012046380) 528-719
LAM2>GFP-Lam2swL4S2	416 LAM2 promoter GFP Lam2p 1-1027 + Lam4 953-1161 + Lam2 1245-1438
LAM2>GFP-Lam2swL4S2GR	416 LAM2 promoter GFP Lam2p 1-1027 + Lam4 953-1161 G1119>R + Lam2 1245-1438
LAM2>GFP-Lam2swL4S2EV	416 LAM2 promoter GFP Lam2p 1-1027 + Lam4 953-1161 E1058>V + Lam2 1245-1438
LAM2>GFP-Lam2swL4S2RI	416 LAM2 promoter GFP Lam2p 1-1027 + Lam4 953-1161 R1025>I + Lam2 1245-1438
RFP-ER	405 RFPx2 Scs2 220-244 (TM domain)
RFP-Tom6p	405 RFPx2 Tom6p

Note: plasmids containing regions of Lam2p were cloned with two extra residues as to facilitate the cloning of full-length Lam2p in five parts. A tyrosine was added after the lysine at position 585, and an arginine was added after the serine at position 1244.

3.2.2 Primers

The primers used for homologous recombination knockouts (KOs) and gap repair strategy for yeast gene cloning are listed in Table 3-2 (see results sections 4.2.3, 4.2.11 and 5.2.8 and Figure 4.5, Figure 4.15 and Figure 5.8 for more details on the KO or cloning strategy).

Table 3-2 List of primers

Primer name	Sequence 5' to 3'
Af LAM KO FD1 F	CCGAGCTCCCAAATCTG
Af LAM KO FU2 R	GAAATCACGCCATGTAGTG
Af LAM KO M2 F	GAGCTTATACCGAGCTCC
Af LAM KO M3 R	CAGCAATCGCGCATATG
AF LamA KO chk F2	CGGTATTCCTCGTGCAG
AF LamA KO chk F3	CCTCGTGTACTGTGTAAG
AF LamA KO chk F4	CAGACTGAACCACAAGG
AF LamA KO chk F5	GTTCACGATGTAGAGCC
AF LamA KO chk R2	CTTCAAGTCAGCCAACTG
AF LamA KO chk R3	CGATAACGTACTTGTGGC
AF LamA KO chk R4	CCGAGGTAGAAGATGTTC
AF LamA KO chk R5	GCACAATTGAGTGGTCAG
Af LamA KO D1 F	CTCCACATCTCCACTCGAGCATGGAATGCATCACAGC
Af LamA KO D2 R	CTTTATTGCGCACTACACC
Af LamA KO FD2 R	GACACCTACCACATGATC
Af LamA KO FU1 R	GTTTCTCTAGCCGGTAACC
Af LamA KO M1 R	GCACTCCGCTATATTCCTTGAATTCCCTTGTATCTCTAC
Af LamA KO M4 R	GCATTCCATGCATGGGCATTCGAGTGGAGATGTGGAG
Af LamA KO U1 F	CAATGGAGGAGGTTTCTC
Af LamA KO U2 R	GTAGAGATACAAGGGAATTCAAGGAATATAGCGGAGTGC
AF LamB KO chk F2	GTACCAGAGGCGTCTTC
AF LamB KO chk F3	GAAGTCCTCGTGTACTGTG
AF LamB KO chk F4	GGAGCTTGCGACCATAG
AF LamB KO chk F5	GTCAGCGATCAAGTGCG
AF LamB KO chk R2	GCAAACAGAATATCCCGCC
AF LamB KO chk R3	GTGCCATGAGCGTAGTC
AF LamB KO chk R4	CATGTTCAGGTCCGACAG
AF LamB KO chk R5	CAAGCTGCTCCTGTTCC
Af LamB KO D1 F	CTCCACATCTCCACTCGAAAGGTACATAGGAGTTGC
Af LamB KO D2 R	GAGCGTAGTCTGGATATG
Af LamB KO FD2 R	GTACGGAATGACGGAGTAG
Af LamB KO FU1 R	CTTCCCACTTGTCATCG
Af LamB KO M1 R	GGAGCTCTCTTCTCGACGAATTCCCTTGTATCTCTA

	C
Af LamB KO M4 R	GCAACTCCTATGTACCTTTCGAGTGGAGATGTGGAG
Af LamB KO U1 F	CCGTTTCTGCATTTCCTC
Af LamB KO U2 R	GTAGAGATACAAGGGAATTCGTCGAGAAGAGAGCTCC
His5 5R chk	CTGGTCGCTATACTGCTG
Lam1 KO F	GGTCTGTTCTTCGATTTAGTACTGCCAATTTCAAGTTTTTCACTTCTATAGCTGGATGGCGGCGTTAGTATC
Lam1 KO R	AGACAAGACGGGGTCCTTCTGATTATTGAAGAGTAGACATTCTGGGGCACGGTCGACGGTATCGATAAGC
Lam1 Prom F	CATGCGAACAGTACCAAG
Lam2 KO F	GAAGCAGCAGCTGTACAGATATCCCTAACCAATGAGGGATGAAGCTACTCGCTGATGGATGGCGGCGTTAGTATC
Lam2 KO R	GTTATTTTATCAAAGTAATTGGTTAGTAGCCGACGTGTTATCCGTTTGGGCCGGTCGACGGTATCGATAAGC
Lam2 Prom F	CTCTGAGCTCGAGCCTACATTTCCTCTGATG
Lam3 C GR F	CACGTTGCTAGCGGCCGCTTAAGACTACGAAAAATTCTTGCTG
Lam3 C GR R	CACTTGGGTACCAATCGAGAGACTTCGTG
Lam3 KO F	GGTGTAACTAAAACATAGCTGCATGAGTAGACCTGTTGATCAATTGACATTGGATGGCGGCGTTAGTATC
Lam3 KO R	CGCTATTGACGAAAGAGAAGTATCTTTCATGAGGTCAATAATAACGTTCAGGTCGACGGTATCGATAAGC
Lam3 N GR F	CTAGTGAAGCTTGCAGGTGCCATGTCCGTTCACGGGAGG
Lam3 N GR R	CACGTTGCTAGCAGTTCTAATAGCGCGGTTG
Lam3 Prom F	TGCCGCCTAGTGGTACAC
Lam4 5f check	GGCTGGCTTTATGCGGC
Lam5 5f chk	GGCCATCCGTGTAGTAGTG
Lam5 KO F	CGCTATCTGAGAAAAGGGTGAAGAAGGCAACTACACAAAAAGATTAGTGGTGGATGGCGGCGTTAGTATC
Lam5 KO R	GCTTATCGATACCGTCGACCATCAACTGGTGAAGCTGCAATTGGTAGAACTGAAGTTGTGATCTG
Lam6 5f chk	GGGTCGGTTGCAGAAGGG
Lam6 KO F	GTGGCATCTAGAGAGAATAATTGAACGCAATGAAGAGAGCATGGTACGTTGGATGGCGGCGTTAGTATC
Lam6 KO R	GCTTATCGATACCGTCGAGGTCAAGACCAAGAAGGGGAGACGTGTTGTAACAGAGTAATCATGTAATATTG

3.2.3 Plasmid miniprep

Transformed MC1601 *Escherichia coli* (*Ec*) strain cells containing a plasmid were spread onto an LB agar plate supplemented with the corresponding antibiotic of the selection marker. The plate was incubated at 30°C overnight. Single colonies from the plate were inoculated into separate sterile culture tubes containing 2.5 ml LB broth with the corresponding antibiotics and incubated at 37°C shaking at 225 rpm for 6

hours. Plasmid Miniprep Kit (Qiagen) was then used to extract plasmid DNA from (*Ec*) according to the manufacturer's instructions.

3.2.4 Diagnostic digests

To check the identity of the vector, a restriction digest reaction was performed with specifically chosen restriction enzymes. A typical reaction was made to a final volume of 10 µl containing approximately 0.75 µg of DNA, 1 unit of enzyme and 1x corresponding enzyme buffer. The restriction digestion mixture was incubated at 37°C for one hour and run out on a 1% electrophoresis agarose gel.

3.2.5 Agarose gel electrophoresis

DNA samples were separated by size using electrophoresis. A typical agarose gel contained 1% (w/v) agarose, 1x TAE buffer and 1x SafeView Nucleic Acid Stain (NBS Biologicals), an ethidium bromide alternative. The gel was submerged in 1x TAE buffer in the electrophoresis tank. DNA size markers and DNA sampled were mixed with 5x loading buffer, loaded onto the gel and run at 100 V for 25 minutes. The DNA bands were then detected and photographed by using a UV imaging system.

3.2.6 Gel purification of DNA

DNA samples were separated on a 1% agarose gel and the correct sized DNA fragments were excised from the gel. The DNA was recovered from the agarose using QiaQuick Gel Extraction kit (Qiagen) following the manufacturer's instruction.

3.2.7 Ligation of DNA fragments

Corresponding DNA fragments with complementary sticky ends were joined together by a ligation reaction using T4 DNA ligase (NEB). A typical ligation reaction was made to a final volume of 5 µl and contained a ratio of 1:2 (backbone:insert), 200 units of ligase and 1x ligase buffer. The ligation was incubated for one hour at room temperature.

3.2.8 Blunting of DNA fragments

After the digestion of the plasmid, if necessary the overhanging ends were blunted with Polymerase Klenow fragment. 2.5 µM dNTPs and 1 unit of Polymerase Klenow fragment (NEB) was added to a 10 µl digestion volume and incubated at 37°C for 5 minutes. The reaction mixture was run on a 1% agarose gel and the relevant fragment was purified. The blunted fragment was then ligated as above.

3.2.9 Polymerase chain reaction (PCR) for regular length products

DNA fragments were amplified by polymerase chain reaction. A typical reaction mixture, for a product length of ~500bp, was made up to 12.5 µl and contained 200 µM dNTPs, 0.4 µM forward and reverse primers, 0.3 units of GoTaq (Promega) and/or

Velocity (Bioline) and/or Q5 (NEB) and the corresponding reaction buffer. A typical PCR cycle was carried out for 6 minutes at 94°C, 30 x (30 seconds at 94°C, 30 seconds at 52°C, 60 seconds per 1 kb at 72°C), 7 minutes at 72°C.

3.2.10 Polymerase chain reaction (PCR) for long products

For DNA fragments >4 kb, a polymerase chain reaction with a typical reaction mixture of 10 µl was used using 1x GoTaq Long Polymerase Master Mix (Promega) and 0.4 µM forward and reverse primers. A typical PCR cycle was carried out for 6 minutes at 94°C, 30 x (20 seconds at 94°C, 30 seconds at 52°C, 60 seconds per 1 kb at 72°C), 7 minutes at 72°C.

3.2.11 Fusion polymerase chain reaction (PCR)

Fusion polymerase chain reaction was used to produce a recombinant DNA fragment with two parts from different DNA sources. The first round of regular PCR was used to generate a DNA fragment from separate DNA sources with primers designed to overlap by 18 bp at the 3' end of the first fragment and the 5' end of the second fragment. The second round of regular PCR or long PCR was used to connect the two DNA fragments together using the purified PCR products from the first round and a set of primers that are inset from the 5' end of the first fragment and the 3' end of the second fragment (see section 5.2.8 and Figure 5.8).

3.2.12 Yeast plasmid isolation

Plasmids from yeast were isolated using buffers from Qiagen Plasmid Miniprep kit. 100 ml of yeast containing the plasmid required was grown overnight in Synthetic Drop out medium at 30°C. The cells were pelleted and resuspended in 500 µl Buffer P1, a resuspension buffer containing RNase A. 500 µl cell wall digestion solution containing 1.2 M sorbitol, 0.1 M $NaPO_4$ buffer, pH7.4 and 0.5 $mgml^{-1}$ Zymolyase 100T was added, and the mixture was incubated at 37°C for 45 minutes. 1 ml of Buffer P2, a high PH lysis buffer containing SDS as a detergent, was added and the mixture was inverted before incubating for 10 minutes at RT. 1.4ml of Buffer N3, a low PH neutralisation buffer containing protein denaturing Guanidinium-HCl was added and the mixture was inverted and incubated on ice for 30 minutes. The cell lysis was then centrifuged for 10 minutes at 10 000 g at 4°C to pellet the cell debris. The supernatant was applied to a Qiagen plasmid miniprep column and washed first with 500 µl of Buffer PB and next with 750 µl Buffer PE. The purified DNA was eluted with 50 µl of TE and subjected to a round of bacteria miniprep isolation before use.

3.3 Yeast

3.3.1 Yeast Strains

Saccharomyces cerevisiae (*Sc*) was the yeast model organism used in this study. The yeast strains used or created in this study are listed in Table 3-3. Delete strains are Mat A with background BY4741 from the Yeast Knockout Collection (Saccharomyces Genome Deletion Project, obtained from Euroscarf) unless otherwise stated.

Table 3-3 List of yeast strains

Strain	Genotype	Source
BY4741	MATa *his3Δ1 leu2Δ0 met15Δ0 ura3Δ0*	Euroscarf
Δ*lam1*	BY4741 *YHR155W*::*KANMX4*	Euroscarf
Δ*lam2*	BY4741 *YDR326C*::*KANMX4*	Euroscarf
Δ*lam3*	BY4741 *YNL257C*::*KANMX4*	Euroscarf
Δ*lam4*	BY4741 *YHR080C*::*KANMX4*	Euroscarf
Δ*lam5*	BY4741 *YFL042C*::*KANMX4*	Euroscarf
Δ*lam6*	BY4741 *YLR072W*::*KANMX4*	Euroscarf
Δ*lam1*Δ*lam3*	BY4741 x BY4742 haploid *YHR155W*::*KANMX4* *YNL257C*::*KANMX4*	This study
RS453C	MATα *ade2-1 his3-11,15 ura3-52 leu2-3112 trp1-1*	[Levine and Munro, 2001]
Δ*lam1*	RS453C *YHR155W*::*HIS5 Sp*	This study
Δ*lam2*	RS453C *YDR326C*::*HIS5 Sp*	This study
Δ*lam3*	RS453C *YNL257C*::*HIS5 Sp*	This study
Δ*lam4*	RS453C *YHR080C*::*HIS5 Sp*	This study
Δ*lam5*	RS453C *YFL042C*::*HIS5 Sp*	This study
Δ*lam6*	RS453C *YLR072W*::*HIS5 Sp*	This study
SEY6210	MATa *leu2-3,-112 ura3-52 his3Δ200 trp1Δ901 lys2-801 suc2-Δ9 GAL*	[Manford *et al.*, 2012]
ANDY198 (*Δtether*)	SEY6210 *ist2Δ::HISMX6 scs2Δ::TRP1 scs22Δ::HISMX6 tcb1Δ::KANMX4 tcb2Δ::KANMX46 tcb3Δ::HISMX6*	[Manford *et al.*, 2012]
CBY924	SEY6210 *osh1Δ::kan-MX4 osh2Δ::kan-MX4 osh3Δ::LYS2 osh4Δ::HIS3 osh5Δ::LEU2 osh6Δ::LEU2 osh7Δ::HIS3 [OSH4, TRP1]*	[Beh and Rine, 2004]
CBY926	SEY6210 *osh1Δ::kan-MX4 osh2Δ::kan-MX4 osh3Δ::LYS2 osh4Δ::HIS3 osh5Δ::LEU2 osh6Δ::LEU2 osh7Δ::HIS3 [osh4-1, TRP1]*	[Beh and Rine 2004]

3.3.2 Zymolyase treatment of yeast

A stock of 3 $mgml^{-1}$ of Zymolyase 100T was prepared in 1x PBS and stored at -20°C. The Zymolyase 100T was diluted 1 in 10 with 1x PBS to a volume of 20 µl with each single colony of yeast and incubated at 30°C for 20 minutes. The mixture was incubated at 99°C for 10 minutes to break the cells open and then stored at -20°C until use.

3.3.3 Yeast transformation

3.3.3.1 *pRS41X series plasmids*

PLATE solution was made using 40% polyethylene glycol 3350, 0.1 M LiAc, 1 mM EDTA and 10 mM Tris-HCl at pH 7.5. Cells were made competent for transformation by harvesting 1 mm^3 of cells from an agar plate and combined with 5 µg of plasmid DNA and 10 µl of single-stranded DNA from salmon sperm and finally resuspending in 100 µl PLATE. After at least 1 hour at RT, the cells were subjected to heat shock at 42°C for 5 minutes, spun down, resuspended in 50 µl PBS and plated on the required selective synthetic drop out agar plates.

3.3.3.2 *pRS40X series and gap repair plasmids*

The necessary plasmids were digested at the relevant homologous recombination site and frozen at -20°C until use. Yeast was grown overnight in 5 ml of YPD at 30°C. The yeast was pelleted and washed in PLATE. 10 µl of ssDNA was added to 1.5 µg of digested plasmids and mixed before adding to the cells. 100 µl of PLATE was used to resuspend the cells and plasmids. The yeast was incubated at RT overnight, heat shocked at 42℃ for 5 minutes and plated on the required selective synthetic drop out agar plates.

3.3.3.3 *Yeast genomic knock-out and knock-in*

A 200 µl PCR of the *HIS5* gene from *Schizosaccharomyces pombe* with primers containing 50 bases before and after from the 5' and 3' untranslated regions of the target gene (see Table 3-2) was concentrated by ethanol precipitation (see section 4.2.3 and Figure 4.5 for details). 200 µl of PCR product to 20 µl of 3M NaAc were mixed, and then 620 µl of 100% EtOH was added before placing at -20°C for ≥30 minutes. The precipitated DNA was centrifuged for 10 minutes at 13 000 rpm (16 kg max, desktop centrifuge at room temperature) and the supernatant was removed. The pellet was dried and resolubilised in 5 µl of TE for ≥10 minutes.

LATE solution was prepared using 0.1 M LiAc, 1 mM EDTA and 10 mM Tris-HCl at pH 7.5. An overnight culture of yeast was grown up in YPD. The culture was diluted 1 in 200 and regrown until 0.5 OD_{600}. The yeast was washed in LATE solution

twice and resuspended at room temperature in 100 µl of the LATE solution. After an incubation of 5 minutes at RT, 5 µl of the PCR marker cassette was added, vortexed and incubated for a further 5 minutes at RT. 280 µl of PLATE solution was added and vortexed before incubating at 4°C overnight. 50 µl DMSO was added to the yeast suspension and mixed by inversion. The yeast was heat shocked at 42°C for 5 minutes, pelleted by brief centrifugation, washed and resuspended in 50 µl water and plated on the required selective synthetic drop out agar plates. Knock-out and knock-in strains were checked by PCR after streaking to single colonies. The first PCR used a primer within the marker cassette and within the genomic DNA upstream or downstream of the integrated marker cassette to check the presence of a successful homologous recombination. The final check PCR used primers within the knocked out gene of interest to check to the absence of the gene.

3.3.4 Growth assays

For yeast strains without plasmids, YPD plates were poured with the relevant drug. For example, Amphotericin B was tested with a range of 62.5 – 1000 ng ml^{-1}. Cells were diluted so that a pin replicator deposited approximately 4000, 200 and 10 cells in 1.5 µl spots onto agar plates and incubated at 30°C for approximately 72 hours.

3.3.5 Microscopy

Yeast strains expressing a fluorescently labelled protein were first grown overnight in the appropriate SD medium, diluted 1 in 100 and grown again until mid-log phase. The cells were pelleted and immobilised between a glass slide and glass coverslip. Images were obtained within 30 minutes of immobilising on a Leica AOBS SP2, a laser scanning confocal microscope, with a 63×/NA1.4 objective lens. Line by line averaging, with each line being exposed 16 times was used for image acquisition.

3.4 Bacteria

3.4.1 MC1601 *Ec*

Competent MC1061 *Ec* was made by growing 5 colonies overnight from a fresh plate to seed a 250 ml culture at 1 in 100 dilution for approximately 4 hours at 37°C until an OD of 0.5-0.55 is reached. The culture was placed on ice for 5 minutes and then centrifuged to collect the cells. The cell pellet was resuspended in 62.5 ml ice-cold 0.1 M MgCl2 and incubated on ice for 10 minutes. The cells were collected by centrifugation and resuspended in 31 ml 0.1 M CaCl2 and incubated on ice for 30 minutes. The cells were collected for a final time by centrifugation and resuspended in

12.5 ml 0.1 M CaCl2 and 13% glycerol. 120 µl aliquots were made and frozen instantly and stored at -80°C

MC1061 cells were transformed by incubating 15 µl on ice with 5 µl of the plasmid or ligation mixture for 20 minutes, incubated at 42°C for 60 seconds and recovered with 90 µl of LB at 37°C for 30 minutes before plating on LB agar with the appropriate antibiotic.

3.4.2 BL21 *Ec*

Competent BL21-DE3 *Ec* cells were made as with MC1601. BL21-DE3 *Ec* cells were transformed by incubating 15 µl on ice with 5 µl of the plasmid or ligation mixture for 30 minutes, incubated at 42°C for 45 seconds and recovered with 90 µl of LB at 37°C for 30 minutes before plating on LB agar with the appropriate antibiotic.

3.5 Protein

3.5.1 Protein expression

Polyhistidine-tagged proteins were purified from BL21 (DE3) *Ec* cells transformed with the relevant plasmids. The bacteria were first grown overnight and in the morning, diluted 1 in 200 before being induced at 0.5 OD_{600} with 0.2 mM IPTG for up to 6 hours. The cells were collected and resuspended in 25 mM Tris-HCl pH 8.0, 300 mM NaCl, 5 mM imidazole, 1 $mgml^{-1}$ egg lysozyme, 0.5 mM AEBSF, complete EDTA-free protease inhibitor cocktail tablet (Roche). The cells were frozen at -80°C until purification

3.5.2 Protein purification

The cells were defrosted at 15°C for 1 hour, and then DNA was sheared using a probe sonicator for 3 x 30 seconds on ice before centrifugation at 17000 rpm to remove cell debris. The bacterial lysate was mixed with Ni-NTA agarose beads for 1 hour at 4°C, and the beads were then washed repeatedly before eluting with increasing imidazole concentration in 25 mM Tris-HCl pH 8.0, 300 mM NaCl. The eluted protein was desalted into 20 mM PIPES, 137 mM NaCl, 3 mM KCl, pH 6.8 using a PD-10 Desalting Column (GE Healthcare) and stored at -80°C. The protein purity was evaluated by SDS-PAGE and was >90% for all preparations other than Hisx6-GFP-LamS1S2. Protein quantification was carried out using NanoDrop (Thermo Fisher Scientific) with the coefficient extinction for each protein.

3.5.3 SDS-PAGE

Proteins were evaluated by SDS-PAGE. A typical acrylamide gel contained 12% acrylamide and was 0.75 mm thick. The resolving gel contained 375 mM Tris-HCl pH

8.9, 0.1% SDS, 0.05 % APS, 0.1% TEMED and 12% acrylamide. The stacking gel contained 125 mM Tris-HCl pH 6.8, 0.1% SDS, 0.05 % APS, 0.1% TEMED and 5% acrylamide. Gels were loaded with protein and sample buffer containing 62 mM Tris-HCl pH 6.8, 1% SDS, 10% glycerol, 0.003% bromophenol blue and 5% β-mercaptoethanol. The gels were run at 200 V for 1 hour in cold running buffer containing 25 mM Tris-HCl, 200 mM Glycine and 0.1% SDS. The gels were stained with warm 0.05% Coomassie Blue R250 in 10% acetic acid, 50% methanol and 40% H_2O for 30 minutes shaking and destained for at least 2.5 hours shaking with 10% acetic acid, 50% methanol and 40% H_2O. The destain solution was changed at least two times with an H_2O rinse in between.

3.6 Lipids

3.6.1 Radioactive lipid binding assay

Carried out by Shamshad Cockcroft: HL60 cells were labelled with 1 $\mu Ciml^{-1}$ [^{14}C] acetate for 72 hours RPMI 1640 medium. 10^7 cells were permeabilised with 0.6 i.u. Streptolysin O, 2 mM MgATP, 20 mM PIPES, 137 mM NaCl, 3 mM KCl, pH 6.8 for 10 minutes at 37°C before incubating on ice for 5 minutes. Cell membranes were pelleted by centrifugation at 3000 rpm for 5 minutes to separate leaked cytosol and resuspended in 5 ml 20 mM PIPES, 137 mM NaCl, 3 mM KCl, pH 6.8.

100 µl of radiolabelled donor membranes and 100 µl of acceptor liposomes PC:PI (98:2 80 nmol PL) were incubated with 50 µl of protein for 30 minutes at 25°C. The reaction was quenched by the addition of 50 µl ice cold 200 mM sodium acetate, 250 mM sucrose pH 5 and samples were incubated on ice for 10 minutes after vortexing. The precipitated donor membranes were separated by centrifugation at 12 000 g for 10 minutes at 4°C, and the supernatant was transferred into clean tubes for analysis. Lipids were extracted from the supernatant by the addition of 3.75 ml chloroform:methanol (1:2), 1.25 ml chloroform and 1.25 ml H_2O, vortexing at each addition. The mixture was dried in a Savant SpeedVac overnight, and the pellet was resuspended in 50 µl chloroform. The samples were loaded on a Whatman Silica Gel 60 TLC plate, which was developed in choloroform:methanol:acetic acid:H_2O (75:45:3:1) for PLs and hexane:diethylether:acetic acid (155:45:2) for neutral lipids. Controls using RdgBα, a known PI/PA transfer protein was used as a positive control, and a small sample of the donor membranes was used to show total lipids. TLC plates were exposed and analysed using Fuji phosphorimaging screens and BAS1000 phohsphorimaging system.

3.6.2 Lipids

Lipids were dissolved in chloroform and stored under argon gas at -20°C in a glass desiccator jar. The majority of lipids were purchased from Avanti Polar Lipid European distributor, Instruchemie (Netherlands) or Lipid Products (Nuffield UK). Table 3-4 lists the supplier, the acyl saturation details in square brackets and the purity in brackets of each lipid.

Table 3-4 Table detailing lipids used

Lipids	Supplier(s)	Details
Dehydroergosterol (DHE)	Sigma	Ergosta-5,7,9(11),22-tetraen-3β-ol (~96%)
Ergosterol (Erg)	MP Biomedicals	3β-Hydroxy-5, 7, 22-ergostatriene (95.5%)
Cholesterol (Chol)	Avanti Polar Lipids	Cholest-5-en-3ß-ol from ovine wool (>98%)
Phosphatidylcholine (PC)	Avanti Polar Lipids, Lipid Products	[33% 16:0, 32% 18.1, 17% 18:2, 12% 18:0] L-α-phosphatidylcholine from egg yolk (>99%)
Phosphatidylethanolamine (PE)	Avanti Polar Lipids, Lipid Products	[18:1] 1,2-dioleoyl-sn-glycero-3-phosphoethanolamine (>99%)
Phosphatidylserine (PS)	Avanti Polar Lipids, Lipid Products	[42% 18:0, 30% 18:1, 11% 22:6] L-α-phosphatidylserine from Bovine spinal cord
Phosphatidylinositol (PI)	Lipid Products	[46% 18:0, 17% 20:4, 13% 20:3] L-α-phosphatidylinositol from Bovine liver
Dansyl-PE (D-PE)	Avanti Polar Lipids	[18:1] 1,2-dioleoyl-sn-glycero-3-phosphoethanolamine-N-(5-dimethylamino-1-naphthalenesulfonyl) (>99%)
Phosphatidylglycerol (PG)	Lipid Products	[33% 16:0, 30% 18:1, 19% 18:2, 12% 18:0] L-α-phosphatidylglycerol from egg yolk (>99%)
Phosphatidic acid (PA)	Lipid Products	[34% 16:0, 32% 18:1, 19% 18:2, 12%, 18:0] L-α-phosphatidic acid from egg yolk (>99%)

3.6.3 Liposome preparation

Lipids stored in chloroform were mixed at the desired molar ratio, dried under argon gas and placed under vacuum for one hour. The lipid film was hydrated in 42°C 20 mM PIPES, 137 mM NaCl, 3 mM KCl, pH 6.8 and rotated at 37°C for at least an hour to obtain a suspension of large multilamellar liposomes. For liposome binding assays, liposomes (detailed in Table 3-5) were made in 20 mM PIPES, pH 6.8 and 280 mM Raffinose in place of 137 mM NaCl, 2.7 mM KCl. The suspension was subjected

to at least five cycles of freezing and thawing using liquid nitrogen and then extruded through Whatman polycarbonate filters (Sigma) of 0.4 μm, 0.2 μm and finally 0.1 μm pore size using a mini-extruder (Avanti Lipids). Liposomes were stored at 4°C under argon in the dark.

Table 3-5 Table showing composition of liposomes used

Liposomes	Other names	Lipid composition
PC_{100}	PC	100% PC
$PC_{70}DHE_{30}$	PCDHE	70% PC, 30% DHE
$PC_{50}PE_{20}DHE_{30}$	PCPEDHE	50% PC, 20% PE, 30% DHE
$PC_{60}PS_{10}DHE_{30}$	PCPSDHE	60% PC, 10% PS, 30% DHE
$PC_{40}PE_{20}PS_{10}DHE_{30}$	PCPEPSDHE, 30% DHE	40% PC, 20% PE, 10% PS, 30% DHE
$PC_{60}PE_{20}PS_{10}DHE_{10}$	10% DHE	60% PC, 20% PE, 10% PS, 10% DHE
$PC_{60}PI_{10}DHE_{30}$	PCPIDHE	60% PC, 10% PI, 30% DHE
$PC_{90}PS_{10}$	PCPS	90% PC, 10% PS
$PC_{80}PE_{20}$	PCPE	80% PC, 20% PE
$PC_{40}PE_7PS_{20}DHE_{30}$ D-PE_3		40% PC, 7% PE, 20% PS, 30% DHE, 3% Dansyl-PE
$PC_{40}PE_{20}PS_{10}Chol_{30}$		40% PC, 20% PE, 10% PS, 30% Chol
$PC_{40}PE_7PS_{20}Chol_{30}$ D-PE_3		40% PC, 7% PE, 20% PS, 30% Chol, 3% Dansyl-PE
$PC_{70}PE_{20}PS_{10}$	PCPEPS, 0% DHE	70% PC 20% PE 10% PS

3.6.4 Lipids in MβCD preparation

5 mM Lipids stored in chloroform were dried under argon gas and placed under vacuum for one hour. The lipid film was hydrated in 25mM MβCD, 20 mM PIPES, 137 mM NaCl, 3 mM KCl, pH 6.8 to obtain a lipid/MβCD ratio of 1:5. This suspension was vortexed for 10 minutes, sonicated for at least 10 minutes and rotated at 37°C overnight. The suspension was then sonicated for another 10 minutes before centrifuging for 10 minutes at 13,000 rpm to remove undissolved lipid. The lipid in MβCD was stored at 4°C under argon in the dark.

3.6.5 Lipids in methanol preparation

5 mM lipids stores in chloroform were dried under argon gas and placed under vacuum for one hour. The lipid film was then re-solubilised in methanol and stored at 4°C under argon in the dark.

3.6.6 Fluorescence assays

3.6.6.1 *DHE binding with MβCD*

A typical reaction used 1 μM of purified LAM StARkin domains incubated for 5 minutes with ~25 μM DHE complexed to MβCD in 1 ml. An emission scan from 320 nm to 420 nm was measured using a PerkinElmer LS50B Fluorescence Spectrometer or Cary Eclipse Fluorescence Spectrometer (courtesy of Professor MF Cordeiro) using an excitation wavelength of 295 nm with 5 nm slit width. After measuring fluorescence, the ratio between the FRET peak and the tryptophan peak was established as the FRET response. The tryptophan peak of 335 nm is the emission of the protein only. The FRET peak of 375 nm is the emission of DHE after the absorption of the tryptophan emission when protein is mixed with DHE.

3.6.6.2 *DHE binding with Methanol*

A typical reaction used 18 μl of 200 μM purified LAM StARkin domains incubated for 5 minutes with 300 μM of lipids added in a volume of 2 μl in methanol. This mixture was then diluted into 2 ml, and an emission scan from 320 nm to 420 nm was measured using a Cary Eclipse Fluorescence Spectrometer using an excitation wavelength of 295 nm with 5 nm slit width. After measuring fluorescence, the ratio between the FRET peak and the tryptophan peak was established as the FRET response.

3.6.6.3 *DHE binding with Liposomes*

1.05 μM of purified LAM StARkin domain was incubated with varying concentrations of $PC_{40}PE_{20}PS_{10}DHE_{30}$ liposomes in 20 mM PIPES, 2.7 mM KCl, 137 mM NaCl pH 6.8 buffer. An emission scan was measured with a Cary Eclipse Fluorescence Spectrometer using an excitation wavelength of 295 nm with 5 nm slit width. After measuring fluorescence, the ratio between the FRET peak and the tryptophan peak was established as the FRET response.

3.6.6.4 *DHE transfer with Liposomes*

1 μM of purified LAM StARkin domain was incubated with 100 μM of donor or acceptor liposomes with varying composition, where both DHE and Dansyl-PE were present (starting either in *cis* or in *trans*). The excitation wavelength used was 340 nm and the emission wavelength used was 525 nm both with 5 nm slit widths. A time course reading was taken to measure the FRET response upon the addition of all reactants, *i.e.* both sets of liposomes and transfer protein. Additions were made with constant stirring, and measurements were made with a Cary Eclipse Fluorescence Spectrometer.

3.6.7 Liposome binding assays

All incubations included 8 µM of purified LAM StARkin domain and liposomes making a total lipid concentration of 400 µM, all Protein and liposomes were incubated for 15 minutes and centrifuged at 50, 000 rpm for 10 minutes using rotor S120AT2. The supernatant was removed carefully, and the remaining pellet of liposomes was resuspended in 20 µl of 20 mM PIPES, 2.7 mM KCl, 137 mM NaCl pH 6.8 buffer. The pellet was then analysed by SDS-PAGE.

3.7 Aspergillus fumigatus

Experiments using *Aspergillus fumigatus* (*Af*) cells were carried out at F2G Ltd. Singling out of colonies was conducted by Nicola Beckmann, and purified genomic DNA for KO fusion PCRs was provided by Jason Oliver.

3.7.1 *Aspergillus fumigatus* strains

The parental *Af* strain used in this study was the KU80Δ strain, deleted for *akuB*^{KU80} in a CEA17 background (da Silva Ferreira *et al.*, 2006). The delete strains generated for this study was *AfLamBΔ* and *AfLamAΔ* which are deleted for AFUB 005770 + 054660 under a hygromycin resistant gene respectively. PCR products for KO homologous recombination were made so that 1500 bp overlapped before and after the gene of interest (see section 5.2.8 and Figure 5.8) and transformed into protoplasts. All strains were maintained on Sabouraud Glucose (SAB) Agar (BD™).

3.7.2 Culture of spores

Unless otherwise stated, an autoclaved cotton swab was dipped into a stock spore solution of *Af* and spread over 5 ml of SAB agar in a 25 ml tissue culture flask. The *Af* was incubated at 35°C for 2-3 days until a layer of spores was observed.

3.7.3 Stock spore solution

Approximately 5 ml of PBS 0.01% PBS was pipetted into the flask, and the lid was closed tightly. The flask was shaken vigorously until the liquid became a green colour from the dislodged spores. The spore solution was then filtered through glass wool in a syringe. A yield of 10^7 to 10^8 spores was obtained depending on the growth of the strain. The spore solution was stored at 4°C or frozen with glycerol at -80°C. Spore concentration was calculated using a 485 nm absorbance reading.

3.7.4 Genomic DNA extraction

Genomic DNA was extracted from *Af* cultures using the FastDNA SPIN Kit (Qbiogene) according to the manufacturer's manual. 3 to 6 ml of 10^6 *Af* spores per ml was incubated for 24 hours in SAB media shaking at 200 rpm at 37°C. The pellet was

harvested and dried for 60 seconds on sterile filter paper. Approximately 25-50 mg of dry weight was obtained. 1 ml of CLS-Y cell lysis solution was added to the cells in a Lysing Matrix A tube containing one ceramic sphere. The FastPrep® Instrument was used to homogenise the sample for two rounds of 30 seconds at a speed setting of 6.0. The debris was pelleted by centrifugation for 10 minutes. An equal volume of the supernatant and binding matrix was added to a 2 ml tube and rotated for 5 minutes. The binding matrix was quickly pelleted and resuspended in 500 µl of SEWS-M before transferred to a spin column. The column was centrifuged for 1 minute to remove the solution and spun again to dry the binding matrix. The DNA was eluted with 100 µl of DES at 55°C for 5 minutes and was spun down into a 1.5 ml tube. To remove any debris, the eluted DNA was centrifuged for 2 minutes, and the supernatant was transferred to a fresh, clean tube. The DNA was stored at -20°C.

3.7.5 Protoplast preparation

50 ml of 10^6 spores ml^{-1} SAB broth was incubated overnight at 37°C in 5 x 90 mm Petri dishes overnight at 37°C. The Aspergillus biomass was collected in a sterile J cloth lined funnel, washed with H_2O and dried on sterile tissue paper. Approximately 1 g of biomass was added to 20 ml of filter sterilised 5% glucanex 0.6 M KCl 50 mM $CaCl_2$ and incubated at 30°C shaking at 100 rpm for approximately 1 hr until protoplasts have formed. The protoplasts were filtered through 4 layers of sterile lens tissue and topped up to 45 ml with cold 0.6 M KCl 50 mM $CaCl_2$ before being pelleted at 1800 rpm at 4°C for 9 mins and resuspended in 1 ml 0.6 M KCl 50 mM $CaCl_2$. The protoplasts were topped up to 25 ml with cold 0.6 M KCl 50mM $CaCl_2$ and slowly 25 ml of cold 10 mM Tris-HCl pH 7.5 50mM $CaCl_2$ 1.2 sorbitol was added. The protoplast solution was pelleted at 1900 rpm at 4°C for 10 mins and resuspended in 200 µl of 10 mM Tris-HCl pH 7.5 50mM $CaCl_2$ 1.2 M sorbitol.

3.7.6 Protoplast transformation

Approximately 100 µl of protoplasts in 10 mM Tris-HCl pH 7.5 50mM $CaCl_2$ 1.2 M sorbitol was added to ~2 µg of transforming DNA in a maximum volume of 20 µl H_20. 200 µl of 60% PEG 6000 10 mM Tris-HCl pH 7.5 50mM $CaCl_2$ 1.2 M sorbitol was added to the protoplasts and transforming DNA and incubated for 5 mins. The protoplast solution was vortexed and plate onto SAB 1.2 M sorbitol with an appropriate antibiotic such as hygromycin.

3.7.7 MIC

The EUCAST standard method for MIC readings was used. RPMI-1640 was used containing 2% Dextrose pH 7 MOPS. A 96 well flat bottom plate was used to

inoculate 100 µl of RPMI-1640 medium with 10^4 spores with an appropriate dilution of drugs over 48 hours at 35°C. The MIC value was taken as the first well concentration where no Aspergillus growth was observed.

3.7.8 Dot assay

10^4 spores in 5 µl were dotted onto a plate of appropriate agar media and incubated at 37°C for 48 hrs. Minimal media was made using ingredients in Table 3-6 by autoclaving glucose and agar before adding filter sterilised Vogel's salts stock solution that contained ingredients in grey and a stock solution of trace ingredients in pink. Complete media was made as 2% glucose, 2% malt extract, 0.1% peptone and 1.5% agar. Images were made after 24 hours and 48 hours. Nicola Beckmann carried out image acquisition.

Table 3-6 List of ingredients for minimal media

Ingredient	Final concentration
Glucose	2%
Agar	1.5%
Sodium citrate	8.5mM
KH_2PO_4	28.7 mM
NH_4NO_3	25 mM
$MgSO_4$	0.8 mM
$CaCl_2$	0.7 mM
Biotin	20 mM
Citric Acid	24 µM
$ZnSO_4$	17.3 µM
$Fe(NH_4)_2(SO_4)_2$	25 µM
$CuSO_4$	10 µM
$MnSO_4$	3 µM
H_3BO_3	8 µM
Na_2MoO_4	3 µM

3.8 Bioinformatics

3.8.1 HHpred

HHpred hidden Markov model sequence homology search was used at toolkit.teubingen.mpg.de. Typical parameters used were: database of Protein Databank (PDB) structures (version pdb70_28Dec16), HHblits, 8 iterations, score with secondary structure, local alignment mode with maximum accuracy (MAC) algorithm.

3.8.2 Predicted Models

For example, Lam4StARkin2 sequence (967-1139) was submitted to HHpred against the PDB database (version pdb70_28Dec16). Parameters used were: HHblits, 8

iterations, score with secondary structure, local alignment mode with MAC algorithm. Modeller was used to create a 3D model based on the top two hits with known ligands and functions, which were human StARD3 and StARD5. The 3D model of the protein was visualised in UCSF Chimera (Pettersen *et al.*, 2004).

3.8.3 LAM StARkin alignment

LAM polybasic regions were submitted to MSAProbs alignment program using default settings accessed via toolkit.teubingen.mpg.de.

3.8.4 Sequence culling

Sequences were culled using PISCES using BLASTDB compiled on 9th January 2017. Bulk sequence renaming in FASTA format was carried out using a program written by Thomas McLean.

3.8.5 CLuster ANalysis of Sequences

Sequences of domains were downloaded from Pfam at pfam.xfam.org, and those with over 150 sequences were culled. Culling rounds were used at 75%, 50%, 40%, 30% and 20% sequence similarity until close to 100 sequences were reached. The CLANS software was used from toolkit.tuebingen.mpg.de/clans using PSI-BLAST using BLOSUM-62, 8 iterations with the filter on for low complexity regions.

3.8.6 Transmembrane helix prediction

Sequences were submitted to the TMHMM, a membrane topology prediction software accessed at cbs.dtu.dk/services/TMHMM. Server v2.0 was used for all predictions of transmembrane helices.

3.8.7 Cleavage site prediction

Sequences were submitted to the SignalIP 4.1 server, a signal peptide cleavage site prediction software accessed at cbs.dtu.dk/services/SignalIP-4.1. Default settings were used with the exception of truncation of sequence for which it was designated 0.

Results

CHAPTER 4

Analysis of the Yeast LAM family

4.1 Introduction

The budding yeast, *Saccharomyces cerevisiae* (*Sc*), is a useful model organism for studying lipid transfer. As it is a eukaryote, yeast has multiple membrane-bound organelles meaning that it is an ideal model to study contact sites. In addition, it is relatively easy to distinguish cellular compartments under a confocal microscope. Another key advantage is the ease of genetic manipulation. Yeast share the same basic mechanism for sterol synthesis as humans. Thus intracellular traffic of sterol is conserved to some degree throughout eukaryotes. In this chapter, I will investigate the effect of removing the LAM (Lipid transfer protein Anchored at Membrane contact sites) protein family in yeast and characterise the cellular localisation and sterol-related function of individual LAM proteins.

4.1.1 Saccharomyces cerevisiae LAM proteins

The *Sc*LAM protein family consists of three paralogous pairs of proteins: Lam1p/3p, Lam2p/4p and Lam5p/6p. This pairing is due to a whole genome duplication, which created two paralogs for each distinct LAM protein type. Each pair shares a higher sequence similarity than with the other LAM proteins. Our group identified this eukaryotic wide family of proteins using a powerful bioinformatics program seeded by a mammalian StART domain (Gatta *et al.*, 2015). This led to the discovery of LAM proteins in yeast, an organism that was not identified to possess a StART-like lipid transfer domain prior to this study. The other domains contained within this family include BAR, PH and transmembrane helices, all of which are membrane-associating modules (see section 1.5.8 for more detailed information on LAMs). Together these suggest that this protein is highly likely to localise, either stably or transiently, to membrane contact sites. The StART domain is a proven lipid transfer domain (see section 1.5.4 for information on StART proteins), and thus the evidence points to LAM proteins being involved in lipid transfer at contact sites.

One piece of evidence pointing to involvement of this novel family in sterol transfer specifically is the growth sensitivity of delete strains on ergosterol affecting drugs. One such drug is Amphotericin B (AmB), a molecule that can disrupt normal ergosterol homoeostasis by sequestering ergosterol from yeast membranes, thus can reveal sterol-affecting genes in mutants that show sensitivity or resistance. Hillenmeyer *et al.* carried out 1144 chemical assays on the whole delete collection of yeast including many hundreds of small molecules (Hillenmeyer *et al.*, 2008). The growth assays for AmB showed that Δ*lam1*, Δ*lam2* and Δ*lam3* were in the top 25 hits of approximately 5000 homozygous delete strains, with Δ*lam2* being slightly less sensitive than Δ*lam1*/Δ*lam3* [Table 4-1]. The positions of Δ*lam5* and Δ*lam6* were within the first third of the delete strains with Δ*lam4* showing no significant effect on growth.

Table 4-1 Table detailing LAMs and their growth defect on Amphotericin B

Names	Other names	ORF	Position /4742	Fitness defect	p-value
LAM1	YSP1	YHR155W	13	10.007	1.04e-10
LAM2	YSP2, LTC4	YDR326C	21	7.83416	1.31e-08
LAM3	SIP3	YNL257C	4	13.4704	< 1e-12
LAM4	LTC3	YHR080C	2605	0	0
LAM5	LTC2	YFL042C/ 43C	1820	0.619275	0.27056
LAM6	LTC1	YLR072W	1479	0.946849	0.17622

4.1.2 Amphotericin B

AmB is an antifungal drug and is used as a last resort for invasive fungal infections [Figure 4.1A]. It is extremely toxic to fungi and resistance against AmB is rare compared to other antimicrobial molecules. Although AmB is effective, it is only used when there is no alternative due to its severe side effects on patients. AmB belongs to the polyene macrolide class of drugs and was found in 1955 as a metabolite of *Streptomyces nodosus* (Oura, Sternberg and Wright, 1955).

During recent decades, there has been a rise in life-threatening fungal-caused disease. It is estimated that 1.5 million sufferers die every year due to invasive fungal infections, a comparable number to tuberculosis caused deaths (Brown *et al.*, 2012). This increased prevalence of fungal diseases is linked to an increased number of immunocompromised patients, such as those with HIV/AIDS, transplanted organs and chemotherapy, and subsequently, drug resistant fungal strains have arisen. Yet after more than half a century of widespread use, the acquisition of resistance to AmB remains rare (Vincent *et al.*, 2013).

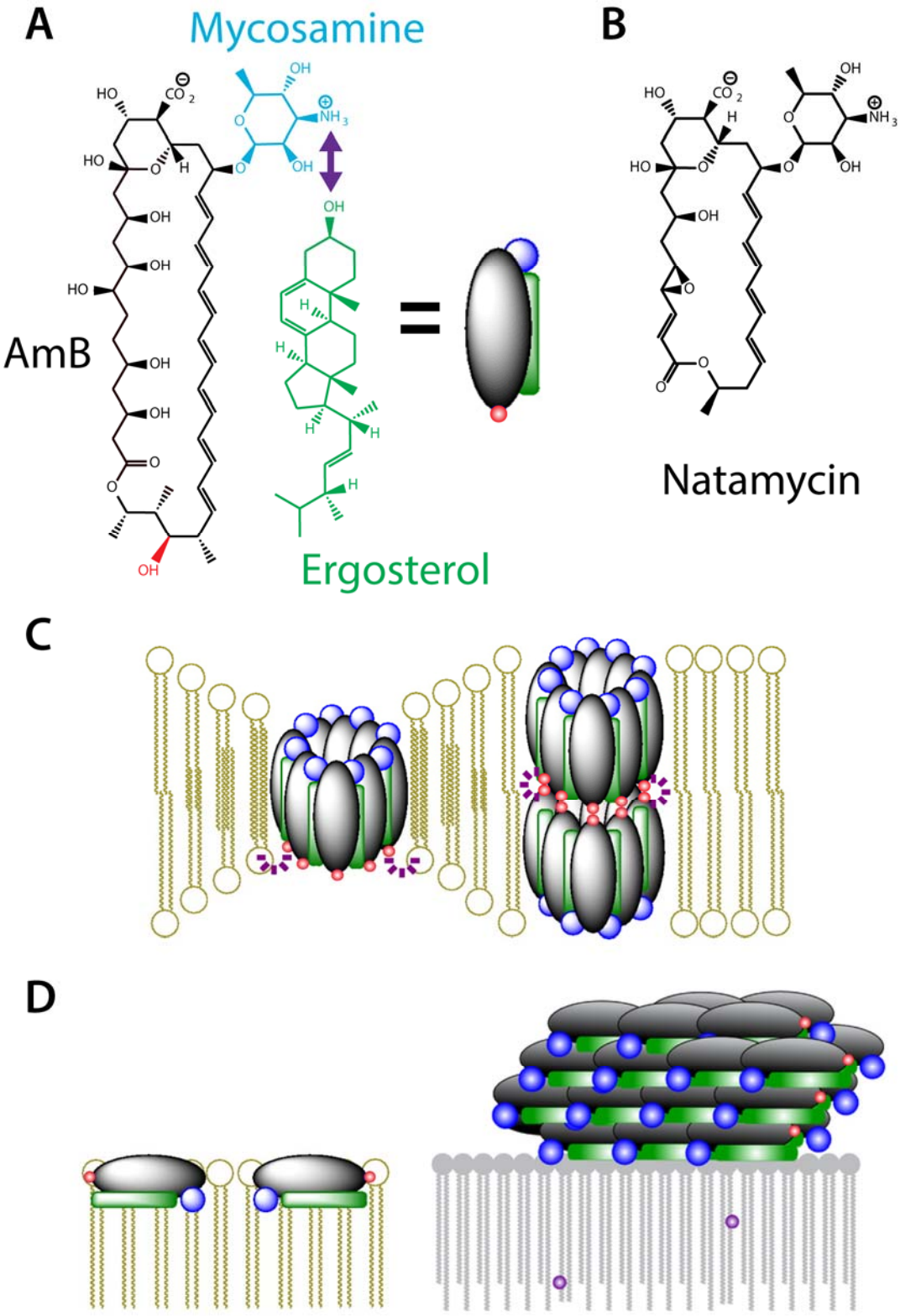

Figure 4.1 **Chemical structure of polyenes and AmB modes of action**
A) Chemical structure of Amphotericin B (AmB) molecule interacting with ergosterol via the mycosamine group. The heptaene structure is also hypothesised to interact with the ergosterol sterene structure. **B**) Structure of Natamycin, a smaller polyene compared to AmB. **C**) Model of pore formation by AmB polymerisation in the bilayer. The length of the AmB requires a double ring to span the thickness of an average membrane. **D**) Model of sterol sequestering by AmB as monomeric and newly proposed sponge model. Red shows the OH group responsible for channel formation, blue shows the mycosamine group thought to be essential for sterol interaction and green shows the sterol molecule. Adapted from (Gray *et al.*, 2012) and (Anderson *et al.*, 2014).

The molecular mechanism of the antifungal action of AmB is still unclear with several different molecular mechanisms proposed thus far. However, it may be that AmB has more than one mode of action against fungi. There are three major models, all of which involve interactions with ergosterol in the PM: formation of channels, aggregation of AmB-sterol complexes and mass absorption of ergosterol from the cell membrane into extracellular sponges [Figure 4.1C+D]. These models all rely on the proposed Van der Waal interactions between the conjugated double bonds of the polyene molecules and the indole rings of the ergosterol molecules (Bagiński, Tempczyk and Borowski, 1989). The mycosamine group on the AmB molecule is suggested to interact with the hydroxyl group of the ergosterol, bringing other areas of the molecules into close enough proximity for Van der Waal's forces to have an effect [Figure 4.1A] (Umegawa *et al.*, 2012). As mammalian and yeast sterols are very similar in structure AmB can also bind cholesterol, though at a lower affinity, which is how AmB acts selectively toward fungi (Baginski, Czub and Sternal, 2006).

Amongst the models for AmB molecular mechanism, the most popular is channel formation in the PM bilayer although there is now strong evidence that ergosterol sequestering is also a key activity. Through their affinity to ergosterol in the PM, AmB molecules are thought to invade the lipid bilayer, polymerising to form a channel through the PM thus permeabilising the cell causing cell death [Figure 4.1C] (Baginski, Resat and Borowski, 2002; Mouri *et al.*, 2008; Umegawa *et al.*, 2012). The pore must consist of two rings of AmB molecules stacked on top of each other to be the correct length to span the bilayer membrane.

However, it has been published that cell death still occurs after removal of the polymerising side chain, therefore suggesting that the pore-forming ability of AmB is not needed for its toxicity (Palacios, Anderson and Burke, 2007; Palacios *et al.*, 2011; Gray *et al.*, 2012). Instead, the sterol binding ability of AmB is essential for its effectiveness as an antifungal. In these studies, AmB was physically altered by removing functional groups and thus was not in its native state. Even without the polymerising side chain, the synthesised AmB analogue was found to be an effective antifungal with no decrease in toxicity, suggesting the lethal effects do not require membrane permeabilisation. An example of a polyene without a channel forming ability is Natamycin (see section 4.1.3 below), another widely used antifungal but one that cannot structurally form pores like AmB. Indeed further investigation found that the essential characteristic of the toxicity of AmB to yeast lies in the ability to bind and

sequester ergosterol (Gray *et al.*, 2012). It is unclear whether these aggregates form within the membranes as is proposed with Natamycin.

A relatively recent model builds on the association of AmB with ergosterol. A subsequent publication by the same group showed that AmB forms a large aggregate termed a 'sponge' on the exterior of the membrane which sequesters the ergosterol from the lipid bilayer (Anderson *et al.*, 2014). Whilst this original theory is proven to occur *in vitro* using liposomes, it is yet to be shown *in vivo*; yeast have thick hydrophilic cell walls that would physically hamper large aggregates of sterol-AmB formation (Kamiński, 2014).

Regardless of the mode of action, what is established is that AmB interacts with ergosterol and resistance to AmB can be acquired through mutants in ergosterol affecting genes such as *ERG2*, an enzyme in the ergosterol biosynthetic pathway (Vincent *et al.*, 2013). It is proposed that due to the defect in ergosterol synthesis, there are reduced ergosterol levels at the PM, instead there is increased levels of structurally different sterol and thus there is a reduced effect of AmB (Munn *et al.*, 1999).

4.1.3 Natamycin

Like Amphotericin B, Natamycin is a polyene antifungal molecule but is made by *Streptomyces natalensi* rather than *Streptomyces nodosus*. The main difference between Natamycin and AmB is the length of the structure, Natamycin is much smaller, and it is unable to form pores in the membrane [Figure 4.1B]. Instead, it is suggested that it aggregates within the membrane through its interaction with sterols, leading to disruption of the membrane without forming pores. This would be similar to Filipin, another small polyene (te Welscher *et al.*, 2008). In addition, Natamycin has been shown to interfere with ergosterol dependent cellular processes including the inhibition of a range of essential PM transport proteins, endocytosis and vacuolar fusion (Van Leeuwen, Golovina and Dijksterhuis, 2009; Te Welscher *et al.*, 2010; te Welscher *et al.*, 2012).

In the study by te Welscher *et al.*, other polyenes were also tested for their effects on vacuolar fusion: Nystatin, which is thought to form channels through the PM similarly to AmB (Marty and Finkelstein, 1975), and Filipin, an even smaller polyene than Natamycin. Both polyenes were shown to be more efficient in inhibiting vacuolar fusion than Natamycin (Te Welscher *et al.*, 2010). Both pore-forming and non-pore-forming polyenes were shown to negatively affect normal vacuolar processes in yeast suggesting that this mechanism might also be shared with AmB.

Natamycin was shown to have an impact on a broad range of membrane transport proteins with different characteristics and transport mechanisms (te Welscher *et al.*, 2012). The authors suggest that Natamycin affects these proteins by affecting the PM properties through its interaction with membrane ergosterol rather than each individual membrane protein. Indeed, there has been evidence that other members of the polyene class of antifungals, including AmB, alter normal cellular function and regulation of membrane transport proteins (Opekarová and Tanner, 1994; L. Zhang *et al.*, 2002; Agarwal *et al.*, 2003; Waheed *et al.*, 2008). Furthermore, the synthesised AmB molecule which was unable to form pores was found to be similar in toxicity to Natamycin (Gray *et al.*, 2012). These are yet additional pieces of evidence showing that the formation of channels through the cell membrane may not be the primary mode of action for AmB and that the general disruption of normal ergosterol function is likely an important requirement of toxicity.

4.1.4 Osh1-7p in yeast

Thus far, the most qualified protein family with the potential to function as bulk sterol transporters in yeast are the OSH proteins. The seven OSBP homologues in yeast together perform at least one essential function; the depletion of all seven yeast OSH proteins results in lethality (Beh *et al.*, 2001). The expression of any single OSH gene can rescue the sevenfold delete, demonstrating overlapping function. Therefore, to maintain a viable sevenfold delete strain, Beh *et al.* created a temperature sensitive copy of Osh4p in the six-fold delete of all other *OSH* members to rescue the lethality of the sevenfold delete (Beh and Rine, 2004). Intracellular sterol transport is reduced but not abolished in *Osh1-7*Δ cells, and there is an accumulation of sterols in this strain (Beh and Rine, 2004; Raychaudhuri *et al.*, 2006). Although the OSH family is thought of as a prime contender for the regulation of intracellular sterol traffic, not all OSH members are able to bind sterol. Osh6p/7p are do not bind sterol, instead, they bind PS (Schulz and Prinz, 2007; von Filseck, Vanni, *et al.*, 2015). Therefore direct sterol transfer cannot be the essential common function between all members of the OSH family

Whilst some OSH members are primarily cytoplasmic, Osh1p strongly targets the Golgi and NVJ, and Osh2p/3p are found at ER-PM contacts (Levine and Munro, 2001; Stefan *et al.*, 2011). Osh6p/7p are found diffuse in the cytoplasm although in one report they are suggested to also concentrate at the punctate structures near the PM where there is PM-associated ER (pmaER) (Wang, Duan, *et al.*, 2005; Schulz *et al.*, 2009). In spite of differences in their localisation, any one protein can compensate for the deletion of all seven. The exact shared essential function is yet undetermined,

though the above evidence suggests it is not direct sterol traffic. *In vitro* assays have revealed PI4P to be a common ligand and thus PI4P maintenance is proposed to be the shared function of OSH proteins (see section 1.5.2 for more detailed information on ORPs and their counter transport function).

4.1.5 Probing the function and localisation of LAM proteins

Using primarily AmB and also Natamycin, I will probe the function of the predicted LAM protein family. A high throughput study has already shown the sensitivity of the delete strain. Thus my investigation starts with corroborating this data and generating knockouts in another common laboratory strain of *Saccharomyces cerevisiae*. Although the StARkin domain was found in LAM proteins by a powerful bioinformatic tool, confirmation of the predicted domain is required, in addition to the predicted TM domain(s). Thus, I will label LAM proteins with GFP to probe their localisations and answer the question of where LAM proteins might reside, along with whether these areas may be membrane contact sites. The growth sensitivity to AmB will also be investigated to find whether the predicted StARkin domain may be specifically responsible for basal resistance to AmB.

4.2 Results

4.2.1 LAM StARkin Bioinformatics

There are six LAM proteins in budding yeast, paired as Lam1p/3p, Lam2p/4p and Lam5p/6p due to genome duplication and three members in the human genome [Figure 4.2]. All LAM members contain a transmembrane helix, a GRAM-like PH domain and at least one newly identified LAM StARkin domain. The majority of LAM StARkin domains are labelled by InterPro as DUF4782 (domain of unknown function 4782), a category label added during this study. However, it was identified by our lab with the use of bioinformatics; HHpred was employed with a mammalian StART protein seed, which targeted members of the LAM StARkin proteins. This tool predicts secondary structure and uses highly sensitive sequence alignments by hidden Markov models that also take into account the predicted structure to identify the structures of domains.

PSI-BLAST searches the sequence database by generating multiple sequence alignments to the seeds and identifying high scoring sequences to the seed alignment. Figure 4.3A shows the highest detected sequence homology of each LAM StARkin member to another using PSI-BLAST. The proportion of sequence that was found to be homologous was shown to be low even between paralogous pairs of protein within the same strain of budding yeast [Figure 4.2 + Figure 4.3]. Of the yeast LAM StARkin domains, the *Sc*Lam1p/3p is the most divergent by sequence compared to *Sc*Lam2p/4p and *Sc*Lam5p/6p. PSI-BLAST was not able to detect any sequence homology between Lam1/3p StARkin domain to any other LAM StARkin domain in three iterations [Figure 4.3A]. In contrast, HHpred searches with the same number of iterations found all members of the *Sc*LAM StARkin family with >99% probability of matched structure [Figure 4.3B].

The core members of the StARkin superfamily include the large family of Bet v1, AHA1 (C-terminal domain) and StAR-like proteins (see section 5.2.3). These proteins established the representative helix-grip fold consisting of β_1-α_1-α_2-β_2-β_3-β_4-β_5-β_6-β_7-α_3 that forms an antiparallel β-sheet wrapped around the face of a long α helix. This same secondary structure arrangement is predicted in the LAM StARkins with a similar helix-grip configuration [Figure 4.3C]. Even though no sequence homology was detected by PSI-BLAST between the Lam1/3p and the other members, HHpred was able to detect high structure homology and predicted 3D models shows the degree of similarity between the structured regions of the domains [Figure 4.3D superimposed 3D structure]. Lam3StARkin has additional insertions seen as unstructured loops where it

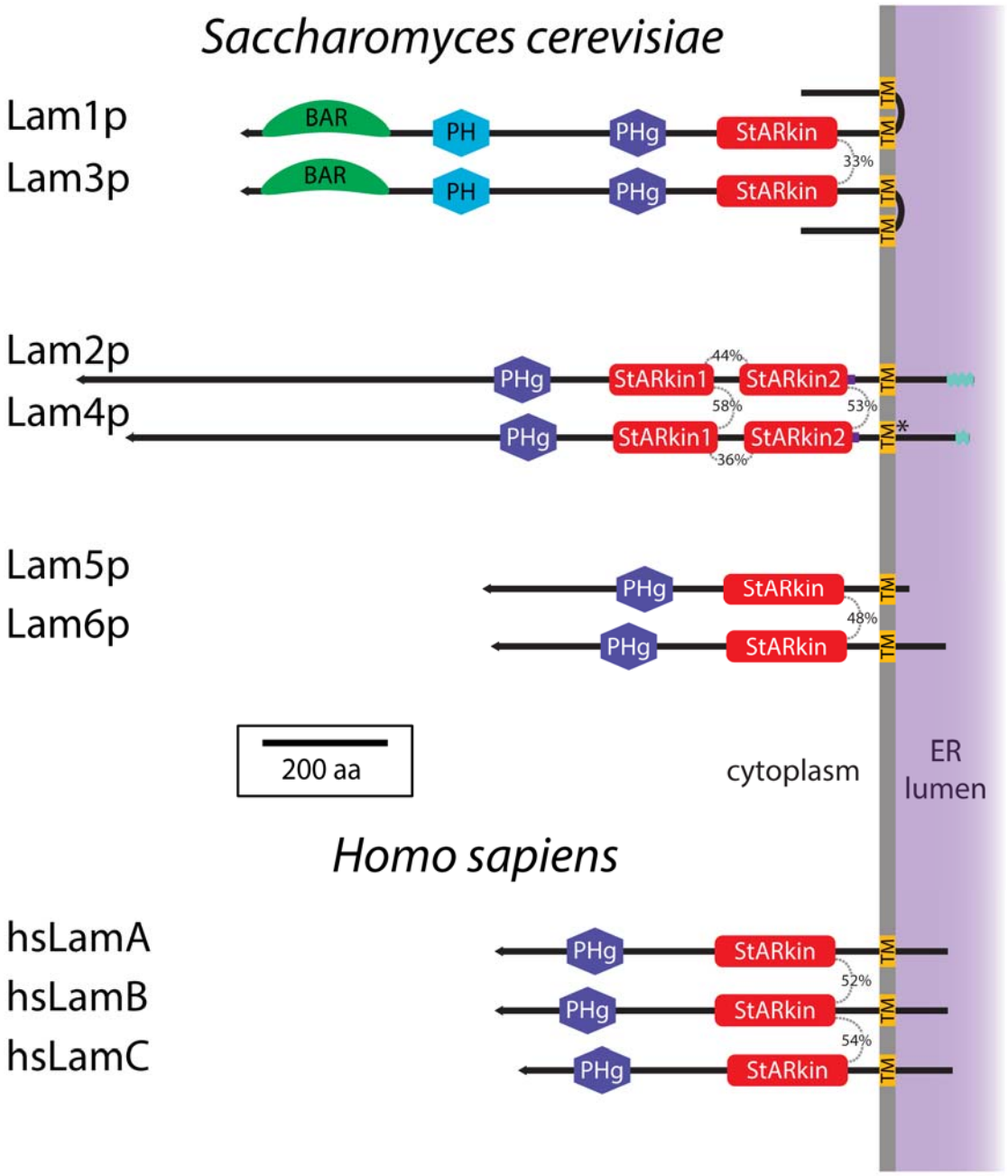

Figure 4.2 **LAM family in yeast and human**
Diagrams of the domain architecture of LAM protein members in *Saccharomyces cerevisiae* and *Homo sapiens*. The sequence similarity between StARkin domains are indicated in percentages. * indicates a transmembrane domain (TM) that is not strongly predicted. Significant predicted coiled coils are illustrated by a light blue irregular shape. The physical lengths of the diagrams are proportional to the sequence length where possible. The tapered end indicates the N-terminus.

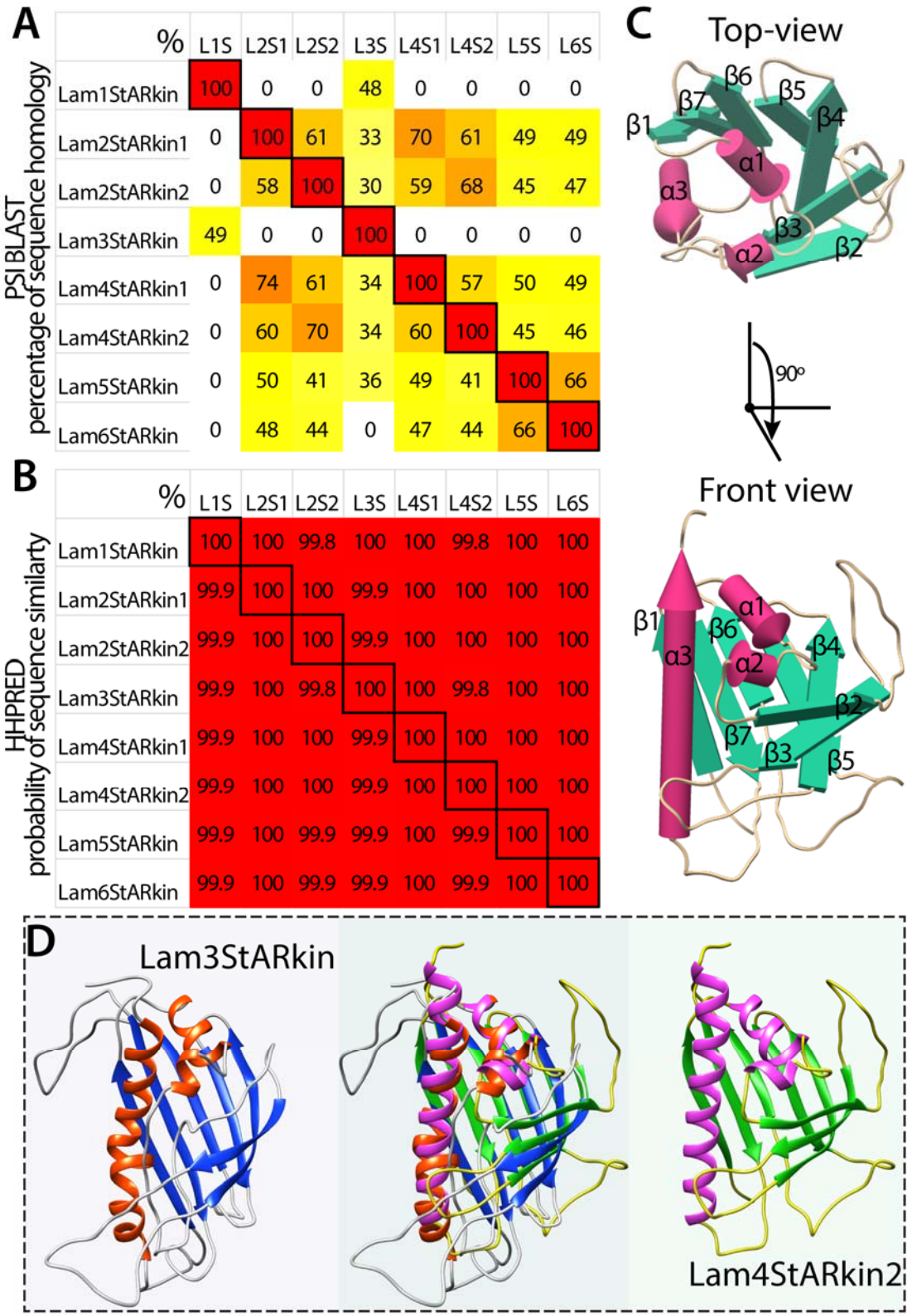

Figure 4.3 **Predicted StARkin domain of LAM proteins**
Probability of **A**) sequence similarity by PSI-BLAST and **B**) probability of a match by HHPred that uses addition secondary structure prediction to the first hit of each type of yeast LAM. The seed sequence is indicated for each row and the target is indicated in each column. The colour is designated as white<yellow<orange<red for 0%<1%<50%<100% respectively. 0% is used to signify that no hit. **C**) Predicted Lam4 StARkin 2 domain depicted as rods (pink) and planks (green) for α helices and β strands respectively. **D)** Comparison of predicted Lam3 StARkin domain (red and blue) on the left and Lam4 StARkin 2 domain (pink and green) on the right. A superimposed image of both structures is shown in the middle.

shows obvious differences to Lam4StARkin 2. The data provided by HHpred places Lam1/3p in the same family as Lam2/4/5/6p by the structure homology.

4.2.2 BY4741 delete strains show sensitivity on AmB

Delete strains of the LAM proteins from the widely available homozygous diploid yeast delete collection show sensitivity on Amphotericin B as reported by the high throughput data compiled by Hillenmeyer (Hillenmeyer *et al.*, 2008). This finding was reproduced [Figure 4.4A+B] with the haploid delete strains BY4741 (mating type A), produced with the same technique as the diploid deletes. 1:20 serial dilutions in 100 µl were made with freshly grown yeast so that there were approximately 4 $x10^6$ per 100 µl in the first dilution and 10^3 in the last. Approximately 1 µl of each dilution was spotted on agar plates to test the growth of yeast strains on AmB.

Δ*lam1* and Δ*lam3* strains displayed the greatest sensitivity to AmB, followed by Δ*lam2* [Figure 4.4A+B]. These three *LAM* delete strains were significantly more sensitive to Amphotericin than Δ*lam4*, Δ*lam5* and Δ*lam6.* There is a similar level of growth deficiency on AmB with Δ*lam1* and Δ*lam3,* a paralogous pair of LAMs, although Δ*lam3* shows slightly worse growth at the higher concentration of AmB. Δ*lam2* shows less vulnerability to AmB, but this is in stark contrast to the lack of any growth defect seen in Δ*lam4*, the strain deleted for the paralog of *LAM2*. In fact, it could be suggested that Δ*lam4* is slightly resistant to AmB as the plate with 810 $ngml^{-1}$ AmB, after only 24 hours, showed slightly more growth than WT [Figure 4.4B]. This suggests that although Lam2p and Lam4p are a paralogous pair of proteins arising from a genome duplication, their exact functions have diverged. One possibility is a different direction of sterol transfer, although we have no evidence for this. Looking closely at the growth of Δ*lam5* and Δ*lam6*, it is visible on the 24 hour plate that the growth of Δ*lam6* cannot be distinguished from WT growth [Figure 4.4B]. However, Δ*lam5* showed visibly more growth, similar to Δ*lam4*. Although Δ*lam4* is consistently slightly resistant (described Section 4.2.4 using the RS453C background), Δ*lam5* growth phenotype is inconclusive due to the slightly higher number of cells in the control plate (average of 19 colonies in the final dilutions compared to WT, Δ*lam4* and Δ*lam6* of 6, 8 and 7 colonies respectively) [Figure 4.4B].

4.2.3 Homologous recombination used to disrupt LAM protein family

In the experiments thus far, the widely available delete strains of the LAM family in the BY4741 background have been used to test the phenotype (Winzeler *et al.*, 1999; Giaever *et al.*, 2002). It has been noted that some commonly used lab strains

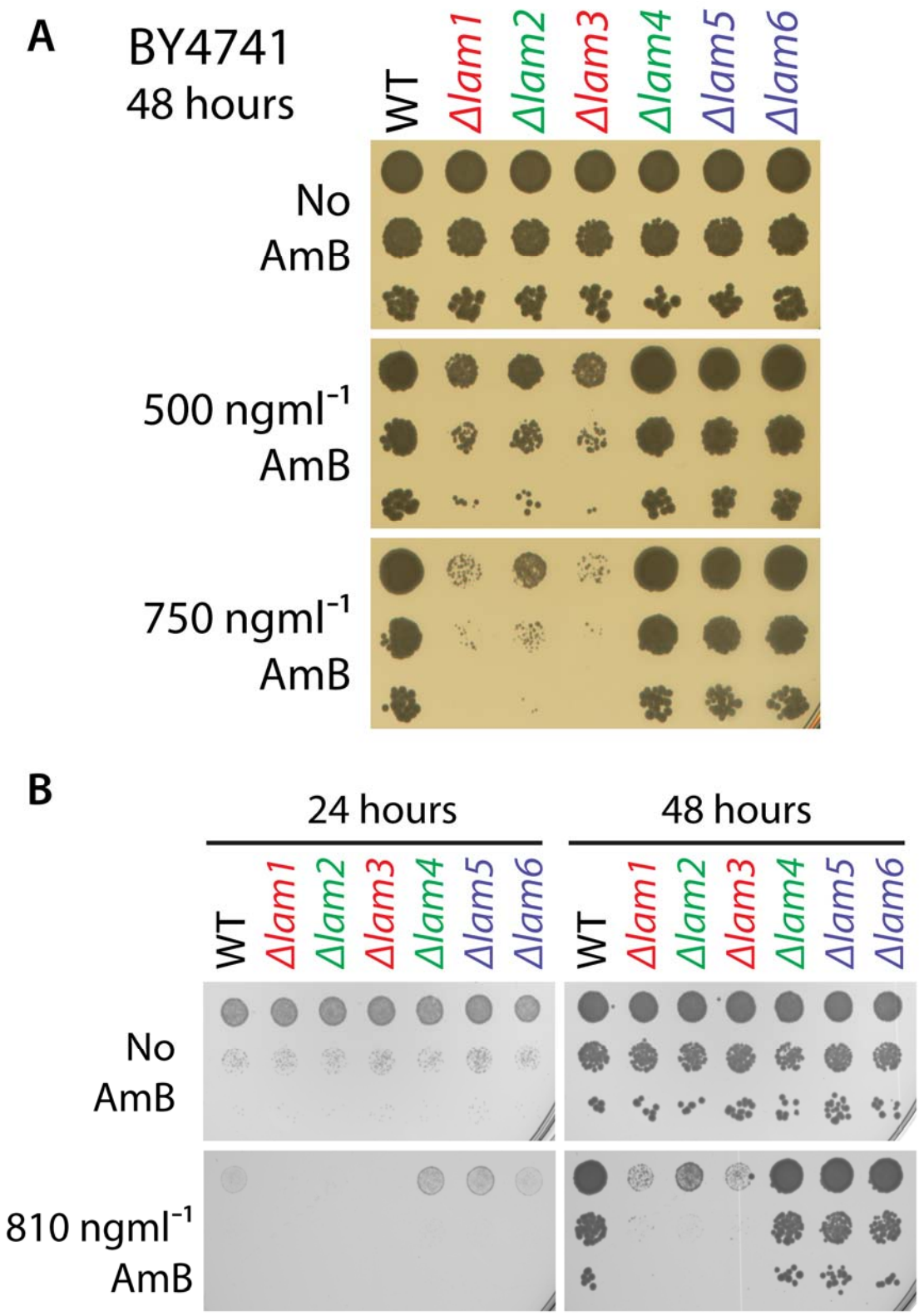

Figure 4.4 **LAMs are important for AmB resistance in BY4741**
Growth assay of BY4741 WT, Δ*lam1-6* on YPD agar with carrying concentration of AmB over **A**) 48 hours at 500-750 ngml^{-1} and **B**) 24 hours and 48 hours at 810 ngml^{-1}. YPD with no AmB was used as a control for cell dilution numbers across the different strains. Δ*lam3* is most sensitive, closely followed by Δ*lam1* and then Δ*lam2*. Knock out strains, Δ*lam4-6,* have a very similar AmB resistance to WT. Delete *LAM* strains are labelled in pairs by colour Δ*lam1* and Δ*lam3* are red, Δ*lam2* and Δ*lam4* are green, Δ*lam5* and Δ*lam6* in blue.

including BY4741 show atypical sensitivity to growth in certain conditions, in addition to potential issues with the high throughput knockouts such as the intact start codon of the deleted open reading frame (ORF) (Cohen and Engelberg, 2007). The systematic delete collection is extensively used in different labs, but to validate the phenotypes observed in the BY4741 delete *LAM1-6* yeast strains an unrelated WT strain was used to knock out the *LAM* genes.

A specific ORF (open reading frame) in the yeast genome can be selectively disrupted in various ways. The technique used here takes advantage of the yeast's own homologous recombination mechanism by using a PCR (polymerase chain reaction) amplified selection marker of amino acid prototrophy, flanked with 50 bp fragments at both ends of the ORF genomic DNA. Using this method, shown in Figure 4.5, each protein from the *LAM* family was knocked out in haploid yeast strain RS453C. The template DNA for the PCR was a plasmid containing the *HIS3MX6* cassette coding for imidazole glycerol phosphate dehydratase (*HIS5* from *Schizosaccharomyces pombe* plus a promoter and terminator, *Pteff* and *Tteff* respectively that are also heterologous to *Sc* (Steiner and Philippsen, 1994; Wach *et al.*, 1994, 1997; Erickson and Hannig, 1995)). *HIS3MX6* can substitute for the endogenous *HIS3* function in histidine biosynthesis, but will not find any part of the genome in which to unexpectedly homologously recombine and thus is ideal as a metabolic marker for yeast. The *HIS3MX6* cassette was amplified with oligonucleotides that extend it 50 bases 5' and 3' to recombine with the sequences immediately upstream and downstream of the target gene ORF, *LAM1-6*. Colonies generated from the transformation were genotyped by PCR. The first PCR genotyping detected the presence of the protein promoter leading to the inserted *HIS5* marker [Figure 4.5]. The second PCR identified the absence of the target gene by using primers within the *LAM*s; the control is WT to show the presence of a thick band where the gene is still present [Figure 4.6]. All knockouts were successful confirming that all six *LAM* genes are not essential genes.

4.2.4 RS453C KO strains show similar growth sensitivity on AmB as BY4741

After the verification of the KO (knockout) RS453C strains by PCR, the KO colonies were tested on AmB to characterise and compare their growth sensitivities [Figure 4.7]. As with the delete BY4741 strains, Δ*lam2*, Δ*lam1* and Δ*lam3* showed the greatest growth sensitivity on AmB. A key observation is the higher sensitivity of the RS453C knockout compared with the equivalent delete BY4741 strains. This shift in sensitivity is also found in the WT, which at 810 $ngml^{-1}$ AmB is more sensitive in the

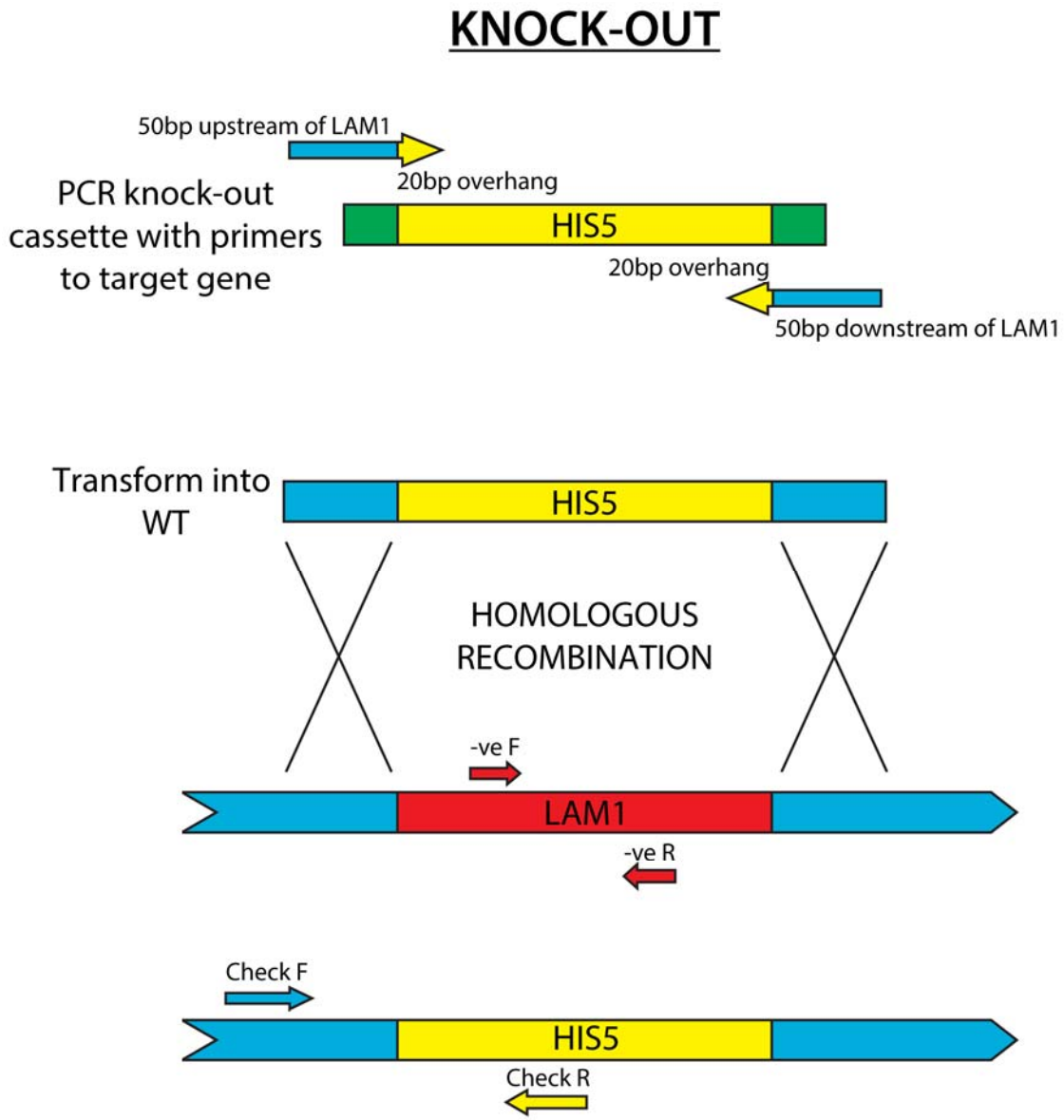

Figure 4.5 **Homologous gene replacement in yeast**
Technique to knock out genes in yeast. The homologous recombination mechanism of yeast is taken advantage to knock out *LAM1-6* using the *HIS5* metabolic marker in the *HIS3MX6* cassette. PCR products were generated with overhangs of ~50 bp up- and down-stream of each gene flanking the *HIS5*-containing cassette. After transformation of yeast, colonies appearing on a –His selection plate were isolated and genotyped. Two genotyping PCRs were carried out to determine successful knockouts. The first (check PCR) used a forward (F) primer in the promoter region of the gene and a reverse (R) primer in the *HIS5* marker to produce a product unique to successful knock out colonies. The second genotyping PCR (negative PCR) used F and R primers within the gene itself to confirm removal of the gene. Arrows shows the approximate positions of the primers used.

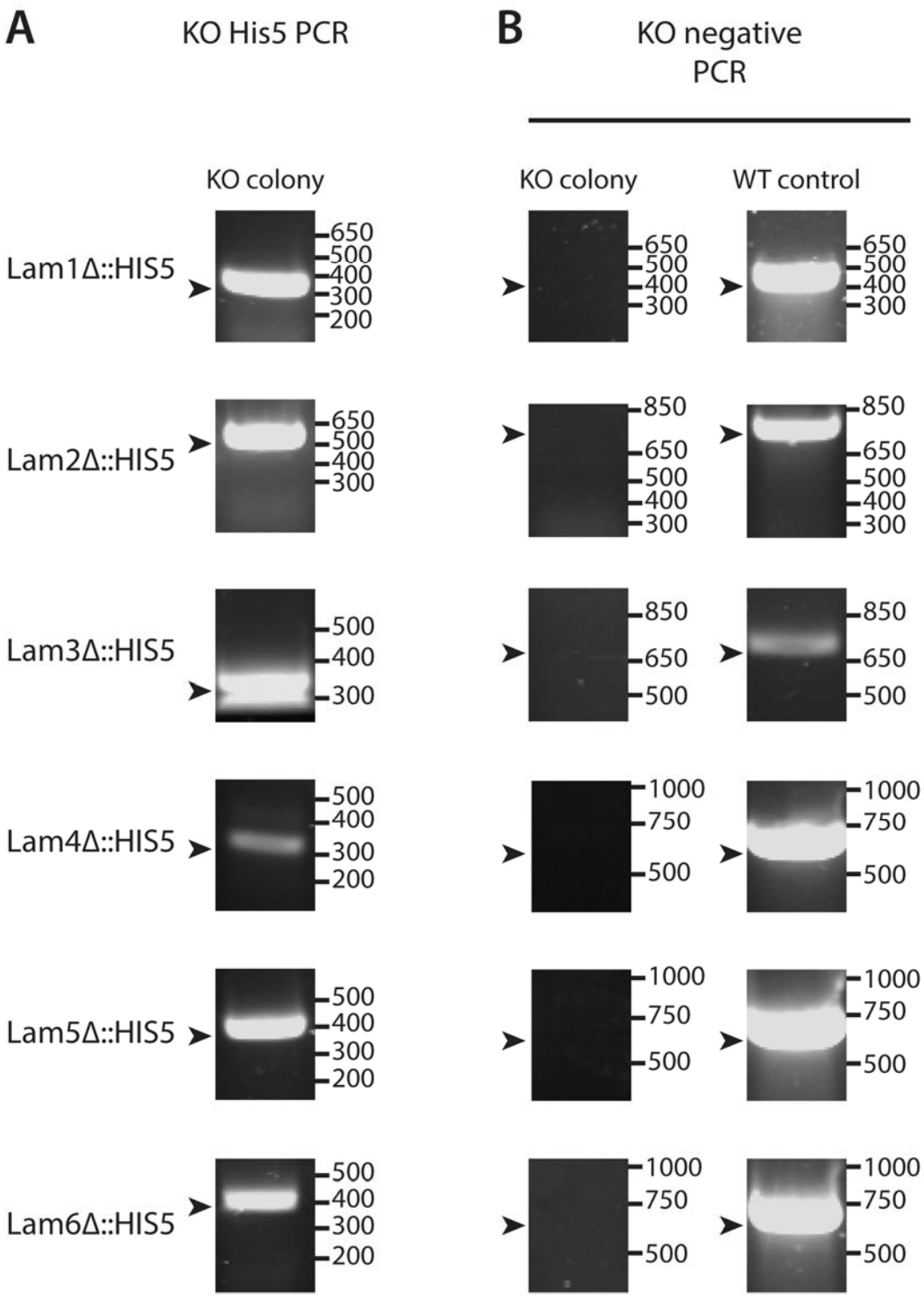

Figure 4.6 **PCR genotyping of Δ*lam1-6* in RS453C**
PCR genotyping of RS453C *LAM1-6* knock-outs run out on 1% agarose gels. **A**) PCRs confirming the presence of the *HIS5* marker were carried out using a primer in the promoter of each gene with a primer within the *HIS5* cassette. Note that the PCR product of Δ*lam3* was run to the end of the agarose gel and thus with imaging restrictions a double band was observed. **B**) PCRs confirming the absence of each gene were carried out using primers within each gene. WT was used as a control to show that the negative PCR primers are functional when the gene is present.

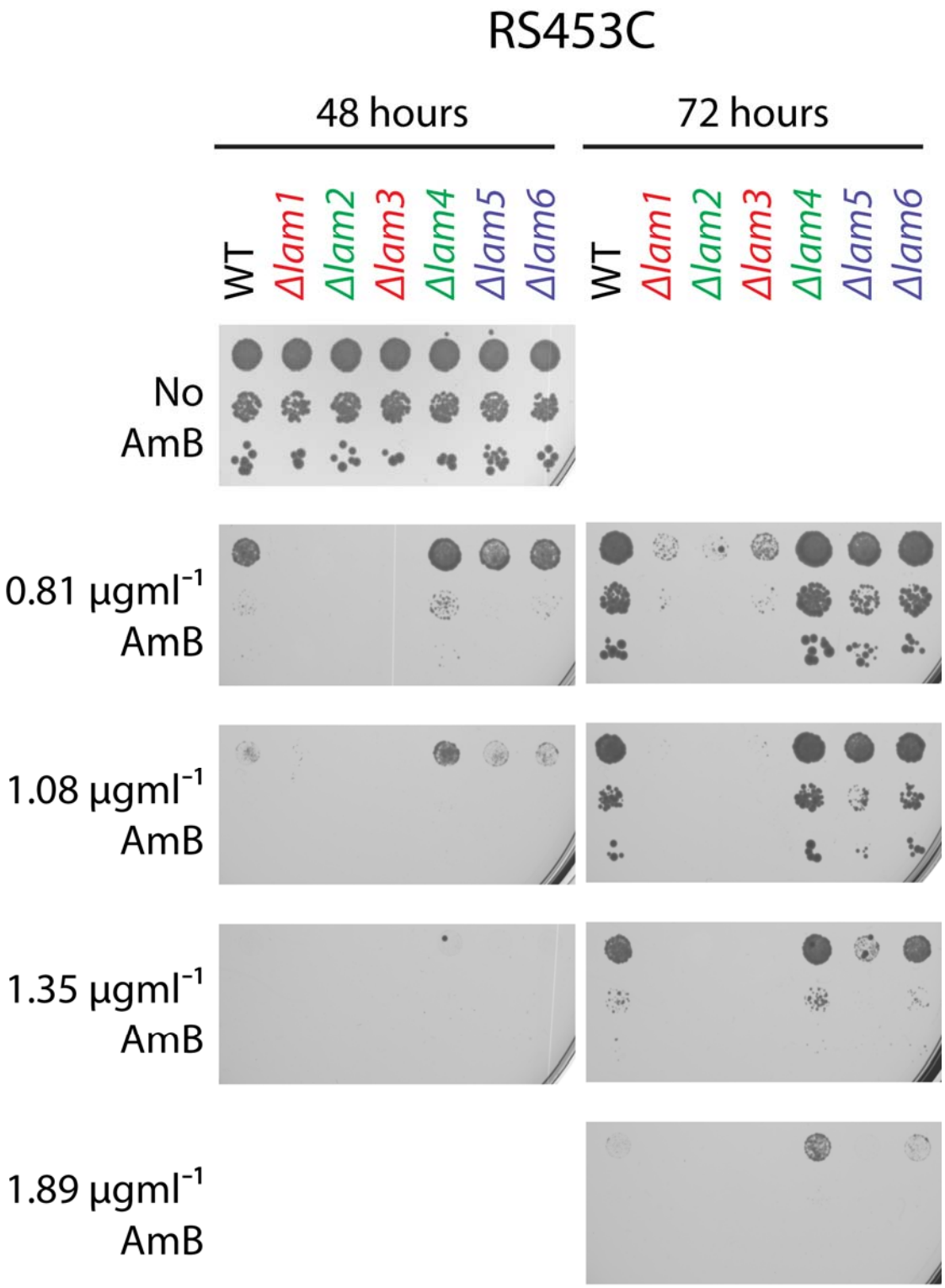

Figure 4.7 **LAMs are important for AmB resistance in RS453C**
Growth assay using RS453C WT and knock out strains for Δ*lam1-6* on YPD agar with varying concentration of AmB over 48 hours and 72 hours. YPD with no AmB was used as a control for cell dilution numbers across the different strains. The RS453C strains have a lower basal resistance to AmB compared to BY4741. With the higher sensitivity, the growth phenotypes of Δ*lam4-6* are revealed. Δ*lam5* is slightly more sensitive than WT, Δ*lam6* is indistinguishable to WT and Δ*lam4* is slightly more resistant than WT. Delete *LAM* strains are labelled in pairs by colour Δ*lam1* and Δ*lam3* are red, Δ*lam2* and Δ*lam4* are green, Δ*lam5* and Δ*lam6* in blue.

RS453C background than the BY4741 [Figure 4.4 + Figure 4.7]. This higher sensitivity to AmB reveals more clearly that Δ*lam5* is sensitive to AmB but to a lesser extent than Δ*lam2*, Δ*lam1* and Δ*lam3*. The growth of Δ*lam6* is not visibly different to that of WT. On the other hand, Δ*lam4* shows resistance to AmB compared to WT, much more clearly than Δ*lam4* in the BY4741 background.

4.2.5 *LAM* delete strains in RS453C show similar growth sensitivity on Natamycin as BY4741

Natamycin is a polyene similar to AmB but is thought not to form channels in the PM. Instead, the toxicity relies solely on its interaction with cellular ergosterol. Growth assays were carried out with BY4741, but high concentrations of Natamycin were required to see a growth phenotype [Figure 4.8]. However, it is easily observed that Δ*lam2* is most sensitive, followed by Δ*lam3*. Again, Δ*lam4* seems to be more resistant than WT.

The Natamycin growth assay was repeated with RS453C knockouts, and growth phenotypes were clearly observed indicating that the RS453C background not only has a lower basal resistance to AmB but additionally to the polyene family of molecules [Figure 4.9]. The greater sensitivity of RS453C knockouts compared to BY4741 allows observation of Natamycin growth sensitivity that would otherwise be harder to reveal with BY4741.

Again, as with BY4741, it is easily observed that the most sensitive strain to Natamycin is Δ*lam2* [Figure 4.9]. The Natamycin plates show that the next most sensitive delete strains were Δ*lam1* and Δ*lam3,* indicating that Lam1-3p are affecting the ergosterol pools which the polyene class of molecules are able to access, regardless of the differences between AmB and Natamycin.

Intriguingly, although the three most sensitive delete strains to Natamycin were the same as AmB (Δ*lam1-3)*, the order of sensitivity was reversed. Δ*lam2* was the most sensitive on Natamycin followed by Δ*lam1* and Δ*lam3*, whereas with AmB, Δ*lam1* and Δ*lam3* were most sensitive. This change of sensitivity order adds to evidence on the differences between the polyene molecules but also raises speculation on the differences in function between Lam2p and Lam1p/Lam3p.

Both drugs are accepted to bind with ergosterol. Therefore it is possible that the elimination of Lam2p, Lam1p and Lam3p affects the ergosterol supply that is available for the polyene molecules to interact. However, the presentation of differences in growth defects between AmB and Natamycin data suggests that there is a divergence of function between Lam1p/Lam3p and Lam2p. Possibilities for this include that they each

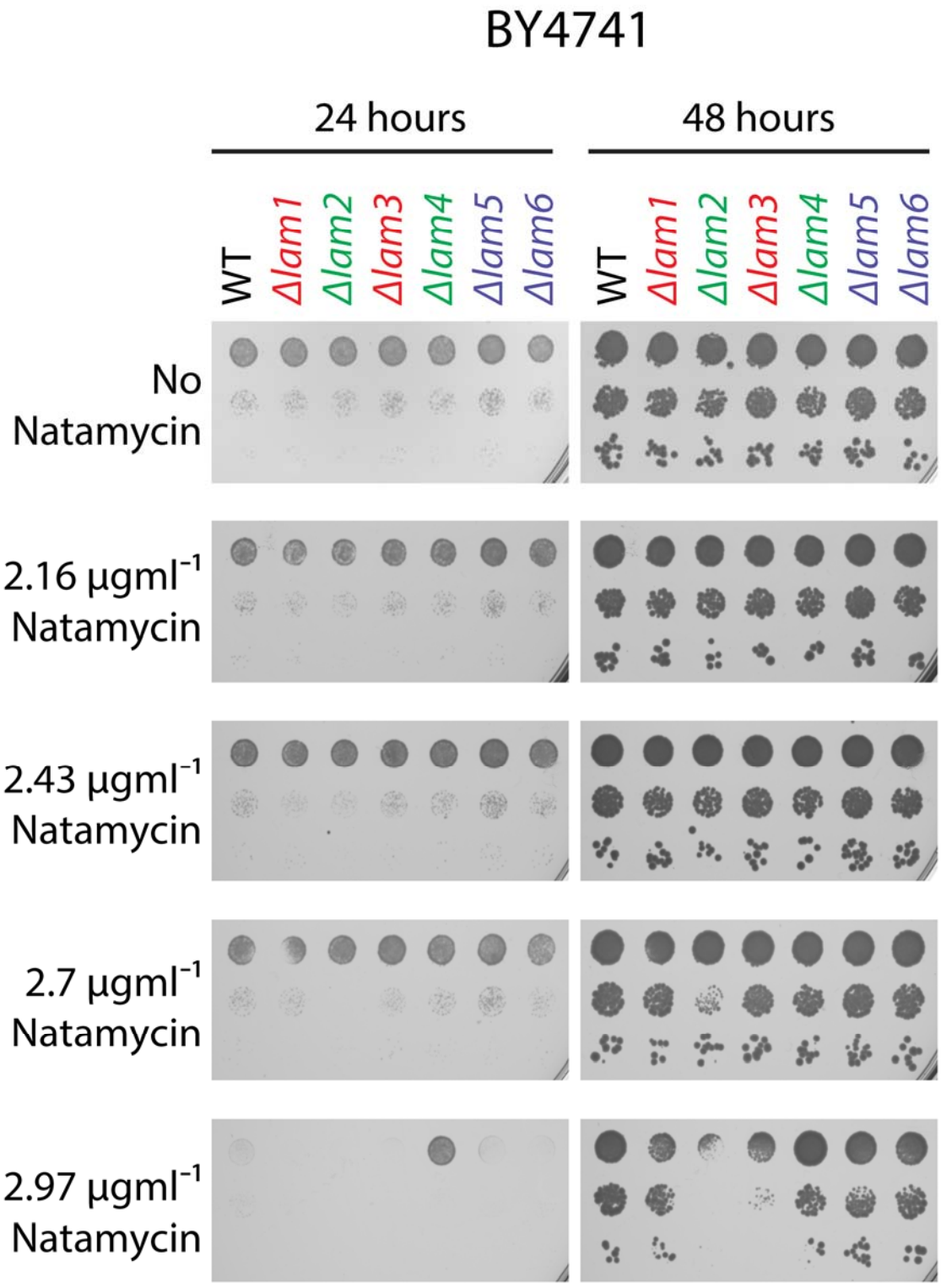

Figure 4.8 **LAMs are important for Natamycin basal resistance in BY4741** Growth assay using BY4741 WT and knock out strains for Δ*lam1-6* on YPD agar with varying concentration of Natamycin over 24 hours and 48 hours. YPD with no Natamycin was used as a control for cell dilution numbers across the different strains. BY4741 has a much higher basal resistance to Natamycin compared to RS453C. Δ*lam2* is most sensitive followed by Δ*lam3* and then Δ*lam1*. Δ*lam5* and Δ*lam6* have similar resistance to Natamycin as WT. Δ*lam4* is visibly more resistant. Delete *LAM* strains are labelled in pairs by colour Δ*lam1* and Δ*lam3* are red, Δ*lam2* and Δ*lam4* are green, Δ*lam5* and Δ*lam6* in blue.

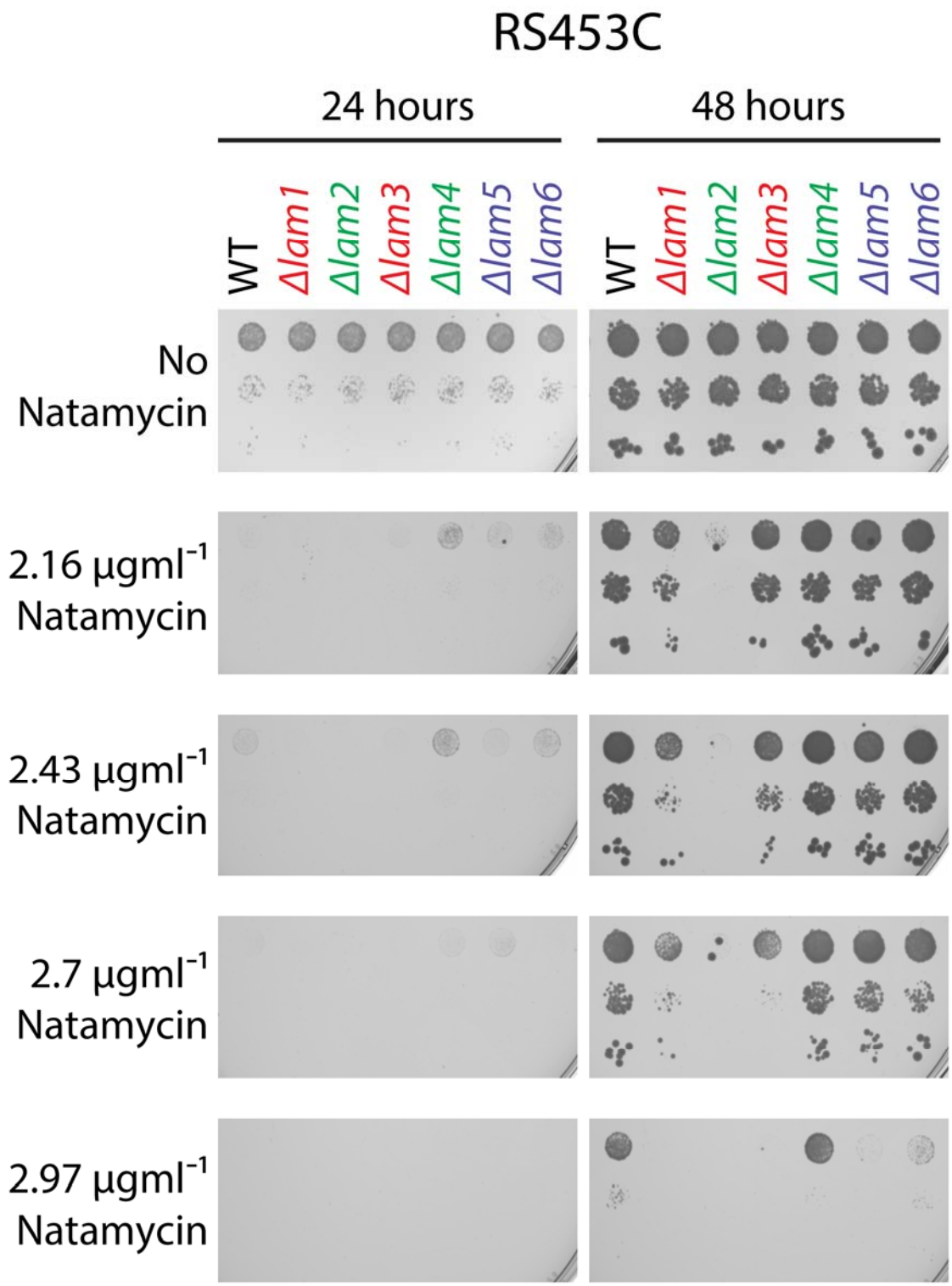

Figure 4.9 **LAMs are important for Natamycin basal resistance in RS453C** Growth assay using RS453C WT and knock out strains for Δ*lam1-6* on YPD agar with varying concentration of Natamycin over 48 hours and 72 hours. YPD with no Natamycin was used as a control for cell dilution numbers across the different strains. The RS453C strains have a lower basal resistance to Natamycin compared to BY4741. With the higher sensitivity, the growth phenotypes of Δ*lam1-6* are more distinct. Δ*lam2* is most sensitive followed by Δ*lam3* and then Δ*lam1*. Δ*lam5* is more sensitive than WT, followed by Δ*lam6* and Δ*lam4* is slightly more resistant than WT, although this is inconclusive. Delete *LAM* strains are labelled in pairs by colour Δ*lam1* and Δ*lam3* are red, Δ*lam2* and Δ*lam4* are green, Δ*lam5* and Δ*lam6* in blue.

affect different sterol pools, or that there are differences in the absolute function, for example, being direct transporters, indirect transporters or sensors.

The reversal of the sensitivity pattern of Δ*lam1/2/3* on AmB and Natamycin also indicates a difference in the mechanism of the drugs on ergosterol. If there were only a difference in ergosterol affinity, it would be likely that the sensitivity pattern of Δ*lam1/2/3* would be the same but the variation would only be the concentration of drug required for lethality would be different. For example, Natamycin could act on mainly on one pool and AmB on either another pool or even both pools. It is reported that four times more Natamycin is needed to see the same effect of AmB (Gray *et al.*, 2012), and indeed a higher concentration of Natamycin is required to reveal growth phenotypes in all strains including WT. One possible explanation is that AmB acts on an additional pool of ergosterol that Natamycin cannot access. It is also possible that without Lam1/3p, AmB can more easily create PM spanning pores.

4.2.6 Lam2p is localised to pmaER

To label Lam2p with GFP, a yeast expression plasmid was constructed to contain *GFP* prior to the *LAM2* gene so that the protein is tagged at the N-terminus [Figure 4.10A]. *LAM2* was expressed under its own endogenous promoter using a stretch of ~300 bases prior to the ORF. In these cells, GFP-Lam2p was found unevenly in punctate areas along the periphery of the cell indicating confined clusters of Lam2p where there are multiple GFP-tagged Lam2p [Figure 4.10B]. Reconstitution of GFP-Lam2p was easily observed in contrast to other LAM members (except the similarly expressed paralogous Lam4p), which were difficult to distinguish unless highly expressed, suggesting a higher endogenous level of Lam2p [data not shown].

The scattered fluorescence of Lam2p along the periphery of the cell was reminiscent of ER-PM contact structures, which occur sporadically around the edge of the cell where a piece of the ER is close to the PM. Further analysis of Lam2p localisation under a *PHO5* promoter, which allows high expression of a protein (carried out by Alberto Gatta), confirmed Lam2p localisation to the pmaER (Gatta *et al.*, 2015). The Δ*tether* strain is deleted for six known tether proteins between the ER and the PM, causing a reduction of 90% of pmaER (see section 4.2.12). Using the Δ*tether* strain, the number of punctate Lam2p also decreased, but more importantly, the remaining Lam2p was only observed at the rare occurrences of RFP-tagged pmaER (microscopy by Alberto Gatta) (Gatta *et al.*, 2015). In addition, the localisation of Lam2p was unaffected in a *SEC18* mutant that has a defective secretory pathway (Gatta *et al.*, 2015). The endurance of localised Lam2p indicates that there is a population of ER-PM

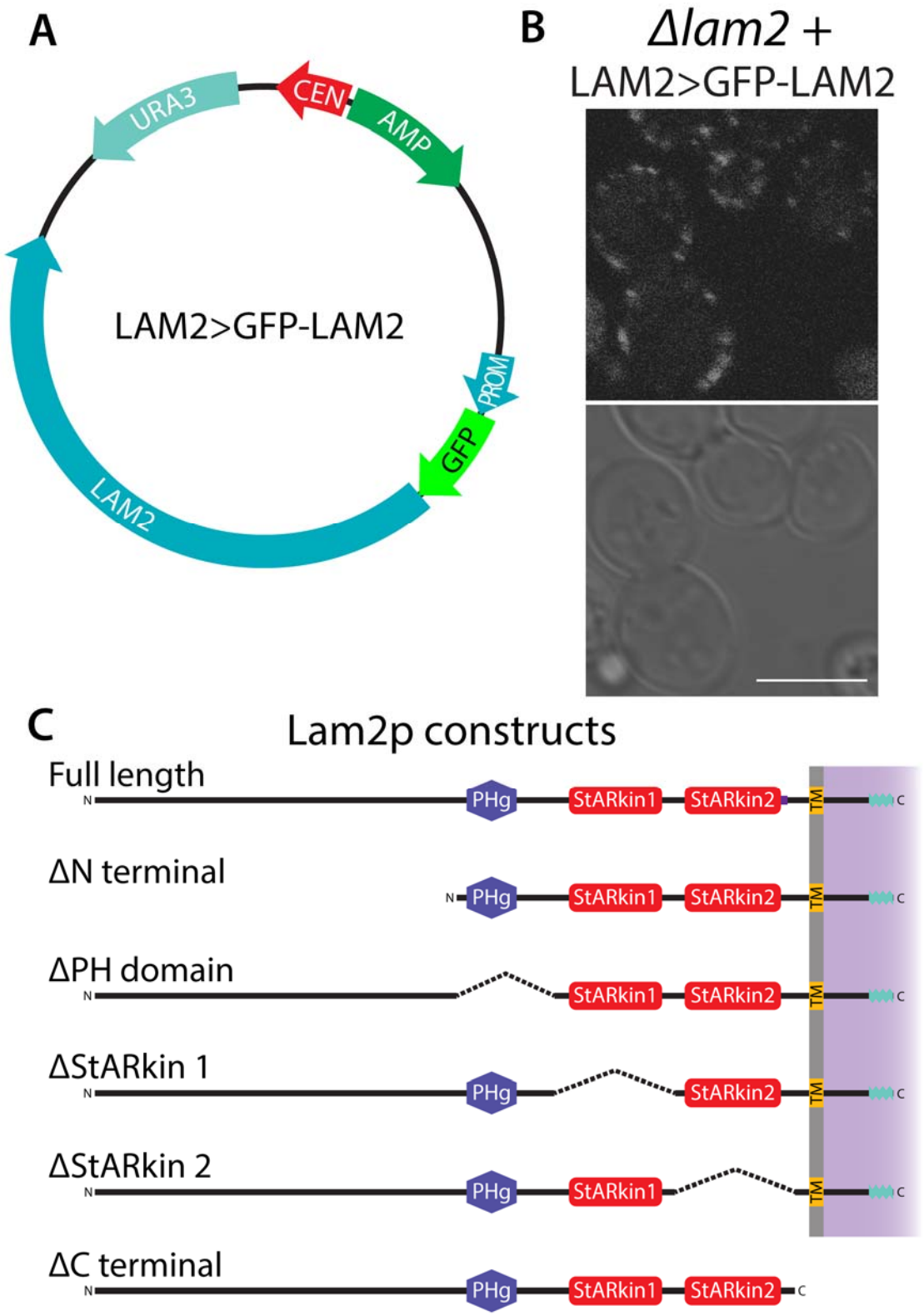

Figure 4.10 **GFP-Lam2p localises to ER puncta and GFP-Lam2p contructs**
A) Approximation of a pRS416 yeast vector expressing Lam2p, GFP-tagged at the N-terminus and under the endogenous *LAM2* promoter. A Uracil metabolic marker is used to retain the vector during strain maintenance on minimum media. **B**) Confocal microscopy of GFP-tagged Lam2p expressed from a plasmid in Δ*lam2*. Lam2p localises to ER puncta around the periphery of the cell. Scale bar shows 5 µm. **C**) Diagrams showing the delete domain constructs of Lam2p used to compare the requirement of each domain.

contact sites independent from the six known tethers to which Lam2p can target.

4.2.7 Deletion of TM domain affects the function

Lam2p is a long protein consisting of 1438 amino acids and is composed of various domains [Figure 4.10C]. In addition to two StARkin domains, it also contains a PH (GRAM-like) domain, a long unstructured N-terminal, a C-terminus TM helix and a short luminal domain. As Lam2p was required for AmB resistance, the phenotype of Δ*lam2* observed on AmB was used to assess the different domains to find the active domain or domains of Lam2p. The full-length Lam2p was re-cloned to delete different domains, and the ability of these to rescue Δ*lam2* strains was assessed in relation to the AmB growth defect [Figure 4.10C + Figure 4.11]. The expression of Lam2p was made on a plasmid using a metabolic selection marker for Uracil. Minimal media was used to retain the plasmid in the yeast, and it is due to the decreased levels of nutrients that a lower basal toleration of AmB is seen across all strains transformed with a pRS416 plasmid with a Uracil marker.

Unsurprisingly the most essential domain of Lam2p is the localising C-terminus, consisting of the transmembrane helix and a short luminal domain [Figure 4.10C + Figure 4.11]. Lam2p localisation required simply this C-terminus domain of Lam2p; microscopy by Tim Levine showed a truncated Lam2p consisting of only the TM domain and remaining C-terminal localising normally (Gatta *et al.*, 2015). The AmB growth assay shows a greater growth defect in cells expressing Lam2pΔCT than not expressing Lam2p, which was reproducible in repeat assays. The phenotype is seen most clearly in the RS453C background grown on 90 $ngml^{-1}$ AmB [Figure 4.11]. The detrimental effect of the mislocalised protein indicates that it is still functional but is acting in an incorrect location preventing resistance against AmB. This action may be the mislocalised normal function of the protein, or another possibility is that there are abnormal protein-protein or membrane-protein interactions with yet unknown partner(s).

4.2.8 Deletion of the second StARkin domain affects the function

The deletion of the second StARkin domain showed the least amount of rescuing effect after the removal of the TM domain [Figure 4.10C + Figure 4.11]. This reveals the key activity of the protein responsible for AmB basal resistance lies in this StARkin domain of Lam2p. Lam2pΔS2 shows no activity and is not detrimental to the yeast (in contrast to Lam2pΔCT); therefore, the protein has lost its activity without the second StARkin. Surprisingly, the deletion of the first StARkin domain had very little

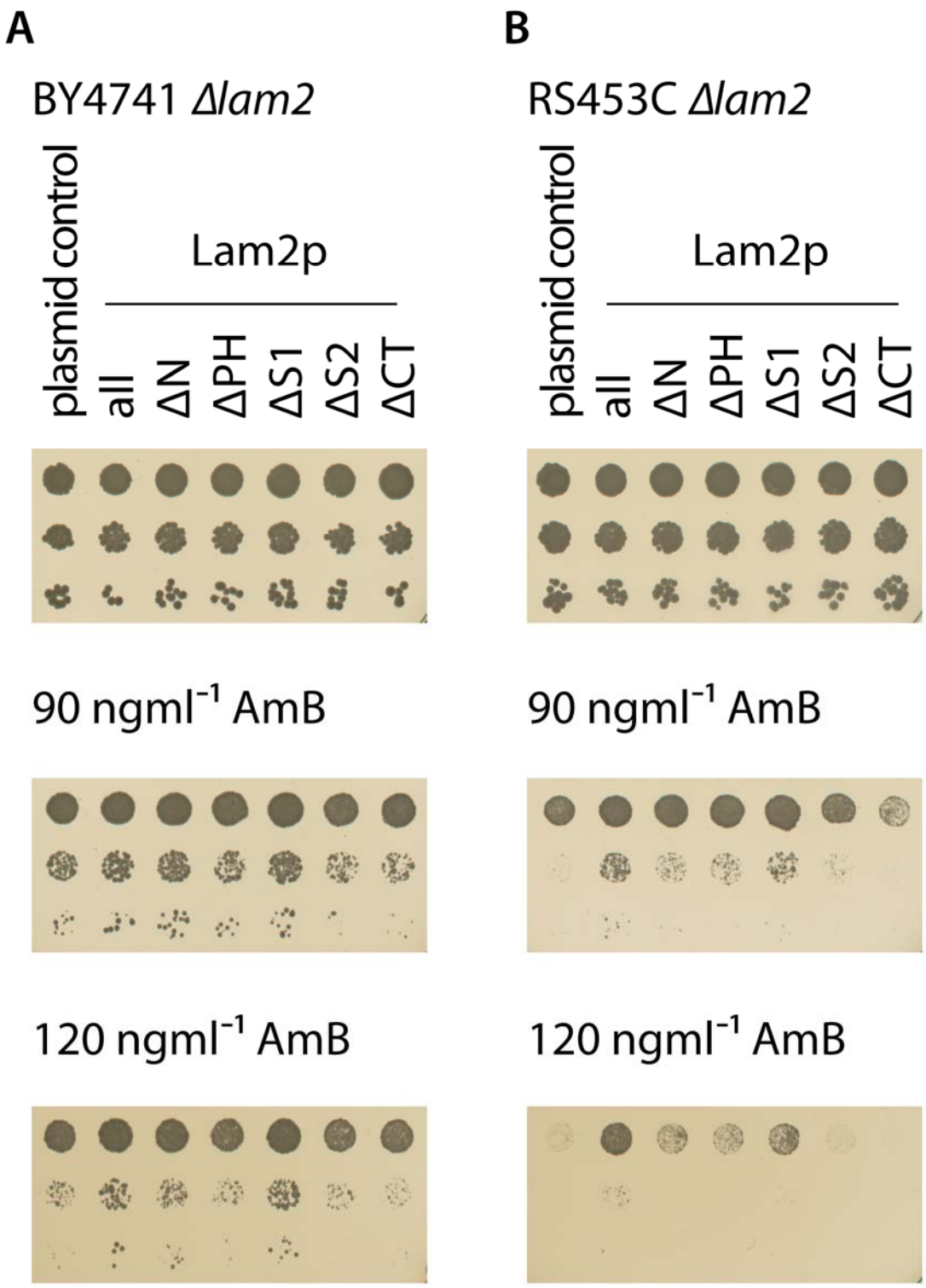

Figure 4.11 **Lam2p function is dependent on correct localisation and StARkin 2** Growth assay of Δ*lam2* genotype in a BY4741 and RS453C background with a plasmid expressing endogenous levels of full length Lam2p or Lam2p deleted for the N-terminal, PH (GRAM-like) domain, StARkin 1, StARkin 2 or the C-terminal including the TM domain. SD + 2 % dextrose agar was used with various concentration of AmB. A plasmid control using GFP expression is used to compare cell number. It is important to note that due to minimal media used, levels of AmB were lower than with YPD media used in previous experiments. Expression levels of the Lam2p with deleted domains were checked by GFP fluorescence of the tagged protein using microscopy and were similar to endogenous protein though Lam2pΔCT was mislocalised.

effect on the function of the protein. Lam2pΔS1 rescues almost as well as full-length Lam2p. In addition, the deletion of the unstructured N-terminal or PH domain showed more defect in Lam2p activity than the deletion of the first StARkin domain. It seems unlikely that yeast evolved to gain a protein with two StARkin domains only to use one StARkin domain, it is more parsimonious to hypothesise that the first StARkin domain is still active but not in regards to the sterol pool that is affected by AmB. It would be interesting to repeat this assay on Natamycin to see if the rescue order of the delete domains would be still be consistent.

4.2.9 Lam4S2 replaces the function of Lam2S2

The deletion of *LAM4* showed no growth defect on AmB, unlike its paralogous gene *LAM2*, which showed high sensitivity to polyene antibiotics [Figure 4.4 + Figure 4.7]. Similarly to Lam2p, the domain architecture is predicted to consist of a long unstructured N-terminal, a PH (GRAM-like) domain, two StARkin domains, a TM domain and a short intraluminal domain at the C-terminus [Figure 4.12A]. In the previous AmB assay, it was shown that the second StARkin domain of Lam2p was the most active domain [Figure 4.11]. To investigate whether the StARkin domain of Lam4p is capable of the same function, the second StARkin domain of Lam2p was removed and replaced with the equivalent domain of Lam4p which shares 53% sequence identity [Figure 4.12A] (Gatta *et al.*, 2015). This recombinant protein is hereafter termed Lam2swapL4S2 (or Lam2swL4S2 in Figure 4.13).

WT Lam2p is typically found in puncta along the pmaER [Figure 4.10B] (Gatta *et al.*, 2015). As the localisation generated by the C-terminal TM helix and short luminal domain of Lam2p is essential for the correct function of the protein, the localisation of Lam2swapL4S2 was verified for correct positioning. Microscopy shows that endogenously promoted Lam2swapL4S2 has an identical localisation to WT Lam2p indicating any differences in the rescue would not be due to the incorrect localisation of the protein [Figure 4.12B].

The AmB growth assay comparing WT Lam2p and Lam2swapL4S2 expressed under the *LAM2* promoter shows little difference between the two [Figure 4.13]. Both are able to rescue Δ*lam2* almost back to WT growth levels on AmB indicating that the second StARkin domain of Lam4p is able to carry out the same function as the equivalent domain of Lam2p. This data adds to the puzzle of the role of Lam4p compared to Lam2p - the second StARkin of Lam4p has the same function as the active StARkin domain of Lam2p. However, Δ*lam4* show no growth defect compared to Δ*lam2*, instead it was slightly resistant to AmB. If the second StARkin domain is also

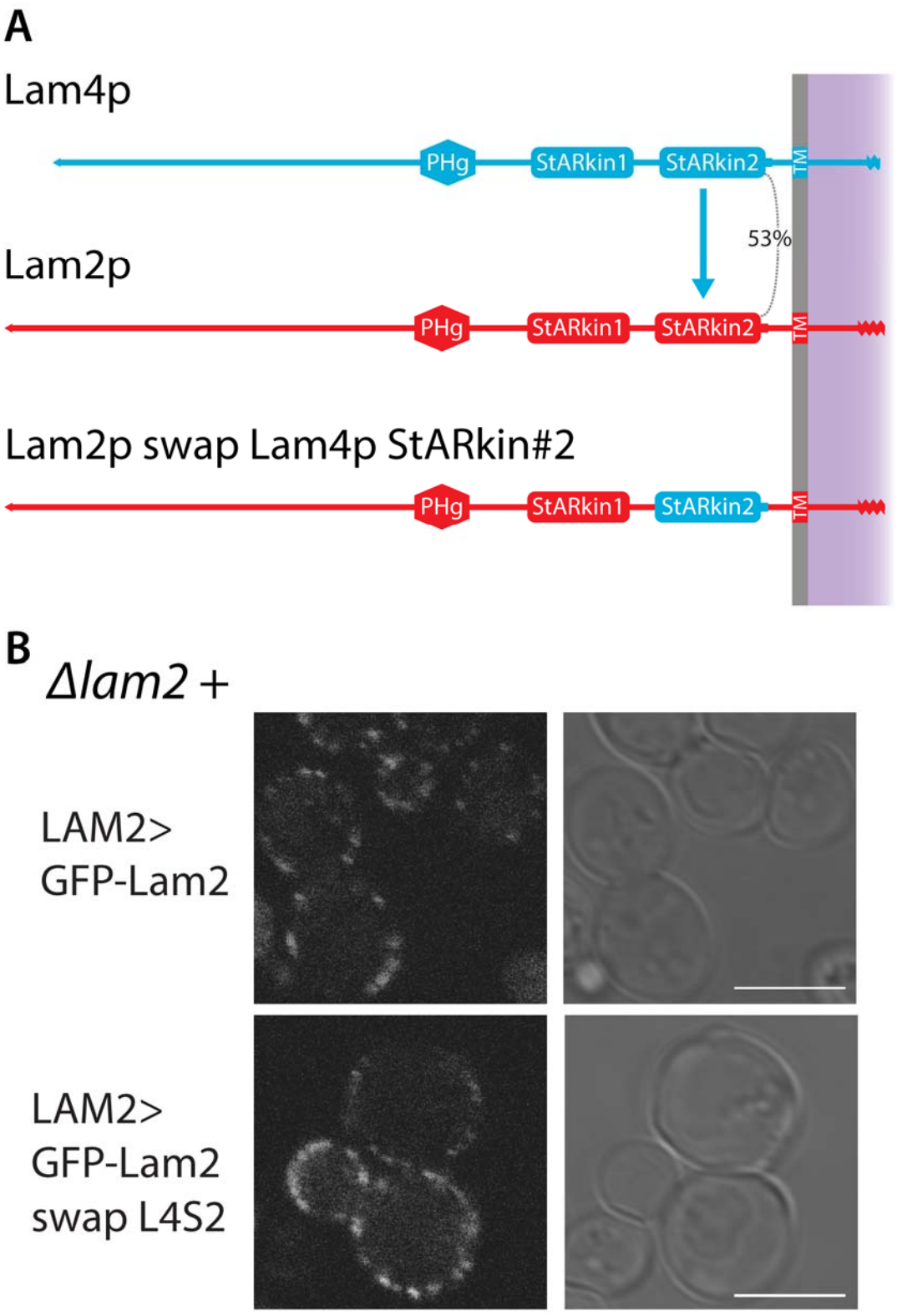

Figure 4.12 **Lam2p with Lam4S2 localises as normal**
A) Schematic of the predicted domains in Lam2p (red), Lam4p (blue) and the recombinant Lam2p with the StARkin2 domain from Lam4p. StARkin 2 domains from Lam2p and Lam4p are 53% similar. This recombinant protein is termed Lam2swapL4S2. The tapered end indicates the N-terminus. **B**) Microscopy showing endogenously promoted GFP-tagged Lam2p with StARkin 2 from Lam4p in log phase Δ*lam2* cells. Lam2p with StARkin 2 from Lam4p localises as WT Lam2p. Scale bar is 5 µm.

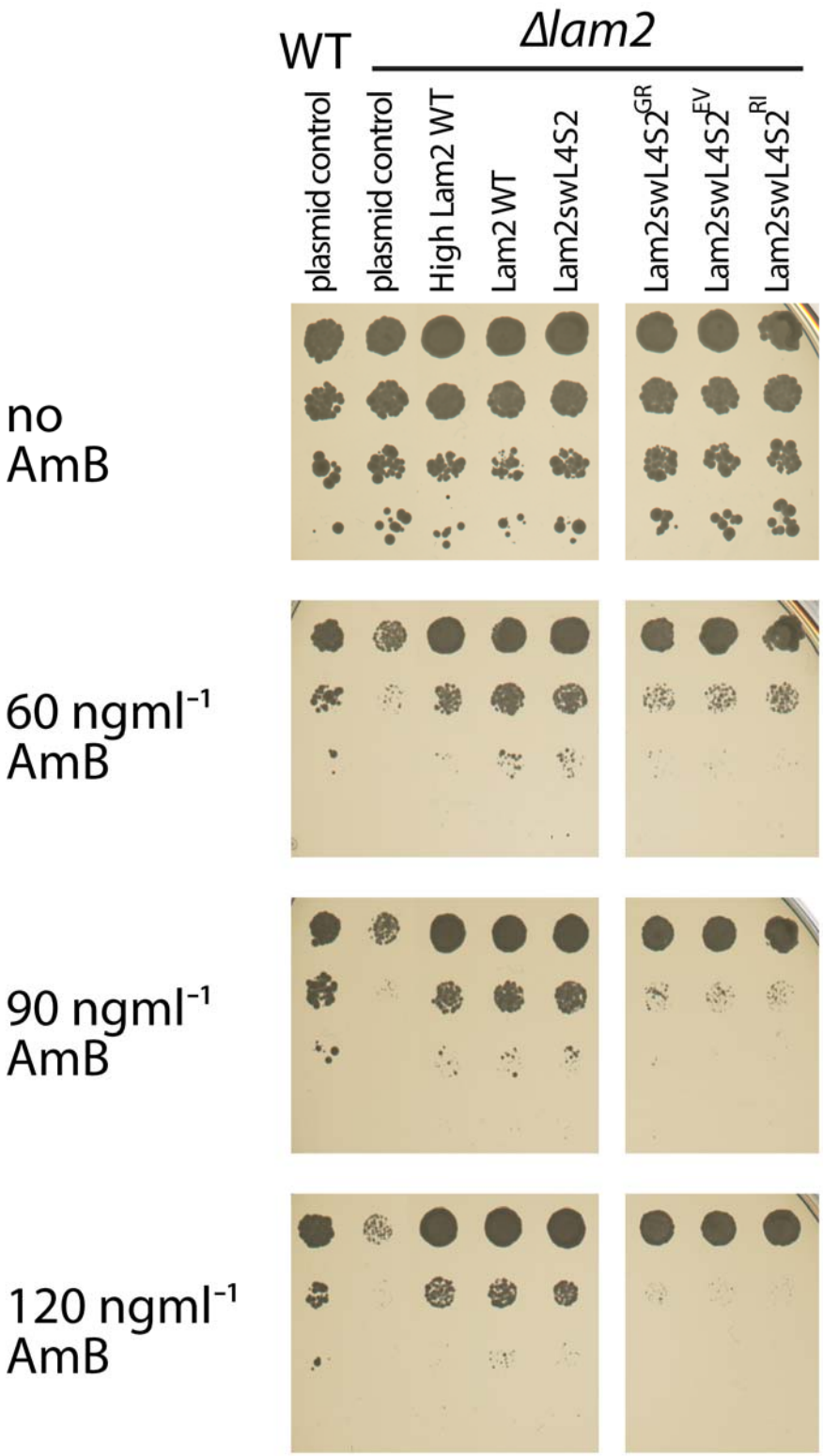

Figure 4.13 **Lam4S2 mutations are detrimental to the function of Lam2p**
Growth assay on SD agar + 2% Dextrose with various concentration of AmB comparing the rescue of Δ*lam2* using high expression levels of WT Lam2p, endogenous levels of WT Lam2p and endogenous levels of Lam2p with StARkin2 from Lam4p WT (Lam2swL4S2) or with mutations. WT cells and Δ*lam2* expressing GFP as a control plasmid were used to compare the extent of rescue and media with no AmB was used to compare cell numbers. The Lam2swL4S2 construct functions as WT Lam2p for basal resistance to AmB. G1119R, E1048V and R1025I mutations in Lam4 StARkin 2 domain suppressed function of Lam2swL4S2.

the active domain of Lam4p, it is feasible that the overall activity of Lam4p is similar to Lam2p even if it does not contribute to the basal resistance to AmB. It is possible that Lam4p affects a pool of ergosterol that is not detected by AmB or its activity is inhibited in this growth condition. Endogenously expressed GFP-tagged Lam4p is expressed at lower but comparable levels of Lam2p when observed under a confocal microscope [data not shown]. This is in contrast to Lam1p/Lam3p, which were difficult to distinguish under an endogenous promoter. Therefore, the difference in expression levels cannot explain why Lam1p/2p/3p are more essential to cellular growth on AmB than Lam4p. It would be interesting to find whether, and in which circumstances, the Lam4p is observed to be functional.

4.2.10 Mutations in StARkin 2 repress rescue of full-length Lam2p

Mutations within the StARkin 2 domain of Lam4p were found to cease the rescue of Lam2swapL4S2 [Figure 4.13]. All substitutions were non-conservative mutations altering the WT residue to an amino acid with different properties, and expression levels were checked with fluorescent microscopy [data not shown].

These mutations were chosen as prior work by Tim Levine on the rescue ability of Lam2p StARkin 2 domain only. The overexpression StARkin domains only of Lam2p/4p/5p/6p were able to rescue the phenotype of delete *LAM* strains on AmB (Gatta *et al.*, 2015). A range of different mutations was introduced to the StARkin domain only expressing plasmid, substituting conserved residues. These mutants tested on their ability to rescue growth of Δ*lam2* cells on AmB (carried out by Tim Levine). The mutants that showed the least amount of rescue were used in this experiment.

The first mutation introduced was a conserved glycine in the C-terminal α-helix predicted to line the cavity, which was mutated to arginine (G1119R) [Figure 4.14A] (Gatta *et al.*, 2015). By disturbing the hydrophobic cavity, the binding of a ligand would be impaired. It is important to note that previous experiments by Tim Levine showed that the mutation of the G1119 to alanine and threonine (small and uncharged amino acids) only partially inhibited function of Lam2p StARkin domain, suggesting that the large charged characteristic of arginine is needed to physically intrude into the binding pocket [Figure 4.14A]. When this mutation was translated to Lam4p StARkin 2 domain, Lam2swapL4S2 was unable to rescue the growth phenotype of Δ*lam2* cells on AmB [Figure 4.13].

The second and third mutations that were tested in Lam2swapL4S2 were of large charged residues in the core β-strands that make up the StARkin fold. These residues were mutated from a charged amino acid to an uncharged amino acid. One

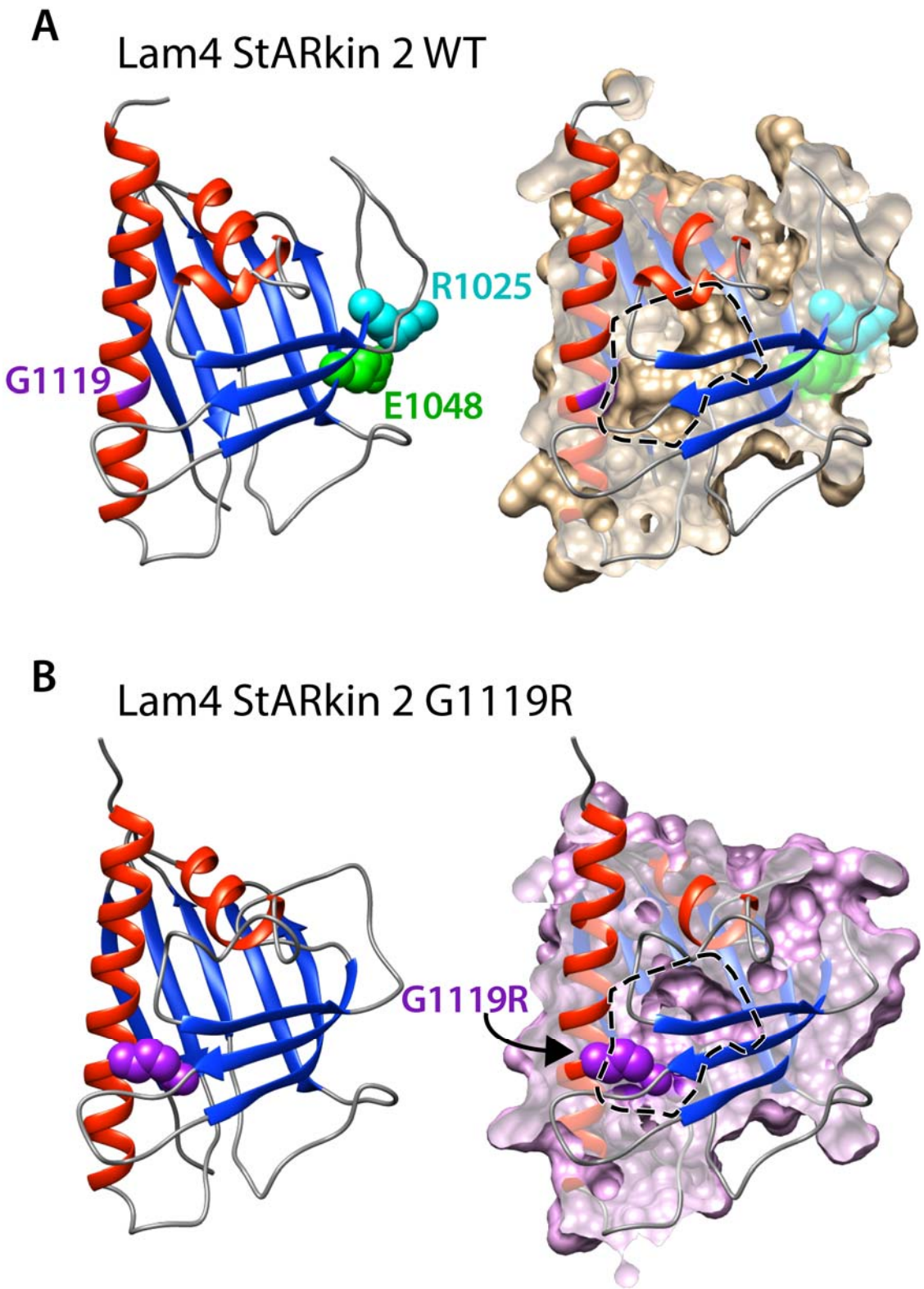

Figure 4.14 **Mutations of residues in Lam4S2 domain**
A) 3D structure of the predicted Lam4 StARkin 2 domain. Glycine^{1119} is highlighted in purple, Arginine^{1025} is highlighted in cyan and Glutamic acid^{1048} is highlighted in green. A cross section of the domain show that the Glycine points inwards towards the cavity. The approximate shape of the WT cavity is indicated with a dotted line. **B**) 3D structure of the predicted Lam4 StARkin 2 domain with a G1119R mutation. The substitute residue Arginine is much bigger and is shown to obstruct the binding cavity. The shape of the WT cavity is superimposed on the cross section to show the Arginine intruding the cavity,

mutation was of a glutamic acid, which was replaced with a valine (E1048V), an amino acid with no charge and a smaller side chain. The other was an arginine to isoleucine (R1025I). Initially these residues were thought to face into the pocket, however, upon generating predicted structures, these residues are proposed to form the outside surface of the domain [Figure 4.14B]. By testing the ability to rescue compared with WT, both of these mutations were shown to be disruptive to Lam4StARkin 2 domain and suppressed its ability to rescue growth phenotype of Δ*lam2* cells on AmB [Figure 4.13].

4.2.11 Lam3p localises to the ER

The cloning of genes from yeast can be done by PCR or by homologous recombination in the yeast itself. The *LAM3* gene is long – approximately 3700 bases. Taking advantage of homologous recombination, the full length of *LAM3* was cloned via transformation of WT yeast. The first and last 150 bp of *LAM3* were cloned via PCR into a plasmid for overexpression (*PHO5* promoter) of N-terminally GFP-tagged sequences [Figure 4.15]. The plasmid was digested between the two fragments and transformed into yeast. The colonies were screened via PCR for a product using a forward primer within the plasmid GFP and the middle of *LAM3*, which would only be present after a successful homologous recombination. Sequencing of plasmid rescued from these yeast cells was used to verify complete cloning of the correct sequence of *LAM3*.

GFP-Lam3p was seen in puncta localised at the periphery of the cell and in the nuclear envelope in all strains tested (WT, Δ*lam1,* Δ*lam2*, Δ*lam3* and Δ*lam1*Δ*lam3)* [Figure 4.16]. The localisation pattern suggests that the protein is located on the ER. In yeast cells, the ER can be classed into three domains - the cortical ER, also known as the pmaER, the nuclear ER and the ER strands that connect them together [Figure 4.17A]. The microscopy clearly shows these three domains, though fragmented due to the punctate distribution of the protein. This localisation appears to be similar in all strains imaged (WT, Δ*lam1,* Δ*lam2*, Δ*lam3* and Δ*lam1*Δ*lam3*). The *PHO5* promoter was used to visualise Lam3p although further microscopy using the endogenous promoter was carried out by Alberto Gatta, which showed very low expression that is hard to visualise clearly (Gatta *et al.*, 2015).

Lam3p and its paralog pair Lam1p were suggested to reside in mitochondria by high throughput microscopy CYCLoPs (Koh *et al.*, 2015). The shortcoming of the high throughput data is that the protein is C-terminally tagged and consequently a large globular GFP domain was added to the relatively small C-terminal domain after ER membrane spanning helices. As ascertained previously for Lam2p (but not repeated

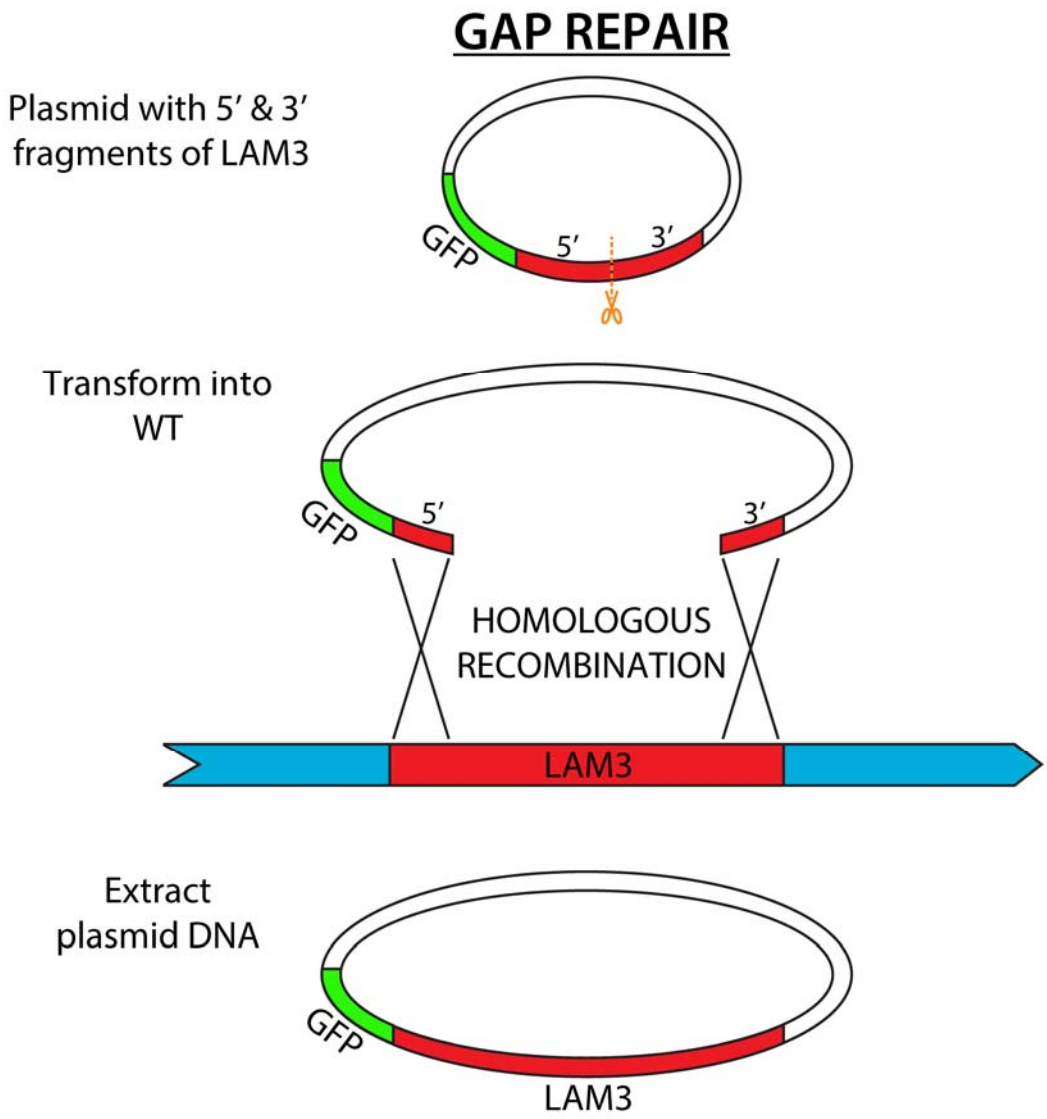

Figure 4.15 **Yeast gene repair in plasmids by yeast homologous recombination** Gap repair technique taking advantage of the yeast homologous recombination mechanism to clone the full length of *LAM3*. A plasmid was constructed with ~100 bp of the start and end of *LAM3* (red) and prior to transformation in WT yeast was digested at the intersection (orange dotted line) between the *LAM3* fragments. Colonies that appeared on the -His selection plate were isolated and plasmids purified from the colonies were sequenced.

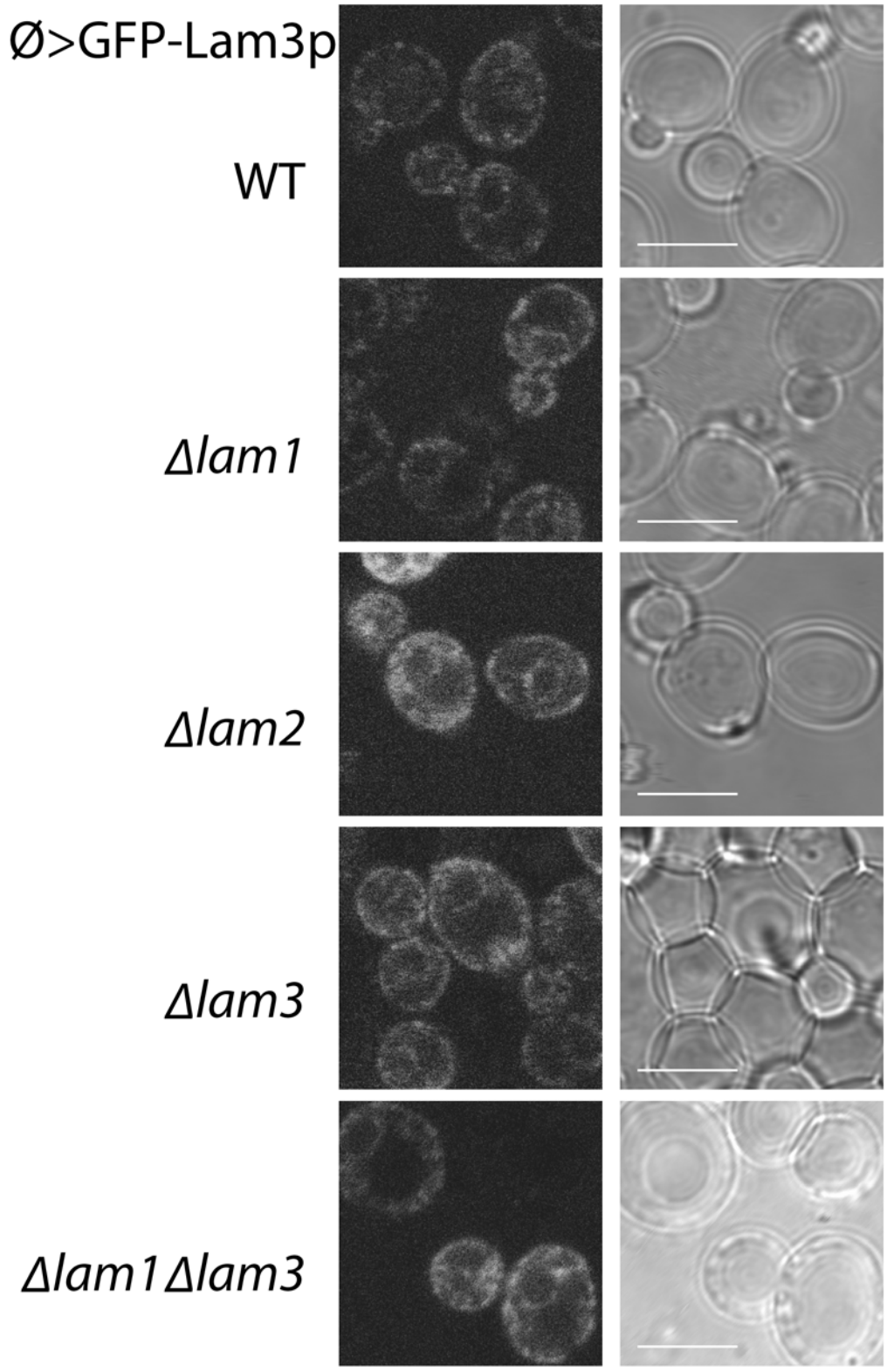

Figure 4.16 **Lam3p localises to ER puncta**
Confocal microscopy of WT cells showing localisation of highly expressed GFP-Lam3p in log phase WT, Δ*lam1,* Δ*lam2,* Δ*lam3* and Δ*lam1*Δ*lam3*. Scale bar shows 5µm. All strains show similar Lam3p puncta which suggests localisation the ER structure in yeast.

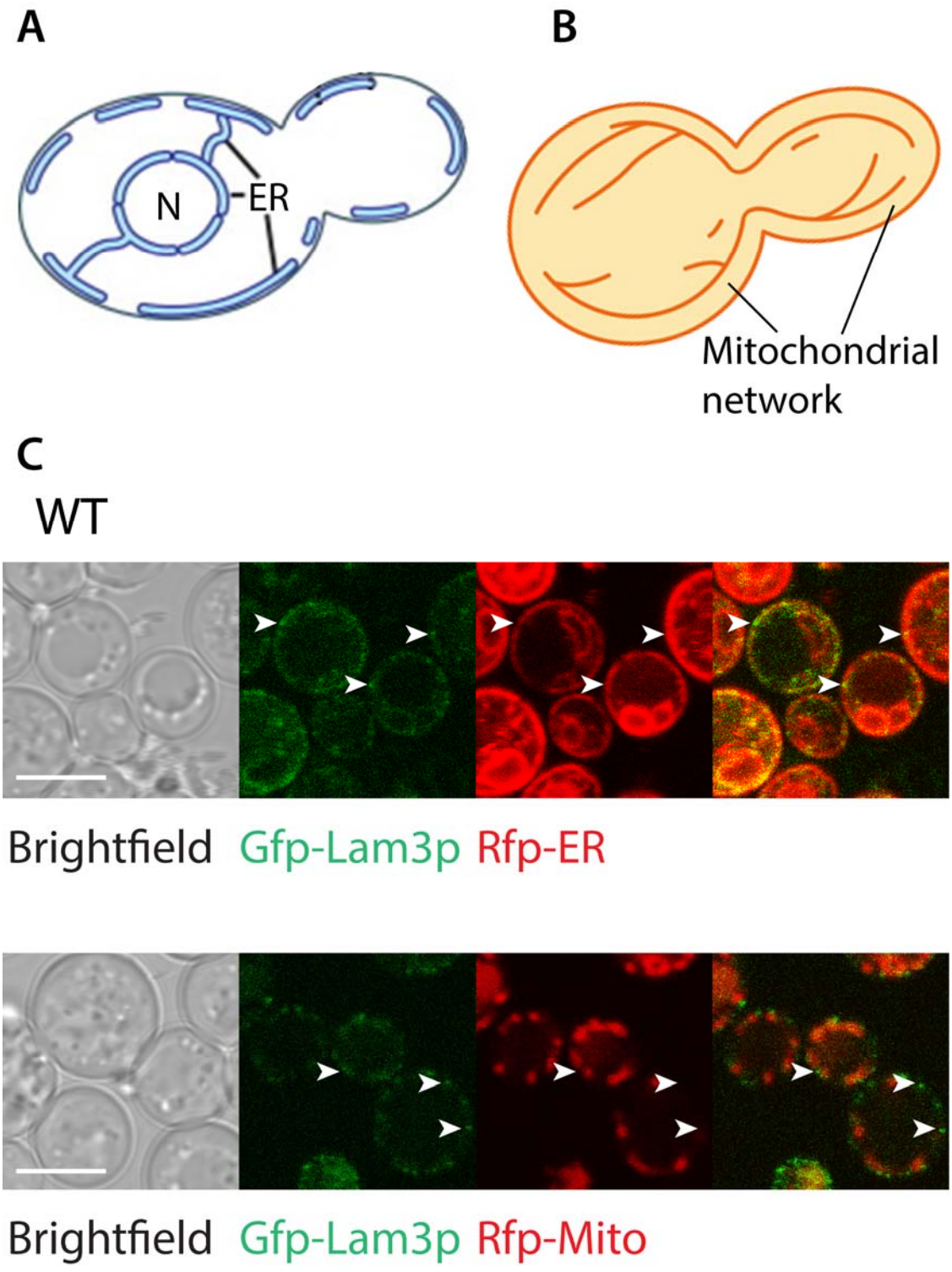

Figure 4.17 **Lam3p colocalises with RFP-ER**
Illustration showing normal distribution of yeast **A**) ER and **B**) mitochondrial network adapted from Manford *et al.*, 2012 and Yaffe *et al.*, 1999. **C**) Confocal microscopy of log phase WT cells showing co-localisation of high expressing GFP-Lam3p and RFP-tagged ER and RFP-tagged mitochondria using the TM domain of Scs2p and Tom6p. GFP-Lam3p shows co-localisation with RFP-ER but not with RFP-mitochondria. Scale bar shows 5µm.

for Lam3p), the C-terminal domain including the TM domain is solely responsible for correct localisation. Thus the addition of the fluorescent group on the C-terminal could affect localisation of Lam3p. In addition, yeast mitochondria are often seen as tubular chains around the cell periphery [Figure 4.17B], and so it is not unlikely that this high-throughput data is incorrect.

To corroborate the localisation of GFP-Lam3p to ER puncta, GFP-Lam3p was expressed in yeast expressing either RFP-ER or RFP-Tom6p. Lam3p co-localises with RFP-ER rather than RFP-Mitochondria [Figure 4.17C]. The co-localisation shows GFP-Lam3p in punctate dots along the red line of cortical ER that is labelled with RFP. Conversely, there is no clear co-localisation with RFP-Mitochondria. There are however green punctate dots, which are not connected to any red mitochondria.

4.2.12 *Δtether* strain to confirm pmaER localisation of Lam3p

In yeast, the pmaER spans over 40% of the cell periphery close to the PM, consequently even with confocal microscopy, it is hard to verify that the localisation is within the pmaER rather than a punctate protein at the PM [Figure 4.17A]. Considering this, a yeast strain with a deletion of six genes thought to tether the ER to the PM was utilised to distinguish between the pmaER and the PM [Figure 4.18A]. Tether proteins are present between organelles to leash the two membranes together, forming the MCS. In yeast, there are six such proteins. Δ*tether* is a strain of yeast that is deleted for all six suggested tether proteins between the ER and the PM (VAP proteins Scs2/22p, Ist2p and tricalbin proteins Tcb1/2/3p) (see section 1.4.3 for information on ER-PM tethers) (Manford *et al.*, 2012). The elimination of all six proteins causes a dramatic loss of approximately 90% of the pmaER, the mass of which is collapsed inside the cell and is seen as a cluster of ER strands. This reduces the proportion of PM in contact with ER from 40% to only 4%. Although there is still the question of what is responsible for the remaining 10% of pmaER contacts, this strain is a useful tool for observing PM-ER contact site localisation of proteins. Thus, if Lam3p localises in the pmaER rather than the PM, the punctate dots will be less frequent and will only appear where the limited pmaER is left.

Indeed, when GFP-Lam3p was visualised in the Δ*tether* strain the number of puncta around the cell periphery was significantly lower [Figure 4.18B]. The small number of puncta that remain coincide with a red strand of ER reaching out from the typical nER. Furthermore, when the mitochondria were also labelled in this Δ*tether* strain, co-localisation was distinctly absent between GFP-Lam3p and RFP labelled-mitochondria.

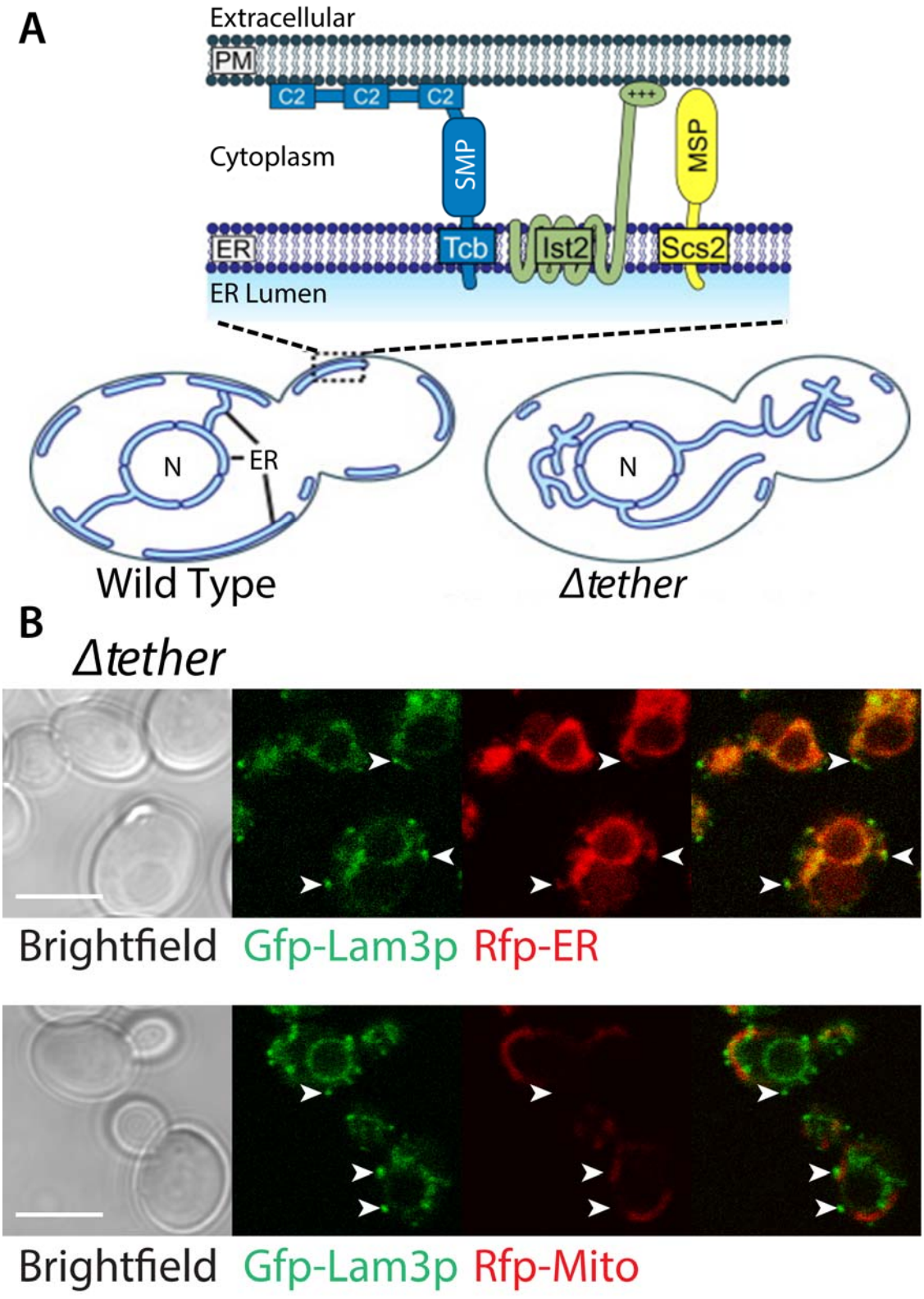

Figure 4.18 **Lam3p colocalises to remaining pmaER in Δ*tether* cells**
A) Diagram of Δ*tether* yeast cells adapted from Manford *et al.*, 2012 showing the extent of ER-PM contact site loss when deleted for six ER-PM tethers (Scs2p/22p, Ist2p Tcb1p/2p/3p). **B**) Confocal microscopy of log phase Δ*tether* cells showing co-localisation of high expressing GFP-Lam3p and RFP-tagged ER and RFP-tagged mitochondria using the TM domain of Scs2p and Tom6p. GFP-Lam3p shows co-localisation with RFP-ER but not with RFP-mitochondria. Scale bar shows 5µm.

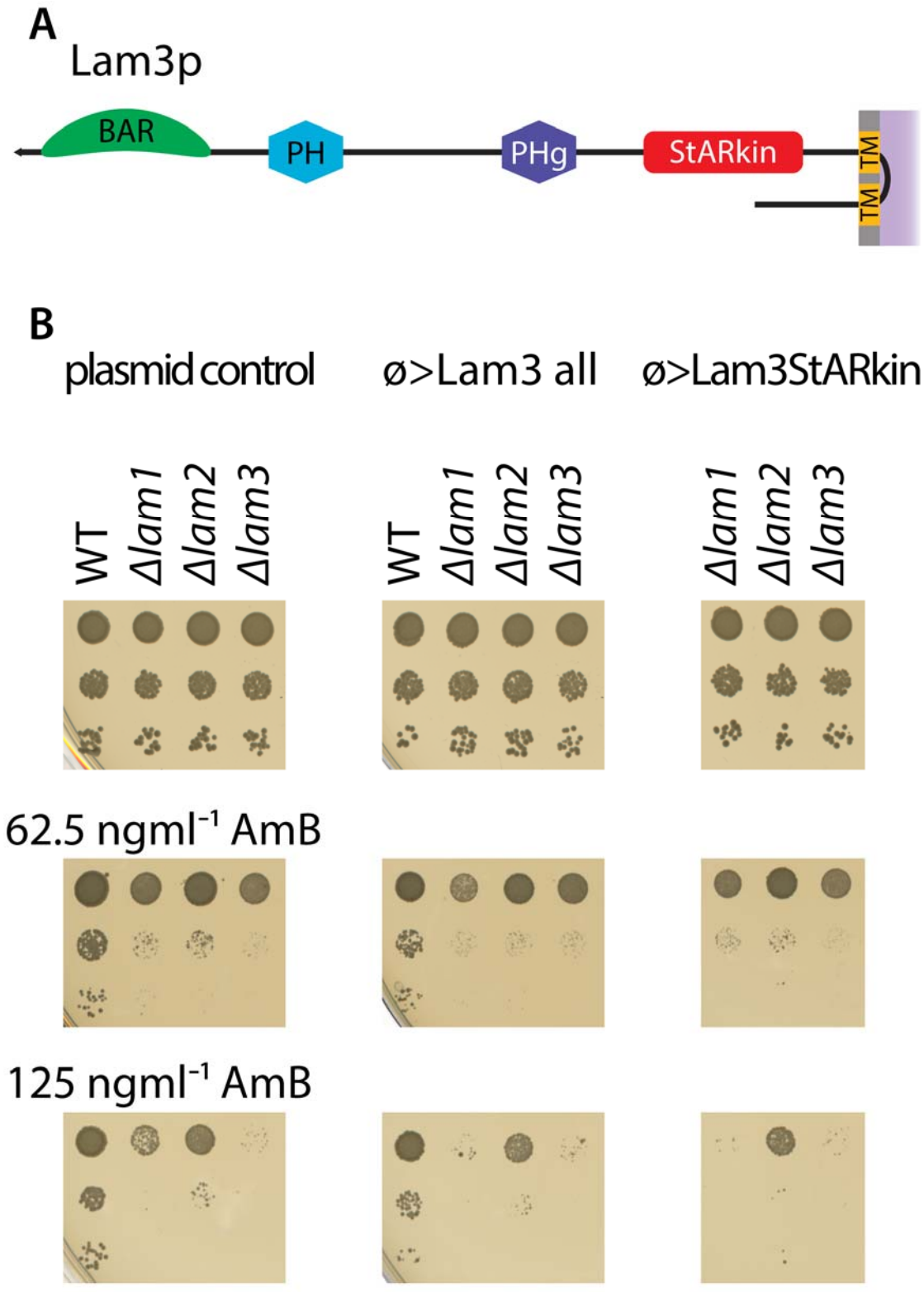

Figure 4.19 **Additional expression of Lam3p is detrimental to AmB resistance** **A**) Diagram of domains predicted to be in Lam3p. The tapered end indicates the N-terminus. **B**) Growth assay on minimal media with AmB of WT, Δ*lam1,* Δ*lam2* and Δ*lam3* expressing high levels of Lam3p full length and Lam3p StARkin domain only after 48 hours. Expression of GFP and media with no added AmB were used as controls for protein expression (not shown) and cell growth respectively. Expression of full length Lam3p and Lam3p StARkin domain is detrimental to the growth of Δ*lam1,* Δ*lam2* and to a lesser extent WT on AmB.

4.2.13 Highly expressed Lam3p hinders growth on AmB

Strains transformed with highly expressed full-length Lam3p were tested on AmB to find whether it can rescue delete strains, Δ*lam1,* Δ*lam2* and Δ*lam3* [Figure 4.19B]. The results show that high expression of full-length Lam3p was unable to rescue Δ*lam3.* There was possibly a very slight improvement in growth from Δ*lam3* expressing GFP as a control or Lam3p under a *PHO5* promoter. In contrast, Δ*lam1* was impaired by co-expression of GFP-Lam3p. Additionally, WT and Δ*lam2* were all slightly impaired in growth on AmB. The increased sensitivity seen in these strains implies that too much Lam3p is detrimental to growth on AmB. As WT, Δ*lam1* and Δ*lam2* strains already have the endogenous Lam3p, the expression of addition Lam3p could be causing an overload in Lam3p leading to harmful effects. Overall, the data implies that levels of Lam3p are highly regulated in the cell. Microscopy of endogenously promoted Lam3p carried out by Alberto Gatta shows a very low expression level at cortical ER dots in contrast to the localisation with highly expressed Lam3p, where it is also present in other parts of the ER [Figure 4.17 + Figure 4.18] (Gatta *et al.*, 2015). The characteristic of overexpression being harmful is also seen with Lam2p where the *PHO5* regulated expression of Lam2p in Δ*lam2* is detrimental to the cell for growth on AmB compared with endogenous levels of Lam2p [Figure 4.13].

4.2.14 Highly expressed Lam3 StARkin affects growth on AmB

In addition to full-length Lam3p being cloned into a high expressing plasmid, the StARkin domain of Lam3 was also cloned into the same plasmid. The StARkin domain was cloned without the transmembrane domain to anchor the protein to its normal localisation on the ER. The Lam3p StARkin was transformed into delete strains Δ*lam1,* Δ*lam2* and Δ*lam3* [Figure 4.19]. As with full-length Lam3p, the expression of Lam3p StARkin domain was detrimental to the growth of Δ*lam1*on AmB. There were much milder reductions of growth for Δ*lam2* and Δ*lam3*, best seen with the higher level of AmB (125 $ngml^{-1}$). Both the expression of Lam3p and Lam3p StARkin domain in Δ*lam1* cells causes a significant reduction in resistance to AmB. This data could be interpreted as a link between levels of Lam3p and Lam1p, where significant expression of Lam3p without Lam1p can cause harmful effects. However, it is not confirmed if the isolated Lam3p StARkin is soluble as attempts to purify this construct failed (correspondence with Alberto Gatta) though there are levels of detectable GFP tagged protein in yeast cells [data not shown].

4.2.15 Expression of LAM proteins impairs Δ*osh* growth on AmB

Yeast OSBP homologs Osh1-7 are implicated in lipid traffic in the cell, in spite of evidence that calls direct involvement in sterol traffic into question. A sevenfold delete of yeast OSH proteins is lethal thus CBY926 *osh1-7*Δosh4^{ts} with a temperature sensitive Osh4p was used to express additional high and endogenous levels of LAM proteins to assess whether additional expression of LAM proteins can rescue the lethality when all OSH proteins are removed. No growth was seen at the restrictive temperature of 37°C for all transformants [data not shown] therefore the function of full-length LAM proteins does not overlap with the essential role of the seven OSH proteins. Localisation of Lam2p and Lam4p were checked to assess for normal expression in the Δ*osh* strain. Localisation at both 30°C and 37°C in the Δ*osh* strain was indistinguishable from wild-type [Figure 4.20 + Figure 4.10 + data not shown], suggesting that there is no requirement for the presence of OSH proteins nor their downstream effects on the correct distribution of LAM proteins. It also indicates that there is no significant upregulation (or downregulation) of LAM proteins as a response to the removal of all OSH proteins, although this is not conclusive without a Western blot to confirm protein levels.

An AmB growth assay was carried out at the permissive temperature of 30°C where Osh4p is still functional [Figure 4.21]. A significant decrease in growth was found with the high expression of Lam2p in the *osh1-7*Δosh4^{ts} strain, which is even observed with no AmB, indicating that high levels of Lam2p are detrimental to the proper growth of yeast.

With the exception of Lam2p, high expression of the LAM proteins has a small negative effect on the growth of the strains on AmB. Surprisingly, ‘low’ expression of LAM proteins (where there are twice the endogenous levels due to two *LAM* genes, a genomic copy and a copy in the expression plasmid) generally had more of an effect on growth than high expression. The *PHO5* promoter is one that ensures high expression in yeast and endogenous levels of LAM proteins are much lower than *PHO5* promoter levels as shown by previous microscopy and personal correspondence with Tim Levine. However, microscopy has only been carried out with yeast grown without AmB. Therefore it has yet to be determined whether as a response to AmB, LAM proteins are upregulated to a level that surpasses the *PHO5* promoter. Further investigation into this is required to find the reason for the discrepancy between *PHO5* promoted, and *LAM* promoted expression when grown on AmB.

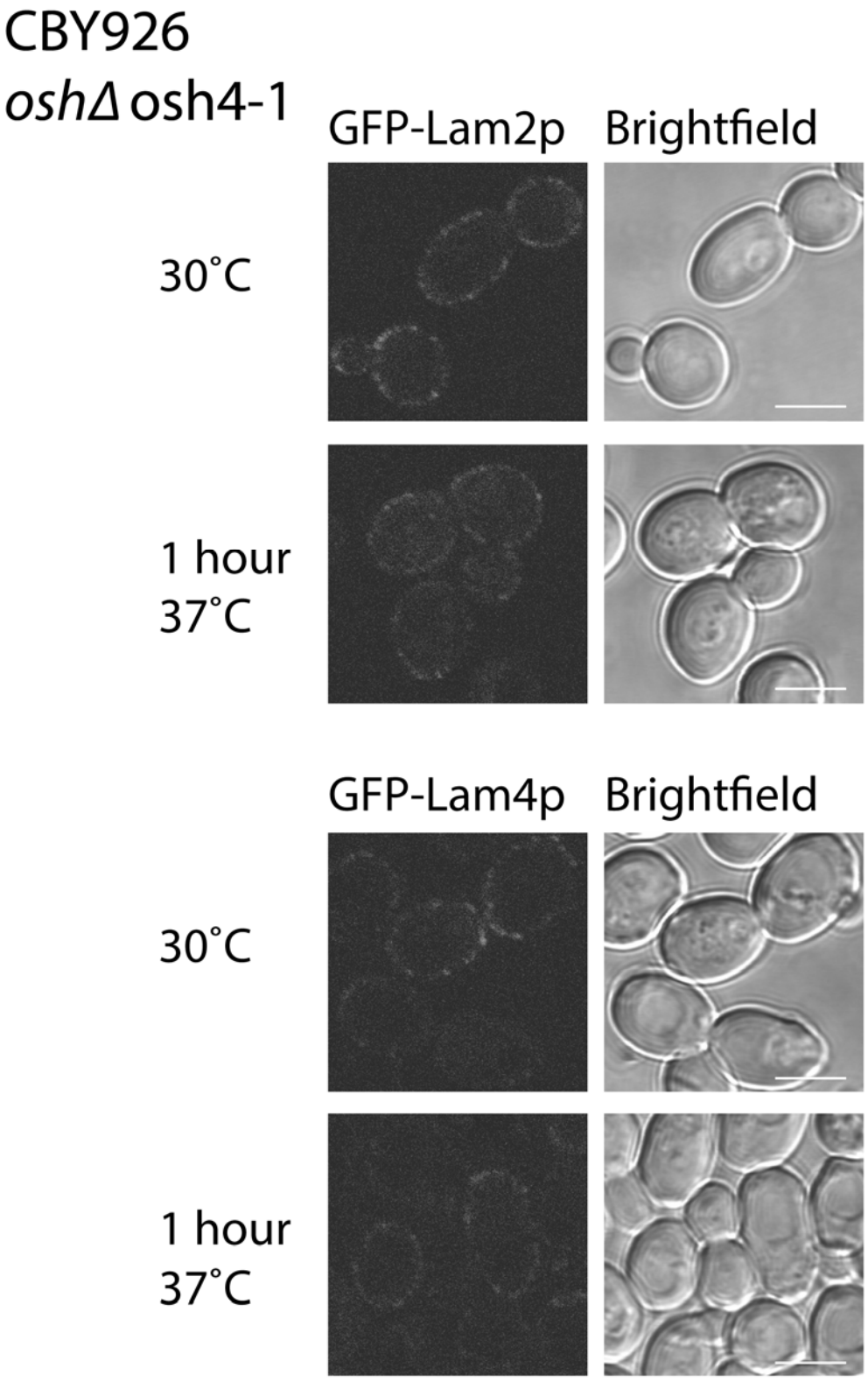

Figure 4.20 **Lam2p and Lam4p localises as normal in CBY926**
Confocal microscopy showing localisation off endogenously promoted GFP-tagged Lam2p and Lam4p in CBY926 *osh1-7*Δosh4^{ts} strain. There is no difference in localisation between growth at 30°C and 1 hour at 37°C where there is complete loss of OSH proteins. Scale bar shows 5 μm.

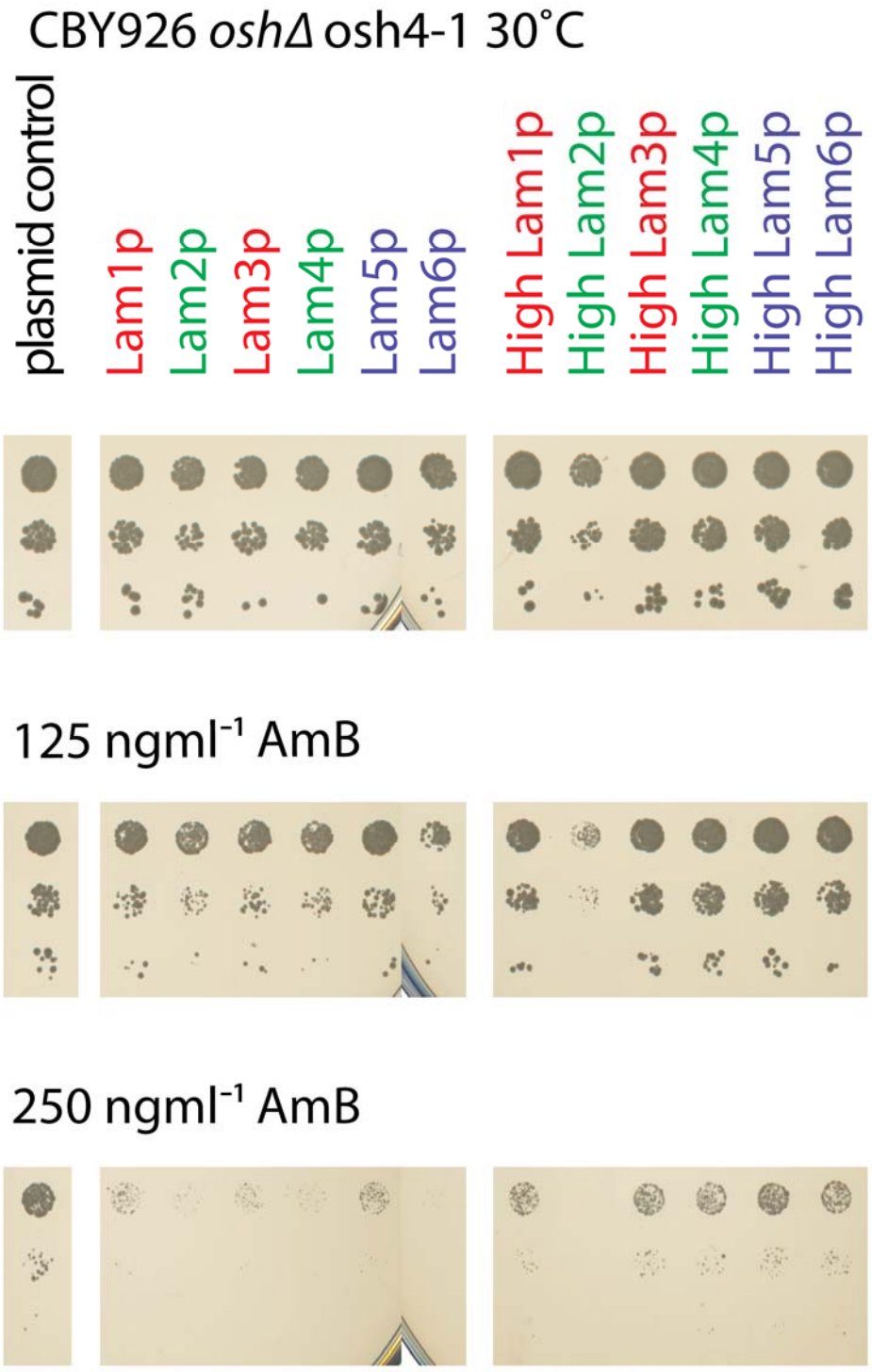

Figure 4.21 **Expression of LAMs affect CBY926 growth**
Growth assay on SD agar + 2% dextrose with various concentrations of AmB comparing the effects of high and low expression of full length LAM proteins in CBY926 *osh1-7*Δosh4^{ts} strain after 48 hours at a permissive temperature of 30°C. All additional expression of LAM proteins decreases basal resistance to AmB with the higher expression of Lam2p being significantly detrimental to basal resistance to AmB.

Notably, low expression of Lam2p, Lam4p and Lam6p shows worse growth than Lam1p, Lam3p and Lam5p. It is not possible to conclude whether the additional copies of the LAM proteins are detrimental to the *OSH* delete strain or to yeast already expressing LAM proteins in general. A repetition of this assay is required with a parallel assay on WT yeast to ascertain whether the detrimental effect on the growth of overexpressing LAM proteins is enhanced in the *OSH* delete strain.

4.2.16 Expression of LAM StARkin impairs Δ*osh* growth on AmB

As full-length LAM proteins are localised to specific contact sites, the growth assay results may differ using LAM StARkins only in Δ*osh1-7*, as the isolated domains are not tethered to particular localisations. This set up would indicate whether the StARkin domains are able to carry out a similar enough function to Δ*osh1-7* to rescue lethality. Any potential lipid binding activity of LAM StARkin domains can theoretically be performed throughout the cell, and if the lipid binding or transfer overlaps with the ORD domains in other locations, the growth of *osh1-7*Δosh4^{ts} cells can occur at 37°C. Previous growth assays in delete *LAM* strains with some isolated LAM StARkin domains have shown various levels of rescue and impairment on AmB (carried out by Alberto Gatta), and thus these domains are proven to perform an active function when expressed alone (Gatta *et al.*, 2015). However, the assay with the *osh1-7*Δosh4^{ts} strain expressing high levels of LAM StARkins showed no growth at the restrictive temperature of 37°C with the *osh1-7*Δosh4^{ts} strain [data not shown]. Therefore, there is no overlap in the function of LAM StARkin domains with the OSH family of proteins that can rescue the lethality of the *OSH* sevenfold delete.

Significant detrimental effects were not observed with the high expression of the isolated StARkins in the CBY926 *osh1-7*Δosh4^{ts} strain at permissive temperature in contrast to that seen with full-length Lam2p [Figure 4.22 + Figure 4.21]. Slight reductions in growth were observed with the expression of LAM StARkin domains, with the exception of Lam1 StARkin and Lam4 StARkin 1 (best seen in [Figure 4.22], 24 hr, no AmB). Interestingly, the expression of Lam2 StARkin 2 showed slight harmful effects on growth compared to the plasmid control on media without drug; however, on AmB the growth is similar to that of the plasmid control. This data suggests that there is a rescuing effect with the expression of Lam2 StARkin 2 on media with AmB but it is detrimental to normal growth. In contrast, Lam4S2, Lam5 StARkin and Lam6 StARkin were unable to rescue growth of AmB (best seen in [Figure 4.22], 24 hr, 45 ngml^{-1}). These differences in growth phenotypes are very slight, and further analysis on higher concentrations of AmB must be carried out for a conclusive

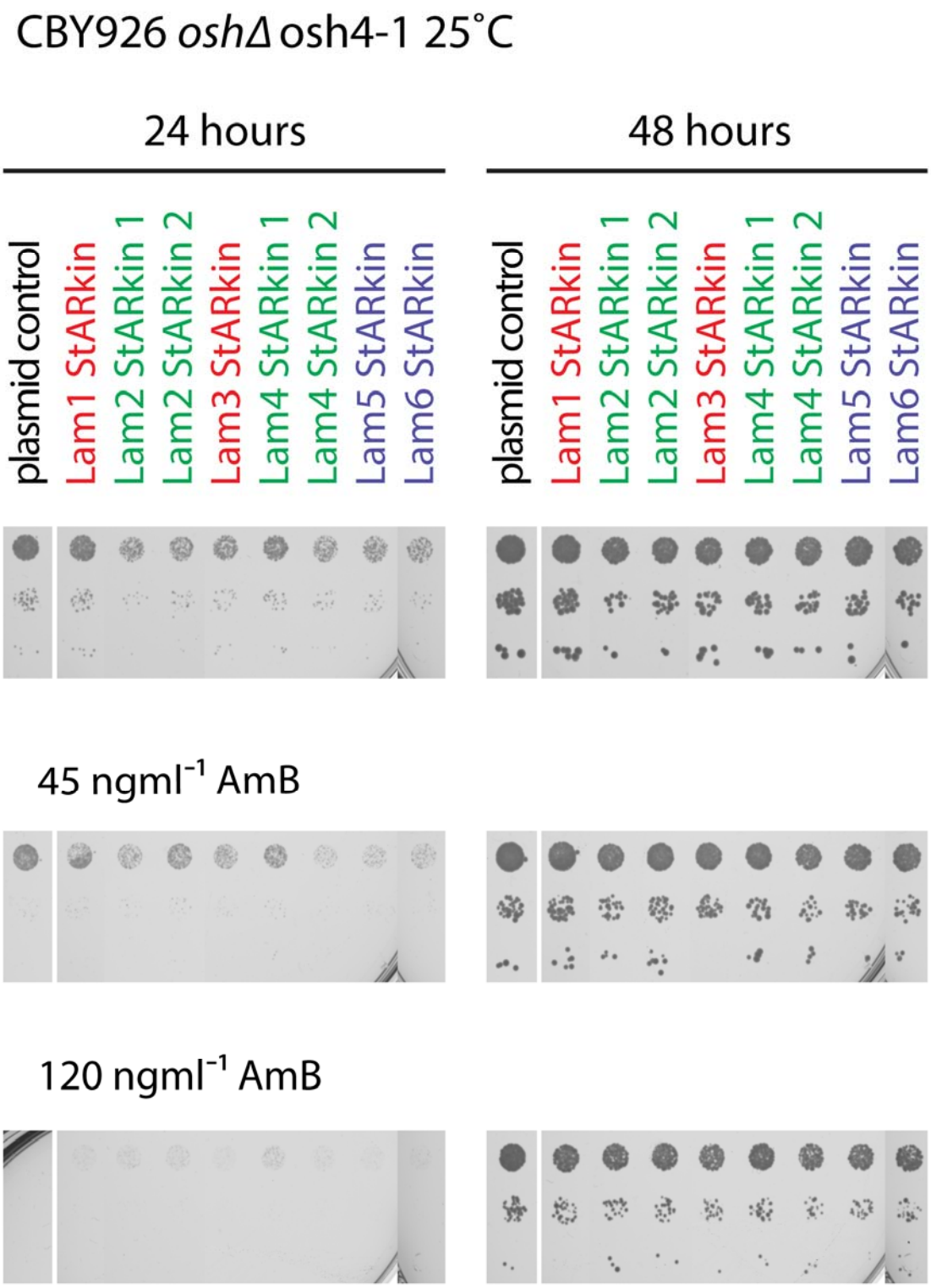

Figure 4.22 **Expression of LAM StARkins has minor effects on CBY926 growth** Growth assay on SD agar + 2% dextrose with various concentrations of AmB comparing the effects of high expression of LAM StARkin domains in CBY926 *osh1-7*Δosh4^{ts} strain at a permissive temperature of 30°C. All additional expressions of LAM StARkin domains, except Lam1 StARkin, are detrimental to the growth of the strain. The most significant decreases correspond to the expression of Lam4 StARkin 2, Lam5 StARkin and Lam6 StARkin, which were also not able to rescue growth on AmB. A slight rescue of growth is observed with the expression of Lam2 StARkin 2 where the growth on clean media fared less well than the plasmid control, but on AmB is seen to be as viable as the plasmid control.

observation on the effects of LAM StARkin domain expression. However, it is clear that the active function of the isolated LAM StARkin domains, whether beneficial or detrimental to the growth is unable to compensate for the loss of OSH proteins and thus the role of LAM StARkin domains are distinct to that of OSH proteins.

4.3 Discussion

4.3.1 Implication of role in cellular sterol transfer

The identification of a conserved StARkin domain, previously determined to be an active lipid transfer domain has implicated the involvement of this novel LAM family in intracellular sterol transport. Initial data included the appearance of *LAM4* deletion for survival in a tritium sterol uptake assay and growth phenotype on ergosterol affecting polyene drugs. During the course of this project, work by the Levine lab in addition to the Nunnari labs has added to this evidence. MLN64, a known sterol transfer mammalian StART protein has been shown to rescue delete *LAM* growth phenotype similarly to the overexpression of isolated LAM StARkin domains but not StART domains with a different lipid ligand (PCTP and CERT) (by Tim Levine (Gatta *et al.*, 2015)). The deletion of *LAM1/2/3* causes a significant decrease in *in vivo* retrograde sterol traffic (by Yves Sere, Cornell University USA) [Figure 4.23] (Gatta *et al.*, 2015). In this assay, the rate in which exogenous DHE is taken up by yeast and deposited as DHE ester is measured [Figure 4.23A]. Each single deletion of *LAM1/2/3* causes a reduction that is comparative to the defect of removing all seven OSH genes [Figure 4.23B] (Georgiev *et al.*, 2011; Gatta *et al.*, 2015).

Finally, deletion of *LAM6* prevents ergosterol-rich domain formation on the vacuole as a response to certain growth conditions (discussed below) (Murley *et al.*, 2015). The intracellular sterol activity of Lam2p has been traced to the StARkin 2 domain both by the deletion of StARkin 2 causing growth defects and by the rescue of growth defect by the isolated overexpressed StARkin 2. However, analysing growth defects on AmB is an indirect source of cellular sterol transfer evidence and therefore a more direct assay similar to *in vivo* retrograde sterol traffic experiments should be carried out with strains expression Lam2p deleted for the StARkin 2 domain.

4.3.2 Analysing activity of LAM proteins on Amphotericin B

The analysis of the activity of LAMs was based upon the phenotype observed when grown on Amphotericin B, an antifungal shown to act on ergosterol found in the PM of the yeast cell. A key consideration of using this anti-fungal to determine the sterol-linked activity of proteins is that low levels of, or the absence of, AmB sensitivity phenotype does not preclude ergosterol transfer activity of the proteins.

Notably, the removal of Lam5p or Lam6p only causes slight growth defect on AmB indicated by high throughput independent data, yet these proteins have been shown to be involved in sterol transport (Hillenmeyer *et al.*, 2008; Murley *et al.*, 2015). Isolated StARkin domains from both proteins are also able to rescue Δ*lam2* growth

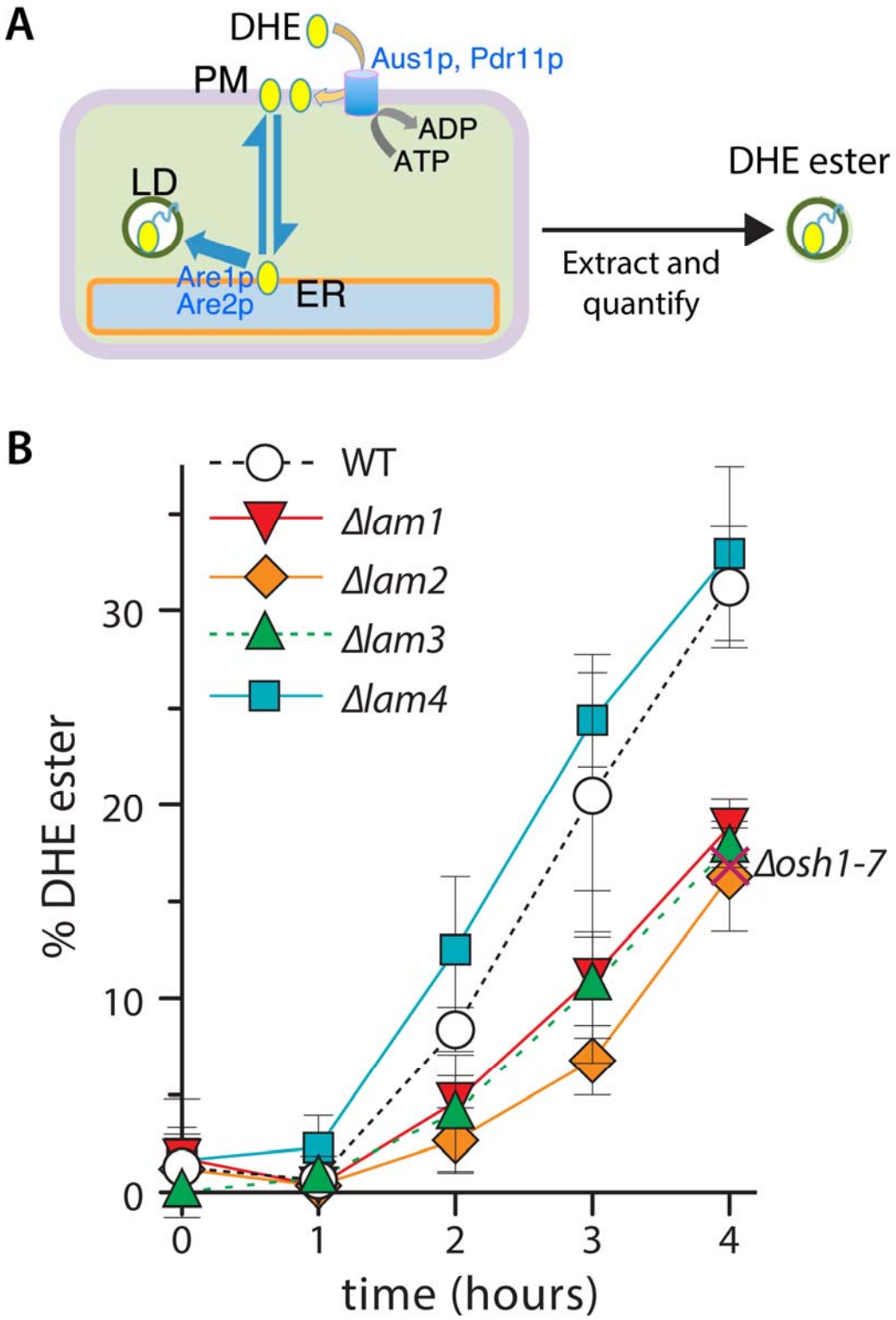

Figure 4.23 **Retrograde traffic of sterol is decreased in Δ*lam* strains**
A) Illustration of a retrograde traffic assay. Yeast are grown in conditions where it can take up exogenous DHE by ABC transporters, Aus1p/Pdr11p at the PM. It is moved to the ER by a yet undetermined mechanism/protein. ACAT enzymes, Are1p/Are2p esterify the sterol prior to storage in lipid droplets (LD). Sterols are extracted and quantified by HPLC to determine the rate in which DHE is redistributed from the PM. Adapted from (Gatta *et al.*, 2015). **B**) Retrograde traffic of DHE in Δ*lam1*, Δ*lam2* and Δ*lam3* decreases by approximately 50% compared to WT. Δ*lam4* has no defect in retrograde traffic. The equivalent defect of retrograde sterol traffic in Δ*osh1-7* compared to WT is indicated by a cross. Data from (Georgiev *et al.*, 2011; Gatta *et al.*, 2015).

phenotype on AmB (by Alberto Gatta (Gatta *et al.*, 2015)). One potential reason for the inconsistency between the AmB related function of Lam5p/6p and their StARkin domains lies with the localisation of Lam5p and Lam6p, which are at contact sites between the ER, mitochondria and vacuole (Elbaz-Alon *et al.*, 2015; Gatta *et al.*, 2015; Murley *et al.*, 2015). AmB has two charged groups and thus is an amphipathic molecule thus it would be difficult for it to cross the cell membrane alone (Baginski, Resat and McCammon, 1997). Therefore logic indicates that AmB would first act on the ergosterol in the PM rather than the intracellular sterol which the antifungal would only encounter if the intracellular sterol is transferred to the PM or if AmB was internalised. Lam5p/Lam6p cannot be directly involved in the sterol-linked activity at the PM due to their localisation, suggesting an explanation for a lesser phenotype on AmB. AmB assays on Lam2p show that the TM domain responsible for localisation activates the function of the LAM domain, as strains expressing Lam2pΔCT grow similarly to complete deletion of Lam2p, reinforcing the suggestion that Lam5p/Lam6p show minor phenotype on AmB due to their localisation and affecting non-PM sterols rather than their lack of sterol transfer activity. As demonstrated by Murley *et al.*, Lam6p is essential for ergosterol enriched regions in the vacuolar membrane which are formed under conditions such as weak acid stress (Murley *et al.*, 2015).

Conversely, the function of Lam4p is unexplained, as it does have a PM vicinity localisation yet deletion does not show a phenotype on AmB. However, the high expressions of Lam4 StARkins are able to rescue Δ*lam2* on AmB indicating a related function of the StARkin domain, as with Lam5p/6p. Therefore, key questions remain about the role and function of cellular Lam4p. Perhaps there are conditional phenotypes that are yet to be assessed (see section 7.1.4 for further discussion).

4.3.3 Natamycin assays versus AmB assays

Lam1p, Lam2p and Lam3p all reside in ER-PM contacts, and their deletions have strong growth defects on AmB and Natamycin. Natamycin is a smaller polyene suggested to act on ergosterol only rather than having other characteristics such as pore formation. It is interesting that the relative strengths of their phenotypes are reversed in order on Natamycin compared to AmB (Δ*lam2* is more sensitive to Natamycin than Δ*lam1/3* whereas Δ*lam1/3* is more susceptible to AmB than Δ*lam2*). This observation of differences on the two polyenes could be informative on the function of the proteins, however, due to the precise mode of action being unknown for both Natamycin and AmB it is hard to come to any conclusion. Derivatives of AmB that are altered for a lack of pore formation ability could be tested in parallel to Natamycin and unaltered

AmB in order to compare growth defects in strains missing LAM proteins (Gray *et al.*, 2012).

4.3.4 Links between Lam2p and Lam3p

The expression levels of the LAM proteins affected the growth of yeast on AmB. High levels of Lam3p were detrimental to growth. In work we published, this manipulation of Lam3p was shown to mislocalise Lam2p (Gatta *et al.*, 2015). It was found that endogenous levels of Lam3p only localise to the pmaER rather than nER (Gatta *et al.*, 2015), which is seen when Lam3p was highly expressed. This mislocalisation of Lam3p to the nER was seen to be responsible for the mislocalisation of Lam2p to the nER which was not seen when Lam2p itself was overexpressed. The additional high expression of Lam3p in strains already expressing Lam3p but not Lam1p or Lam2p was detrimental to growth on AmB compared to the same in Δ*lam3* where there is no endogenous Lam3p, but there is still a presence of Lam1p and Lam2p. A precise balance of LAM protein levels could be required for normal function of Lam1p/Lam3p and Lam2p. Due to the common localisation of these three LAM proteins, perhaps the co-regulation is indicative of a complex involving all or a combination of these LAMs.

4.3.5 Functions of Lam2p domains

Deletions of specific domains in Lam2p show that the activity of Lam2p relies on the second StARkin, which can be replaced with the second StART of Lam4p. Confirmation that the predicted StARkin domain is functional and active during growth on AmB reinforces the idea that sterol transport occurs via the StARkin domains. However, it is still unclear what function the other domains have. Even less obvious is the long N-terminus in Lam2p that is predicted to be largely unstructured.

In addition to the removal of StARkin 2, loss of function of endogenous Lam2p also occurred with the deletion of the localising C-terminus (including the TM domain) indicating that a significant aspect of the activity of the protein is the correct localisation. Overexpression of isolated Lam2 StARkin 2 rescues the growth defect on AmB (shown by Alberto Gatta) (Gatta *et al.*, 2015). Targeting this domain to membranes that are not the PM or the ER membrane (where Lam2p normally localises at ER-PM contacts), for instance to mitochondria, removed its rescuing functionality (shown by Tim Levine (Gatta *et al.*, 2015)). This evidence indicates that the functionality works only at the correct position – at ER or PM. Adjacent to the first StARkin domain on Lam2p is a PH-like domain in the GRAM family. The most studied function of PH domains is their ability to interact with PI lipids in different membranes,

therefore directing proteins to a specific membrane localisation. Despite having this membrane interacting domain, localisation of Lam2p is reliant only on the transmembrane and C-terminal domain (shown by Alberto Gatta (Gatta *et al.*, 2015)) suggesting that there is one or more docking or scaffold protein involved in a LAM to protein interaction via the C-terminal rather than a LAM to membrane interaction via the PH domain. If the lipid-binding domains (PH or StARkin domains) were involved, the Lam2p C-terminus only should not be localised in punctate dots. Instead, it should be diffuse in the ER. This data implies that the localisation of the Lam2p at contact sites between the two membranes is due to the C-terminus that is localised within the ER when it is in contact with the PM. It is likely that there is an interaction between the C-terminus of Lam2p and a yet unidentified protein, which can regulate and localise Lam2p.

4.3.6 Possible interactions between Lam3p and Lam2p

The overexpression of Lam3p is shown to mislocalise Lam2p, leading to speculation of an interaction between the two proteins (Gatta *et al.*, 2015). If Lam3p and Lam2p do indeed interact, the interaction must be strong enough to overcome the localisation of Lam2p, which raises the question of the role of Lam3p in the localisation of Lam2p. However, there may be a third party to this interaction. It would be beneficial to test the localisation in Δ*lam3* or a Δ*lam1*Δ*lam3* double delete. If Lam3p does localise Lam2p via Lam2p C-terminus, it remains to be seen how Lam3p localises itself to contact sites. Lam3p has a PH domain-like Lam2p. However, Lam3p also has a BAR domain that might target the plasma membrane. Analysis of Lam3p deleted for its various domains would be required to test for domain activity and protein localisation. In addition, there is a question of the existence of additional interactor(s) of Lam2p/Lam4p and Lam1p/Lam3p at ER-PM contact sites. Lam6p has been studied in detail in two recent papers, and it is suggested that Lam6p dynamically interacts with Vac8p, a vacuolar protein, and Tom70/71p, mitochondrial proteins (Murley *et al.*, 2015). Lam6p was also found to co-purify with members of the ERMES complex (Elbaz-Alon *et al.*, 2015; Murley *et al.*, 2015). It is likely that there are ER or PM proteins that the Lam1p/Lam3p and Lam2p/Lam4p can interact with in a similar fashion. Possible investigations using co-purifications of Lam1-4p may yield the identities of protein interactors.

4.3.7 Lam1p/3p membership of the LAM family

The StARkin domains of Lam1p and Lam3p are quite varied compared to the remaining LAM members, such that both Khafif *et al.* and Murley *et al.* identified the

StARkin domains of only Lam2p, Lam4p, Lam5p and Lam6p (Khafif *et al.*, 2014; Murley *et al.*, 2015). The isolated StARkin domains of Lam1p and Lam3p do not show rescuing effects in delete *LAM* strains (demonstrated by Alberto Gatta (Gatta *et al.*, 2015) and in Figure 4.19) and as such the evidence suggests a divergence in function between the StARkin domains of Lam1p/3p and Lam2p/4p/5p/6p. However, there is a significant growth defect of Lam1p/3p on ergosterol sequestering polyenes, which indicates a role with cellular ergosterol levels. For a more complete data set, Lam1p/3p domains can be tested for function by sequential deletion. It is possible that Lam1p/3p are more dependent on their accessory domains for function, for example, due to an interaction with a yet unknown partner that can activate Lam1p/3p, or that Lam1p/3p itself activates a protein partner. It is important to note that bacterial expression of Lam1/3p StARkin domains failed due to the formation of insoluble aggregates within the cells (carried out by Alberto Gatta, personal communication) and thus the inactivity of Lam1/3p StARkin could be due to problems with the constructs.

4.3.8 Lam5p/6p

During this investigation, microscopy carried out by Tim Levine and Alberto Gatta showed that Lam5p/Lam6p targeted contact sites at the NVJ, mitochondrial-ER contacts and also ER-vacuole (VancE) contacts (Gatta *et al.*, 2015). In other studies that occurred simultaneously in the Schuldiner lab and the Nunnari lab, Lam6p was found to interact with ERMES, but the regulation of Lam6p localisation depends on other interactions (Elbaz-Alon *et al.*, 2015; Murley *et al.*, 2015). When Lam6p is located between at VancE contacts or the NVJ, it interacts with Vac8p, and when Lam6p is located at ER-mitochondrial contacts, it interacts with Tom70/71p (Murley *et al.*, 2015). Overexpression of Lam6p causes all these contacts to enlarge, though the formation of these contacts is not dependent on the presence of Lam6p (Elbaz-Alon *et al.*, 2015; Gatta *et al.*, 2015). It is suggested that Lam6p is a regulator of these contact sites and that the excess of Lam6p at any contact encourages enlargement of the contact site (Elbaz-Alon *et al.*, 2015). Indeed, ER-mitochondria contact enlargement that occurs as compensation due to the absence of vCLAMP does not occur when Lam6p is also removed (Elbaz-Alon *et al.*, 2015).

As with other members of the LAM family, Lam5p/Lam6p consists of the StARkin domain along with a transmembrane domain and a PH domain. It is this PH domain that is found to mediate the interaction with Tom70/71p on mitochondria (Murley *et al.*, 2015), though it is unknown how it interacts with Vac8p. In normal growth conditions, Lam6p is found at these ER-mitochondria contacts, but when these

contacts are disturbed with the deletion of one component of the ERMES complex or when the removal of the Tom70/71p interacting PH domain disrupts the mitochondrial targeting, Lam6p is rerouted to ER-vacuolar contacts. Under certain stress situations such as glucose starvation, ergosterol-rich domains are formed on the vacuolar membranes. This stress response cannot occur without the presence of Lam6p, and the genetic redirecting of Lam6p to ER-vacuole contacts promotes the spontaneous formation of these ergosterol-rich domains when yeast are not stressed. In addition, full-length Lam6p minus the TM C-terminal domain shows transfer activity with *in vitro* transfer assays and together, the evidence implicates a strong link between Lam6p (without the PH and TM C-terminal domain) and ergosterol accumulation (Murley *et al.*, 2015).

4.3.9 LAMs, a contender to OSH as the major sterol transporter

The active LAM StARkin domains are unable to substitute for the essential shared function of OSH proteins. Therefore, the shared function of OSH proteins does not overlap with the LAM StARkin domains. Previously, the most likely candidate for intracellular sterol transport was the family of OSH proteins. However, studies have suggested that OSH proteins cannot be solely responsible for cellular sterol transport as the sevenfold *OSH* delete strain shows only a 50% decrease in *in vivo* retrograde sterol transfer (Georgiev *et al.*, 2011). Alternatively, deletion of only one LAM protein (Lam1p, Lam2p, or Lam3p) also causes a 50% fall in *in vivo* retrograde sterol transfer [Figure 4.23B] (Gatta *et al.*, 2015).

The evidence of altered sterol regulation in delete strains, along with the presence of a shared StARkin domain enables the novel LAM protein family to become a strong contender for the cellular ergosterol traffic role. The creation of a sixfold *LAM* delete strain may further decrease measured *in vivo* sterol transfer, which would indicate that LAM protein indeed has a major role in sterol traffic.

Major questions remain about the cellular function of LAM and OSH proteins. Nonetheless, these two protein families both have strong claims for roles in intracellular sterol transport. Further definition of intracellular sterol transport will involve resolving these questions, as any discoveries in either family would aid the knowledge of the other.

4.3.10 Key results

This chapter probed the cellular functions of the novel LAM family of six proteins in budding yeast. The conserved StARkin domain of Lam2/4/5/6p is active and responsible for the basal resistance to ergosterol sequestering AmB. Mutations in

Lam4S2 including G1119R prevented the activity which activates AmB resistance. The localisation of Lam2p at ER-PM contacts is also fundamental to its activity most likely due to directing its activity to the PM or ER membranes where it is found. Though Lam1/3p is essential for growth on AmB and has an ER-PM localisation, unlike the other LAM members, Lam1/3p StARkin alone cannot substitute for the full-length protein. Sequence homology of Lam1/3p is also the most removed from the other members. In addition, evidence suggests a distinct function to the essential role of the OSH family.

CHAPTER 5

Fungal LAM characterisation

5.1 Introduction

Deletions of LAM proteins from laboratory strains of *Saccharomyces cerevisiae* (*Sc*) showed a decrease in tolerance to polyene antifungals including AmB. Budding yeast is not known for causing invasive disease, however, other fungi strains are involved in serious and deadly infections of animals and plants. The growth phenotype of delete *LAM*s on AmB invites speculation on whether this growth sensitivity would be relevant for pathogenic fungal strains. There are a limited number of antifungal agents and reports of resistance to many of these antifungals have increased in recent years. The polyene class of antifungals seems to be a robust molecule with very rare reports of resistance and further investigations show that these mutations usually coincide with a decrease in pathogenicity of the fungi themselves (Vincent *et al.*, 2013). AmB is one of the most effective antifungals but is used as the last resort treatment for patients suffering from Aspergillosis as the detrimental side effects from the drug itself often cause fatality. In fact, a focus of many pharmaceutical investigations is to find ways to deliver Amphotericin B to patients in a safer and more efficient system. Therefore, it is tempting to hypothesise that if the LAMs can be disrupted, the dosage of Amphotericin B (AmB) used in patients could be decreased thus lowering detrimental side effects. In this chapter, the LAM protein family will be explored in the wider fungi kingdom to identify any homologous function.

5.1.1 Aspergillus infections

Aspergillus is a genus of fungus that is found worldwide, growing as a filamentous mould on organic matter, usually in the soil, on plants or on decomposing organic debris (Segal, 2009). Although there are hundreds of species, only a handful causes human illness with most infections caused by *Aspergillus fumigatus* (*Af*). Other species include *Aspergillus flavus*, *Aspergillus terreus*, *Aspergillus niger*, and *Aspergillus nidulans*.

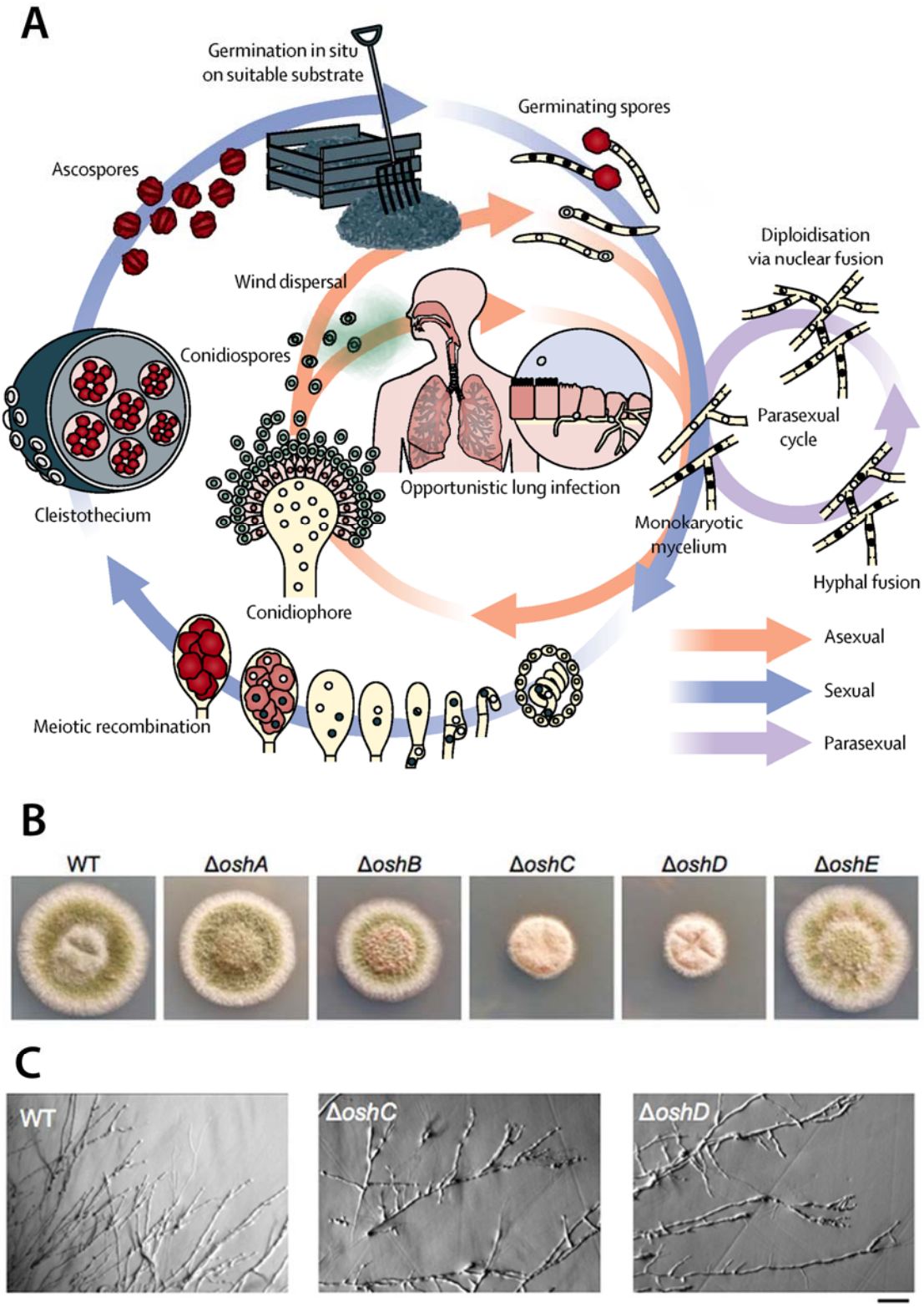

Figure 5.1 **Life cycle of *Aspergillus* and phenotypes of Δ*osh Aspergillus nidulans*** **A**) Diagram of the life cycle of *Aspergillus*. Figure from (Verweij *et al.*, 2016). **B**) Colonies are WT and *oshA-E*Δ strains grown for 3 days on minimal medium glucose. **C**) Hyphal morphology of WT, Δ*oshC* and Δ*oshD*. Scale bar shows 100 µm. Figures from (Bühler, Hagiwara and Takeshita, 2015).

Inhalation of spores, also known as conidia, is the usual route of infection [Figure 5.1A]. Clinical illness following inhalation of conidia is dependent on the health of the host. A normal individual inhales several hundred *Af* conidia per day, which would be harmless to those with a healthy immune system. However, immunocompromised patients do not have a sufficient defence mechanism, rendering them vulnerable to infection by opportunistic fungi. These infections can be fatal even with treatment with mortality rates being as high as 95% (Brown *et al.*, 2012). In fact, invasive aspergillosis is the leading infectious cause of death in immunocompromised patients (Garcia-Vidal *et al.*, 2015).

In individuals without severe impairment of the immune system, *Af* can cause a variety of pulmonary diseases, including asthma, invasive aspergillosis, aspergilloma, hypersensitivity pneumonitis and allergic bronchopulmonary aspergillosis. Long-term exposure to fungal spores can cause inflammation in sensitive individuals, which can develop into allergic conditions such as asthma.

5.1.2 Cryptococcus infections

Much like *Aspergillus* infections, exposure to *Cryptococcus* occurs via the inhalation of spores. This fungal infection usually presents as meningoencephalitis due to its specificity of targeting the central nervous system (Taylor-Smith and May, 2016). Cryptococci cells are able to survive alveolar macrophage phagocytosis allowing access to the blood system and thus the blood brain barrier. Cryptococci cause over 1 million life-threatening infections yearly. As with Aspergillosis, Cryptococcosis infections are increased in immunocompromised individuals with mortality rates reaching as high as 70% in AIDS patients (Brown *et al.*, 2012).

5.1.3 Treating invasive fungi

Fungal infections are harder to treat than bacterial infections. The difficulty in fighting fungi as human pathogens is due to fungal kingdom members being eukaryotic and thus more evolutionarily close to humans than prokaryotes. Therefore, there is an additional complexity for finding molecules that are toxic to fungi but not humans. Ergosterol is a fungal-specific sterol lipid (cholesterol is the human form), and thus many antifungals target ergosterol or ergosterol synthesis.

5.1.4 Evolution of ergosterol

Ergosterol is thought to have developed with the emergence of the fungi kingdom. There are rare species of fungi thought to be evolutionally less advanced which synthesise cholesterol rather than ergosterol (Weete, Abril and Blackwell, 2010). These primitive members of the fungi kingdom are usually flagellated and are aquatic

dwelling species. Ergosterol requires additional steps that are not involved in cholesterol biosynthesis. Intermediate sterol molecules such as C-24 methyl and ethyl sterols are found in some fungi species thus it is suggested that the ability to synthesise ergosterol evolved through progressive steps. As such, it is possible that ergosterol is specifically advantageous for the survival of higher, more complex fungi in a solid environment or a solid-air interface. It is likely that pathogenic fungi, such as Aspergillosis causing species, require very specialised homoeostasis of ergosterol to counter air, liquid and solid surfaces such as within a lung environment.

5.1.5 Sterol in biofilm formation

In addition to the universal function of sterol in the plasma membrane as a lipid component that increases the rigidity of the cell barrier (see section1.2.2 for more details on the role of sterols in membranes), it has been suggested that ergosterol is also essential to several characteristics of invasive and filamentous fungi.

Biofilms are multicellular communities composed of layers of cells, hyphae and a protective exopolysaccharide matrix which adhere to the surface of medical implants and cause persistent infections with increased mortality as opposed to free floating yeasts (Uppuluri *et al.*, 2010; Ramage *et al.*, 2012). Ergosterol is necessary for biofilm formation of *Candida,* as shown by the inhibition of growth and formation of biofilms upon treatment with statins, a molecule which prevents ergosterol synthesis. The addition of exogenous ergosterol reverses this effect suggesting it to be specifically sterol or a downstream event that allows this distinctive growth (Chandra *et al.*, 2001; Mukherjee *et al.*, 2003; Westermeyer and Macreadie, 2007; Liu *et al.*, 2009).

5.1.6 Sterol in growth of infectious fungi

Sterol is uniformly distributed in the unicellular growth of *Saccharomyces cerevisiae,* the main model organism used in this investigation. However, there are some controversies regarding the schmoo formation, a specialised mating growth type of budding yeast, where some groups suggest that there is a higher concentration of sterol at the tips (Bagnat and Simons, 2002; Valdez-Taubas and Pelham, 2003). Hyphal growth in filamentous fungi requires extreme growth at the tip allowing invasion of the host by the fungi. The Spitzenkorper structure located at the hyphal tip is responsible for the extreme polarisation of growth and supplies a concentration of secretory vesicles at the tip (Grove and Bracker, 1970; Howard, 1981; Harris *et al.*, 2005).

Regions of high sterol content observed in actively growing plasma membrane are termed ‘sterol-rich domains’. For example, in *Aspergillus* the tips of the invading hyphae are enriched in sterol (Li, 2005). The size of these domains (3-15 μm^2) is

distinct to so-called ‘lipid rafts’ which proposed to be on average 75 nm^2 (Alvarez, Douglas and Konopka, 2007). Sterol-rich regions at hyphal tips have been linked to cell polarisation, cytoskeleton rearrangement, endocytosis and membrane strength during penetration of host cells. However, their exact role in pathogenicity remains elusive. It is important to note that although filipin is often used to detect sterol-rich domains, it is also widely accepted that there is potential to cause detrimental effects on membrane structure. However, there has been attempt to minimise the formation of artefacts by altering staining protocols as well as using dyes such as Laurdan which show differences in lipid packing to verify the presence of membrane domains (Proszynski *et al.*, 2006; Van Leeuwen *et al.*, 2008).

Studies with *Cryptococcus neoformans* suggest that virulence factors such as superoxide dismutase are localised to detergent-resistant membranes which are displaced by extracting ergosterol (Siafakas *et al.*, 2006). Other proteins that are involved in pathogenicity such as laminin-binding protein, an adhesion protein necessary for fungal-host interaction, are suggested to also to be displaced by ergosterol extraction (Tagliari *et al.*, 2012). Thus there is importance for ergosterol-rich domains in the pathogenicity of infectious fungi. In addition, the deletion of Erg4 homologues in *Af*, proteins responsible for the final step of ergosterol biosynthesis, caused severe impairment to the formation of conidia which was reversed with extracellular ergosterol but there was no effect on hyphae phenotype (Long *et al.*, 2017). In another fungus, *Fusarium graminearum*, a plant pathogen, the deletion of *ERG4* showed changes in conidia structure and hyphal growth (Liu *et al.*, 2013). Some anti-fungal drugs disturb this distribution of sterol at the hyphal tips, indicating that sterol-rich domains can be a target for antifungal action (Mania *et al.*, 2010).

Additionally, the genetic manipulation of *ARV1* in *Candida albicans* perturbed normal ergosterol homoeostasis, affected normal hyphal formation and caused the strain to be avirulent (Gallo-Ebert *et al.*, 2012; McCourt *et al.*, 2016). In yeast, Arv1p is an essential gene when Are1/2p are also removed and has been proposed to affect sterol homoeostasis but not carry out direct intracellular sterol transport (Georgiev *et al.*, 2013). The association between the virulence of *Candida* and proper sterol homoeostasis indicates that the maintenance of normal sterol distribution is essential for the infectious growth of pathogenic fungi.

Three widely used antifungal drug categories are azoles such as Voriconazole, polyenes such as AmB and Allylamines such as terbinafine (Ghannoum and Rice, 1999; Alcazar-Fuoli and Mellado, 2012). These drugs target ergosterol or the biosynthesis of

ergosterol in disease-causing fungi. This indicates that targeting ergosterol is an effective way of treating fungal infections.

5.1.7 OSH homologues in *Aspergillus*

The OSH protein family, which has been linked to intracellular sterol transport, is composed of seven members in *Sc*. *Aspergillus nidulans* (*An*) has five such OSH proteins. ER morphology of *Aspergillus* is similar to that of budding yeast in that there are clear regions of nuclear ER and plasma membrane-associated ER around the periphery of the cell (Maruyama, Kikuchi and Kitamoto, 2006). However, the distribution of pmaER strands increases towards the hyphal tips in *Aspergillus* (Maruyama, Kikuchi and Kitamoto, 2006). *Sc*Osh3p is clearly localised to ER-Golgi contacts, which was observed to be the case for *An*OshB in *Aspergillus* including in the hyphae (Bühler, Hagiwara and Takeshita, 2015). All other *An*OSH are also localised to their *Sc*OSH homolog equivalent including *Sc*Osh6/7p equivalent, *An*OshD, which was diffuse with occasional puncta at the edge of ER strands at the PM.

Deletions of *An*OSH proteins showed various phenotypes such as growth rate reduced down to 50% with the removal of *An*OshC/D (homologous to sterol binding *Sc*Osh4p/5p) and impaired conidiation down to 70% spores in Δ*An*OshD (Bühler, Hagiwara and Takeshita, 2015). Hyphal morphology was also altered in *ΔAnOshC/D* corresponding to the strains with the most severe growth defect [Figure 5.1B+C]. In these strains, there were more branches formed in the hyphae, and *ΔAnOshD* suffered cell lysis at the hyphal tips when grown without osmotic stabilisers. It is likely that the reduction in growth colony diameter is due to the defect in long hyphal formation of the strain. Instead, multiple branching would reduce the colony size compared to WT hyphal morphology.

In contrast to *ScOSH* deletion where cellular sterol levels were seen to increase, *AnOSH* deletes show reductions in ergosterol levels up to 60% compared to WT and their sensitivity to azoles and polyenes was altered. However, sterol-rich domains at hyphal tips were not affected in *An*OshA-D. Interestingly, *An*OshE with no budding yeast homologue was found to be necessary for sterol-rich domains of hyphae and although there was no growth defect, the delete strain had the most severe decrease in conidiation.

It is noteworthy that the strains with the most defective growth are *ΔAnOshC* and *ΔAnOshD*, homologous to Osh4/5p and Osh6/7p thought to transport sterol and PS respectively with PI4P. Though it is untested, it is feasible that *Aspergillus OSH* deletes may have lowered pathogenicity due to the growth defects. If the OSH protein family

has a role in ergosterol (discussed in section 1.5.2 on ORPs), it is possible that loss of pathogenicity is caused by ergosterol disruption. Understanding the role of ergosterol and ergosterol regulation would be beneficial for investigations for further antifungal discovery. It would be interesting to investigate these characteristics in *Aspergillus* deleted for LAM proteins, which we have suggested to be an alternative candidate for cellular sterol transport to the OSH family.

5.1.8 Aspergillus KU80 strain

In the previous chapter, homologous recombination was used to replace genes in *Sc* strains with marker cassettes to create delete strains. Though homologous recombination is the primary DNA-break repair pathway in yeast, other processes can be utilised such as non-homologous end joining. The rate of homologous integration in *Af* is highly inefficient due to the activation of other DNA repair pathways. The Ku70-Ku80 heterodimer is part of the machinery that mediates non-homologous end joining. By removing one of either *KU70* or *KU80*, homologous recombination is boosted due to the loss of non-homologous end joining (da Silva Ferreira *et al.*, 2006; Krappmann, Sasse and Braus, 2006). In a *KU80*Δ strain, homologous integration increased to 80% from 3% in the WT strain (da Silva Ferreira *et al.*, 2006). The *KU80*Δ strain showed no loss of virulence, and so its creation has been used in many studies as a parental strain to delete genes (Krappmann, 2006; Paul, Diekema and Moye-Rowley, 2013; Bruder Nascimento *et al.*, 2016). In this investigation, I will use the *KU80*Δ strain to delete endogenous *LAM* genes in *Af.*

5.1.9 StARkins superfamily

Bioinformatic tools which also score secondary structure revealed the presence of a subfamily, named LAM, of conserved StARkin domains which is also present in yeast (Khafif *et al.*, 2014; Gatta *et al.*, 2015; Murley *et al.*, 2015). The StARkin superfamily is proposed by us as a replacement name for the SRPBCC superfamily that groups proteins with the distinct helix-grip fold. SRPBCC is an abbreviation for StART/ RHOαC /PITP/Bet v1/CoxG/CalC which are all members of this superfamily. However, it is suggested that the RHOαC subfamily is different to that of the StART and Bet v1 folds due to differences in sequence homology (Iyer, Koonin and Aravind, 2001).

5.1.10 Investigation of StARkins in fungi

Members of the LAM family have yet to be investigated in fungi other than in budding yeast (in this study and recent studies by Elbaz-Alon *et al.* and Murley *et al.)*. In this chapter, I will explore the LAMs in other fungal species to investigate whether the characteristics of *Sc*LAM proteins are shared across the fungi kingdom.

5.2 Results

5.2.1 LAM family in fungi

There are six members of the LAM family in budding yeast, characterised as three pairs. The duplication of the whole genome results in the protein pair formation so there are only three different domain architectures. However, not all of these LAM types are found in fungi. In *Af* there are two LAM proteins. One is similar to *Sc*Lam1p/3p, and the other has similar domain order to that of *Sc*Lam5p/6p. On the other hand, *Cryptococcus neoformans* has only the *Sc*Lam5p/6p-like LAM protein [Figure 5.2]. *Candida albicans* has four LAM family members with domain architecture akin to *Sc*Lam5p/6p and *Sc*Lam1p/3p [data not shown].

It is important to note that the domain structure of *Sc*Lam2p/4p, being highly specific to the Saccharomycetes class of fungus, is not a common occurrence across the kingdom. Although *Aspergillus, Cryptococcus* and *Fusarium* have LAM members with similar domain architecture to *Sc*Lam5p/6p, the StARkin domains themselves are equally similar to both *Sc*Lam2p/4p and *Sc*Lam5p/6p pairs. This suggests that the earliest Lam2p/4p developed from Lam5p/6p-like proteins.

The *Sc*Lam1/3p LAM type is unique to the fungi kingdom though not all fungi possess this protein and are the most divergent by sequence compared to the *Sc*Lam2p/4p and *Sc*Lam5p/6p. The coexistence of *Sc*Lam1p/3p and *Sc*Lam2p/4p/5p/6p in most fungi suggests that the event of a double LAM StARkin domain structure in *Sc*Lam2p/4p came after the event of *Sc*Lam1p/3p. Lam5p/6p is universal to eukaryotes with humans having three homologous (*Hs*LamA/B/C). Thus the earliest form of the LAM protein would be the Lam5p/6p-like.

5.2.2 DUF3074

The LAM proteins are a newly identified family of proteins containing StART-like domains identified in the StARkin superfamily. Among these LAM members in the fungi and plants, there are various domain architectures that are slightly different to that of the six *Sc*LAM members. One such domain architecture belonging to *Fusarium oxysporum* is *Fo*LamB, which is largely homologous to *Sc*Lam1p/3p. However, it is extended to contain an additional StARkin labelled as DUF3074 [Figure 5.2]. Bioinformatics shows that DUF3074 has a similar predicted structure to StARkin, although, the DUF3074 domain is fungus-specific with no members in *Sc*.

5.2.3 StARkin domain clustering

To better gauge the relationship between the LAM family of StARkin domains and the DUF3074 family of StARkin domains, a sequence clustering was carried out

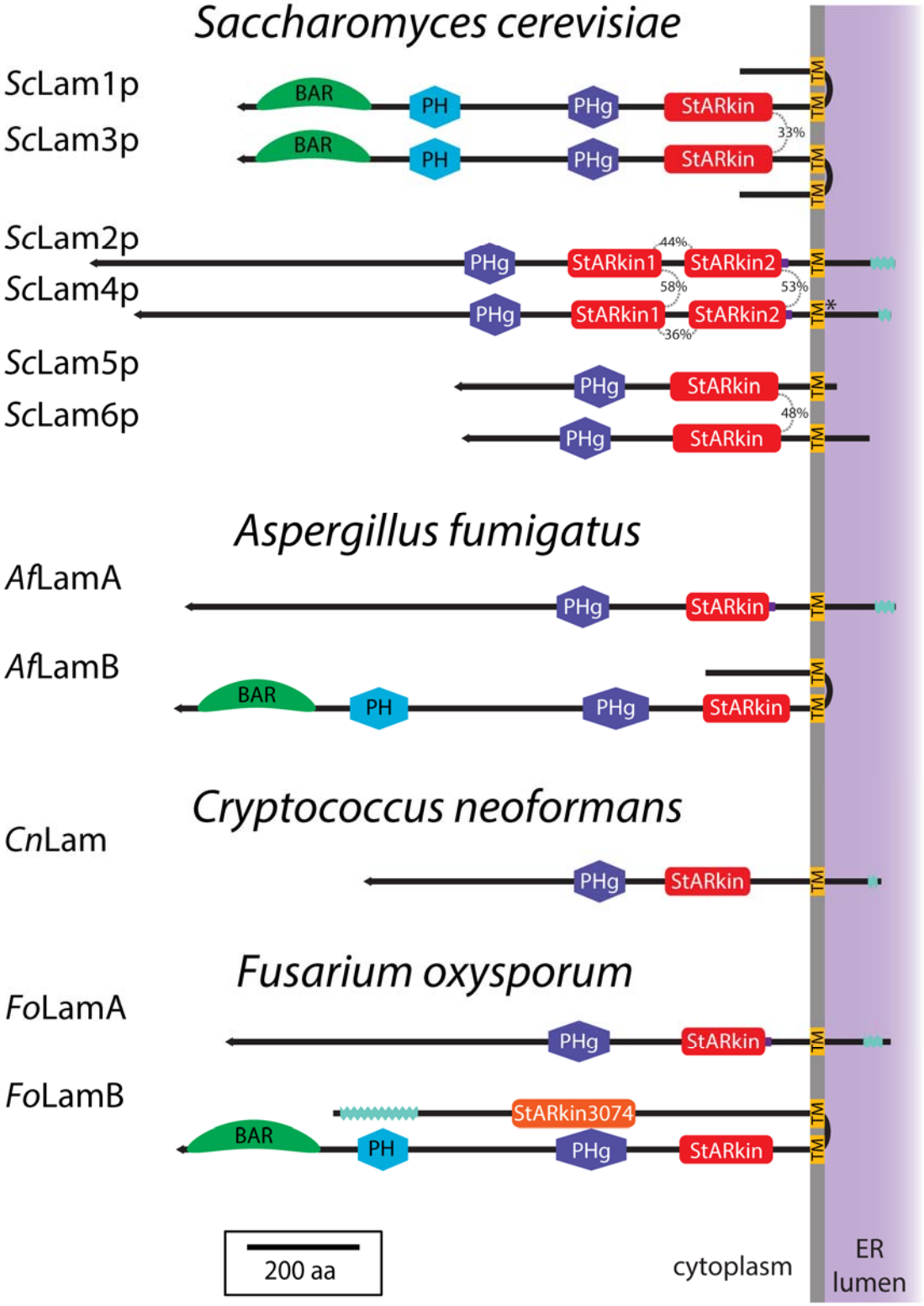

Figure 5.2 **LAMs in yeast and filamentous fungi**
Diagrams of the domain architecture of LAM proteins in *Saccharomyces cerevisiae, Aspergillus fumigatus, Cryptococcus neoformans* and *Fusarium oxysporum.* The sequence similarity is indicated for *Sc*Lams. * indicates a transmembrane domain (TM) that is not strongly predicted. Significant predicted coiled coils are illustrated by a light blue irregular shape. LAM StARkin domains are indicated in red whereas the StARkin domain belonging to the DUF3074 is coloured orange. The physical lengths of the diagrams are proportional to the sequence length where possible. The tapered end indicates the N-terminus.

with CLANS (Cluster Analysis of Sequences) (Frickey and Lupas, 2004). The advantage of using CLANS is that a comparison can be made with large numbers of proteins and be shown efficiently on a single image. In comparison, a phylogenetic tree would be difficult to arrange with large numbers of sequences and a linear relationship would be shown where the rooting would be a major source of error. CLANS visually shows all versus all PSI-BLAST searches and arranges each sequence as a function of their similarity to all other sequences in 3D space, allowing multiple relationships with a large number of other sequences (images were acquired as 2D maps for clarity).

Sequences of members of each subfamily in the SRPBCC and StARkin superfamily were collected and culled so that a total of 2000 sequences were obtained. The culling kept the most divergent of sequences in each subfamily, and these sequences were clustered using the CLANS (Cluster Analysis of Sequences) program [Figure 5.3]. Each sequence is illustrated as a dot and PSI-BLAST was carried out with 8 iterations using BLOSUM62. The p-values are shown by the shade of line connecting each sequence – the lower the p-value, the darker the line.

Using this tool, a map is generated using a p-value cut-off of $1x10^{-5}$. This p-value is still significant to indicate no links with a control group of proteins of similar length (TBOX). At this p-value, DUF1731 does not show sequence homology with any other StARkin domain subfamily, however, 3D structure suggests that it has a helix-grip fold, similar to that of the StARkin family.

RhoαC has been proposed to be excluded from the StARkin domain due to an altered structure where the β-sheet does not grip around the elongated α-helix. However, it shows very low levels of sequence homology to some StARkin members demonstrated by links indicated on the CLANS clustering. At a higher p-value cut-off of $1x10^{-15}$, the RhoαC/Pf11723 cluster disconnects from the main cluster map as do RCAR and PaO [data not shown]. As confirmed with 3D structure, RCAR has a clear StARkin domain. However, PaO domains (found at the C-terminus of Rieske-type enzymes) are very short and do not form a full StARkin fold [Figure 5.4].

The cluster map shows a concentration of most StARkin members at one centre. Figure 5.5 shows a CLANS clustering using a higher p-value cut off of $1x10^{-20}$ with all sequences unconnected to the 'core' group removed for clarity (sequences within the dotted of Figure 5.3 and DUF3809). At this higher p-value cut-off of $1x10^{-20}$, sequence similarity between LAM StARkin domains and the core StARkin group was not detected [Figure 5.5]. This family was only detected as StARkins with the use of a structural homology program and the predicted 3D structure clearly shows a helix-grip

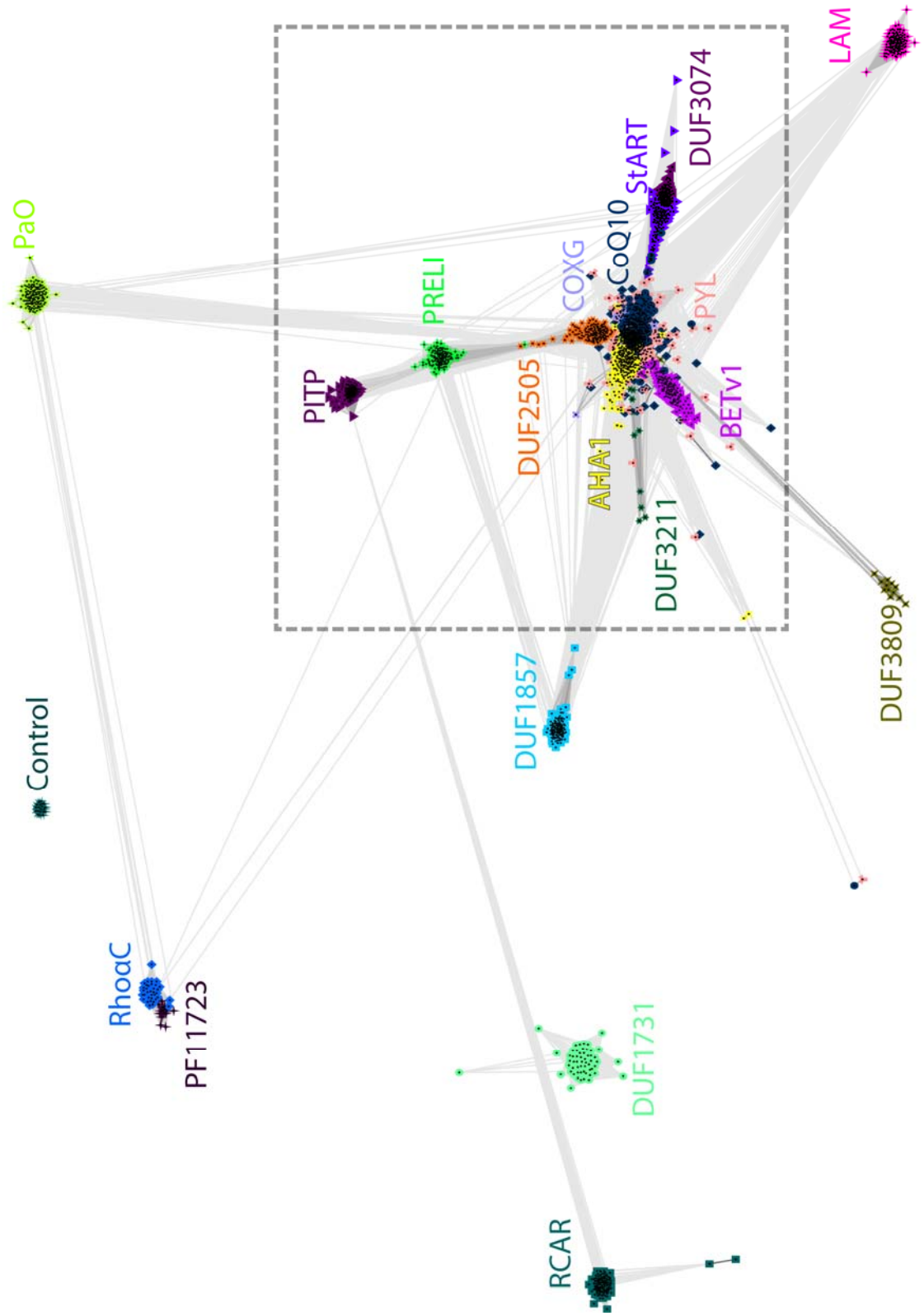

Figure 5.3 **CLANS clustering of StARkin superfamily**
CLANS clustering of the StARkin domain superfamily with all-against-all pairwise similarities as measured by PSI-BLAST. A maximum of ~140 sequences from each subfamily were obtained by PISCES culling to keep the most divergent. The total number of sequences was ~2000. p-value = $1x10^{-5}$. Control proteins were TBOX, a domain of similar size to StARkins (~150 aa). The dotted box shows where Figure 5.5 is zoomed in to use a higher p-value threshold. Each dot represents one sequence. Sequences within each subfamily are indicated by the same colour. Lines represent a hit and the intensity in dictates the p-values. The lightest line indicates a p value of $1x10^{-5}$ and the darkest line represents a p-value $1x10^{-324}$.

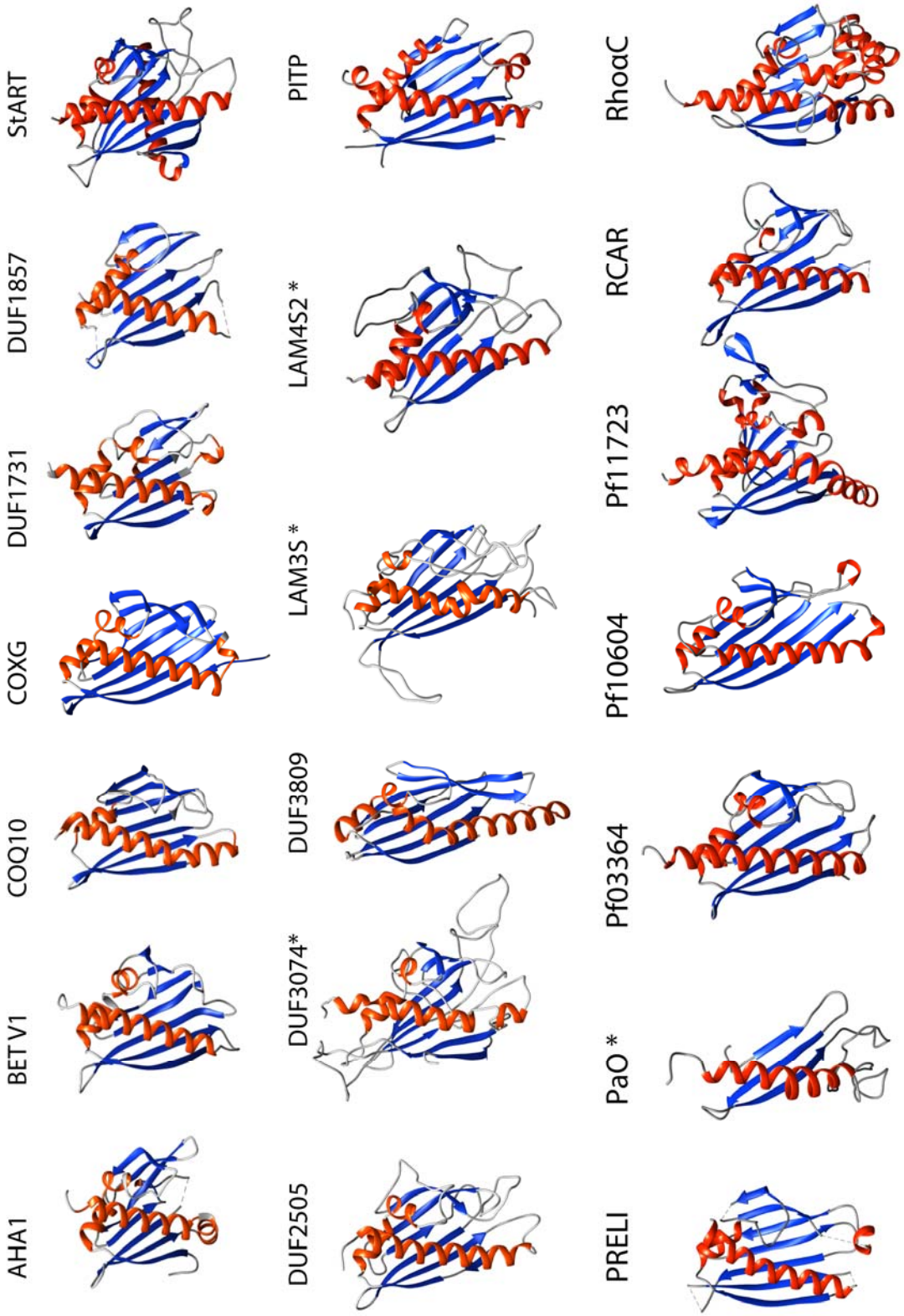

Figure 5.4 **3D structures of StARkin superfamily members**
3D models of an example of all subfamilies used in the StARkin CLANS clustering. * denotes a predicted structure using alignments by HHPred and Modeller. AHA1: 1XFS, Bet V1: 1BV1, CoQ10: 1T17, COXG: 2NS9, DUF1731: 3OH8, DUF1857: 2FFS, StART: 1EM2, DUF3809: 3NQN, PITP: 1UW5, PRELI: 4XZV, PaO: predicted, Pf03364: 2RER, Pf10604: 3PQV, Pf11723: 4NBA, RCAR: 3K9O, RHOαC: 3EN1A

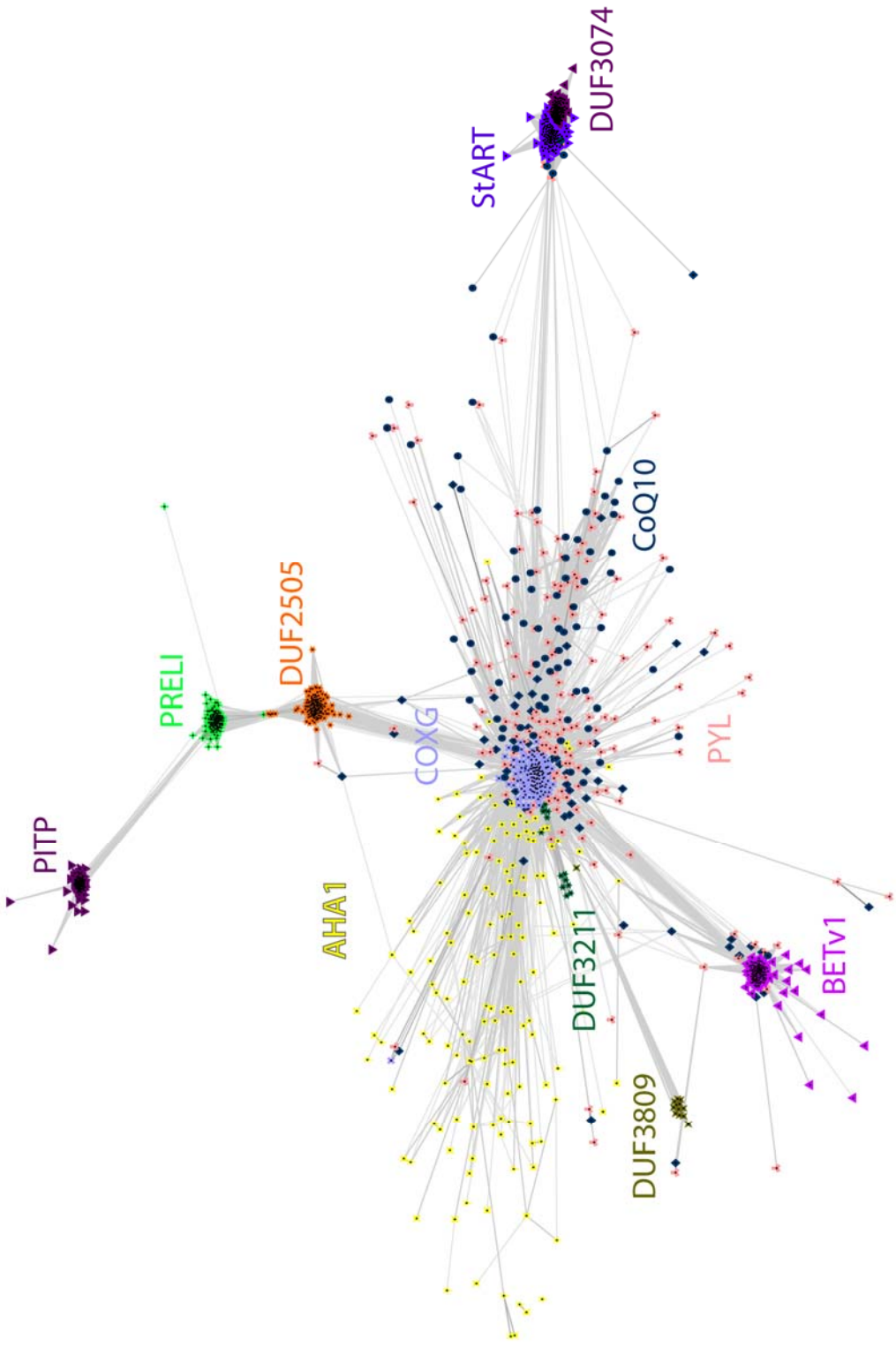

Figure 5.5 **CLANS clustering of select StARkin subfamilies**
CLANS clustering of a subset of the StARkin domain superfamily with all-against-all pairwise similarities as measured by PSI-BLAST. The subset of sequences used includes all sequences in the dotted box from Figure 5.3 and also DUF3809 which after the use of a higher p-value threshold moved into the vicinity of the core groups. p-value = $1x10^{-20}$. Each dot represents one sequence. Sequences within each subfamily are indicated by the same colour. Lines represent a hit and the intensity in dictates the p-values. The lightest line indicates a p value of $1x10^{-20}$ and the darkest line represents a p-value $1x10^{324}$

fold.

The ‘core’ group of StARkin members of the most similar by sequence includes COXG, PYL, CoQ10, AHA1 and DUF3211 subfamilies. The AHA1 StARkin domain is at the C-terminal of the full-length proteins. Of these subgroups, COXG is most central, and the sequence is fairly well conserved. AHA1, CoQ10 and PYL subfamilies show more dispersion, perhaps due to the large size of these families. Radiating out from this core group are DUF2505, DUF3809, Bet v1, and finally the StART/DUF3074 cluster. The group of sequences of StART and DUF3074 is extremely close indicating very high similarity between the two subgroups. DUF2505 is the intermediate group between the core and PRELI, a recently confirmed StARkin member where the StARkin fold is dependent on TRIAP1 (Miliara *et al.*, 2015; Watanabe *et al.*, 2015; Yu *et al.*, 2015). PITP is linked to the other StARkin members by only via connections to PRELI.

5.2.4 DUF3074 compared to StARkin

CLANs clustering of SRPBCC/StARkin family members show that DUF3074 is very closely related to the StART subfamily of proteins [Figure 5.5]. This is in contrast to the LAM StARkin domains (DUF4782) which are one of the most removed subfamilies of StARkins from the ‘core’ group. There is no similarity hit between LAM StARkin domains and DUF3074 StARkin domains by CLANS even at p-value cutoff of $1x10^{-1}$ suggesting that there is no sequence homology link between these StARkin domains [data not shown]. However, both domains show links to the StART, CoQ10, CoxG and DUF2505 subfamilies. LAM sequence homology is weighted towards DUF2505, mostly found in bacteria, whereas DUF3074 is weighted towards the StART subfamily.

Most DUF3074 StARkin containing proteins are short with only the DUF3074 domain being annotated in contrast to LAMs, which have various membrane-associating domains such as BAR and transmembrane helices. Bioinformatic searches for other domains or transmembrane helices yielded no results, with the exception of the combined LAM and DUf3074 protein [Figure 5.2 *Fo*LamB]. However, a common feature is a predicted coiled coil of varying length. It is perhaps surprising that there is an occurrence of the DUF3074 domain in some Lam1/3p which would restrict the localisation of this otherwise short protein to specific contact site localisation. SignalIP, a program detecting sequence homology to known signal peptide cleavage sites detected no cleavage sites, and thus this DUF3074 domain would be targeted to ER-PM contact sites, similar to *Sc*Lam1p/3p.

5.2.5 Expression of StARkin domain from *Cn*LAM Rescues AmB Phenotype

In the infectious fungi*, Cryptococcus neoformans* (*Cn*), there is one LAM family member with a domain order similar to that of the Lam5p/6p protein pair found in *Sc* [Figure 5.1]. Using purified genomic DNA, the StARkin domain of the single *Cn*LAM family member was cloned without introns and transformed into *Sc*. The growth defect of WT, Δ*lam1,* Δ*lam2*, Δ*lam3* and Δ*lam1/2/3* was assessed on Amphotericin B with a GFP-expressing plasmid as a control or highly expressed StARkin domain from *Cn*LAM protein [Figure 5.6B]. Δ*lam1/2/3* is a strain produced by Diana Calderón-Noreña (Cornell University USA), which has *LAM1*, *LAM2* and *LAM3* deleted in the BY4741 background. This strain has a severe growth defect on AmB, which is more serious than any of the single *LAM* deletes [Figure 5.6B].

All strains expressing *Cn*Lam StARkin were less sensitive to AmB than the same strains expressing the control plasmid. Not only was it able to rescue the *ScLAM* deletes, it was also able to increase the growth of the WT strain on Amphotericin B. This demonstrates the shared role of the LAM StARkin domain across the fungi kingdom for the basal resistance to ergosterol sequestering AmB. However, it does not clarify if the *Cn* gene is orthologous to *LAM2/4* or to *LAM5/6*, since domains from all of these rescues, and phylogenetic trees put the *Cn* protein equally distant from all these *Sc*LAMs (Gatta *et al.*, 2015).

5.2.6 Expression of StARkin domain from *Cn*DUF3074 does not rescue AmB phenotype

The second protein possessing a StARkin domain is a short protein consisting of only the DUF3074 domain [Figure 5.6A]. The DUF3074 StARkin domain sequence was also extracted without its introns and introduced in budding yeast strains, WT, Δ*lam1,* Δ*lam2*, Δ*lam3* and Δ*lam1/2/3*. There was no significant difference between the strains expressing a plasmid control or the DUF3074 StARkin domain with or without AmB, though it could be argued that there is a marginal increase of growth in WT and the single deletion strains [Figure 5.6B]. Repeats of this assay would determine whether this slight rescue is reproducible. Nevertheless, it is clear that DUF3074 shows functional differences to the LAM domain. The CLANS sequence clustering suggested that the DUF3074 subfamily of StARkin domains is very different to the LAM StARkin subfamily. However, *Sc*Lam1p/3p StARkins are homologous to other yeast LAM StARkins yet do not rescue AmB growth (see section 4.2.14 + Figure 4.19 for experiments using *Sc*Lam3p). Therefore, further investigation will be required to confirm that LAM StARkins and DUF3074 StARkins have distinct, unrelated functions.

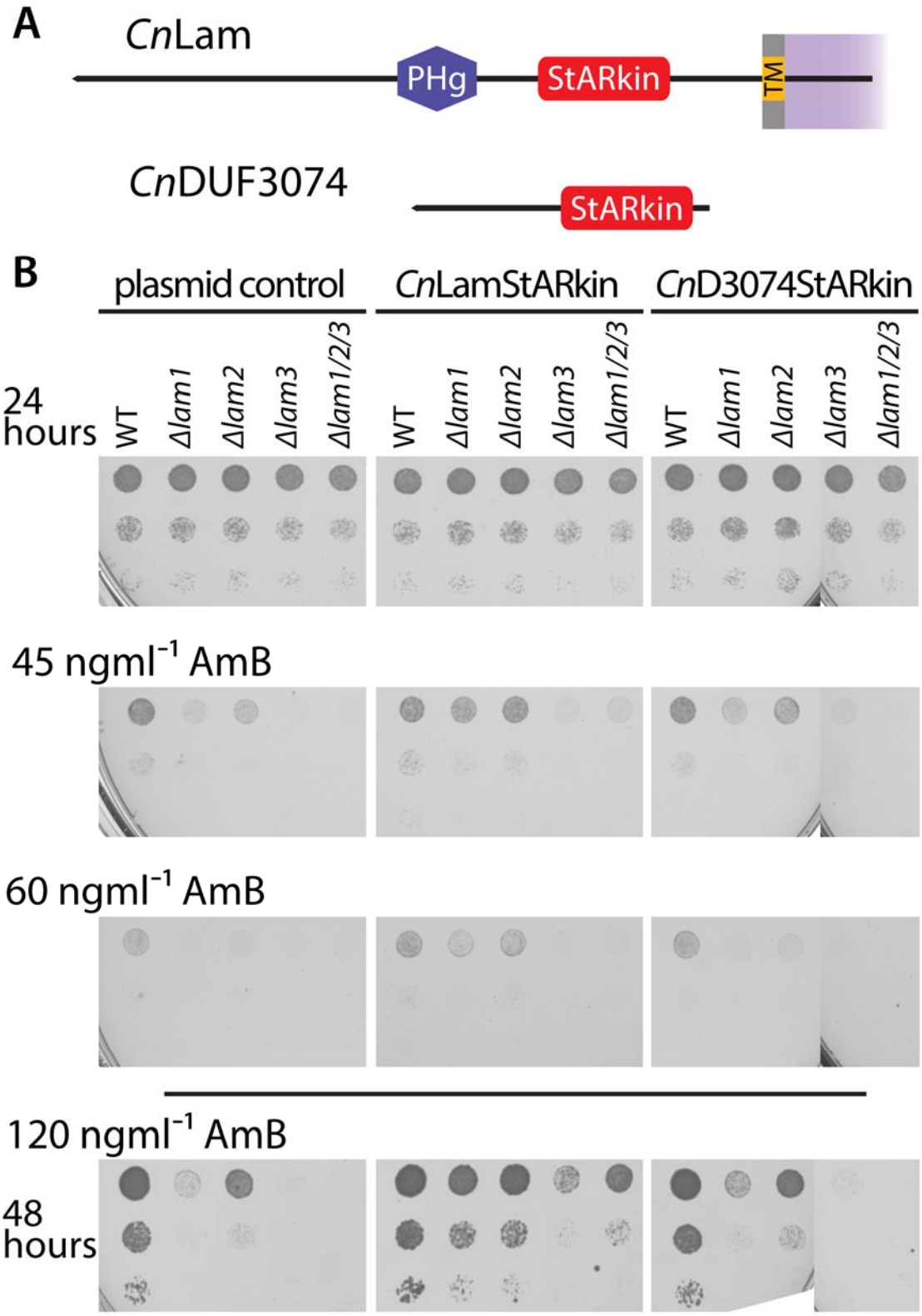

Figure 5.6 ***Cryptococcus* LAM StARkin functions similarly to *Sc*LAMs**
A) Diagram showing domains of *Cryptococcus neoformans* LAM protein and DUF3074. Both proteins contain a StARkin domain; however there is no DUF3074 homologue in *Sc*. *Cn*Lam is homologous to *Sc*Lam2p/4p/5p/6p. The tapered end indicates the N-terminus. **B**) Growth assay on SD agar + 2% dextrose with various concentrations of AmB comparing the effects of high expression of *Cryptococcus neoformans* LAM StARkin and DUF3074 StARkin in BY4741 *Saccharomyces cerevisiae* strain. There is significant rescue of growth on AmB with the expression of the isolated *Cn*Lam StARkin domain compared to the plasmid control. The expression of the StARkin domain of DUF3074 did not rescue growth on AmB.

5.2.7 Expression of StARkin domain from *Af*LAM Rescues AmB Phenotype

ScLAM delete growth assays show that the most sensitive strains are Δ*lam1,* Δ*lam3* and Δ*lam2.* To further characterise LAM proteins in other fungi *Af*, another filamentous fungus, was used. In this species, there are two LAM proteins. *Af*LamA has a similar domain structure to *Sc*Lam5p/6p and *Af*LamB is homologous to *Sc*Lam1p/3p [Figure 5.7A]. Again, the StARkin domains from both *Af*LAM proteins were cloned without introns from genomic DNA and expressed in *Sc* strains deleted for *ScLAM*s. The isolated *Af*LamA StARkin domain was significantly rescued growth of all the yeast delete strains on AmB. The expression of *Af*LamA StARkin could completely substitute for the removal of full-length *Sc*LAM proteins. All delete *ScLAM* strains grew as well as WT when expressing *Af*LAM StARkin.

In contrast, the StARkin domain from *Af*LamB showed no rescue or even slight impairment to growth in all strains except for Δ*lam3* where there is a marginal increase in growth. This follows the same data seen when expressing *Sc*Lam3 StARkin domain, the homologous yeast StARkin that showed minor detrimental effects to the growth of yeast on AmB.

5.2.8 Fusion PCR strategy for *Aspergillus* gene deletion

Budding yeast LAM proteins are essential for the AmB resistance. This characteristic has been taken advantage of for the analysis of this family and their StARkin domains [CHAPTER 4 + Figure 5.6 + Figure 5.7]. It is attractive to hypothesise that if this phenotype is shared across the fungi kingdom, LAM proteins could be targeted as a secondary target alongside AmB treatment for fungal infections. To expand the investigation into the role of LAMs in *Aspergillus*, further experiments were carried out in *Af*.

As homologous recombination is not as efficient in *Aspergillus* as in *Sc*, a *KU80*Δ parental strain was used (labelled as WT from hereafter). This strain is deleted for a subunit in a complex responsible for non-homologous end joining process thus stimulating the rate of homologous recombination. This boosts the success of homologous gene replacement. 1-2 kbp homologous regions flanking the ORF are required in the PCR knockout product, greatly increased from *Sc,* which only requires 50 bp. As such, fusion PCR was carried out to produce the product whereby two separate PCR products were combined in a second PCR run [Figure 5.8A]. The hygromycin selection cassette was utilised as the metabolic marker, which replaced the targeted *Af* genes [Figure 5.8B]. 1.5 kbp upstream and 1.5 kbp downstream of the

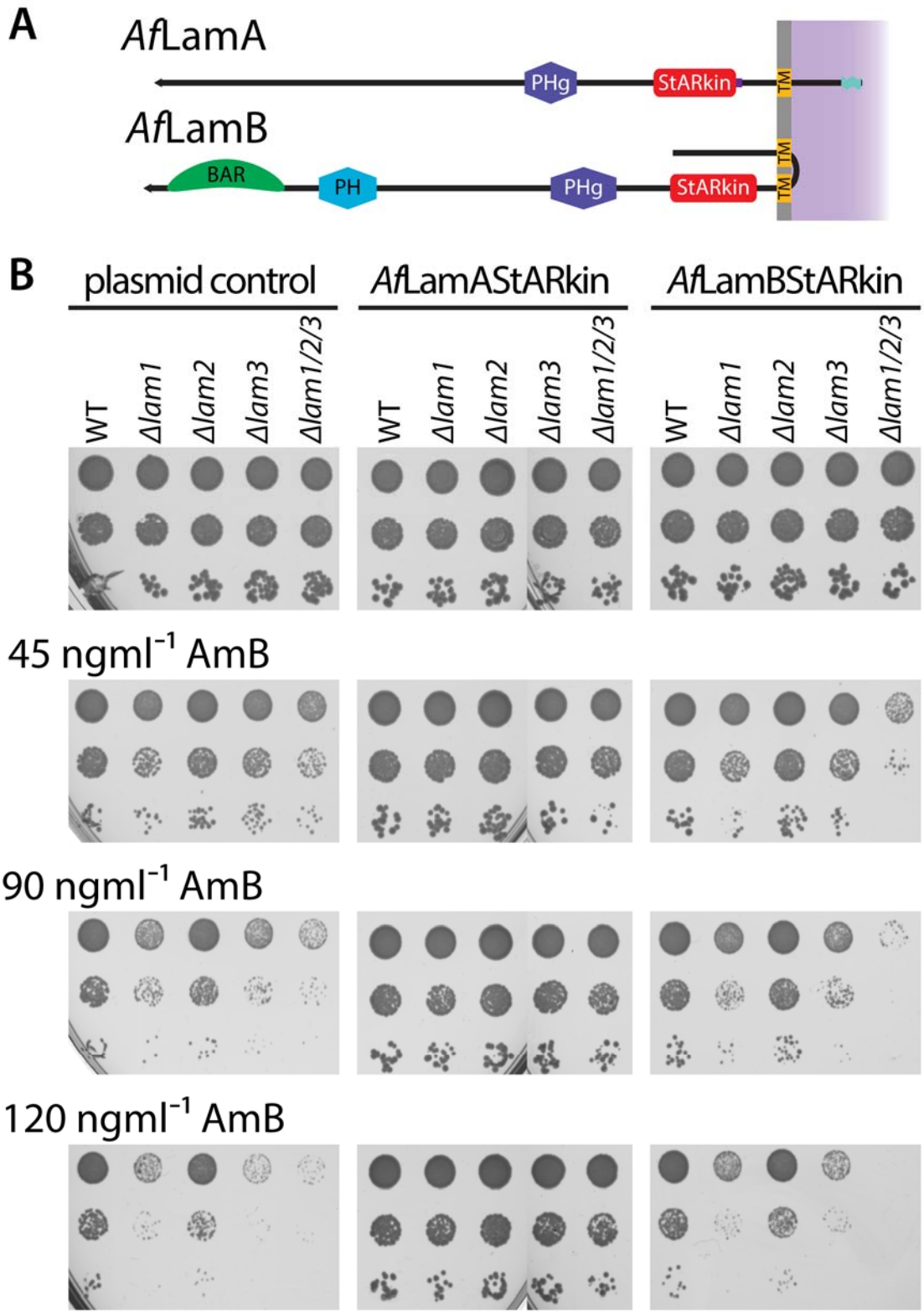

Figure 5.7 ***Aspergillus* LAM StARkin functions similarly to *Sc*LAMs**
A) Diagram showing domains of *Aspergillus fumigatus* LAM proteins. LamA is homologous to *Sc*Lam2p/4p/5p/6p and LamB is homologous to *Sc*Lam1p/3p. The tapered end indicates the N-terminus. **B**) Growth assay on SD agar + 2% dextrose with various concentrations of AmB comparing the effects of high expression of *Aspergillus fumigatus* LamA StARkin and LamB StARkin in BY4741 *Saccharomyces cerevisiae* strain. There is significant rescue of growth on AmB with the expression of the isolated *Af*LamA StARkin domain compared to the plasmid control. The expression of the *Af*LamB StARkin domain did not rescue growth on AmB.

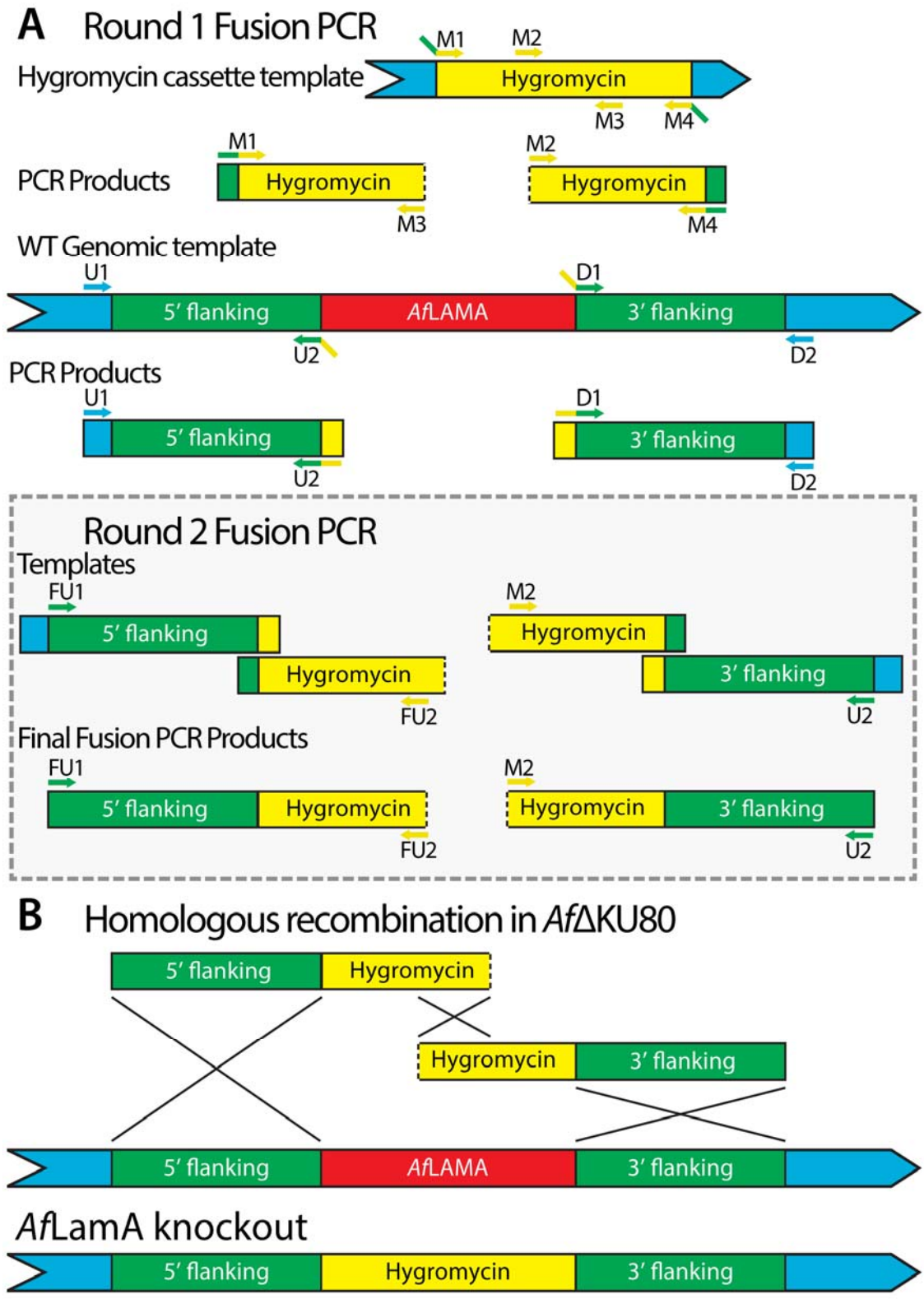

Figure 5.8 **Fusion PCR for *Aspergillus* gene deletion**
A) Diagram showing the process of fusion PCR for the gene replacement product to be used in *A. fumigatus KU80*Δ strain. The first round of PCR isolates 1.5 kbp genomic DNA flanking either side of the target gene and the hygromycin cassette. The second round of PCR joins the genomic DNA and the hygromycin cassette together. **B**) Diagram showing the homologous recombination that allows gene replacement of *Af*LamA for the hygromycin selection cassette. 1.5 kbp either side of the gene is involved in homologous recombination with the genome and 1.5 kbp of the two hygromycin sections overlap for homologous recombination to complete the hygromycin cassette.

AfLAM was fused with the majority of either end of the hygromycin cassette so that two final products were obtained with the marker overlapping by approximately 1.5 kbp. During successful transformation, the 3' and 5' flanking DNA integrates with genomic DNA and the hygromycin areas of the insert overlaps generating a complete marker cassette thus replacing the endogenous *AfLAM* (Nielsen *et al.*, 2006).

Af prepared protoplasts were transformed with the purified PCR knockout products and colonies were obtained within 48 hours. After two successions of isolating single colonies, genomic DNA was extracted for genotyping.

5.2.9 *Af*LamA and *Af*LamB are not essential genes

PCR genotyping of DNA extracted from single colonies twice isolated from the initially transformed colony was carried out to minimised chances of colonies with both WT and transformed nuclei. The presence of both WT and mutant nuclei can occur in *Af* due to the nature of filamentous fungi allowing coenocyte formation when nuclear division occurs without cytokinesis. It is important to note that Southern blotting is the gold standard for *Af* genotyping because of its high accuracy (though it is not always used (Paul, Diekema and Moye-Rowley, 2013)). Due to laboratory restrictions, it was not carried out for genotyping these colonies. However, the PCR genotyping strategy was designed to minimise PCR genotyping inaccuracies. Multiple reactions were performed to confirm the homologous replacement of *Af*LamA and *Af*LamB [Figure 5.9A + Figure 5.10A]. One reaction (primers F1 + R1) confirmed the presence of the hygromycin cassette. Two reactions (primers F2 + R2 and F4 + F3) confirmed successful incorporation of both sections knockout DNA by testing for the unique recombined DNA otherwise not found in WT. The last reactions (primer F4+ R4 and F5 + R5) detect the presence of WT DNA by producing products found within the *AfLAM* genes themselves.

Both *Af*LamA and *Af*LamB were successfully deleted from the parental strain [Figure 5.9A + Figure 5.10A]. Colony 1.2 *AflamA*Δ and colony 2.1 *AflamB*Δ were used in experiments from here on. Two additional rounds of colony isolation were carried out, and a glycerol stock was kept for routine strain refreshment.

5.2.10 AmB MIC is reduced in *Aflam*Δ

In some *ScLAM* delete strains, there was severe growth phenotype on AmB. To test the growth of *AfLAM* delete strains, MICs (minimal inhibitory concentrations) were determined using the EUCAST method [Figure 5.11 + Table 5-1].

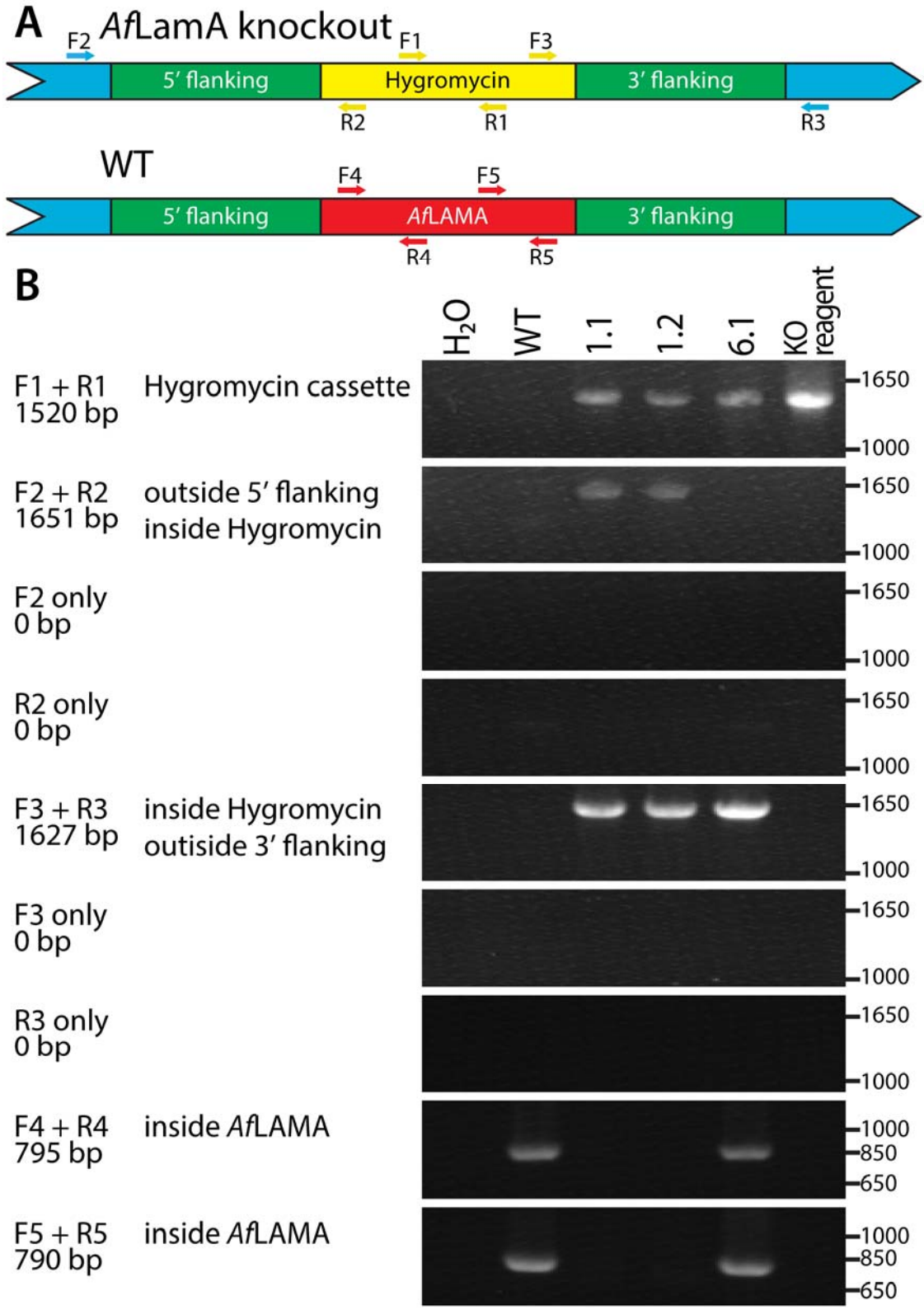

Figure 5.9 **PCR genotyping of *AfLamA*Δ**
A) Diagram showing the positions of the genotyping primers for genotyping *AfLamA*Δ colonies. F1 + R1 test for the presence of the hygromycin cassette. F2 + R2 and F3 + R3 would only be present in colonies where homologous recombination was successful. F4 + R4 and F5 + R5 would be present in colonies with WT DNA. **B**) PCR genotyping of colonies obtained after transformation. Colonies were singled out twice for DNA extraction. Colonies 1.1 and 1.2 were successful transformants with no residual WT DNA.

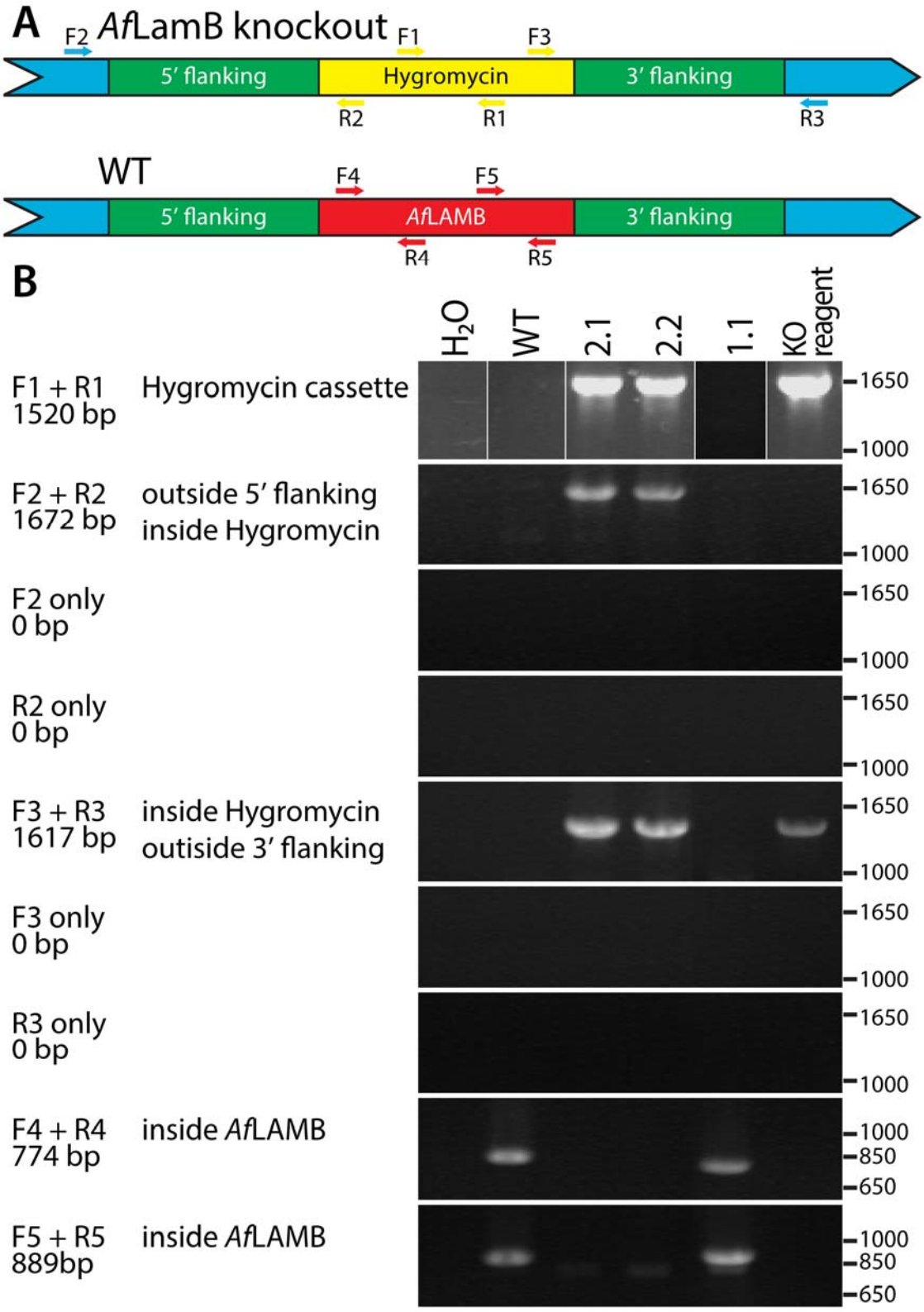

Figure 5.10 **PCR genotyping of *AfLamB*Δ**
A) Diagram showing the positions of the genotyping primers for genotyping *AfLamB*Δ colonies. F1 + R1 test for the presence of the hygromycin cassette. F2 + R2 and F3 + R3 would only be present in colonies where homologous recombination was successful. F4 + R4 and F5 + R5 would be present in colonies with WT DNA. **B**) PCR genotyping of colonies obtained after transformation. Colonies were singled out twice for DNA extraction. Colonies 2.1 and 2.2 were successful transformants with no residual WT DNA.

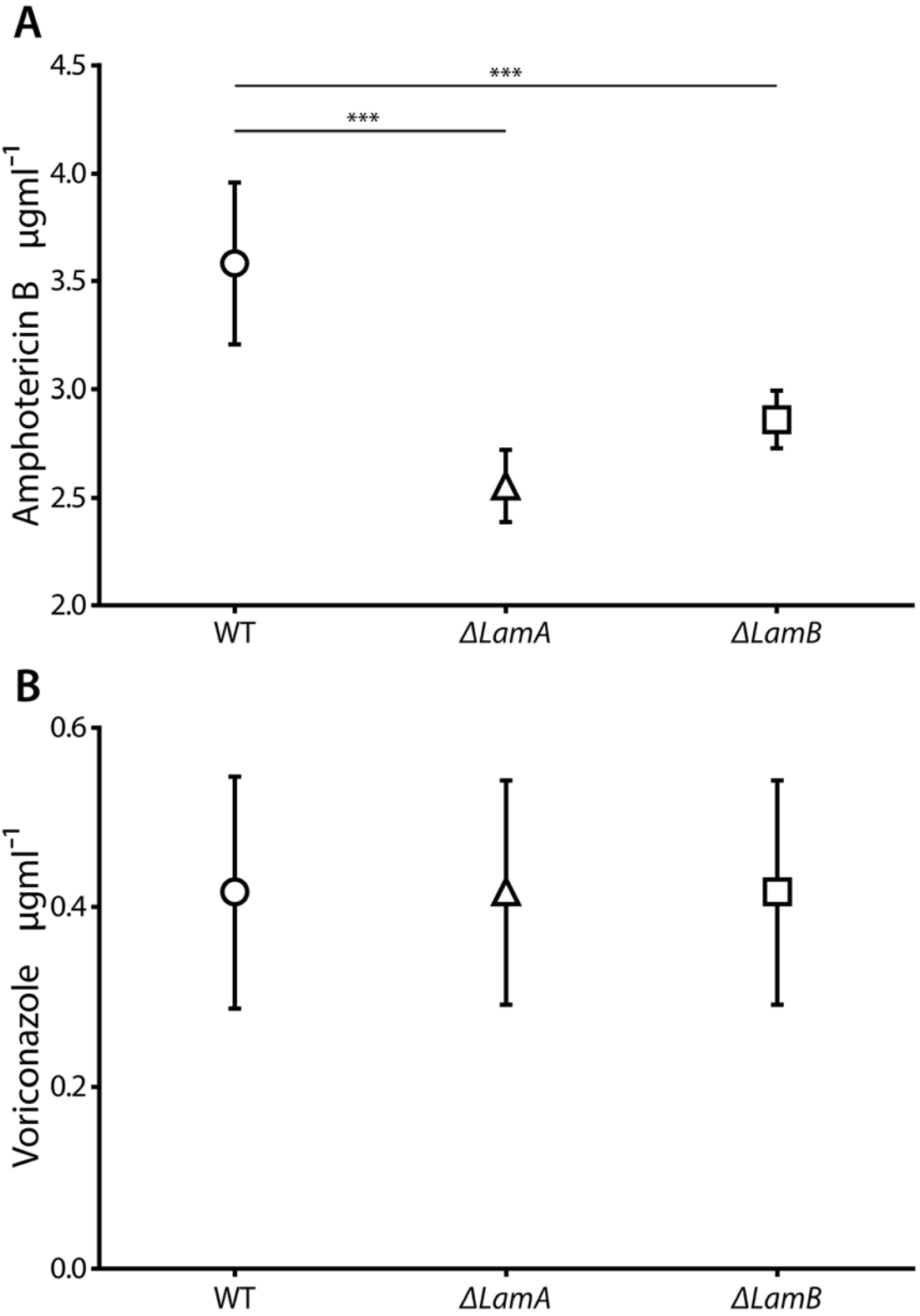

Figure 5.11 **AmB MIC is lower in *AfLam*Δ**
A) Graph showing the MIC ± SD of WT (circle), Δ*LamA* (triangle) and Δ*LamB* (square) in RPMI with Amphotericin B after 48 hours. There is significant difference between the MIC of WT and the MIC of Δ*LamA* and Δ*LamB*. The well columns for WT were between 2 - 4, for Δ*LamA* were between 5 - 7 and for Δ*LamB* were 4 – 5. The range tested was between 5-1µgml^{-1}. For WT n = 6, Δ*LamA* n = 9 and Δ*LamB* n = 9. **B**) Graph showing the MIC ± SD of WT (circle), Δ*LamA* (triangle) and Δ*LamB* (square) in RPMI with Voriconazole after 48 hours. There is no difference between the recorded MIC for WT, Δ*LamA* and Δ*LamB*. The range tested was 8-0.0075µgml^{-1}. For WT n = 6, Δ*LamA* n = 9 and Δ*LamB* n = 9.

Table 5-1 Table showing MIC (EUCAST) for AmB and Voriconazole

	MIC μgml^{-1}	
Strain	Amphotericin B	Voriconazole
WT	3.583±0.376	0.417±0.129
*AflamA*Δ	2.556±0.167	0.417±0.125
*AflamB*Δ	2.861±0.132	0.417±0.125

The MIC value of AmB for *AflamA*Δ was significantly reduced from the WT MIC [Table 5-1]. This decrease was observed consistently across different wells, plates and repeats of the assay. The fall in the MIC value of AmB for *AflamB*Δ was less severe but still significant. In contrast, the MIC value of Voriconazole was not affected. Azole antifungals inhibit Erg11, an enzyme involved in ergosterol synthesis during the step converting lanosterol (Ghannoum and Rice, 1999; Lupetti *et al.*, 2002).

5.2.11 Growth of *Aflam*Δ is reduced on solid media

The growth of *AflamA*Δ was observed to be slower than WT and *AflamB*Δ during routine maintenance. To investigate the extent of growth defect, a colony growth assay was carried out where 1x10^5 conidia were spotted onto a plate and grown for 48 hours. Only one image was obtained after 24 hours to minimise spore contamination due to opening the plate; two images of each side of the plate were made after 48 hours [Figure 5.12]. In all three media types tested (minimal, SAB and complete with low, medium and high nutrients respectively), *AflamA*Δ had visibly less growth. The difference was greater on complete medium though it was also obvious on SAB agar.

*AflamB*Δ did not visually show significant growth changes compared to WT. However, each colony was measured, and the radius plotted [Figure 5.13A-C]. Consistently across the different media, the data indicates that *AflamB*Δ grows slightly less well than WT. In comparison, *AflamA*Δ was also similar to WT on minimal media; however, on SAB media, colony diameter was reduced to ~60%, and on complete media, it decreases to ~40% of WT. Two measurements were made of only one colony, so to confirm this finding the growth assay must be repeated to show that this slight decrease is replicable.

5.2.12 Filamentous growth of *Aflam*Δ is reduced on solid media

Another significant difference between the growth of WT and *Aflam*Δ strains

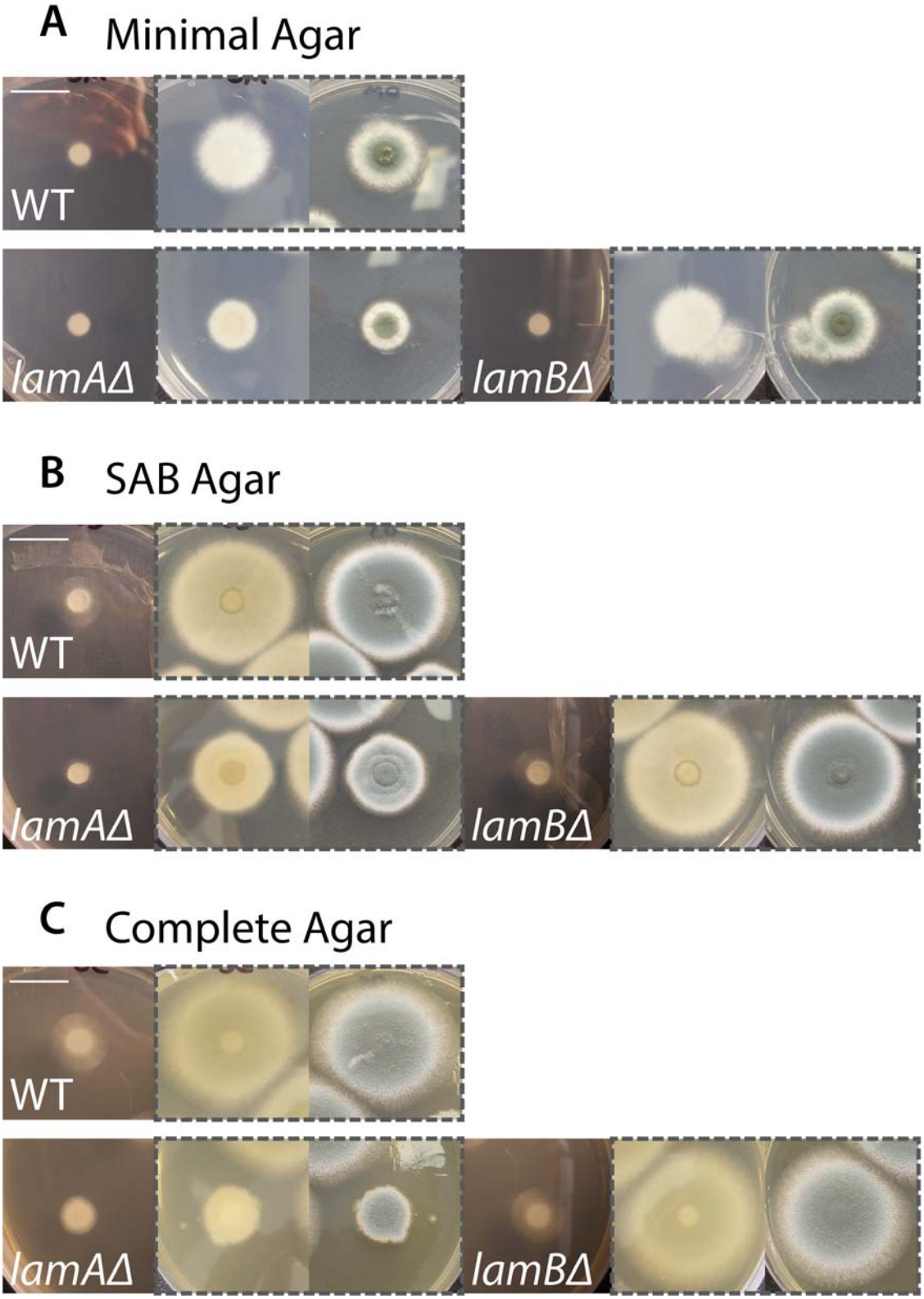

Figure 5.12 ***Af*ΔLamA has a significant growth phenotype**
Images of the growth of WT, Δ*LamA* and Δ*LamB* on **A**) minimal, **B**) SAB and **C**) complete media after 24 hours (no outline) and 48 hours (dotted outline). Δ*LamA* is observed to have much less growth especially of the filamentous growth observed at the edge of the WT and Δ*LamB* growth. There are also less visible spores observed as a lighter green. There is no obvious difference between WT and Δ*LamB*. Scale bar shows 2 cm.

was the filamentous growth of the colony. This is especially observable in *AflamA*Δ on SAB and complete media compared to the WT after 24 hours [Figure 5.12]. To quantify this difference, the filamentous mycelium was measured as a proportion of the total growth [Figure 5.13D + Equation 3].

Equation 3: Equation for filamentous growth

$$filamentous\ growth\ \% = \frac{r_2}{r_1}$$

The measurements were carried out on the colony after 48 hours to minimise the effect of the area where the conidia were initially applied (~40-50 mm diameter). The hyphal growth of *AflamA*Δ was much lower in all media tested, and *AflamB*Δ hyphal growth was less reduced [Figure 5.13E]. On minimal media, the filamentous growth of *AflamA*Δ was ~35% of WT whereas *AflamB*Δ was ~50%. On complete media, *AflamA*Δ filamentous growth was also ~30% of WT, and on SAB media, it was ~50%. Again, the filamentous growth of *AflamB*Δ was less reduced than *AflamA*Δ at ~70% and ~80% respectively. This data points to defective filamentous growth, which is possible considering the role of ergosterol in membrane rigidity and concentration at hyphal tips in connection to the ergosterol function of LAM proteins. In addition, the total growth difference between WT and *AflamA*Δ was more apparent on media with excess nutrients [Figure 5.13A-C]. It is important to note that this data were an average of two measurements of only one colony so to confirm these findings, the growth assay must be repeated to show it is replicable.

Filamentous fungi grow hyphae when nutrients are more abundant and sporulate earlier when nutrients are sparse as a survival strategy. This is illustrated with WT on minimal media where there is less growth, but a darker colour due to increased sporulation compared to on complete media where there is more growth but a lighter colour for less sporulation [Figure 5.12]. Time-lapse microscopy of the germination of a single spore would show the growth structure of hyphae, which would show any differences in growth rates between WT and delete strains.

The removal of some *AnOSH* members causes increased branching in the hyphae, including *An*OshC which is homologous to ergosterol transfer protein, *Sc*Osh4p [Figure 5.1C]. A similar situation could be occurring in the *AflamA*Δ strain where increased branching would decrease the observable area of filamentous growth around the colony. The MIC assay previously showed little difference between the strains when grown in RPMI with Voriconazole. Although there is a presence of the antifungal

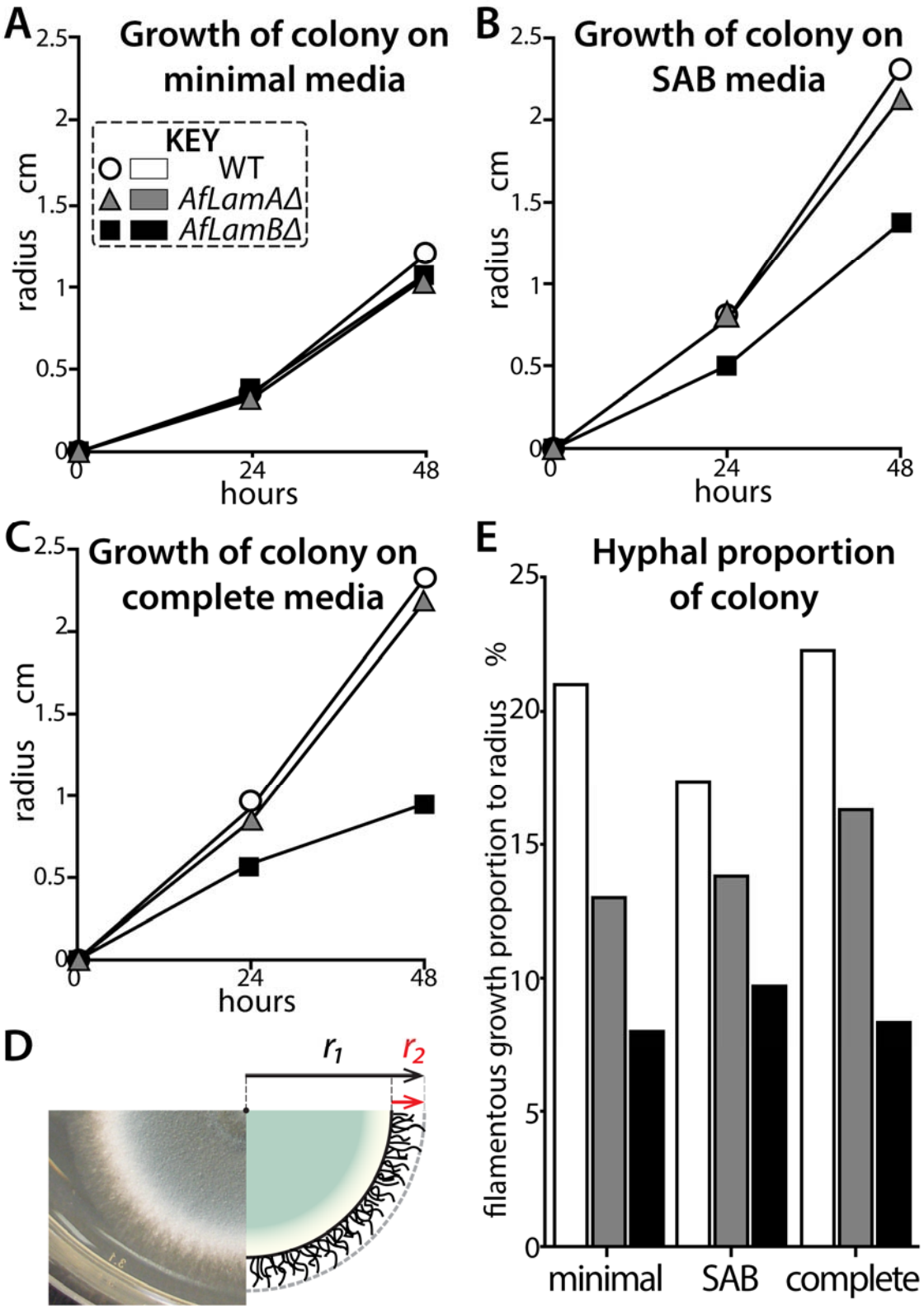

Figure 5.13 **Quantification of colony growth of *Af*Δ*LamA* + *Af*Δ*LamB***
Graph showing the radius in millimetres from the centre of the growth for WT (circle), Δ*LamA* (triangle) and Δ*LamB* (square) after 24 and 48 hours on **A**) minimal agar, **B**) SAB agar and **C**) complete agar. There is observable decrease in growth in the Δ*LamA* strain in SAB and complete media. However, there is also a consistent slight decrease in Δ*LamB* growth across all plates in this study. **D**) Diagram showing the total growth radius (r_1) and the filamentous growth radius (r_2). The average of two radius measurements was used in all graphs. **E**) The radius of filamentous growth as a percentage of total growth of all strains on minimal, SAB and complete media after 24 hours. There was consistently less filamentous growth of Δ*LamA* and Δ*LamB* compared to WT.

molecule, it can also be interpreted that the deletion of *AfLAMA* has no effect on the growth in liquid culture and that it specifically has a role in invasive growth on solid media. Equally, it may be indicative of hyper-branching of the hyphae, similar to some *AnOSH* deletes which would be masked in liquid cultures (Bühler, Hagiwara and Takeshita, 2015). Further microscopy to determine any changes in branching or physical differences such as shape and size would be informative regarding the function of the proteins.

5.2.13 Sporulation of *Aflam*Δ is defective on solid media

Another visual difference between the WT and *AflamA*Δ growth was in the conidia formation. *AflamA*Δ took much longer to sporulate during routine maintenance, which could be due to the lower growth rate. However, the colour of *AflamA*Δ growth did not obtain the dark green colour of WT and *AflamB*Δ indicative of spore formation. The colour of *AflamA*Δ did not reach that of WT even after additional time and the formation of exudates. Some filamentous fungi including *Af* form exudates, which are droplets of liquid on top of sporulated growth containing extrolites, such as mycotoxins (Colotelo, 1978).

At x50 magnification [data not shown], visual observation indicated that *AflamA*Δ did not form a thick layer of spores as WT and the spores themselves were often white in colour. The conidiophore structure that forms the spores was rarely observed in *AflamA*Δ. Instead, there were many visible thread-like hyphae. In contrast, WT had scores of dark spores covering conidiophores such that hyphal growth was not visible. The lack of a dark green colour formation and few normal conidiophores suggest a defect in spore formation. However there is no accurate assay to measure the number of spores formed in proportion to biomass. Additionally, there was no significant drop in spore viability as the number of colonies was similar between *AflamA*Δ and WT.

*AflamB*Δ showed no difference in spore formation, conidiophore structure or spore viability. Further characterisation of the spores via electron microscopy and of the conidiophore structure by a higher-powered light microscope in a suitable laboratory would yield more information between the differences between these strains.

5.2.14 *Aflam*Δ strains have decreased AmB resistance

The growth of *Aflam*Δ strains was tested on Amphotericin B containing solid media. As indicated by the MIC data, *AflamA*Δ showed a lower basal resistance to AmB; there was a complete lack of growth on AmB even at a concentration of 2 $\mu g ml^{-1}$ [Figure 5.14 + Figure 5.15]. This is in comparison to WT and *AflamB*Δ both of which

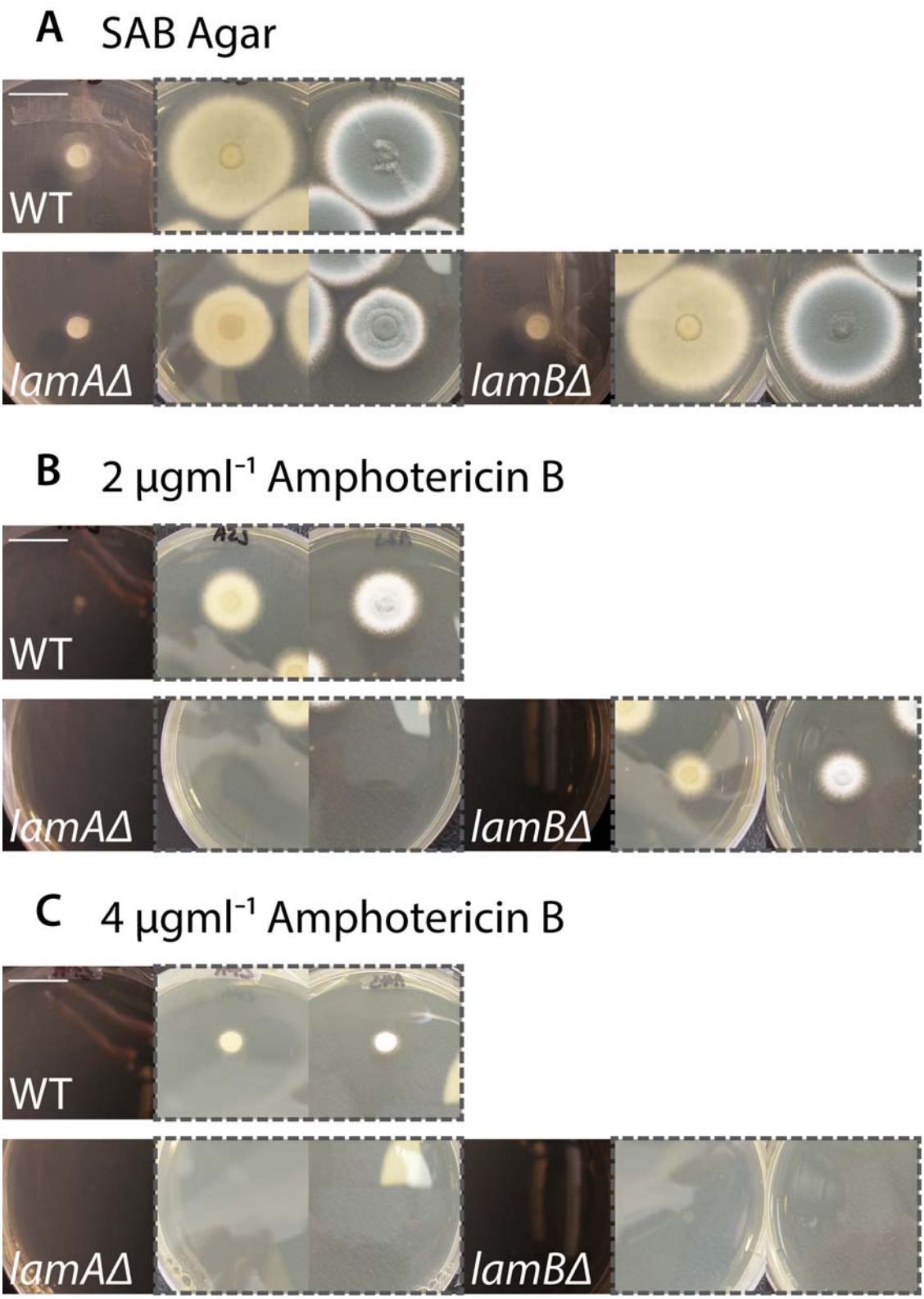

Figure 5.14 ***Af*ΔLamA + *Af*ΔLamB have reduced AmB resistance on SAB**
Images of the growth of WT, Δ*LamA* and Δ*LamB* on SAB media with **A**) 0 μgml^{-1}, **B**) 2 μgml^{-1} and **C**) 4 μgml^{-1}Amphotericin B after 24 hours (no outline) and 48 hours (dotted outline). Δ*LamA* does not show growth on either plates with Amphotericin B. Δ*LamB* shows less growth than WT on plates containing Amphotericin B. Scale bar shows 2 cm.

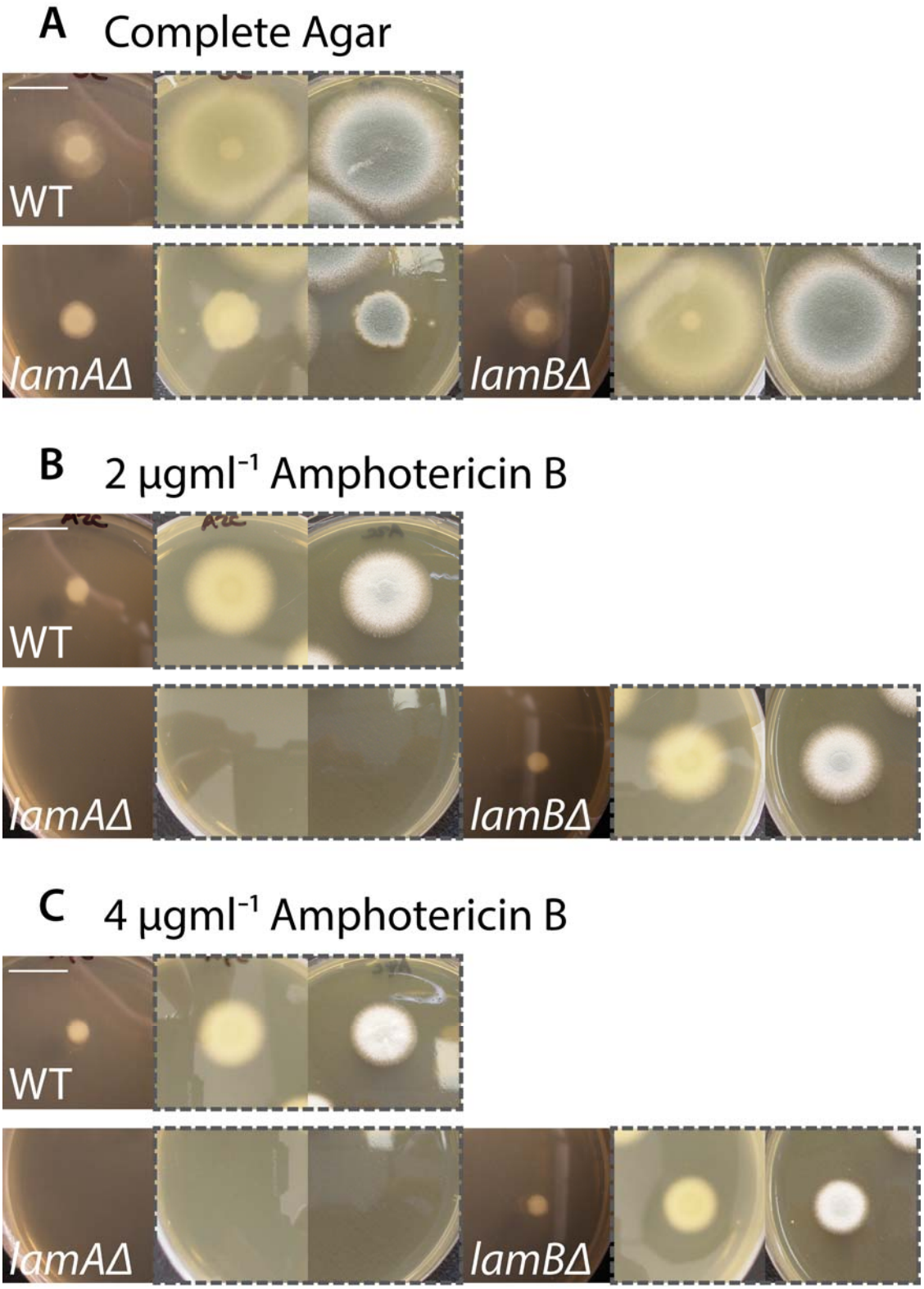

Figure 5.15 ***Af*Δ*LamA* has reduced AmB resistance on complete media**
Images of the growth of WT, Δ*LamA* and Δ*LamB* on complete media with **A**) 0 µgml^{-1}, **B**) 2 µgml^{-1} and **C**) 4 µgml^{-1}Amphotericin B after 24 hours (no outline) and 48 hours (dotted outline). Δ*LamA* does not show growth on either plate with Amphotericin B. Δ*LamB* shows slightly less growth than WT on plates containing Amphotericin B. Scale bar shows 2 cm.

showed growth on all plates containing AmB after 48 hours. There was a slight visible decrease in growth in the *AflamB*Δ strain compared to WT. This could be due to effects of the removal of the LAM protein. However, it is equally possible that it is a further effect of the slightly lower general growth of *AflamB*Δ shown on media without AmB [Figure 5.13A-C].

5.2.15 Growth of *Aflam*Δ strains on Voriconazole containing agar

For the growth assay, $1x10^5$ spores in 5 µl were applied to the agar. Initial *Af* growth is usually observed evenly over the area in which the liquid was dropped before the colony expands [Figure 5.12, Figure 5.14 + Figure 5.15]. This characteristic was observed with WT growth on complete media 0.5 μgml^{-1} Voriconazole [Figure 5.16]. However, *Aflam*Δ strains did not show uniform growth in that area. At 48 hours, *AflamA*Δ showed the beginnings of three individual colonies where WT shows homogenous growth at both 24 and 48 hours [Figure 5.16B]. *AflamB*Δ also showed individual colonies. However it is possible that growth would be similar to WT after additional time. On the other hand, the largest colony of *AflamA*Δ is of a similar size to that of *AflamB*Δ, suggesting that a significant portion of *AflamA*Δ spores are unable to grow on Voriconazole agar. It is also possible that due to lower growth on complete media even without the antifungal, significantly lower growth would be seen regardless of the effect of the lack of LAM proteins on Voriconazole.

5.2.16 *Aflam*Δ growth severities are reversed compared to *Sclam*Δ

In *Sc*, the growth defects on AmB were most severe in Δ*lam3* and Δ*lam1* followed by Δ*lam2* and then Δ*lam6* and Δ*lam5*. *Af*LamB is homologous to *Sc*Lam1/3, yet the removal of this protein showed little defects compared to WT. On the other hand, removal of *Af*LamA, which has a similar domain architecture to *Sc*Lam5/6, showed severe growth defects on AmB. Surprisingly, *AflamA*Δ showed growth deficiency even during normal growth with no antifungal present. A possible reason for this would be due to *Af*LamA being equally homologous to *Sc*Lam2/4p and *Sc*Lam5/6p and therefore would function in place of all four yeast proteins. Therefore, a similar growth defect in budding yeast may be observed in a strain removed of all Lam2p/4p/5p/6p.

It is important to note that for any confirmation of observed phenotypes, reconstitution of the whole gene must be carried out to validate that the phenotypes are due to the removal of the *LAM*s. Strains with restored LAMs should revert the phenotypes back to WT.

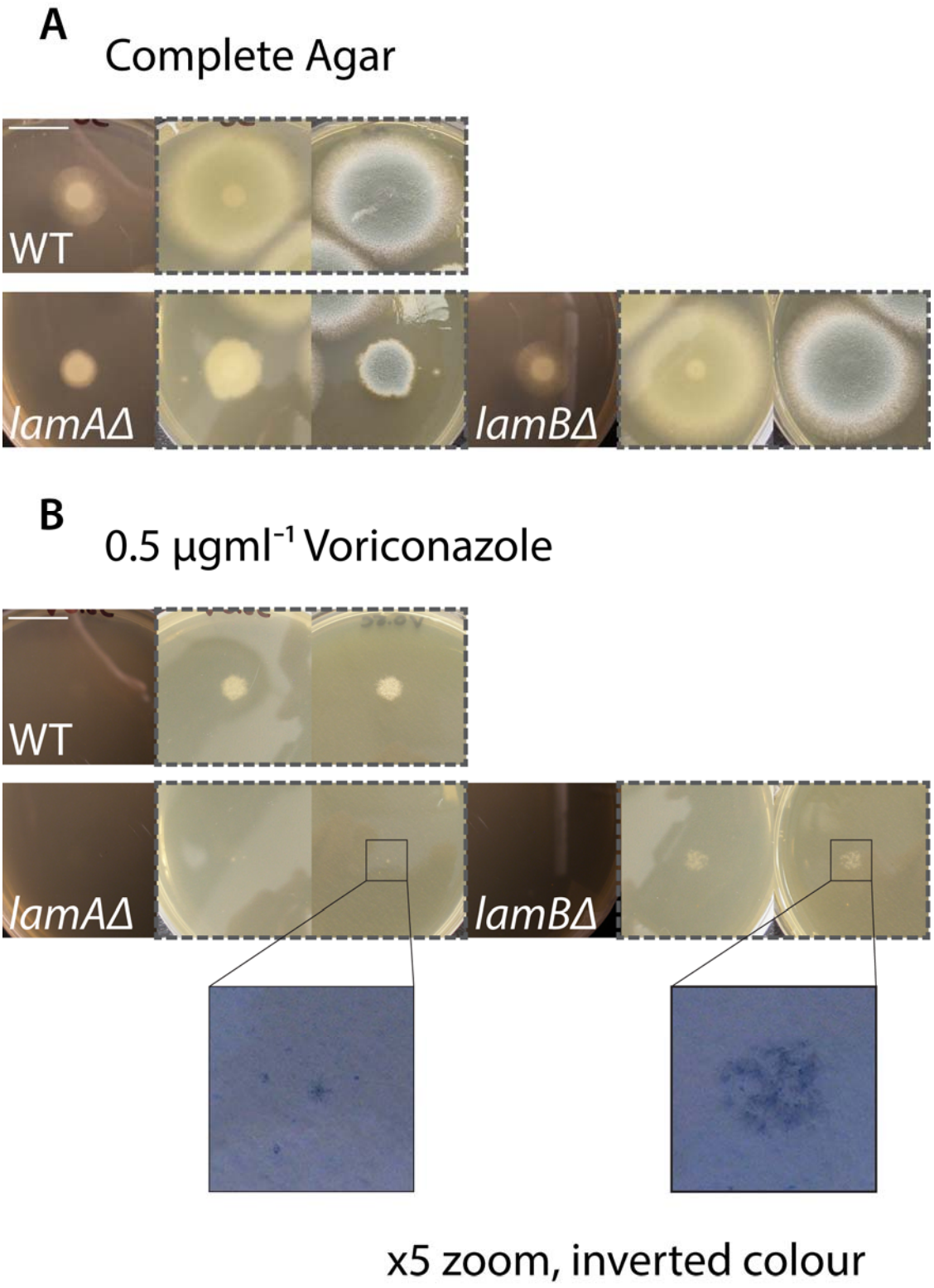

Figure 5.16 ***Af*ΔLamA + *Af*ΔLamB slight growth phenotypes on AmB**
Images of the growth of WT, Δ*LamA* and Δ*LamB* on complete media with **A**) 0 µgml^{-1} and **B**) 0.5 µgml^{-1} Voriconazole after 24 hours (no outline) and 48 hours (dotted outline). Δ*LamA* shows minute growth on media with Voriconazole. Δ*LamB* showed slightly more growth but is still significantly less than WT on Voriconazole. The growth of Δ*LamA* and Δ*LamB* is zoomed in (inset) and colours inverted to better show the colony formation of individual spores. Scale bar shows 2 cm.

5.3 Discussion

5.3.1 DUF3074 and LAMs in fungi

During this study, a large eukaryotic family of LAM proteins containing a conserved StARkin domain was identified. The *Sc*Lam2/4p-like proteins are unique to the Saccharomycetes fungal class having evolved most recently. The *Sc*Lam1/3p-like proteins are present only in fungi and are the most divergent branch of LAMs. The most abundant member is the *Sc*Lam5/6p-like proteins found in all eukaryotes including humans and plants.

Alongside these StARkin domains, another subfamily is found in many fungi termed DUF3074. This domain is occasionally found in conjunction with *Sc*Lam1/3p-like proteins although they share little sequence homology. As most DUF3074 are found as short isolated proteins, it is likely that the combined Lam1/3p-DUF3074 architecture was formed after the separate development of both *Sc*Lam1/3p and DUF3074 in fungi. The presence of DUF3074 within the Lam1/3p protein restricts it to specific contact site localisations due to the transmembrane domain of Lam1/3p tethering the protein to ER-PM contacts. This raises questions of how this domain architecture has formed. It is possible the typical localisation of the short DUF3074 could also be at these contact sites by a yet unknown membrane and/or protein partner. It is also feasible that there is an interaction or dependency of the DUF3074 for Lam1/3p. If DUF3074 is indeed localised to contact sites, it adds to the growing number of StARkin domains at ER-PM contact sites as some yeast species have homologs to all *Sc*Lam proteins in addition to DUF3074. However, the contact site localisation has only been confirmed in budding yeast and not been investigated in other fungi.

5.3.2 DUF3074 function

*Af*DUF3074 was shown to have a distinct function compared to *Sc*Lam2/4/5/6p StARkin domains due to the unsuccessful recovery of growth of yeast Δ*lam* strains on AmB compared to the StARkin domain of *Af*LAM. *Sc*Δ*lam2* was partially rescued by a human StART domain able to bind and transport cholesterol, MLN64, but not by StART domains with a different lipid ligand (PCTP and CERT) (carried out by Tim Levine (Gatta *et al.*, 2015)). As the cluster diagram shows a very close relationship with StART domains, but the isolated DUF3074 StARkin domain is unable to rescue yeast Δ*lam2*, it is possible that DUF3074 has a lipid ligand that is not sterol, for example, PC or ceramide. It would be interesting to find the extent of the link between StARTs and DUF3074, thus discovering whether DUF3074 is a fungal branch of StARTs and thus should be included within this subfamily. The rare proteins with the combined Lam1/3p

and DUF3074 suggest that DUF3074 would be active at the same localisation as Lam1/3p. Identifying the localisation of these proteins and versions of the short DUF3074 members without transmembrane domains would yield important clues to the role of DUF3074.

5.3.3 Cellular characteristics of LAMs in fungi

The ability of *Cryptococcus* and *Aspergillus* LAM StARkin to rescue yeast delete strains similar to that of the yeast own LAM StARkin domains suggests a shared function throughout the fungi kingdom. Indeed, it is suggested the LAM StARkin function is conserved in all eukaryotes indicated by human LAM domain having the same rescuing function (carried out by Alberto Gatta (Gatta *et al.*, 2015)).

In budding yeast, all LAM members were localised to specific membrane contact sites – Lam1/3p and Lam2/4p at ER-PM contact sites and Lam5/6p at ER-vacuole and ER-mitochondria contact sites. Membrane contact sites have yet to be characterised in detail in Aspergilli. However, it would be extremely beneficial to find the localisation of the *Af*LAM proteins to confirm the conserved localisation at contact sites. The localisation cannot be deciphered from their budding yeast homologs as *Sc*Lam2/4p and *Sc*Lam5/6p localise differently. The domain architecture of *Af*LamA is the same as *Sc*Lam5/6p. *Sc*Lam5/6p has multiple localisations at both ER-vacuole and ER-mitochondria contacts. This dual localisation is regulated by interaction to either vacuolar Vac8p or mitochondrial Tom70/71p (see section 1.5.8. for a more detailed description) (Murley *et al.*, 2015). It is possible that *Af*LamA retains all three localisations at ER-PM/vacuolar/mitochondrial contact sites and that additional interactions could regulate where the LAMs locate. In addition, the three human homologs, *Hs*LamA-C, which are also homologous to both *Sc*Lam2/4p and *Sc*Lam5/6p, localise to multiple contacts (microscopy by Alberto Gatta, personal communication).

5.3.4 Growth phenotypes of Δ*lam* strains in *Aspergillus*

As with yeast LAM proteins, *Af* LAMs are not essential for viability, however, contrary to yeast *LAM* delete strains, *Aflam*Δ showed growth defect even in media without AmB. *AflamA*Δ had the most severe growth phenotype. It is possible that due to the role of ergosterol in invasive growth and its high concentration at hyphal tips, the removal of LAM proteins is detrimental during normal growth. Infectious fungi invade their hosts by their hyphae formed during filamentous growth. *Sc* is usually found on the surface of fruit and rarely shows this growth pattern, however, pseudohyphal growth does occur in rare situations (Loeb *et al.*, 1999; Zaragoza and Gancedo, 2000), similar to the ability of *Candida* cells to switch between yeast-like and filamentous growth. It is

plausible that this specialised growth phenotype is poor or even impossible in *Sc*Δ*lam* strains. The growth of yeast on ergosterol synthesis affecting antifungal (azoles) was shown to prevent *Sc* from entering pseudohyphal growth (Kontoyiannis, 2000). Indeed, growth assays using *Af* Δ*lam* strains show a decrease in filamentous growth on solid media. Further characterisation of this phenomenon in *Aspergillus* will shed light of the function of LAMs for filamentous growth as will investigating budding yeast pseudohyphal growth. It is important to note that laboratory yeast strains with an S288C background, including BY4741, do not form pseudohyphae easily.

Sporulation was also reduced in *AflamA*Δ*,* although it is unclear whether this is related to the decrease in filamentous growth. Sporulation of budding yeast BY4741 was carried out to produce double delete strains (conducted by Tim Levine), but no significant defect in the rate of sporulation was noted. However, these were only single delete strains and as LAM proteins are duplicated in budding yeast, the second paralog may have substituted for any essential sporulation function.

5.3.5 Phenotype comparison with budding yeast

The growth phenotype of *AflamB*Δ, homologous to ScLam1/3p was mild compared to *AflamA*Δ, similar to *Sc*Lam5/6p. In contrast, there was a significant growth defect on AmB by yeast delete *LAM*s where the removal of Lam1p or Lam3p showed the greatest AmB phenotype. It would seem that although *Sc*Lam1/3p are part of the LAM family and localisation is similar to that of *Sc*Lam2p/4p; the function is distinct from the other LAM members. It is unclear whether the roles of *Sc*Lam1/3p and *Af*LamB are similar, but as *ScLAM1/3* delete strains show variable growth phenotypes with different polyenes, it would perhaps be informative to test *Af*LamB on a larger variety of drugs and conditions. In *Sc*Δ*lam6*, the stress response of membrane rearrangement to situations such as glucose starvation and cycloheximide treatment failed but was unaffected in response to weak acid stress (Murley *et al.*, 2015). Therefore it very probable that there is an effect in certain situations that is yet unidentified. Though this is a broad line of inquiry, conditions known to affect ergosterol homoeostasis should be tested initially.

5.3.6 LAM as a drug target

Initially, the aim of this focus of the study was to probe the viability of LAM proteins as a secondary drug target alongside Amphotericin B due to the severe growth phenotype of yeast Δ*lam* strains. However, the *Af*LamA was shown to be critical for growth on solid media without the presence of Amphotericin B. This suggests that *Af*LamA could be a target independent of Amphotericin B.

Once the phenotype of Δ*Aflam* strains has been pinpointed to the removal of LAM proteins by reconstitution of WT phenotype upon re-expression of *LAMs*, it would be of interest to measure the virulence of Δ*AfLamA* in a host model. This would reveal whether the decrease in growth and defect of hyphal growth could translate to a weakened invasive infection. A typical virulence assay involves the infection of *Galleria mellonella* as an alternative to mammalian models (Champion, Wagley and Titball, 2016). Spores are injected in *Galleria* larvae, and the rate of death is evaluated.

The LAM StARkin domains have been determined to be responsible for the AmB-resistant activity. If the StARkin domain is also responsible for the proper growth of *Aspergillus,* the domain could be a potential target for the design of a drug to block the predicted cavity.

5.3.7 Key results

Not all *Sc*LAM proteins are conserved in eukaryotes. However, *Sc*Lam5/6p and *Sc*Lam1/3p are found throughout the fungi kingdom. Some versions of Lam1/3p are extended to include another StARkin domain, DUF3074. DUF3074 is highly related to StARTs, a subfamily of the StARkin superfamily. However, like Lam1/3p StARkin domains, the DUF3074 StARkin cannot substitute for the function full-length *Sc*Lam proteins during growth on AmB. The removal of LAM proteins in *Af* affected the ability to grow on AmB. As well as the importance for the basal resistance to AmB, *Af*LamA is also critical for the proper growth of the filamentous fungi, showing severe phenotypes on solid media without antifungals. As such, the StARkin domain of *Af*LamA becomes an appealing antifungal drug target.

CHAPTER 6

In vitro studies of sterol binding and transfer by LAM StARkin domains

6.1 Introduction

Deletion strains of three out of the six members of the *LAM* family were shown to be sensitive to Amphotericin B (AmB). Other genes which when deleted cause AmB sensitivity include *ERG4*, a gene responsible for the synthesis of ergosterol. However, not all *ERG* gene deletions increase polyene sensitivity; for example, *ERG3* and *ERG6* deletion cause polyene resistance rather than sensitivity, contrary to the removal of *ERG4* (Young, Hull and Heitman, 2003). AmB is known for its ergosterol interaction, and so the phenotype associated with the removal of *LAM*s suggests that these proteins must affect cellular ergosterol in some way. This investigation focuses on the essential 'active' domain for AmB resistance, established as the predicted StARkin domain, which is shared amongst all LAM proteins. The StARkin domain may bind and transfer ergosterol, though they might also interact with sphingolipids or other key plasma membrane (PM) lipids that have effects on sterols indirectly. In this investigation, controlled *in vitro* fluorescent assays were used to measure the activity of the purified protein for sterol binding and transfer. Traditional techniques such as radioactive transfer assays are highly invasive, requiring harsh conditions to extract lipids or proteins. A significant advantage of fluorescent assays is that the protein and fluorescent ligand are not destroyed and therefore can be used to probe the real-time dynamic binding of a lipid transfer protein.

6.1.1 Fluorescent sterols

Fluorophores absorb specific wavelengths of light and then emit a different specific longer wavelength. Proteins are generally made of distinct domains, so the addition of a separate fluorophore such as GFP does not greatly interfere with the function or activity of the protein. However, the function of a lipid depends on the properties of the whole lipid, and therefore the addition of a fluorophore may alter

normal lipid functionality. There are many different fluorescent sterol analogues available for use as a lipid probe. With the exception of dehydroergosterol (DHE), the fluorescent probes are labelled with various synthetic chemical tags, which are bulky in comparison to the sterol molecule. Sterol is a small lipid, so even a minor addition to the structure will have large effects on the properties.

Nitrobenzoxadiazole (NBD) is an example of a fluorescence group often added to lipids. The molecular weight of ergosterol is 396.65 $gmol^{-1}$ compared to NBD, which is 294.27 $gmol^{-1}$. Thus the addition of an NBD tag increases the sterol to almost double the size of untagged lipid. NBD-tagged cholesterol has been used *in vivo* and was shown to partition, orientate and behave differently in the cell (Mattjus *et al.*, 1995; Mukherjee *et al.*, 1998; Loura, Fedorov and Prieto, 2001; Scheidt *et al.*, 2003). It is likely that NBD tagged sterol would also have adverse effects in *in vitro* studies by affecting the binding of the sterol into a specific sized hydrophobic pocket of a protein.

On the other hand, DHE is naturally occurring in yeast and is one of the ergosterol species produced in yeast as part of the ergosterol synthesis pathway in the presence of oxygen and glucose (Aries, 1978; Novotny *et al.*, 1987). It does not have an additional bulky fluorescent group but instead has an extra double bond in the C-ring of the structure in comparison to the non-fluorescent ergosterol [Figure 1.3C], which allows it to be excited at 325 nm to emit a peak of 375 nm. The fluorescent spectrum of DHE is very distinctive with the emission spectrum exhibiting three peaks at 354, 371 and 390 nm when in a hydrophobic environment such as in organic solvents or within membranes [Figure 6.1A]. However, in an aqueous environment, the fluorescence spectrum shifts to the right, causing the emission maxima to move to 375, 404 and 426 nm.

6.1.2 Fluorescent amino acids

The primary sequence of a protein can dictate the levels of intrinsic fluorescence, which is dependent upon the presence of three aromatic amino acids acting as fluorophores– tryptophan, tyrosine and phenylalanine. The aromatic amino acids all have different absorption and excitation wavelengths (Teale and Weber, 1957). Tryptophan, having the longest excitation wavelength of 280 nm and the highest quantum yield, dominates the other two aromatic amino acids. In addition, tryptophan is uniquely excitable by UV light at 295 nm and fluoresces at 300-355 nm depending on the environment [Figure 6.1B]. Due to its aromatic structure, Tryptophan is often found buried in the hydrophobic core of a protein and will exhibit a blue-shifted emission which typically will be ~335 nm for a partially buried conformation compared to 355

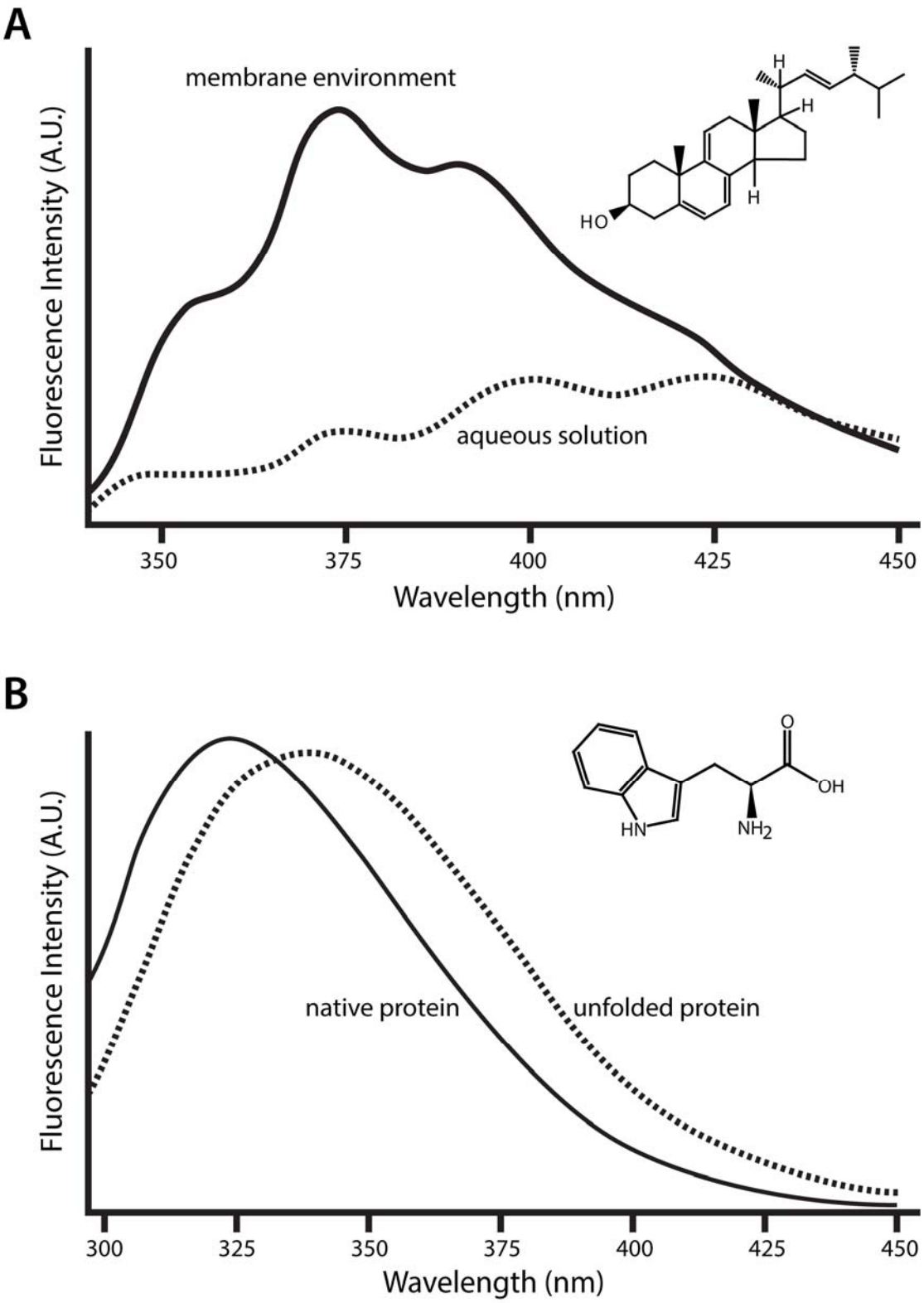

Figure 6.1 **Fluorescent spectra of DHE and tryptophan**
A) Emission spectra of dehydroergosterol in multilamellar vesicles composed of PC:cholesterol:DHE at a 75:24:1 ratio (solid line) and in aqueous solution 4 μgml^{-1} in 0.1% DMSO (dotted line). Data from (Lorent *et al.*, 2013). **B**) Emission spectra of tryptophan fluorescence of cAMP-dependent protein kinase C-subunit in a native, folded form and in a denatured unfolded state induced by 4M urea. Data from (Steichen *et al.*, 2010).

nm for tryptophan in water (Royer, 2006). These characteristics of tryptophan can be taken advantage of to probe LAM StARkin domain binding as the binding pocket of the predicted domain contains a tryptophan residue.

6.1.3 Intrinsic Förster resonance energy transfer

Förster resonance energy transfer (FRET) occurs when there is a non-radiative transfer of energy between an excited donor fluorophore to an acceptor molecule in the ground state [Figure 6.2A]. This dipole-dipole coupling happens if the FRET pair is between 1-10 nm of each other, with most fluorophore pairs showing significant FRET by 6 nm [Figure 6.2B]. The two fluorophores in the FRET pair must have an overlap in emission and excitation spectra [Figure 6.2C]. Intrinsic FRET, utilises the endogenous tryptophan within the protein itself as a fluorophore (Ghisaidoobe and Chung, 2014). The DHE excitation spectrum overlaps with the tryptophan emission spectrum allowing energy transfer between the two fluorophores. In this investigation, the intrinsic tryptophan fluorescence of protein within the binding pocket is used to test the DHE binding ability by measuring the DHE emission signal using the tryptophan excitation wavelength [Figure 6.2C.] This method allows a non-invasive method to probe the binding properties of proteins to sterol.

6.1.4 Using lipids in an aqueous reaction

Sterol has very poor solubility in water (<1 $\mu g ml^{-1}$) and thus requires artificial solubilisation or incorporation into an artificial membrane (Saad and Higuchi, 1965). Cyclodextrins are an example of an agent that is able to solubilise sterols. These molecules are synthetic rigid conical oligosaccharides structure with a hydrophilic exterior and hydrophobic core, which allows binding to (thus solubilisation of) a range of molecules including sterol. The heptamer methyl-β-cyclodextrin (MβCD) is especially good at solubilising cholesterol, having the ability to extract cholesterol from the PM of cells and such is used to deplete cells of and present cells with sterols in *in vivo* assays (Ohtani *et al.*, 1989). This investigation initially uses MβCD to introduce sterols to protein to probe binding and finally uses MβCD as a positive control of a sterol transfer agent (Mukherjee *et al.*, 1998; John *et al.*, 2002).

Another way of solubilising lipids is to synthesise artificial membranes. In addition to binding a lipid ligand, there are other requirements of an efficient lipid transfer protein, for instance, the docking of the protein to an acceptor and donor membrane. Artificial membranes such as liposomes can replicate the cellular membrane environment to test the affinity of proteins to membranes and the proteins ability to detect and extract out the specific lipid in question.

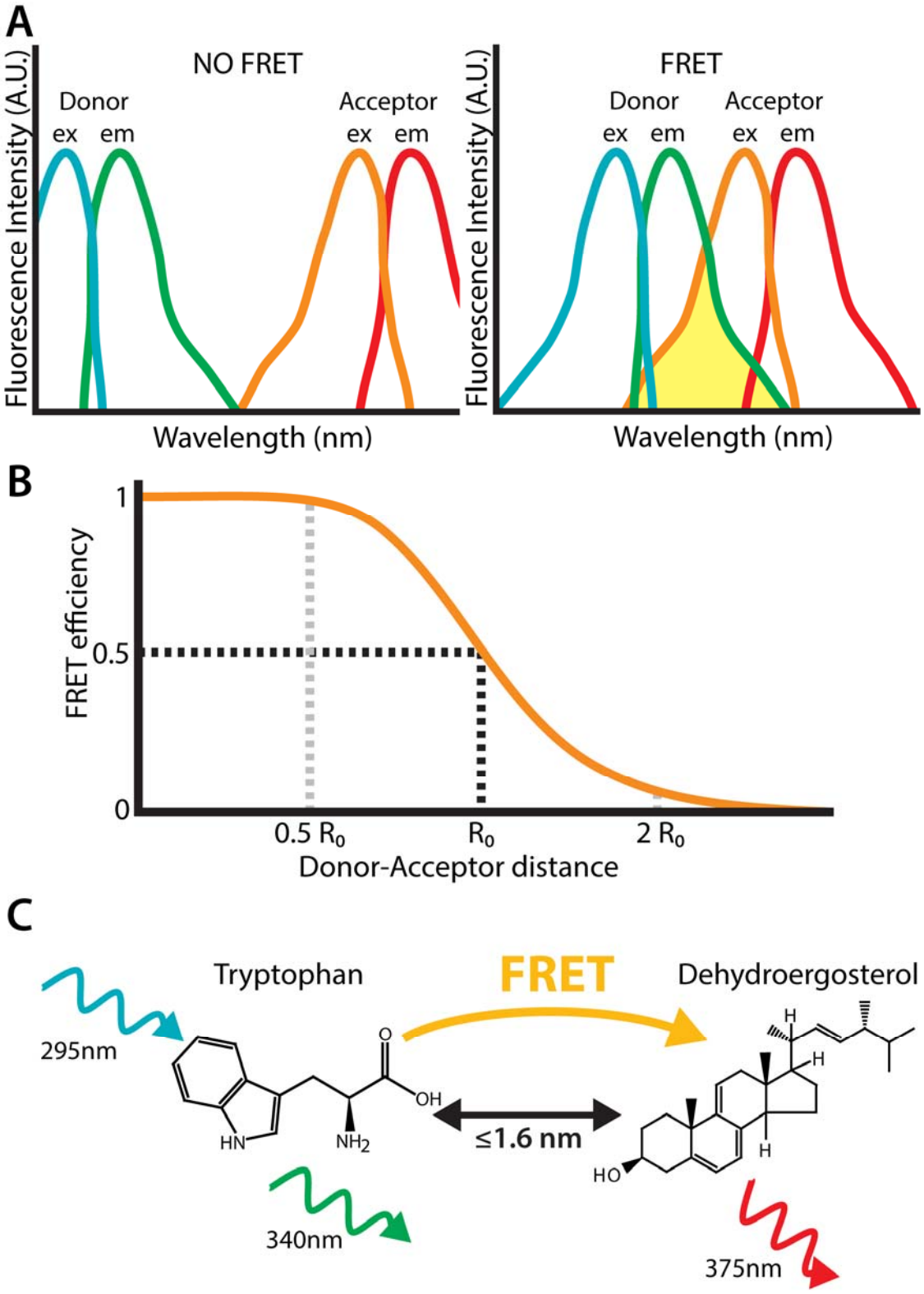

Figure 6.2 **Förster resonance energy transfer (FRET)**
A) A FRET pair is characterised by one fluorophore whose emission spectra overlaps the excitation spectra of the second fluorophore. The spectral overlap is highlighted in yellow. No FRET can occur if there is no overlap. **B**) FRET efficiency is dependent on the distance between the FRET pair. At the Förster distance, R_0, efficiency is 50%. This is ≤1.6 nm for DHE and Tryptophan. Efficiency is inversely proportional to the sixth power of the distance. **C**) Depiction of FRET between tryptophan and DHE.

Liposomes consist of a lipid bilayer surrounding a sphere of an aqueous volume, formed when amphipathic molecules energetically favourably arrange themselves in aqueous solution. By artificially producing these membranes, the lipid composition can be defined and used as a controlled system to test the binding and transfer of the potential lipid transfer protein. The main lipid components of a liposome are various PLs, but sterol can also be included up to 60% (Huang, Buboltz and Feigenson, 1999). The charge of the liposomes can be altered depending on the composition of the lipids used. Liposomes are extensively used as *in vitro* biomembrane models and have been used with DHE to study ergosterol-binding and transfer by proteins (Papahadjopoulos *et al.*, 1973; Yang *et al.*, 2015).

6.1.5 Transfer assays using FRET

An ability to bind a ligand does not necessary translate to an ability in transferring a ligand. For instance, a protein may bind with such high affinity to a ligand that it cannot easily release the molecule and therefore does not transfer the ligand between membranes. Another possibility is the protein is unable to dock to membranes and therefore will be lacking in its ability to extract lipids from membranes and deposit them in another. A lipid transfer protein was first designated as such by the capacity to move lipids between membranes *in vitro* (Helmkamp *et al.*, 1974). Since then, breakthrough studies in the lipid transfer field include data generated by *in vitro* transfer assay using lipid FRET pairs. One FRET pair is DHE, a fluorescent sterol and Dansylated PE, a fluorescently tagged phospholipid. Different to the excitation of FRET pair tryptophan and DHE which is 295 nm, the wavelength used to excite FRET pair DHE and Dansyl-PE is 340 nm. *In vitro* assays probing DHE transfer utilises this FRET pair by the addition of Dansyl-PE only in one membrane which cannot be moved. Any positive transfer of DHE would then be recorded as a change in FRET output, in other words, Dansyl-PE emission using DHE excitation wavelength.

6.1.6 Binding and transfer of DHE by LAM StARkin domains

The ‘active’ domains of LAMs that are responsible for basal resistance to AmB, an ergosterol interacting antifungal, are the predicted StARkin domains found using bioinformatics. This ‘active’ domain, which is predicted to be very similar in structure to known lipid binding and transfer domains of the StART family, is likely to bind ergosterol specifically. This investigation starts with producing constructs containing the StARkin domains of interest from Lam2p/4p and purifying. Using the conveniently placed endogenous tryptophan within the binding pocket of LAM StARkin domain, FRET can be used to detect binding to DHE, a fluorescent molecular analogue of

ergosterol, also present naturally in fungi. Once binding to ergosterol has been established, extraction and transfer of DHE can be detected between two liposomes to simulate two different membranes.

6.2 Results

6.2.1 GFP-tagged Lam2p-StARkin 1+2 does not bind lipids

One plasmid construct containing both of the StARkin domains of Lam2p were cloned and expressed in bacteria with a tag of six Histidines and GFP. The architecture of the protein from the N-terminus to the C-terminus was His x6, GFP, Lam2p StARkin 1 and Lam2p StARkin 2 (referred to as Lam2S1S2). The purified product was ~45% pure with a significant amount of contaminants or degraded protein [Figure 6.3B]. An initial transfer assay of a single LAM StARkin construct purified by Tim Levine and carried out by Shamshad Cockcroft with 50 μg protein had indicated minute PC transfer activity. It was suggested that the very low activity might indicate the requirement of both StARkin domains in tandem as well as more protein. Therefore the transfer assay was repeated with both StARkin domains with more protein. The transfer assay incubated the purified protein with donor cellular membranes containing radiolabelled lipids and acceptor liposomes. Human HL60 cells are grown in 1 $\mu Ciml^{-1}$ [^{14}C]-acetate, allowing the cells to synthesise radioactive lipids and incorporate them into the membranes of the cell and organelles. The membranes were purified and incubated with the recombinant protein and acceptor liposomes to allow any binding and transfer to occur. The radiolabelled membranes were aggregated to quench the reaction and to separate the two membrane populations. The bound lipids were then extracted from the acceptor liposomes and separated on a TLC (thin-layer chromatography) plate [Figure 6.3A]. Controls using no protein and a known PA/PI transfer protein RdgBα showed background lipids and a positive control respectively. A sample of radiolabelled membranes was used as a lipid standard. The background of this assay was very high. However, transfer of the control protein showed a definitive additional band for PA and a much stronger band for PI [Figure 6.3C red arrowheads]. A problem with this transfer assay was the addition of the GFP tag, which was cloned with the StARkin1 and StARkin 2 fragment of Lam2p [Figure 6.3A]. GFP is ~30 kDa, and this could interfere with the two small ~25 kDa StARkin domain by shielding the protein and preventing access to the binding pocket (communication with Shamshad Cockcroft). Therefore, Lam2S1S2 purified from now on were constructed without the GFP tag.

6.2.2 Lam2pS1S2 (without GFP) does not bind lipids

In addition to the potential problem of a GFP, the purification of the protein was not of a high quality. There was a significant amount of contaminant, which may indicate

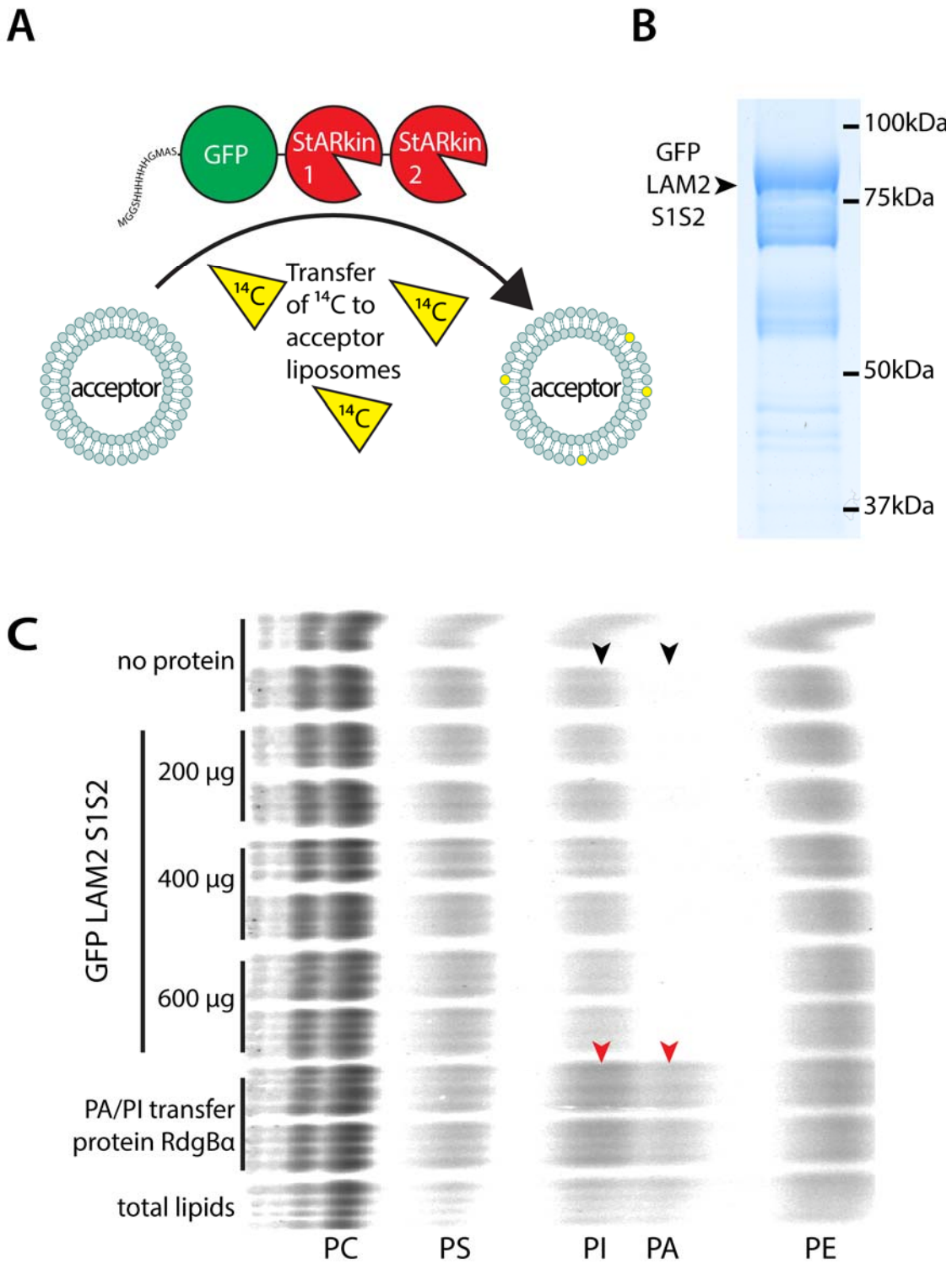

Figure 6.3 **Radioactive lipid transfer with Hisx6 GFP-Lam2S1S2**
A) Schematic of a lipid transfer assay where radiolabelled lipids (yellow) are transferred to non-labelled acceptor membranes. **B**) SDS-PAGE of purified Hisx6 GFP-Lam2S1S2 at ~80kDa of ~45% purity. **C**) TLC separation of radioactive phospholipids extracted from acceptor liposomes after incubation with GFP-Lam2S1S2 and RdgBα, a known PA/PI transfer protein. Samples of the radiolabelled membranes were run out as a standard. This method gave a high background but showed a positive result for RdgBα (red arrows) compared to the negative (black arrows). No transfer was seen for GFP-Lam2S1S2.Abbreviations: PA, phosphatidic acid; PI, phosphatidylinositol; PS, phosphatidyl serine; PC, phosphatidylcholine; PE, phosphatidylethanolamine.

instability of the protein, or additional proteins, which interfere with the function of the domains. Therefore, a version of the protein excluding the GFP was cloned and the Histidine tag, which is used with Ni^{2+} purification beads, was increased from six Histidines to eleven Histidines at the N-terminus. The larger histidine tag was able to enhance the purity of the protein to ~99% [Figure 6.4C]. Contaminants were not seen in an SDS-PAGE run with a sample of the purified product. The radioactive lipid transfer assay was repeated with the pure Lam2S1S2 with no GFP tag [Figure 6.4A+B]. In addition to the PLs separation, the neutral lipids were also separated on a parallel TLC plate [Figure 6.4B]. As with the previous experiment, there was a high amount of background lipids. However, the positive protein control, RdgBα, gave clear indications of correct transfer [Figure 6.4A red arrowheads].

The method used for the radioactive lipid transfer assay is both time and material consuming in addition to having a high background. Furthermore, it is a highly specialised and hard to control technique, which also requires a suitable laboratory for the radioactive material. Therefore, an alternative method was pursued to test *in vitro* LAM StARkin function. Due to the unsuccessful transfer of LAM StARkin domains, binding assays using FRET were carried out for subsequent protein purifications to confirm that these domains are able to bind lipids before proceeding further with transfer assays. Another alteration for subsequent assays was to purify individual StARkin domains to allow full access to the binding pocket.

6.2.3 Tryptophan within the pocket

LAM StARkin domains from Lam2p/4p/5p/6p have two conserved tryptophan residues (Gatta *et al.*, 2015). One tryptophan residue is exposed and faces outside of the domain away from the predicted binding pocket [Figure 6.5A-top tryptophan]. On the other hand, the second tryptophan residue is inside the predicted binding pocket of the fold, exposed to the cavity space of the domain [Figure 6.5A-bottom tryptophan].

The majority of evidence thus far, most prominently the phenotypic assays on ergosterol affecting drugs, suggests that LAM proteins are involved in cellular ergosterol homoeostasis and so the FRET binding assays were carried out with DHE, a naturally occurring fluorescent ergosterol in yeast. The donor emission of the tryptophan spectrum overlaps with the excitation of DHE. The tryptophan can be excited by a wavelength of 295 nm so as to not excite the tyrosine amino acids. The

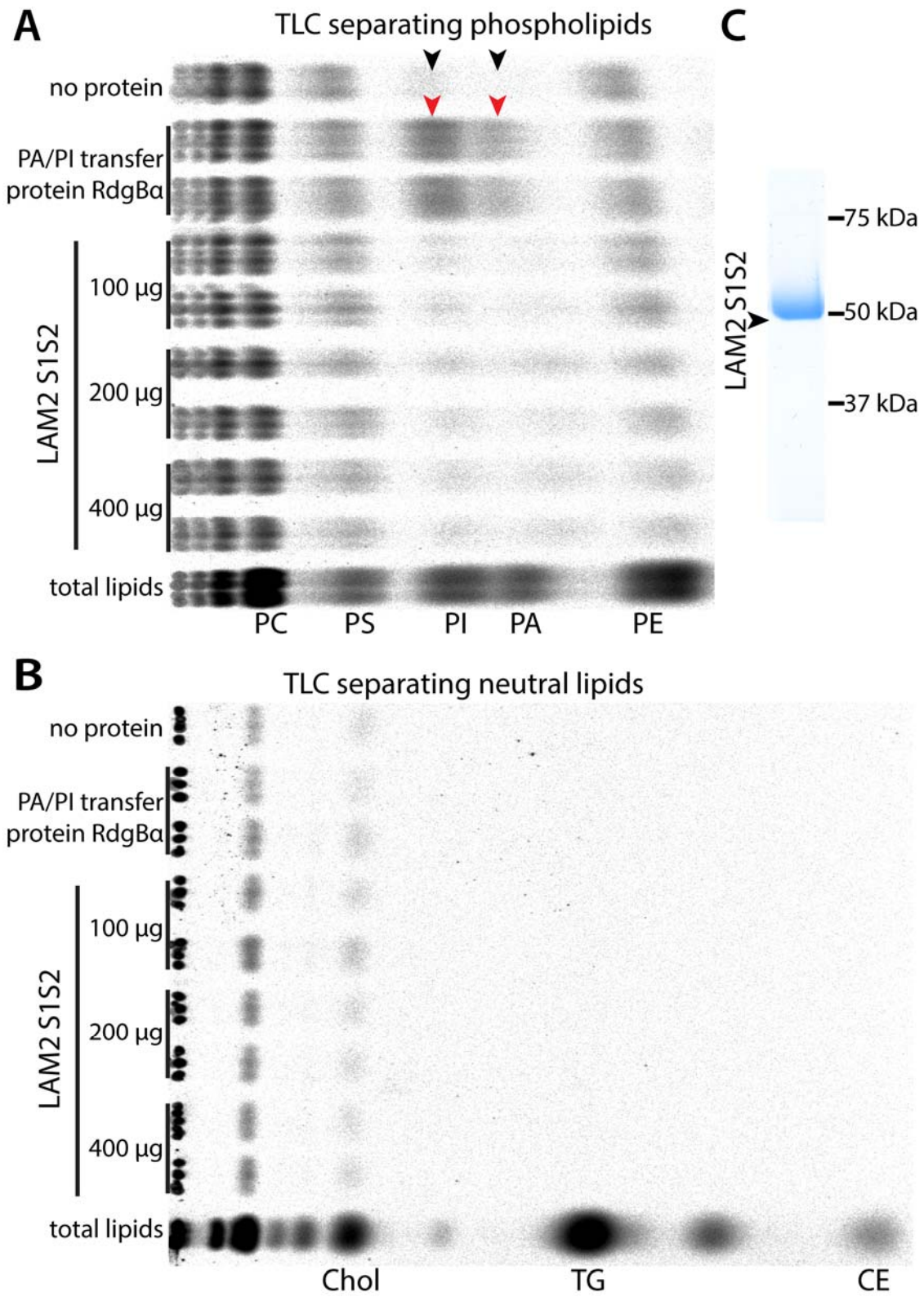

Figure 6.4 **Radioactive lipid transfer with Hisx11 Lam2S1S2**
TLC separation of radioactive **A**) phospholipids and **B**) neutral lipids extracted from acceptor liposomes after incubation with Lam2S1S2 with controls of RdgBα, a known PA/PI transfer protein. Samples of the radiolabelled membranes were run out as a standard. This method gave a high background but showed a positive result of PA and PI transfer for RdgBα (red arrows) compared to the negative (black arrows). No transfer was seen for Lam2S1S2. **C**) SDS-PAGE of purified Hisx11 Lam2S1S2 at ~50kDa of ~99% purity. Abbreviations: PA, phosphatidic acid; PI, phosphatidylinositol; PS, phosphatidylserine; PC, phosphatidylcholine; PE, phosphatidylethanolamine; Chol, cholesterol; TG, triglycerides; CE, cholesteryl esters.

tryptophan will emit a wavelength of 340 nm, but the energy can transfer to the DHE if the latter is very nearby, to then produce a signal at a higher wavelength 375 nm that would otherwise not be seen with the tryptophan alone [Figure 6.2C]. The Förster distance of these two fluorophores (tryptophan and DHE) is ≤1.6 nm (Schroeder *et al.*, 1990; Raghuraman and Chattopadhyay, 2004) and is indicative of the distance that produces 50% maximal FRET efficiency, which falls off inversely proportional to the distance to the power 6, so at 3.2 nm it will be <1% efficient [Figure 6.2B]. The StARkin domains are approximately 2-2.5 nm across, meaning that any measurable FRET signal would require direct binding of the DHE molecule within the cavity.

6.2.4 Histidine x11 increases purity of the protein

Previously, an N-terminal His x6 tag was used to capture proteins onto the Ni^{2+} beads for protein purification. However, the purity was low (<50%) with concentrations of the total protein mix being 1-2 $mgml^{-1}$ [Figure 6.3B]. Increasing the histidine tag from six to eleven residues improves the purity up to ~99% [Figure 6.4C] and concentrations up to 12 $mgml^{-1}$ were achieved. The N-terminal His x11 tag was used to express StARkin 1 and StARkin 2 separately from both Lam2p and Lam4p [Figure 6.5B]. The plasmid constructs were designed so that the full core StARkin domains are expressed with several additional residues either side to facilitate solubility and expression in bacteria. By separating the StARkins, any *in vitro* function could be pinpointed to the *in vivo* function of AmB resistance seen in growth assays with yeast.

All expressed His-tagged StARkin domains from the bacterial cell lysates were fully captured by the Ni^{2+} beads after incubation [Figure 6.5C]. Both LAM StARkin domains from Lam4p (Lam4S1 and Lam4S2) were straightforward to purify at high concentrations (up to 12 $mgml^{-1}$). The StARkin domains from Lam2p (Lam2S1 and Lam2S2) were obtained at lower concentrations, and Lam2S2 had a tendency to precipitate when exchanging buffers from high salt to the storage buffer. AmB growth assays show that Lam4p StARkin domains can rescue delete strains similarly to Lam2p StARkin domains with Lam4S2 being more active than Lam4S1. Due to the StARkin domains from Lam4p being more soluble than Lam2p StARkin domains, Lam4S2 was the most analysed in the following FRET assays of this investigation.

6.2.5 Tryptophan in StARkin domain FRETs with DHE

Lam4S2 has one tryptophan that directly points into the cavity of the domain [Figure 6.5A]. Excitation at 295 nm of Lam4S2 produced a single peak of emission at 340 nm [Figure 6.6A - solid blue line], which varied in intensity dependent on the

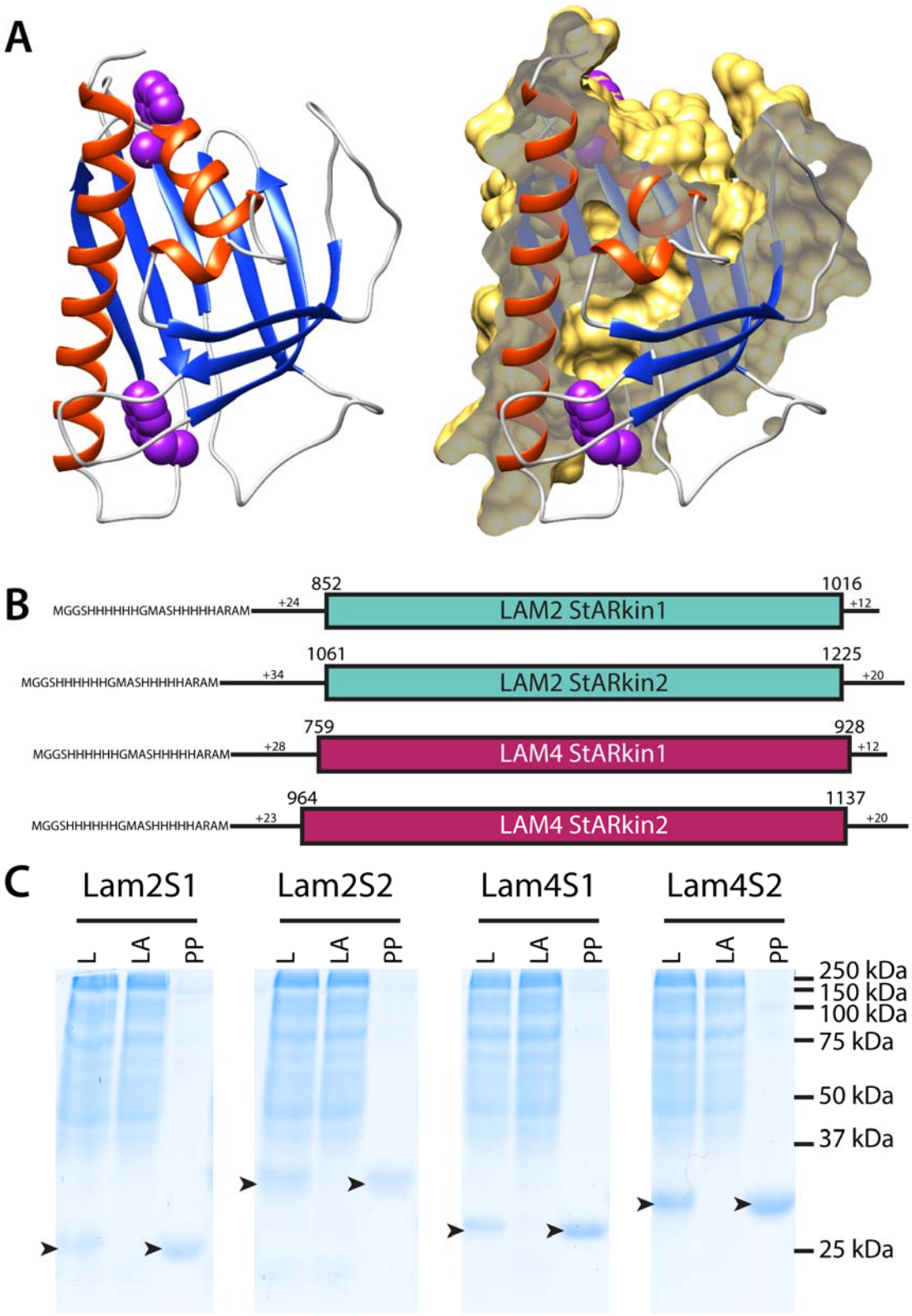

Figure 6.5 **Purification of isolated StARkin domains of Lam2p and Lam4p**
A) Ribbon depiction of Lam4S2 predicted model. The tryptophan residues are indicated in purple. A clipped surface model (yellow) shows the internal cavity surface where ligands may bind. **B**) LAM StARkin constructs labelled with the first and last residue of the core StARkin domain from each Lam2p (cyan) and Lam4p (pink). The numbers of additional residues either side of the StARkin domain constructs are indicated. **C**) SDS-PAGE of purified (PP) Lam2S1, Lam2S2, Lam41 and Lam2S2 of ~99% purity. The cell lysate before (L) and after (LA) incubation with Ni^{2+} was also run showing complete extraction of protein.

concentration of protein added to the cuvette [data not shown].

Sterols, in general, have a low solubility in water; therefore, methyl-β-cyclodextrin (MβCD) was used as a carrier in the aqueous buffer. This method is suggested for loading DHE into cells, so could also be used to load DHE into a protein cavity (Maxfield and Wüstner, 2012). When DHE:MβCD complex was added, a significantly different emission spectrum was observed [Figure 6.6A-blue dotted line]. The new spectrum shows the characteristic emission of DHE when excited at 340 nm; there are three peaks with 375 nm being the highest peak. This new spectrum indicates that FRET has occurred between the tryptophan and DHE:MβCD that has been added. The addition of MβCD alone did not produce any signal. Thus it is the DHE that is involved with the production of the strong FRET signal [Figure 6.6B]. In addition, there is a noticeable decrease in tryptophan fluorescence at 340 nm likely to be a transfer of energy during the FRET to excite the DHE molecule.

6.2.6 FRET requires correct folding of the StARkin domain

To show that FRET between the tryptophan and DHE only occurs when the protein is intact and folded with a binding cavity, an abolishment of FRET is demonstrated when the protein is unfolded and denatured. Guanidinium-HCl is a standard strong denaturing agent, and a 7M concentration was used to denature Lam4S2 [Figure 6.6A]. The same FRET assay was carried out on the denatured Lam4S2. The emission spectrum of the tryptophan is now shifted to the right with a peak of ~355 nm, indicating successful denaturation of the protein. Depending on the hydrophobicity of the tryptophan environment, the emission spectrum can shift [Figure 6.1B]. Previously the tryptophan was in a hydrophobic environment being folded within the cavity and the protein itself. In denaturing conditions, it is exposed to the aqueous environment with an emission peak at 355 nm similar to the emission of tryptophan in water [Figure 6.8A – red solid line]. The addition of DHE to the denatured protein produced no FRET signal showing that the presence of the protein (with its tryptophans) and the fluorescent lipid alone are insufficient for FRET. The requirement of the intact structure of the StARkin domain for FRET indicates that the correct folding of the protein is needed to allow the lipid and the tryptophan residue to come close together *i.e.* to interact.

6.2.7 DHE is bound within the binding pocket

The positive FRET spectrum recorded with native Lam4S2 shows a maximum peak at ~375 nm with secondary peaks at ~ 355 nm and ~390 nm [Figure 6.6A – dotted blue line]. This pattern is similar to that of DHE in a hydrophobic environment such as within a membrane rather than the pattern of DHE in an aqueous solution which shows

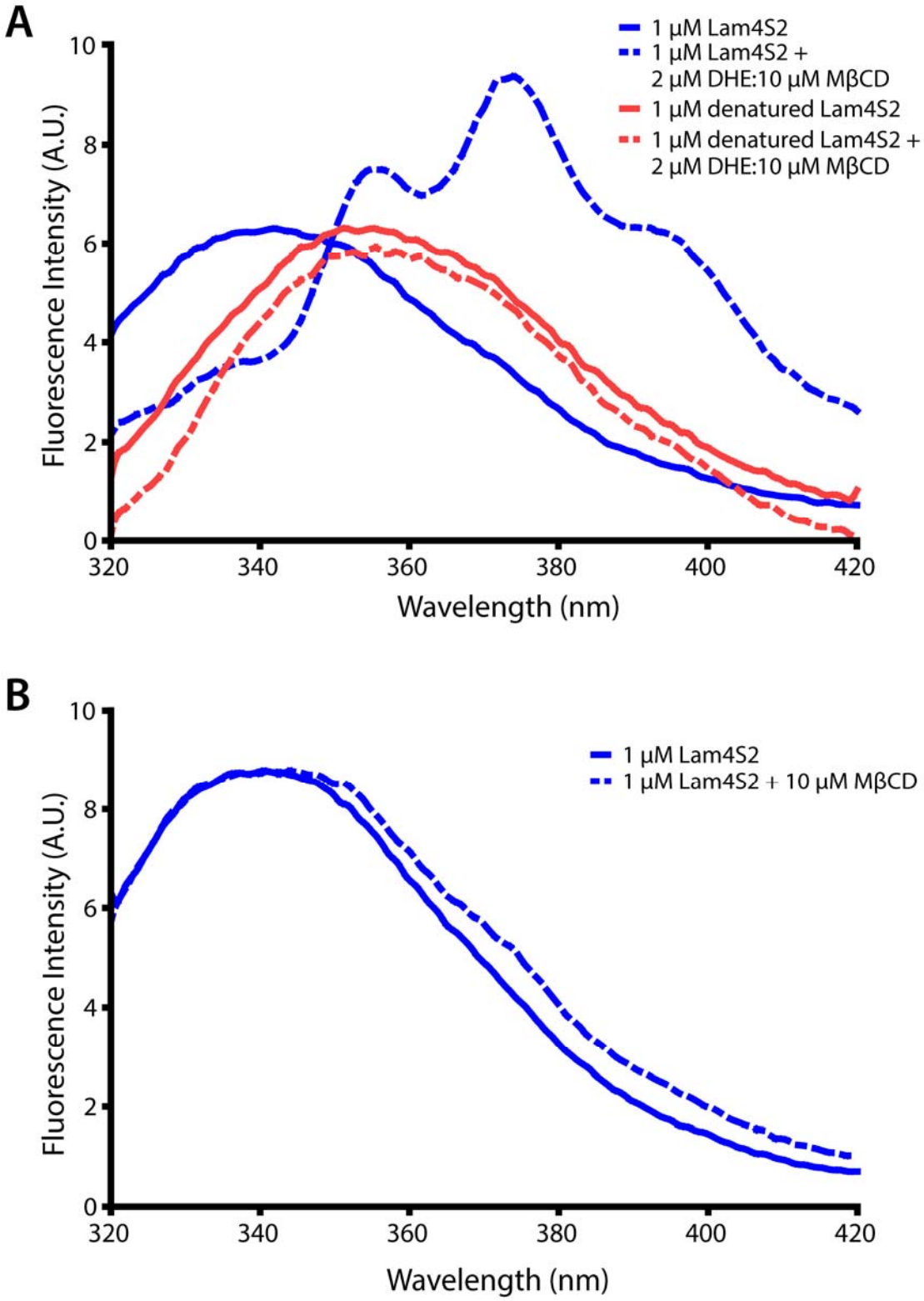

Figure 6.6 **Lam4 StARkin 2 shows binding to DHE**
A) Emission spectra of native folded Lam4S2 (blue) and denatured Lam4S2 in 7M guanidinium HCl (red), with (dotted) and without (solid) DHE:MβCD complex, excited at 295 nm. Background DHE:MβCD and buffer signal are subtracted. A significant change in spectra is recorded upon the addition of DHE:MβCD to native Lam4S2, which is not seen with denatured protein. **B**) Control spectra of Lam4S2 (solid) with MβCD (dotted) show that DHE must be present for FRET signal. All spectra are representative of one experiment though similar results were seen in multiple variants of these experiments.

a prominent peak at 425 nm [Figure 6.1A]. It is likely that this is due to the DHE being bound within the hydrophobic cavity of the StARkin domain, which protects the lipid from the aqueous solution around it.

The assay with the denatured Lam4S2 also indicates that the FRET signal is specifically due to the tryptophan inside the pocket. The exposed tryptophan does not face the binding pocket and is instead facing the solvent [Figure 6.5A] implying that any exposure to DHE when the protein is intact would be similar to the exposure when the protein is denatured. As there is no FRET signal when the protein is denatured, it signifies that the external tryptophan does not contribute to FRET with DHE.

6.2.8 FRET is specific to the StARkin fold

Further control FRET assays were carried out as a negative control, Soybean trypsin inhibitor, which is not known to bind lipids [Figure 6.7] (Koide, Tsunasawa and Ikenaka, 1972). Like Lam4S2, Soybean trypsin inhibitor contains two tryptophan residues and is approximately the same size as Lam4S2, being ~21.5 kDa. No significant difference between the Soybean trypsin inhibitor spectrums was observed either with DHE:MβCD or MβCD alone. This result further indicates that the FRET signal is due to StARkin domain-specific structure and the DHE molecule rather than coincidental proximity of the DHE to a protein containing tryptophan.

Additional FRET assays were also carried out with monomeric tryptophan alone [Figure 6.8]. To replicate the same number of tryptophans as Lam4S2, the concentration of free tryptophan was double that of Lam4S2. As with the denatured Lam4S2, the spectrum of tryptophan has a peak of ~355 nm, indicating the free tryptophan molecules in the aqueous solvent rather than within a folded protein [Figure 6.8A – red solid line]. The addition of DHE:MβCD or MβCD alone did not produce any FRET signal [Figure 6.8]. Again, this supports the FRET signal being specific to the tryptophan inside the cavity of a folded StARkin domain.

6.2.9 StARkin domains from Lam2p and Lam4p binds with DHE

The FRET assays were carried out with the remaining StARkin domains that were purified. Each protein emitted a characteristic tryptophan emission spectrum and upon addition of DHE:MβCD, a strong FRET signal was observed [Figure 6.9+ Figure 6.10]. The positive signals indicate that all four StARkin domains can bind DHE within the cavity of the folded StARkin domain in addition to confirming that there is a conserved tryptophan residue within the internal binding pocket, facing the cavity. The wavelength of 375 nm was consistently the most statistically significant signal as

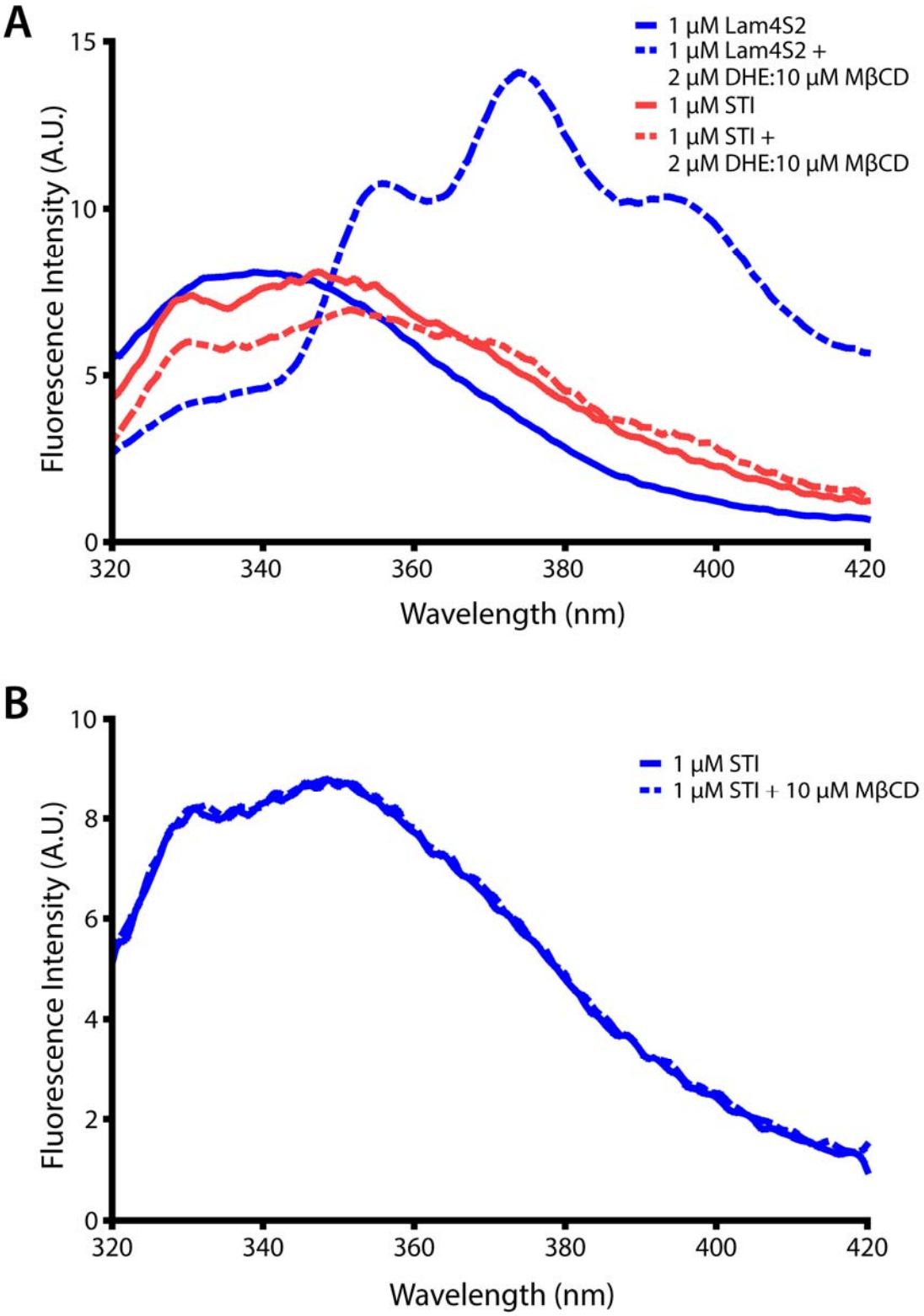

Figure 6.7 **Control protein STI shows no binding to DHE**
A) Emission spectra of Lam4S2 (blue) and Soybean trypsin inhibitor (STI) (red), with (dotted) and without (solid) DHE:MβCD, excited at 295 nm. Background DHE:MβCD and buffer signal are subtracted. A FRET signal is recorded upon the addition of DHE:MβCD to native Lam4S2, which is not seen with STI. **B**) Emission spectra of STI (solid) with MβCD (dotted) show similar spectra to that of STI with DHE:MβCD. All spectra are representative of one experiment though similar results were seen in multiple variants of these experiments.

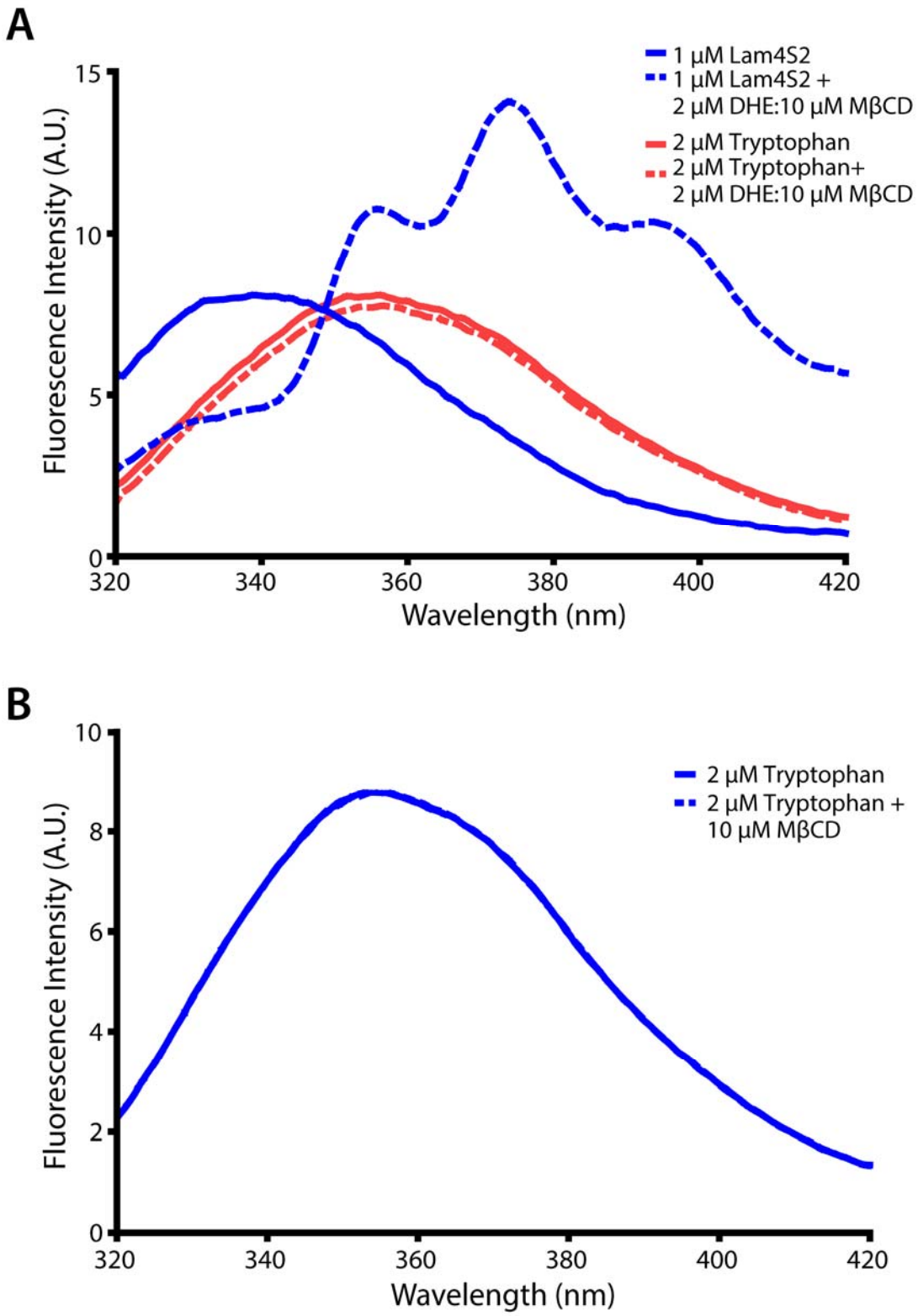

Figure 6.8 **Free tryptophans show no binding to DHE**
A) Emission spectra of Lam4S2 (blue) and free tryptophan (red), with (dotted) and without (solid) DHE:MβCD complex, excited at 295 nm. Background DHE:MβCD and buffer signal are subtracted. The concentration of free tryptophan was double that of Lam4S2 to replicate the number of tryptophans in the protein. A FRET signal is recorded upon the addition of DHE:MβCD to native Lam4S2, which is not seen with free tryptophan. **B**) Emission spectra of free tryptophan (solid) with MβCD (dotted) show similar spectra to that of free tryptophan with DHE:MβCD. All spectra are representative of one experiment though similar results were seen in multiple variants of these experiments.

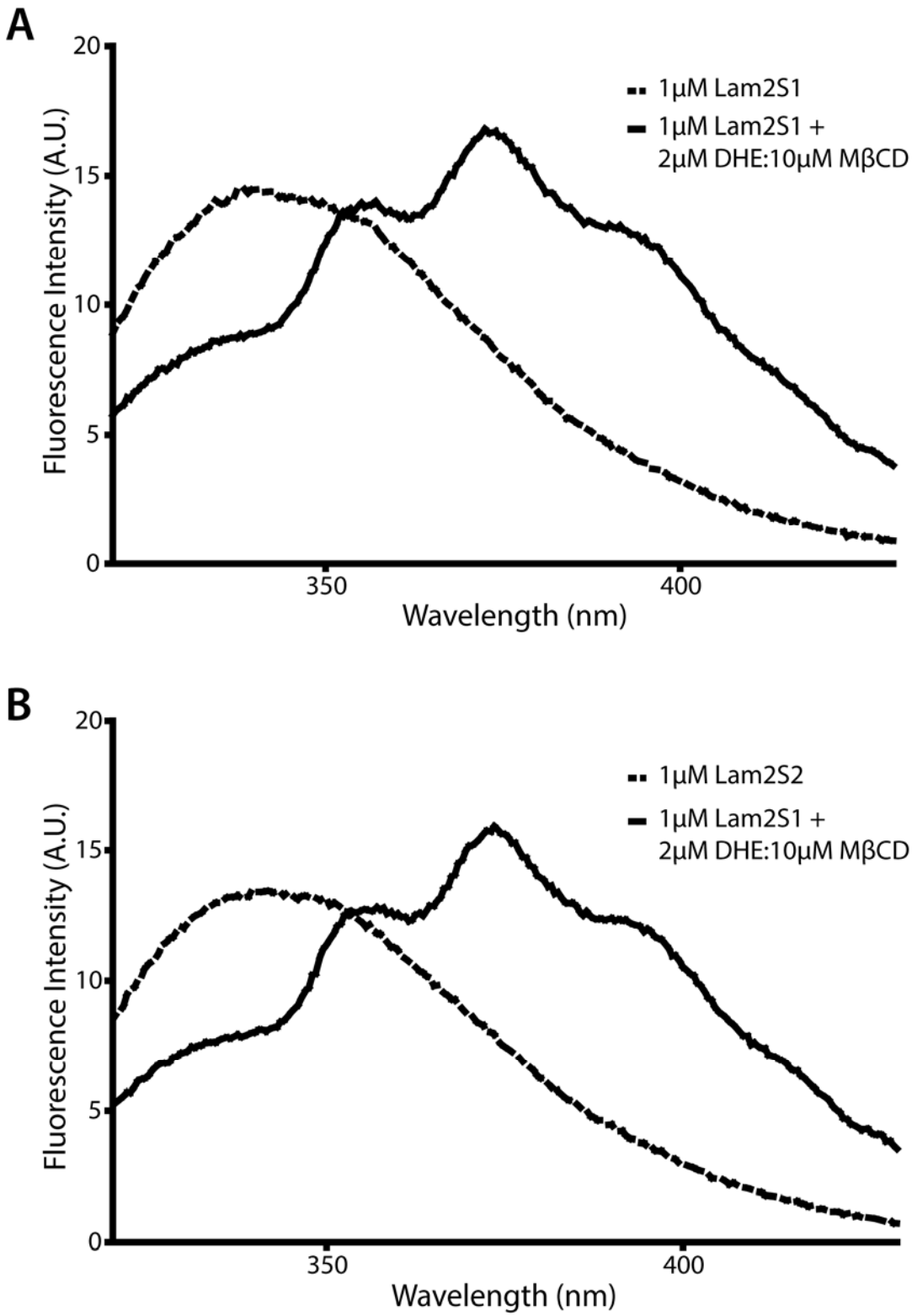

Figure 6.9 **Lam2S1 and Lam2S2 show binding to DHE**
A) Emission spectra of Lam2S1 with (solid) and without (dotted) DHE:MβCD complex with background DHE:MβCD and buffer subtracted. **B**) Emission spectrum of Lam2S2 with (solid) and without (dotted) DHE:MβCD complex with background DHE:MβCD and buffer subtracted. Both purified StARkin domains from Lam2p shows a positive FRET response upon excitation at 295 nm.

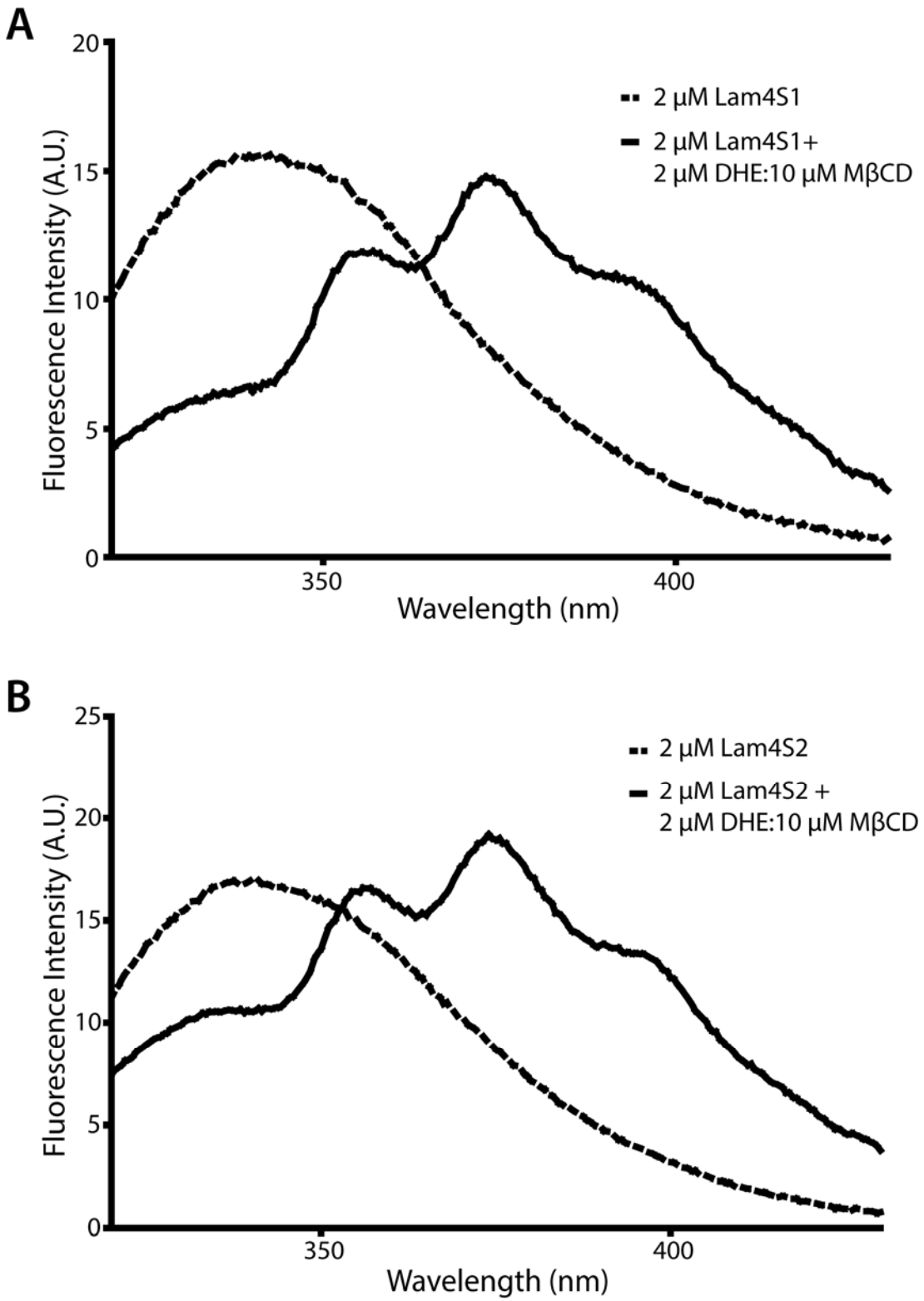

Figure 6.10 **Lam4S1 and Lam4S2 show binding to DHE**
A) Emission spectra of Lam4S1, with (solid) and without (dotted) DHE:MβCD complex. The background DHE:MβCD and buffer signals have been subtracted. **B**) Emission spectrum of Lam4S2, with (solid) and without (dotted) DHE:MβCD complex. The background DHE:MβCD and buffer signals have been subtracted Both purified StARkin domains from Lam4p shows a positive FRET response upon excitation at 295 nm.

expected with DHE in a hydrophobic environment in the binding cavity. Therefore, a ratio of 375 nm:340 nm, the emission peak ratio, was used to quantify the signal. A range of ±2.5 nm either side of the peaks was used to average the signal of each peak before calculating the FRET signal. The FRET signal of protein alone was defined as 0, and the FRET signal of protein and DHE was defined as 1 to standardise the FRET signal for the following assays.

6.2.10 Cholesterol:MβCD competes out the DHE:MβCD

Non-fluorescent cholesterol is very similar in structure to DHE, and it is likely that the StARkin domains from LAM proteins could bind with very similar affinity to cholesterol as it does with DHE. A competition assay was carried out with Lam4S2 where the protein is presented with both DHE and cholesterol at equal concentrations [Figure 6.11A]. Lam4S2 binding to DHE would produce a FRET signal whereas, with non-fluorescent cholesterol, no FRET will occur. It is important to note that this assay presumes full or close to full occupancy even with DHE alone. When Lam4S2 was presented with equal amounts of cholesterol:MβCD and DHE:MβCD, only half the FRET signal was produced compared to DHE:MβCD alone [Figure 6.11B]. This suggests that the affinities of the StARkin domain to these two sterols are very similar in addition to confirming that during this assay most if not all StARkin cavities were filled with a ligand.

As the binding affinities to DHE and cholesterol are similar, the ratio of Lam4S2 that binds to DHE compared to cholesterol will be proportional to the ratio of DHE to cholesterol. When the availability of cholesterol to Lam4S2 was raised by adding increasing cholesterol:MβCD with a fixed concentration of DHE:MβCD, the FRET signal could indeed be competed out [Figure 6.11C]. However, there was a consequence that caused anomalies toward the higher concentrations of cholesterol that were added. A problem with the addition of cholesterol:MβCD is the increasing concentration of MβCD also added, which is evident at the highest concentration of cholesterol:MβCD where the control of MβCD is seen to reduce the FRET [Figure 6.11C]. This reduction in FRET between Lam4S2 and DHE in the absence of cholesterol is possibly due to excess MβCD extracting out the DHE from the cavity of the StARkin domain. A reduction in FRET occurs when there are over 30-fold more MβCD molecules to Lam4S2 indicating that Lam4S2 binds to DHE at a much higher affinity than MβCD.

6.2.11 Excess MβCD disrupts competition of lipids for the StARkin cavity

Assays based on the addition of equimolar concentration of competitor lipids other than sterols were carried out using MβCD as a solubilising agent. Although the competition

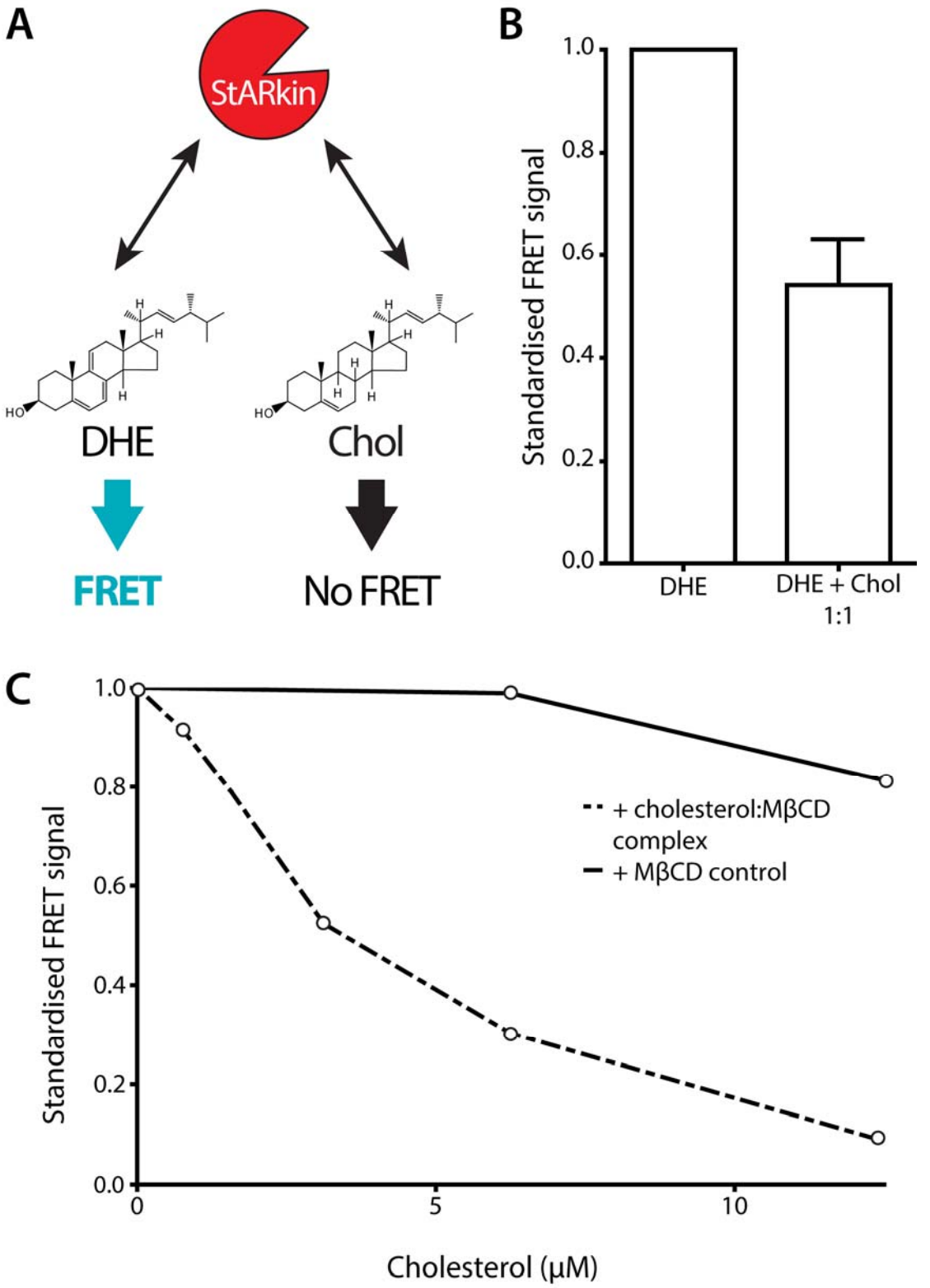

Figure 6.11 **Lam4S2 binds with similarly to both DHE and Cholesterol**
A) Schematic of competition binding assay of 1μM LamS2 to fluorescent DHE and non-fluorescent cholesterol. Binding with DHE results in a FRET signal. **B**) FRET signal of 1 μM Lam4S2 with 2.7 μM DHE:MβCD only is defined as 1. FRET decreases by ~50% with 2.7 μM DHE:MβCD and 2.7 μM Chol:MβCD indicating equal binding to DHE and cholesterol. n =3. **C**) FRET signal decreased with increasing concentrations of cholesterol: MβCD with 2.7 μM DHE: MβC. However, an adverse effect of excess MβCD was observed at the highest concentrations. The ratio of 375 nm to 340 nm was used to standardise the FRET signal. The FRET signal of protein alone was defined as 0 and the FRET signal of protein and DHE was defined as 1.

of the cholesterol could be consistently replicated, the assays with PLs were variable [Figure 6.12A and data not shown]. The spectrum was erratic and significant background emission was observed for some scans. In addition, the MβCD complex for some of the competitor lipids contained precipitants, which was removed from the solution by centrifugation. The removal of solids indicates that there was some loss of lipid, which cannot be quantified easily. Whilst the competition between cholesterol:MβCD and DHE:MβCD was straightforward, the competitions with other lipids complexed with MβCD were unreliable. MβCD has a high affinity to all sterols (Ohtani *et al.*, 1989; Ohvo and Slotte, 1996; Christian *et al.*, 1997; McIntosh *et al.*, 2008). However, the affinities to other lipids are not documented. MβCD is used to extract sterol molecules from cell membranes; therefore, affinities to other lipids such as glycerophospholipids must be lower than that of sterol. This creates a complicated mixture of carriers and lipids as the MβCD will extract sterols from the StARkin more readily than the competitor lipid and donate sterols much less frequently [Figure 6.12B]. In addition, different lipids have different solubilities in solution, with some PLs being able to spontaneously form liposomes which means an unfair and inaccurate comparison of lipid affinity as to the protein's ability to extract lipids from liposomes is a factor with PLs but not sterol. Therefore, this approach is unfeasible to test the competition of different lipids to sterol with the StARkin domains.

6.2.12 Lipids solubilised in methanol binds to StARkin

An alternative approach was developed from a method used by Schauder *et al.* where E-Syt2 was bound with phosphatidylethanolamine *in vitro* after addition of a low concentration of a solution of the lipid in methanol (Schauder *et al.*, 2014). Im *et al.* also used lipids dissolved in alcohol (in this case ethanol) to test the *in vitro* cholesterol binding of Osh4p (Im *et al.*, 2005). In Figure 6.13, DHE solubilised in methanol was incubated with protein so that the methanol was 10% of the total volume and then diluted for the spectrum scan so that methanol was <0.1% of the total volume. The low methanol concentration reduced undesirable effects to the protein. Although the FRET signal was not as strong as with DHE:MβCD, the signal was still significant, and cholesterol was able to compete out the DHE as expected. Equal concentration of cholesterol to DHE produced a FRET signal of 50% of the signal with DHE alone [Figure 6.13A]. The two-fold reduction of FRET in the presence of equal molar of cholesterol indicates that Lam4S2 has similar affinity to cholesterol and DHE. This result is consistent with assays using DHE:MβCD complex.

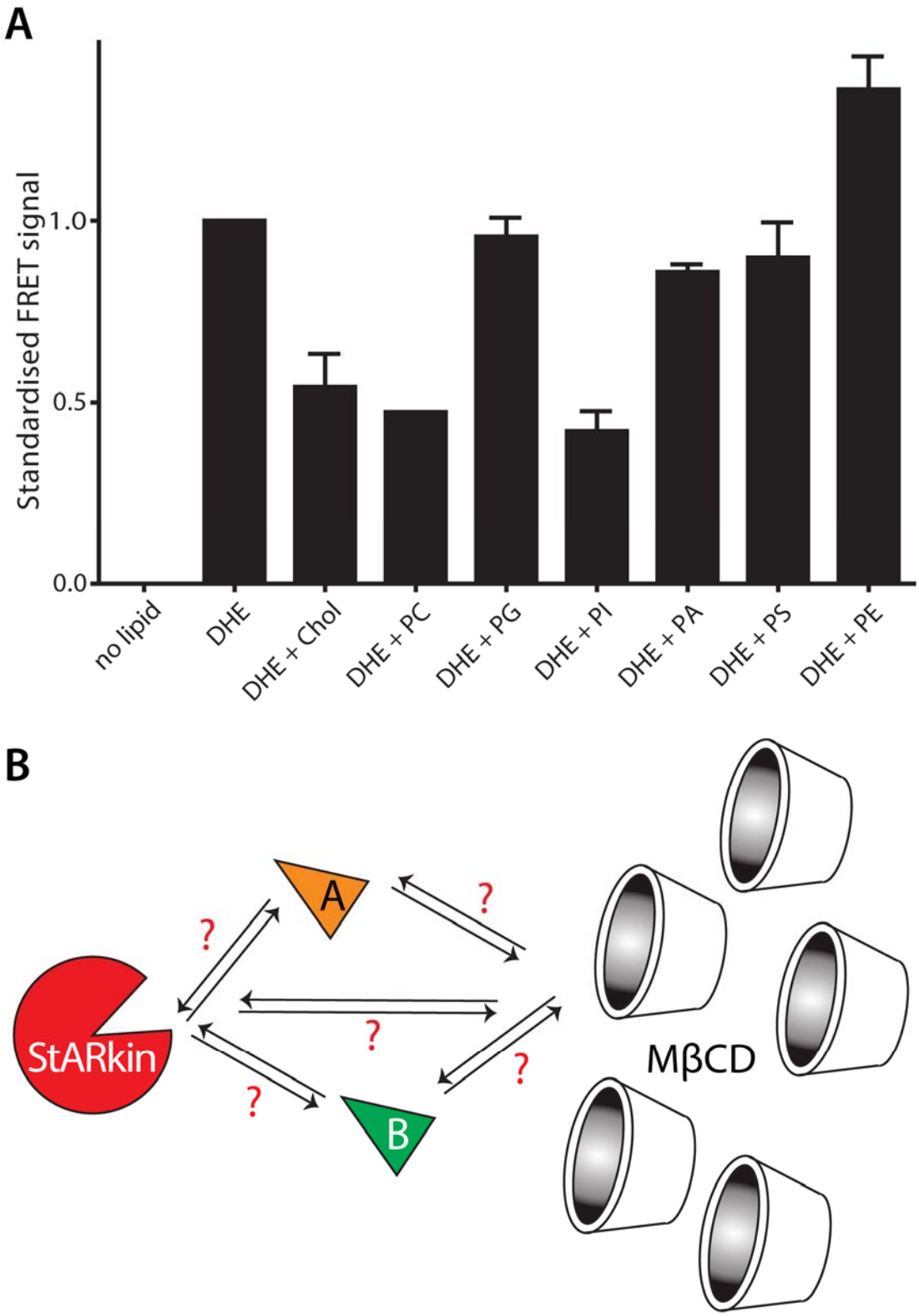

Figure 6.12 **Excess MβCD causes uncontrolled effects on binding assays**
A) FRET signal of 1 µM Lam4S2 with 2.7 µM DHE:MβCD only is defined as 1. FRET assays with equimolar DHE and competitor lipid MβCD complexes. A significant number of spectra scans showed anomalies such as abnormal curve shape that was not used for this graph. n = 1 – 5. The ratio of 375:340 nm was used to standardise the FRET signal. The FRET signal of protein alone was defined as 0. **B**) Illustration showing the unknown affinities involved in the competition assays using MβCD as a solubilising agent. Triangles A and B indicates two different lipids. Abbreviations: Chol, cholesterol; PC, phosphatidylcholine; PG, phosphatidyl glycerol; PI, phosphatidylinositol; PA; phosphatidic acid; PS, Phosphatidylserine; PE, phosphatidyl ethanolamine.

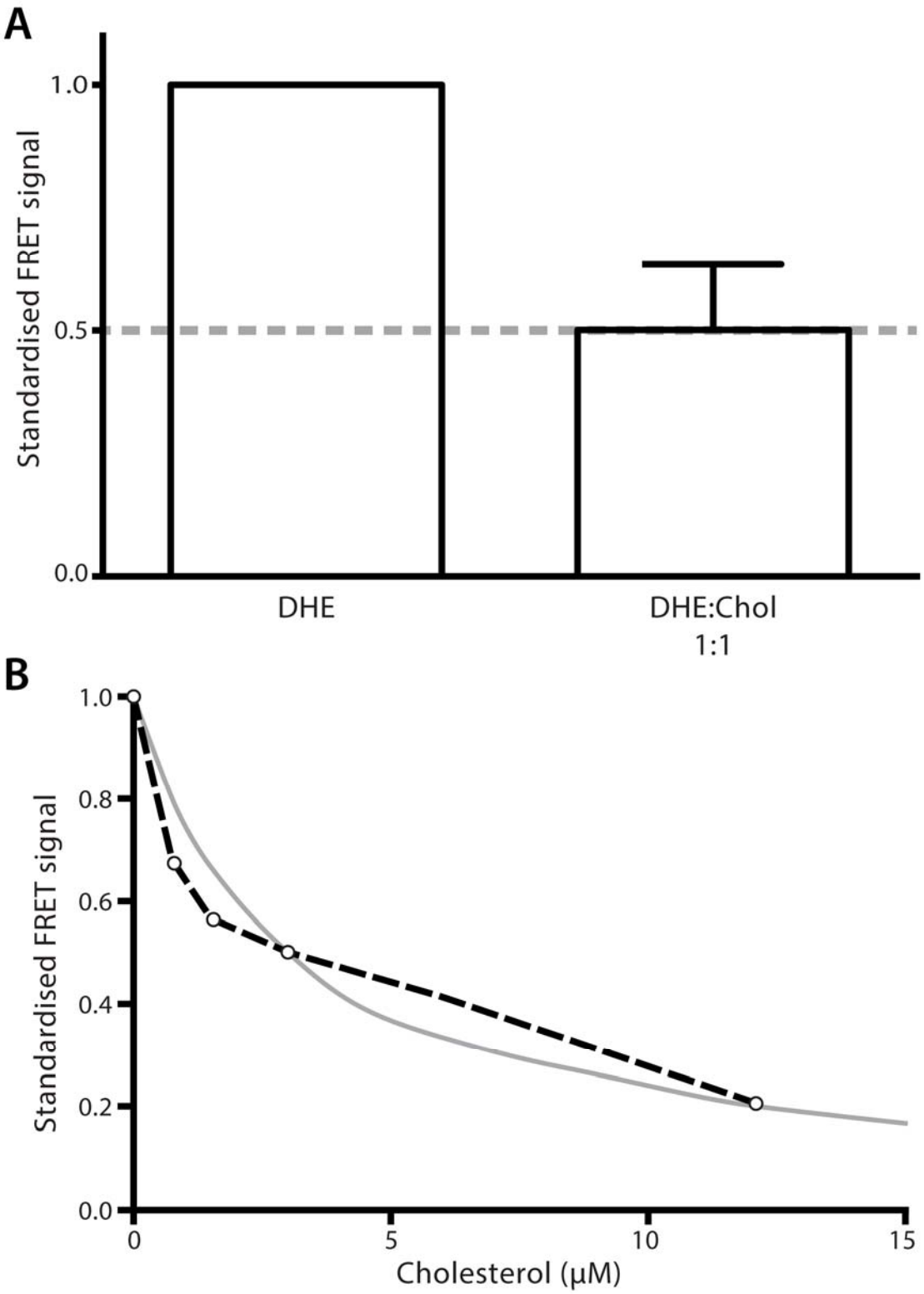

Figure 6.13 **Lam4S2 binds with similar affinity to both DHE and Cholesterol**
A) FRET signal of 2 μM Lam4S2 with 3 μM DHE only is defined as 1. FRET decreases by ~50% with 3 μM DHE and 3 μM Chol indicating equal binding to DHE and cholesterol. 50% is indicated in grey. n =10. **B**) FRET signal decreased with increasing concentrations of cholesterol with 3 μM DHE (dotted). The predicted FRET signal is indicated in grey. The ratio of 375:340 nm was used to standardise the FRET signal. Lipids are solubilised in methanol which consists of <0.1% of the total volume. The FRET signal of protein alone was defined as 0 and the FRET signal of protein and DHE was defined as 1.

This method was used to with various concentrations of cholesterol. As the methanol volume that was added remained the same, there is no additional background to account for in contrast to increasing concentrations of MβCD used in Figure 6.11. Using this solubilising method of cholesterol in methanol, a clear and consistent decrease of FRET was seen with increasing concentrations of DHE:methanol [Figure 6.13B]. The predicted FRET signal dependent on the proportion of fluorescent and non-fluorescent sterol is an inverse exponential curve. For example, where there is equal molar cholesterol to DHE (3 μM:3 μM) the signal is predicted to be 50%, however, when cholesterol concentration is raised to 12 μM, the ratio is 1:4 and therefore predicted FRET is 20%. The measured FRET signal during increasing concentration of cholesterol closely matches the predicted FRET signal, suggesting that this binding assay is efficient and also that there is close to full occupancy when there is ~3 μM of sterol for every 1 μM of protein.

6.2.13 All StARkin domains bind sterols with similar affinities

Both StARkin domains from Lam2p and Lam4p were tested for binding with DHE, cholesterol and ergosterol, and consistently showed a 50% drop in FRET signal [Figure 6.14A]. This suggests that the StARkin domains all bind sterols in a similar manner. There was no binding to PC and PS, two common PLs found in the cell membranes indicated by no recorded decrease in the FRET signal with the addition of PC or PS. The lack of FRET change suggests that the StARkin domain is unable to bind PLs in the cavity where the bound DHE is located. However, this does not rule out binding of lipids outside the protein cavity which would not affect the DHE binding and therefore FRET changes would not be documented.

Lam4S2 was extensively tested with other PLs such as phosphatidic acid [Figure 6.14B]. However, none of the other PLs tested showed binding implying that the specificity of the StARkin domain cavity is to sterols.

Cholesterol is not found in yeast. However, the StARkin domains of the LAM proteins are able to bind to cholesterol in addition to DHE and ergosterol, the native yeast sterols. It is likely that the LAM proteins of yeast bind to mammalian sterol due to its similarity to ergosterol. In addition, it is proposed that ergosterol biosynthesis evolved from ergosterol (Weete, Abril and Blackwell, 2010). Another group of mammalian specific molecules that is structurally similar to sterols is the steroidal hormones for which cholesterol is a precursor. Sterols are a type of steroid and share the common four rings sterene structure. Progesterone is one such steroid hormone and compared to cholesterol/ergosterol, it has a very short functional group attached to the

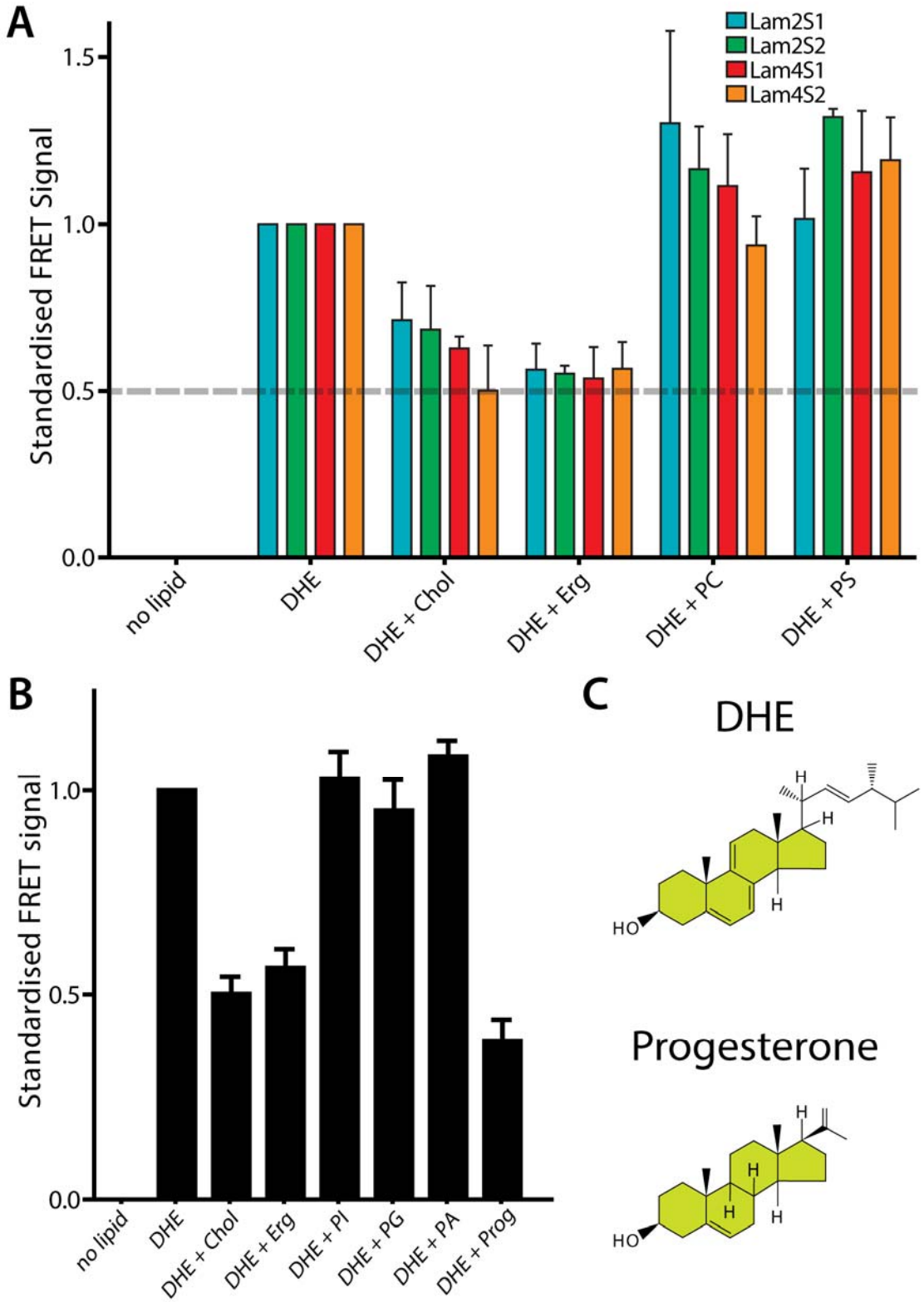

Figure 6.14 **Lam2/4p StARkins binds sterols but not phospholipids**
A) FRET signals of Lam2S1 (blue), Lam2S2 (green), Lam4S1 (red) and Lam4S2 (orange) without lipids, with DHE and with DHE and competitor lipids. 50% signal is indicated in grey. n = 3-10. **B**) FRET signals of Lam2S2 without lipids, with DHE and with DHE and competitor ligands. The ratio of 375:340 nm was used to standardise the FRET signal. 3 µM of lipids were added to 2 µM protein. Lipids are solubilised in methanol which consists of <0.1% of the total volume. The FRET signal of protein alone was defined as 0 and the FRET signal of protein and DHE was defined as 1. **C**) DHE and progesterone chemical structure shows that both molecules are based on the steroid ring structure (light green).

D-ring [Figure 6.14C]. When tested for binding with Lam4S2, Progesterone was able to compete out the DHE to approximately 50%. This is interesting to note that there are many more defined StART domains found in mammalians and all have specific binding to various lipids including but not limited to cholesterol. However, mammalian StART domains are not documented to bind steroid hormones. The StART family in mammalian cells have diverged from the LAM proteins so much that PSI-BLAST was unable to detect the similarity of the domains. This could potentially be due to evolutionary pressures to alter the StARkin domains such that overlaps with steroid binding are prevented. However, binding assays are yet to be carried out with human LAM StARkin domains to test their sterol and steroid binding ability.

6.2.14 StARkin domain binds to DHE in liposomes

The assessment of DHE and sterol binding carried out thus far has been via free lipids not situated within a membrane. In the cellular environment, to facilitate sterol transfer between membranes, the protein must be able to associate with the membrane and be able to extract the sterol from beneath the hydrophilic heads of the PLs present in the membrane, as envisaged by the "umbrella model" (see section 1.2.5 for more information on sterol interaction with other membrane lipids). For instance, there is a possibility that there is a yet unknown protein partner which can pass on its lipid ligand to LAM proteins thus there is no need for LAM StARkins to associate with a membrane. To test the ability of the LAM StARkin domain to extract and bind sterols, an artificial membrane model must be used. Liposomes are small spherical shaped bilayers of which the composition can be defined in the process of production. A composition of a mixture of PC, PE and PS was used to produce the liposomes due to the lack of binding to the StARkin cavity shown in the previous assays.

Initially, a low signal was detected, but troubleshooting tests showed that using both a high DHE content and a small diameter produced high levels of binding. Significantly, more FRET was detected using liposomes with a diameter of 100 nm than with 200 nm suggesting that high membrane curvature is required for the StARkin domain to efficiently extract the sterol from the membrane [Figure 6.15A]. One possibility is that this is more reflective of ER tubule strands where diameters are 50-100 nm [Figure 6.15B]. However, the smaller diameter of the liposomes could be increasing the favourability of the sterol being exposed caused by packing defects, and so could be reflecting the requirements of other domains of the LAM protein or other proteins at the contact site to disrupt the membrane order to allow efficient extraction by

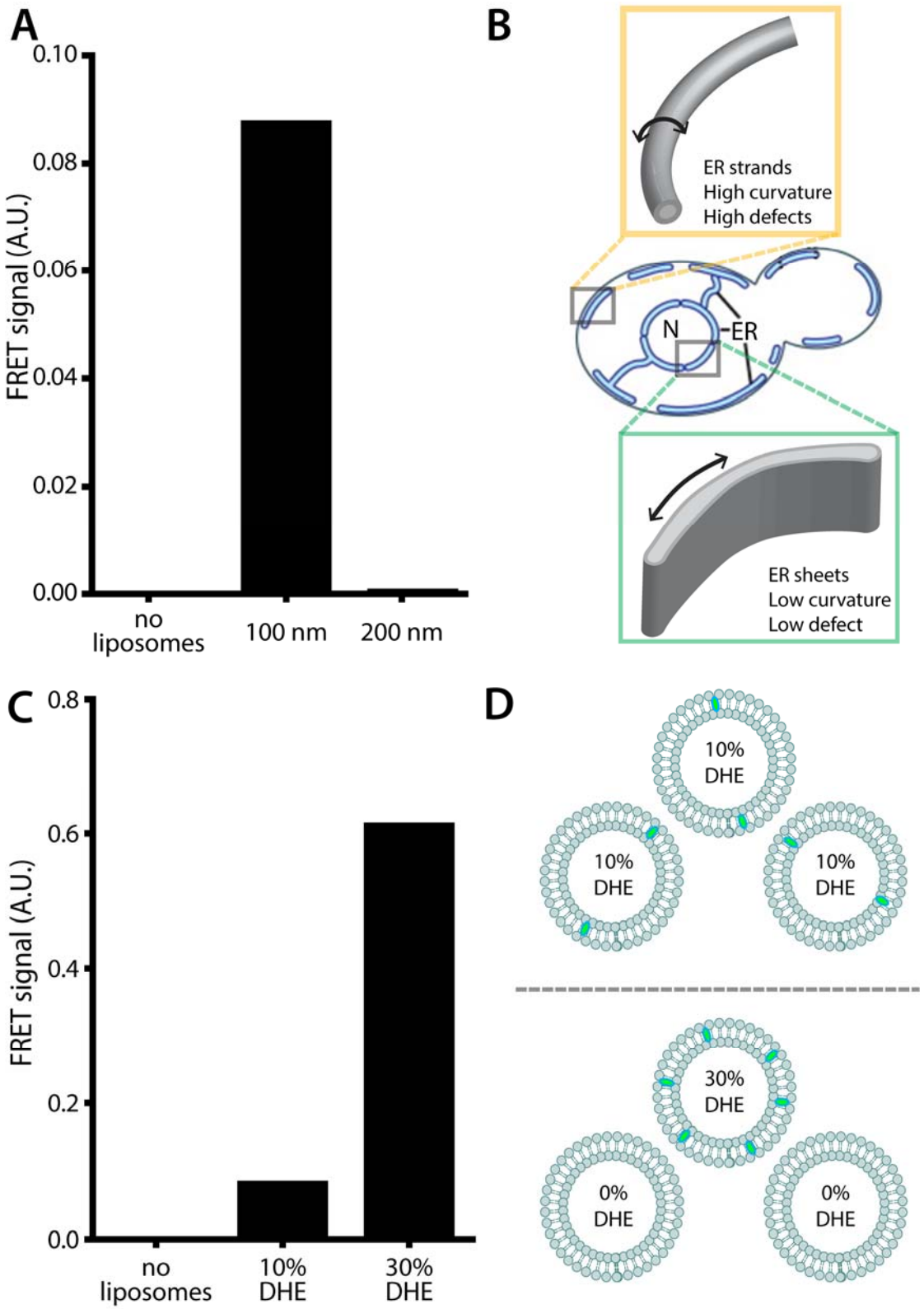

Figure 6.15 **Lam4S2 extracts DHE from liposomes**
A) FRET signal of 1 μM Lam4S2 bound to 20 μM $PC_{60}PE_{20}PS_{10}DHE_{10}$ liposomes of 100 nm and 200 nm diameters. FRET was higher with 100 nm liposomes. **B**) Diagram showing membrane curvature on two possible ER structures. **C**) FRET signal of 1 μM Lam4S2 to 20 μM $PC_{60}PE_{20}PS_{10}DHE_{10}$ liposomes and 20 μM $PC_{40}PE_{20}PS_{10}DHE_{30}$:$PC_{70}PE_{20}PS_{10}$ (1:2) liposomes where both reaction contained equivalent concentrations of each lipid. FRET was higher using liposomes with higher %mol DHE. **D**) Illustration showing liposome population of mixtures in **C**). A and C represents data from one experiment, though unquantified data [not shown] was seen to indicate a similar result. The 375:340 nm ratio was used to standardise the FRET signal. The protein alone was defined as 0.

the StARkin domain. For the advantage of the FRET assay, liposomes of 100 nm in diameter are used in the following experiments.

The optimum DHE content of the liposomes was also tested. Previously, low concentrations of DHE were unable to produce FRET signals [data not shown]. A comparison between different DHE % liposomes was carried out. In one mixture, 10% DHE liposomes were used, and in another 30% DHE:0% DHE liposomes at a 1:2 ratio were used so that both mixtures had the same available DHE molecules for the protein to bind to [Figure 6.15D]. In this assay, the mixture with high DHE content liposomes produced a higher FRET signal indicating that the StARkin domains can only extract sterol from a high sterol content membrane [Figure 6.15C]. This could be an indication of the potential regulatory mechanism for transfer – there could be a requirement of high sterol content or different pools of sterol within the liposomes, which the protein can extract from with varying efficiencies. There are multiple pools of cholesterol with varying accessibility in cell membranes suggested to form due to sequestering by specific membrane lipids (see section 1.2.5 for more details). However, cholesterol pools in liposomes of this composition have not been proven, and thus this hypothesis must be carefully explored. It would be most interesting to use lipid composition more indicative of the cellular composition of the ER or PM where Lam2p/4p localises. For example, the use of sphingomyelin will reflect cellular sterol pools more accurately. Nonetheless, these binding assays show that Lam4S2 is capable of associating to membranes and extracting DHE from under the polar heads of PLs. Due to the success of DHE binding from membranes, further studies were carried out using these artificial membranes to better simulate cellular conditions.

6.2.15 G1119R mutant Lam4S2 is soluble and can be purified

Previously mutations introduced in the StARkin domain of Lam4S2 prevented the rescue of full-length Lam2p when substituted for the endogenous Lam2S2 (see section 4.2.10 for the data). However, when the mutated StARkin domain of Lam4S2 was expressed alone without the rest of the protein, the R1025I and E1048V mutant proteins were found to aggregate inside the cell [Figure 6.16B-lower panel] suggesting that the mutations prevent the correct folding of the domain. The problems with the folding of the mutated domain could explain the functional defect when transformed into yeast to rescue delete LAM phenotype on AmB. In addition, the incorrect folding would lead to difficulties with purifying the protein in bacteria. Indeed, attempts to purify Lam4S2 with R1025I and E1048V mutations were unsuccessful. However, the G1119R mutation was found to be diffuse in the yeast cell, and it was readily produced

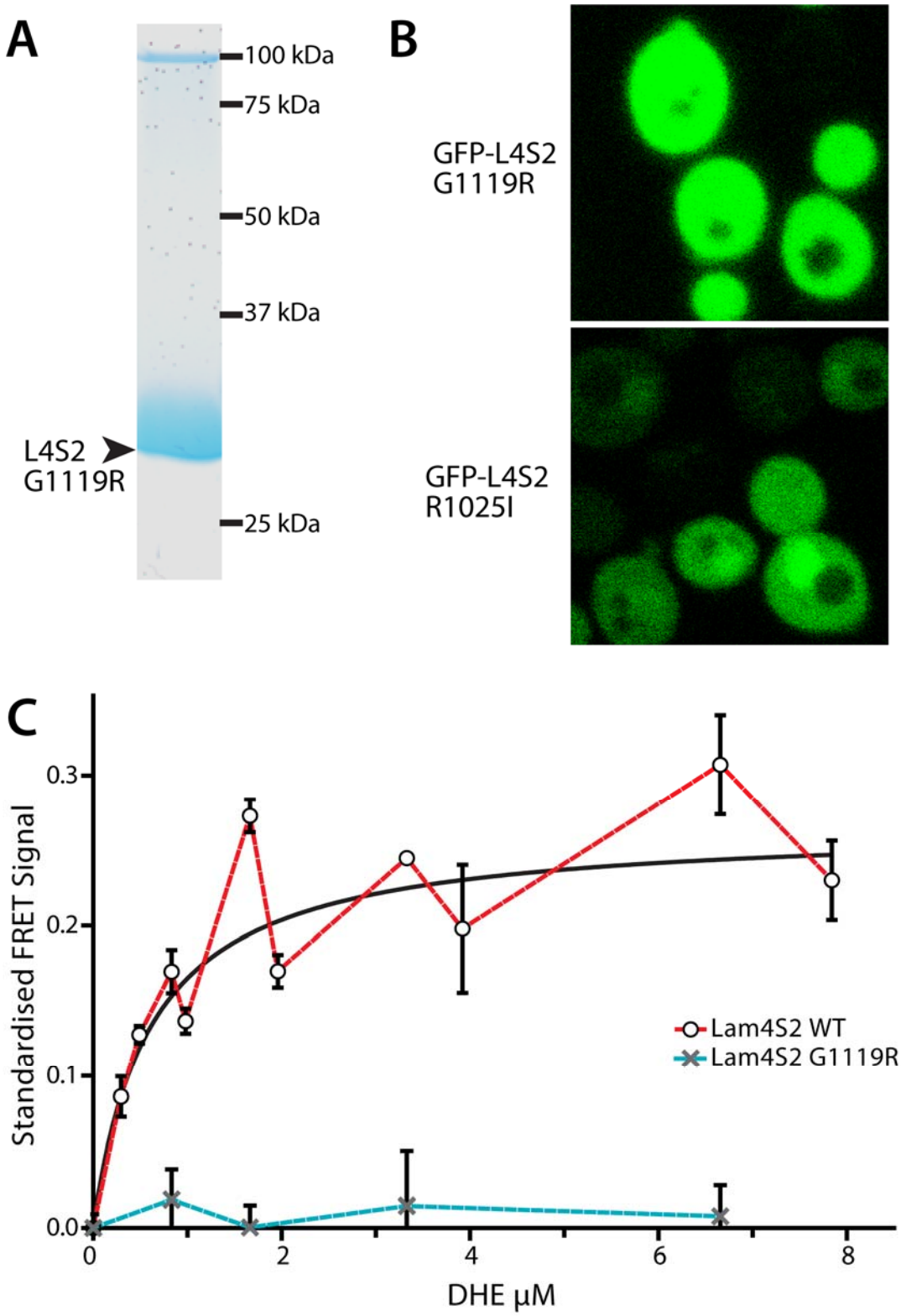

Figure 6.16 **Lam4S2 G1119R mutation prevents binding of DHE**
A) SDS-PAGE of purified His x11 Lam4S2 G1119R at ~95 purity. **B**) Microscopy of GFP-tagged Lam4S2 mutant G1119R diffuse in yeast cells and mutant R1025I in concentrated areas in yeast cells. **C**) Binding curve of Lam4S2 WT (red) and G1119R (blue) to liposomes $PC_{40}PE_{20}PS_{10}DHE_{30}$ of 100 nm diameter. The ratio of 375 nm to 340 nm was used to standardise the FRET signal. The FRET signal of protein alone was defined as 0. A curve was fitted to the WT data for one binding site using PRISM software (black). K_d of WT was calculated to be 0.6161±0.18 µM DHE.

in bacteria. Consequently a high concentration of very pure protein was made with the G1119R mutation similar to that of WT Lam4S2 [Figure 6.16A+B].

6.2.16 Lam4S2 WT, not G1119R mutant can bind to DHE containing liposomes

DHE binding assays with 100 nm diameter 30% mol DHE liposomes showed successful FRET with Lam4S2 WT which increased with increasing concentration of liposomes [Figure 6.16C]. On the other hand, the mutant G1119R Lam4S2 showed no FRET signal. Using the data points from purified WT, a binding curve was produced with increasing concentration of 100 nm diameter $PC_{40}PE_{20}PS_{10}DHE_{30}$ liposomes [Figure 6.16C]. The K_d of the binding with WT was 0.6161±0.18 μM DHE using a non-linear curve fitting of one binding site [Equation 4]. B_{max} (maximum binding signal) is calculated to be 0.2653 and background to be 0.0009626.

Equation 4 Total binding for one site

$$Y = \frac{B_{max}X}{Kd + X} + background$$

The 0.616 μM binding affinity of Lam4S2 for DHE is similar to that of Osh4p to cholesterol, which is reported to be 0.725 μM (Im *et al.*, 2005). When the mutant Lam4S2 G1119R was tested, no significant signal was detected, the algorithm was unable to fit a curve to the data. The absence of FRET binding suggests that the conserved glycine residue is essential for the binding of DHE in the cavity of the StARkin domain. The glycine residue is predicted to form part of the cavity wall (see section 4.2.10 and Figure 4.14 for details on this prediction). As the mutation was altered to a larger residue, it is predicted to physically obstruct the space for DHE binding. Structural data confirming structure and positions of these residues would be required to further investigate these predictions and to confirm that protein folding is as normal.

6.2.17 Lam4S2 and Lam2S2 transfers sterol between membranes

The StARkin domains of Lam4p and Lam2p have been shown in previous experiments to bind and extract sterols from membranes [Figure 6.17A – Steps 1 + 2]. However, the ability to bind is distinct from the capacity to transfer. A very strong binding affinity to a ligand would mean that the protein cannot release the ligand and therefore will not be able to carry out the function of a ‘transfer’ protein. In addition, the protein must have a balanced affinity to both the donor membrane and the acceptor

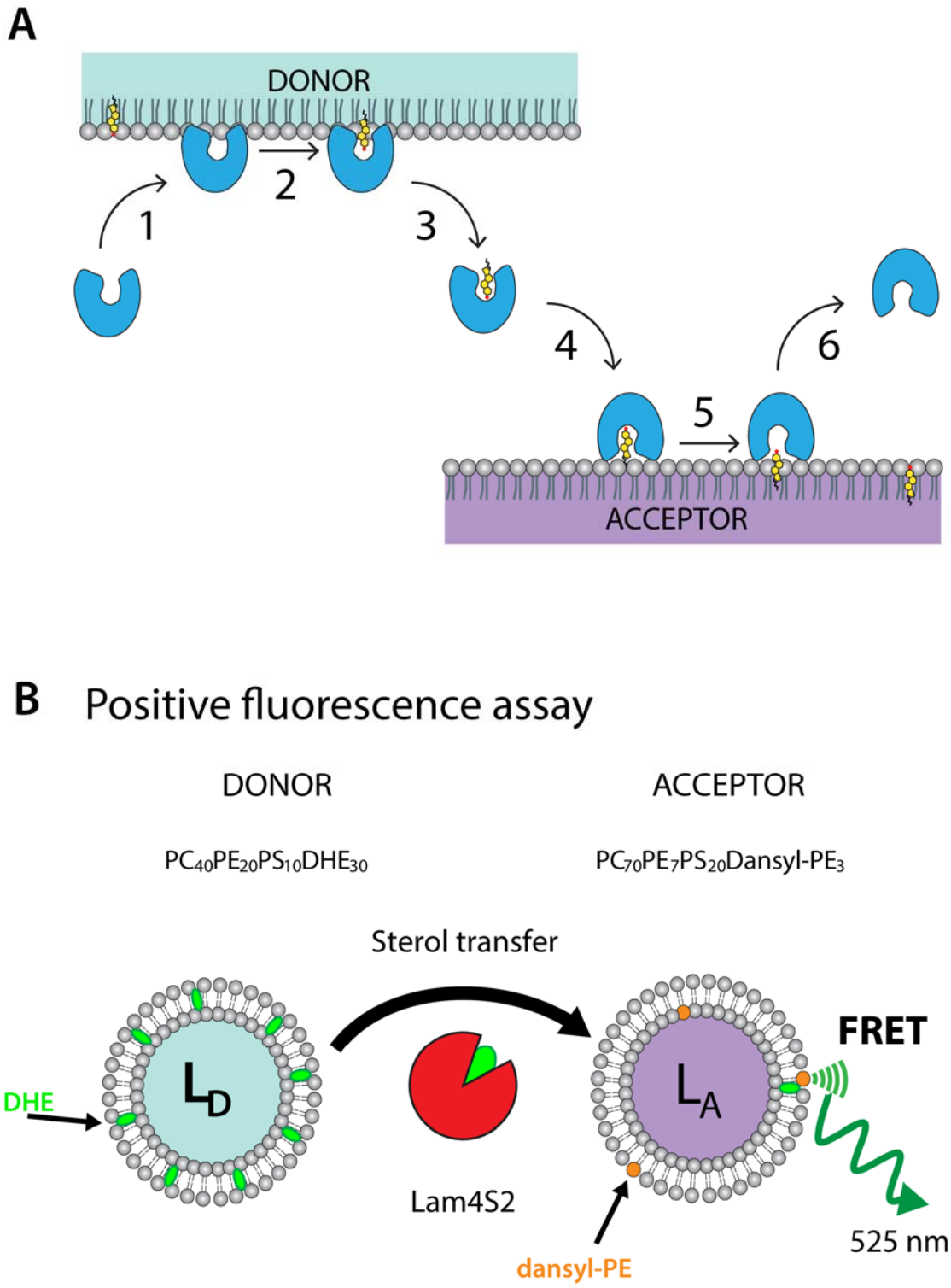

Figure 6.17 **Lipid transfer protein activity in positive transfer assays**
A) Illustration of the basic six steps for lipid transfer between two membranes. 1- associate with donor membrane. 2- extract specific lipid. 3- dissociate with donor membrane. 4- associate to acceptor membrane. 5- release lipid ligand. 6- dissociate from acceptor membrane. **B**) Schematic of a transfer assay where a positive transfer is observed as an increase of FRET between Dansyl-PE in the acceptor liposome (L_A) and the DHE transferred from the donor liposome (L_D) by Lam4S2. An excitation wavelength of 340 nm was used which produces no FRET in L_D and FRET in L_A only upon successful transfer.

membrane – again, too strong an affinity to either will prevent transfer due to the protein remaining on the membrane and being unable to desorb and move to another to transfer. Lam4S2 has been found to be able to bind to DHE that is presented to it buried in a membrane, *i.e.* in a liposome. Transfer proteins must be able to extract ligands from the membrane and deposit it into another membrane [Figure 6.17A]. It is important to note that whilst lipid transfer only requires steps 1-5, any meaningful transfer would require the transfer protein to dissociate from the acceptor membrane to carry out its function repeatedly. To test for the transfer ability of the purified StARkin domains, an assay was set up using the FRET pair, DHE and Dansyl-PE. This FRET pair has been used in transfer assays on other sterol transfer proteins such as Osh4p (Mesmin *et al.*, 2013; von Filseck, Čopič, *et al.*, 2015; von Filseck, Vanni, *et al.*, 2015).

The initial transfer assay measured an increase in FRET as an output recorded as the fluorescence of Dansyl-PE at 525 nm due to the transfer of DHE emission upon excitation at 340 nm [Figure 6.17B]. The lipid ligand, DHE, begins in the donor liposome and upon successful transfer, is moved to the acceptor liposome where Dansyl-PE is located. Therefore, the FRET signal will increase if the StARkin domain extracts the DHE from the liposome, dissociates from the donor liposome, associates with the acceptor liposome and inserts the DHE within the membrane allowing FRET with the Dansyl group attached to PE [Figure 6.17A].

Donor liposomes were composed of $PC_{40}PE_{20}PS_{10}DHE_{30}$, the same composition as those used for sterol binding assay which showed successful binding by Lam4S2. Therefore, step 1, donor liposome association, and step 2, sterol extraction, of basic transfer steps will surely be carried out using this donor liposome composition. The acceptor liposomes composition of $PC_{70}PE_{7}PS_{20}$Dansyl-PE_3 was chosen, as it was effective with transfer assays with a mammalian StART domain, StARD4 (Iaea *et al.*, 2015).

A control transfer assay was carried out with 1 mM MβCD, a sterol extracting and delivery agent, to show a positive transfer signal observed as an increase in the fluorescence of Dansyl-PE emission at 525 nm due to FRET with DHE [Figure 6.18 – orange]. A negative control showing a small bleaching effect for the duration of the assay was carried out without an addition of protein or MβCD [Figure 6.18A – pink]. Compared to the control data, Lam4S2 was shown to transfer DHE between donor liposomes containing and acceptor liposomes [Figure 6.18 – light green]. Most significantly, the transfer rate of Lam4S2, observed by the slope of the curve after the

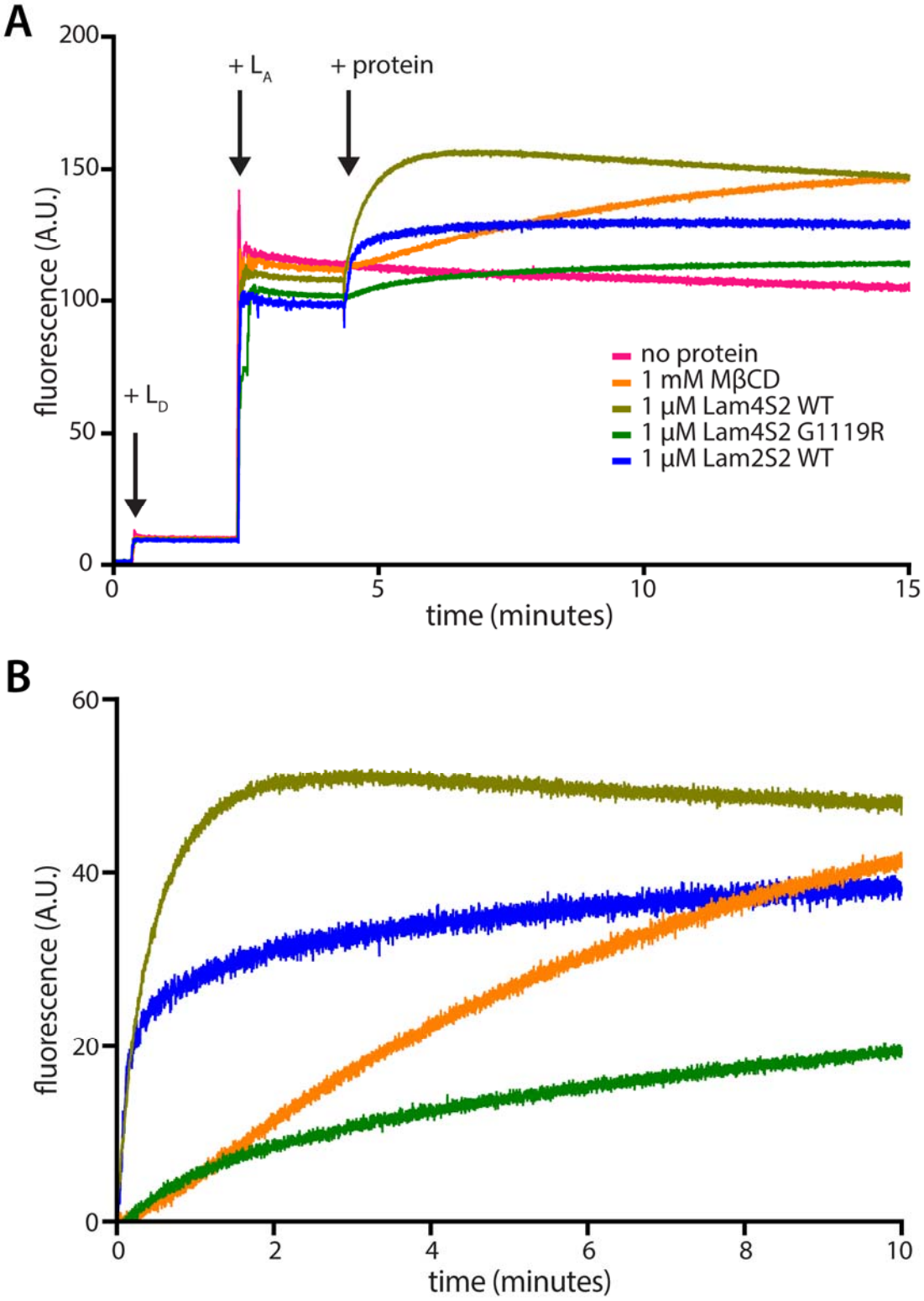

Figure 6.18 **Lam4S2 transfers DHE between membranes**
A) Time course of transfer assay measuring FRET signal at 525 nm emission from 340 nm excitation. The additions of donor liposomes (L_D), acceptor liposomes (L_A) and protein is indicated. There is a base level of bleaching observed when neither protein nor MβCD is added. MβCD is used as a control for transfer of DHE. **B**) Time course of transfer assay with background and base bleaching removed. T_0 is readjusted to when the protein is added. All proteins have a higher transfer rate than 1000x MβCD. Mutant Lam4S2 G1119R has a significantly reduced transfer rate to WT Lam4S2. L_D is composed of $PC_{40}PE_{20}PS_{10}DHE_{30}$ and L_A is composed of $PC_{70}PE_7PS_{20}$Dansyl-PE_3. Data for Lam4S2 WT and G1119R represents 3 individual repeats and for L2S2 is from one experiment. MβCD shows 2 repeats.

addition of protein, is considerably higher than 1000-fold more MβCD (1 mM compared to 1 μM of protein).

The positive transfer signal brings a need to revisit the liposome binding assay with different liposome compositions in one binding assay [Figure 6.15C + D]. It can be assumed that transfer would occur between $PC_{40}PE_{20}PS_{10}DHE_{30}$ and $PC_{70}PE_{20}PS_{10}$ liposomes (ratio 1:2, total 20 μM of lipids) would equilibrate to $PC_{51}PE_{26}PS_{13}DHE_{10}$ and $PC_{63}PE_{18}PS_{9}DHE_{10}$. However, it is important to note that readings were taken within minutes. It is likely that some transfer would have occurred. However, as there was a strong signal with 30% DHE liposomes, it is likely that the predicted transfer equilibrium was not reached. A possible explanation for this would be that not enough time had elapsed for the equilibrium. This would indicate that binding efficiency of 30% DHE compared to 10% DHE could be even greater than measured as the initial extraction was not measured. Another possibility would be due to the PLs being unable to flip between the two leaflets of a bilayer membrane to account for increase or decrease in liposome material (see section 1.3.1 for information on transverse exchange of membrane lipids). In addition, it is unclear whether the composition equilibrates to 10% sterol as is predicted above as the characteristics of the liposomes may be different with different ratios of PC:PE:PS which may affect sterol extraction/deposition. However, Figure 6.15 was only carried out as an optimisation experiment to probe the feasibility of sterol extraction of LAM domains.

6.2.18 Analysis of sterol transfer by LAM StARkin domains

The negative-control fluorescence of both liposomes with no protein appears to bleach during the duration of the time course shown as a gradual decrease in fluorescence after the addition of the acceptor liposome to the donor liposome [Figure 6.18A – pink]. This slight decrease is consistent between all data sets recorded on the time plot. To account for this bleaching, a non-linear equation based on a one phase decay was subtracted from the data with added protein or control MβCD [Equation 5]. K was calculated to be -0.1648±0.0014 min^{-1}.

Equation 5 One phase decay used to fit bleaching

$$Y = \left(Y_0 - (\lim_{t\to\infty} Y)\right) \times e^{(-kt)} + (\lim_{t\to\infty} Y)$$

The resulting data of transfer by protein and MβCD after consideration of bleaching was fitted to one phase association or two phase association and compared for the best fit

[Figure 6.18B]. t = 0 was adjusted to the point where both liposomes and protein or MβCD were present in the reaction, and Y_0 was constrained to zero to remove the background of the liposomes. P_{Fast} is the fraction of the difference between Y_0 and the maximum value as t tends to infinity ($\lim_{t\to\infty} Y$) due to the influence of the faster reaction, with M_F and M_S representing the max value of the fast and slow activities respectively, producing Equation 6 and Equation 7. The generated data is shown in Table 6-1.

Equation 6 One phase association

$$Y = (\lim_{t\to\infty} Y)\,(1 - e^{-Kt})$$

Equation 7 Two phase association

$$M_F = \left((\lim_{t\to\infty} Y) - Y_0\right) P_{Fast}$$

$$M_S = ((\lim_{t\to\infty} Y) - Y_0)(1 - P_{Fast})$$

$$Y = M_F(1 - e^{-K_{Fast}t}) + M_S(1 - e^{-K_{Slow}t})$$

Table 6-1 Table showing comparison of fit for transfer assays

	MβCD	Lam4S2 WT	Lam4S2 GR	Lam2S2 WT
Null hypothesis	One-phase association	One-phase association	One-phase association	One-phase association
Alternative hypothesis	Two phase association	Two phase association	Two phase association	Two phase association
P value		< 0.0001	< 0.0001	< 0.0001
Conclusion	Other fit is ambiguous	Reject null hypothesis	Reject null hypothesis	Reject null hypothesis
Max (A.U.)	54.75±0.07	51.27±0.04	32.29±0.95	39.20±0.04
K min^{-1}	0.1323±0.0003	-	-	-
K_{Fast} min^{-1}	-	6.012±0.115	0.725±0.017	6.592±0.051
K_{Slow} min^{-1}	-	1.750±0.019	0.068±0.004	0.264±0.003
P_{Fast}		24.54	21.53	62.76

It should be noted that even after taking into account bleaching of the liposomes background signal, Figure 6.18B shows that there is some bleaching that remains that is observable after equilibrium is reached for the Lam4S2 WT. The binding curve for Lam4S2 WT shows that the reaction ended by ~2.5 minutes. It is likely that this additional bleaching is due to effects when DHE has been moved to Dansyl-PE containing liposomes which may affect the accuracies of these values and analysis. Measurements with liposomes containing DHE and Dansyl-PE together (see section 6.2.22 for quenching assays) show that there is bleaching similar to the decline seen in this assay. For the purposes of this analysis, the Lam4S2 WT data was truncated at the point where the reaction has ended at 2.5 minutes.

For all transfers by StARkin domains, the model of two-phase association was preferred with $P<0.0001$, in contrast, MβCD was not found to be biphasic. The two-phase association equation models the transfer rate in proportion to the amount that is left, based on a fast rate and a slow rate. The biphasic model for the proteins suggests a different transfer rate depending on either how much sterol is left in the donor liposome or how much sterol is in the acceptor liposome. The fast rate occurs first and could be due to the StARkin domain being able to detect or bind sterol in a membrane with a high content of sterol as was observed in the DHE liposome binding assay [Figure 6.15C]. After an amount of sterol has left the donor liposome, the affinity of the protein to this membrane is lower, hence can result in an observed second, slower rate in the transfer assay. In WT Lam4S2, the first rate, K_{Fast} is 6.01 min^{-1} compared to the second, K_{Slow} of 1.75 min^{-1}, an approximate 3-fold reduction. Theoretically, the concentration of sterols in the donor liposome will drop rapidly from 30%, but the nearer the concentration is to 15%, there is less sterol that is readily available. The liposome binding assay, measuring steps 1 and 2 of transfer showed that Lam4S2 was less able to bind sterol in 10% DHE liposomes compared to 30% DHE liposomes [Figure 6.17A + Figure 6.15]. This difference between sterol extraction rates in high and low % mol sterol membranes would explain the two phases, one for when DHE levels are high, and one when DHE levels reach a threshold where binding, i.e. transfer steps 1 and 2, decreases significantly [Figure 6.17A]. It is important to note that though two phase association was modelled, it is possible the true binding kinetics is multiphasic in nature.

The transfer rates are significantly different between Lam4S2 WT and the mutant Lam4S2 G1119R. With the WT protein, it is observed that the equilibrium is rapidly reached at around one minute; however, the mutant protein is much slower.

Both K_{Fast} and K_{Slow} of Lam4S2G1119R are significantly lower. It is perhaps surprising that there was any transfer with the mutant protein as there was a seemingly lack of binding of the protein [Figure 6.16C]. However, this binding assay was carried out to a maximum of 6 μM of DHE, whereas the transfer assay has 30 μM of sterol available in the donor liposome. This increase in DHE used in the transfer assay suggests that the mutant protein could be binding DHE at a consequential level when it is between the levels of 6 μM and 30 μM, which would not be distinguishable in the previous binding assay. This minute affinity to the sterol of >18 μM would translate into a relatively active transfer since the mutant protein can easily deposit ligand if it reaches the acceptor membrane.

The transfer carried out by the StARkin domain of Lam4p is different to Lam2p. The K_{Fast} transfer rate of Lam2S2 is similar to that of Lam4S2. However, K_{Slow} is 10-fold slower. This low K_{Slow} transfer rate is recorded as a very gradual increase in Dansyl-PE fluorescence after ~ 20 seconds. This is in contrast to Lam4S2 transfer data, which indicates that the transfer equilibrium is achieved much earlier and the K_{Slow} is much faster. The reason for this difference between Lam2p and Lam4p could be due to physiologically relevant differences in the StARkin domains, hinting again at the possibility of the LAM proteins affecting different sterol pools in the plasma membrane.

6.2.19 Lam4S2 transfers sterol at a rate of 2 s^{-1}

The initial transfer assay resulted in a biphasic model where a changing composition of liposomes affected the transfer rate. In addition, it is unknown how much the increasing levels of DHE changes the transfer rate due to the proportion of PLs remaining the same in the liposomes. Thus to prevent the effects of phases, a pseudo-symmetrical transfer assay was designed where the lipid composition was the same in both donor and acceptor liposomes to simplify the reaction [Figure 6.19A]. Both donor and acceptor liposomes contained 30% sterol with non-fluorescent cholesterol in the acceptor membranes and DHE in the donor membranes. Previous binding assays suggest that cholesterol is a suitable non-fluorescent analogue of DHE as Lam4S2 has a similar binding affinity to both sterols. This setup designed so there will not be a net movement of sterol. Thus the total sterol concentration in liposomes will be constant over the duration of the experiment. As there should be no phase transition between high %mol sterol to low %mol sterol, the hypothesis of the biphasic model caused by the % mol sterol in membranes can be probed. Indeed, a two-phase association was unable to be fitted to the data, and the preferred model was the one phase association [Table 6-2].

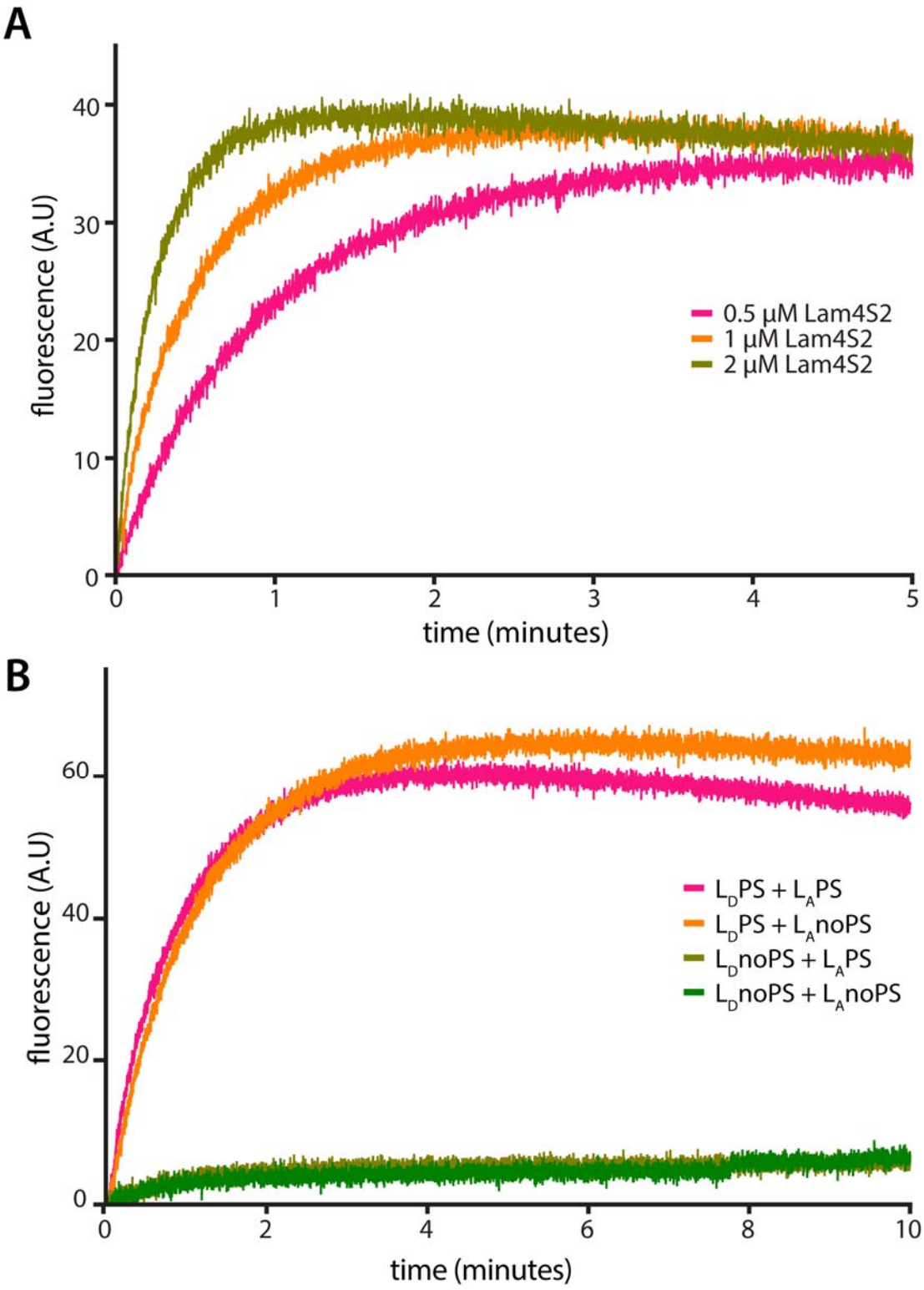

Figure 6.19 **Lam4S2 transfers 2 DHE s^{-1} and requires PS**
A) Time course of a symmetrical transfer assay measuring FRET signal at 525 nm emission from 340 nm excitation, with background and base bleaching removed. T_0 is readjusted to the time that Lam4S2 is added. Transfer rate increases proportionally to the concentration of Lam4S2 added. L_D is composed of $PC_{40}PE_{20}PS_{10}DHE_{30}$ and L_A is composed of $PC_{40}PE_{17}PS_{10}$Dansyl-PE_3Chol_{30}. **B**) Time course of transfer assay measuring FRET signal at 525 nm emission from 340 nm excitation, with background and base bleaching removed. T_0 is readjusted to the time that Lam4S2 is added. Successful transfer requires presence of PS in donor liposomes. L_DPS = $PE_{45}PE_{20}PS_5DHE_{30}$, $L_D$noPS = $PE_{50}PE_{20}DHE_{30}$, L_APS = $PC_{75}PE_{17}PS_5$Dansyl-PE_3 and $L_A$noPS = $PC_{80}PE_{17}$Dansyl-PE_3. n = 1.

Table 6-2 Table showing one phase association of symmetrical transfer assays

	0.5 µM Lam4S2	1 µM Lam4S2	2 µM Lam4S2
Max (A.U.)	34.44 ±0.03	37.25±0.04	38.96±0.04
K min^{-1}	1.126 ±0.004	2.183 ±0.008	4.108 ±0.014
Rate at t_0 µMs^{-1}	1.126±0.004	2.183±0.008	4.108±0.014

In addition to the curve fitting, the rate of sterol transfer was calculated from the initial rate of DHE signal at t_0. The reaction is assumed to equilibrate to L_D = $PE_{40}PE_{20}PS_{10}DHE_{15}Chol_{15}$ and L_A = $PC_{40}PE_{17}PS_{10}DHE_{15}Chol_{15}$Dansyl-$PE_3$. The aim was to calculate not just the rate at which DHE was transferred from donor to acceptor, but also the total rate of sterol transfer. Therefore, the calculated rate of DHE transfer from donor to acceptor was multiplied by four, which takes two assumptions into account; (1) 50% of the protein binds/transfers cholesterol in L_A rather than DHE in L_D and (2) 50% of the sterol picked up from L_D is transferred back to L_D, and similarly L_A can go back to L_A. Using these assumptions, the initial rate at t_0 was calculated with the differential of the one-phase association equation [Equation 6].

Equation 8: Differential of one phase association

$$\frac{dy}{dx} = k\,(\lim_{t\to\infty} Y)\,e^{-kx}$$

Using Equation 8, the rate at t_0 was calculated for 0.5 µM protein = 1.126 µMs^{-1}, 1 µM protein = 2.183 µMs^{-1} and 2 µM protein = 4.108 µMs^{-1}. The increases in rate constants are consistent with the increase in protein concentration, and therefore an average of these rates is calculated to obtain the rate of sterol transfer to be 2.163±0.013 s^{-1} per molecule of Lam4S2.

6.2.20 Lam4S2 requires PS to extract sterol from donor liposomes

StARD4 has been found to require PS to bind to liposomes and thus allowing faster transfer (Mesmin *et al.*, 2011; Iaea *et al.*, 2015). To see if this is the case for the StARkin domain of LAM proteins, a transfer assay was set up with donor and acceptor liposomes with no PS and with 5% PS [Figure 6.19B]. The transfer assay clearly shows that the Lam4S2 requires PS in the donor liposomes for transfer to occur. No significant

increase is observed when 0% PS is raised to 5% PS in acceptor liposomes. Perhaps like StARD4, the StARkin domain 2 of Lam4p requires the negatively charged lipid in the membrane to associate and extract the sterol molecule, but it appears from these results that the unbinding reaction has no such requirement. As the addition of 5%, PS made no visible difference, further lipid transfer assays were carried out to test other acceptor lipid compositions including a higher % of PS more similar to the high PS levels of yeast PM.

6.2.21 Lam4S2 requires high PS to deposit sterol to liposomes

The previous experiment showed no significant preference for the acceptor liposome to have 0% PS or 5% PS. A dequenching experiment [Figure 6.20A] was used to test various acceptor liposome compositions: PC_{100}, $PC_{90}PS_{10}$, PC_{80} PE_{20} and $PC_{70}PE_{20}PS_{10}$. In these transfer assays, both Dansyl-PE and DHE originate in the donor liposome.

When the acceptor membranes contained only PC, a very low amount of transfer was seen [Figure 6.20B – pink]. This was increased with the addition of 20% PE but was substantially increased when 10% PS was added independent of PE levels [Figure 6.20B – orange, green, light green]. This suggests that the rate has saturated with the biggest effect being the addition of higher concentrations of PS. This assay compares the difference between liposomes with 10% PS and liposomes with no PS in contrast to the 5% PS-containing liposomes tested previously. This requirement of specifically for 10% mol PS for the transfer of sterol may be related to the membranes it acts upon. The PM of yeast contains a much high level of PS (~25 % mol) compared to the ER (~5 % mol). One might hypothesise that the StARkin domain is active and depositing its ligand only in the vicinity of the PM where PS levels are > 5% mol.

However there are inconsistencies where L_A with no PE in Figure 6.19B shows very little transfer whereas the L_A with the same composition ($PC_{80}PE_{20}$) shows moderate transfer. Further transfer assays will also be required to test the requirements of PE for depositing sterol by Lam4S2. PE has a small headgroup and thus it is ‘cone’ shaped which can cause membrane instability. It is possible that PE may affect the transfer ability of an LTP.

6.2.22 Construct of LAM4S2 with tether

The addition to PS to the acceptor or donor liposomes increases the rate of transfer of sterol suggests that the lipid does not compete with the binding site of sterol, confirming the findings I have obtained from direct binding studies competing out the DHE within the cavity of the domain [Figure 6.14]. Instead, there is an implication that

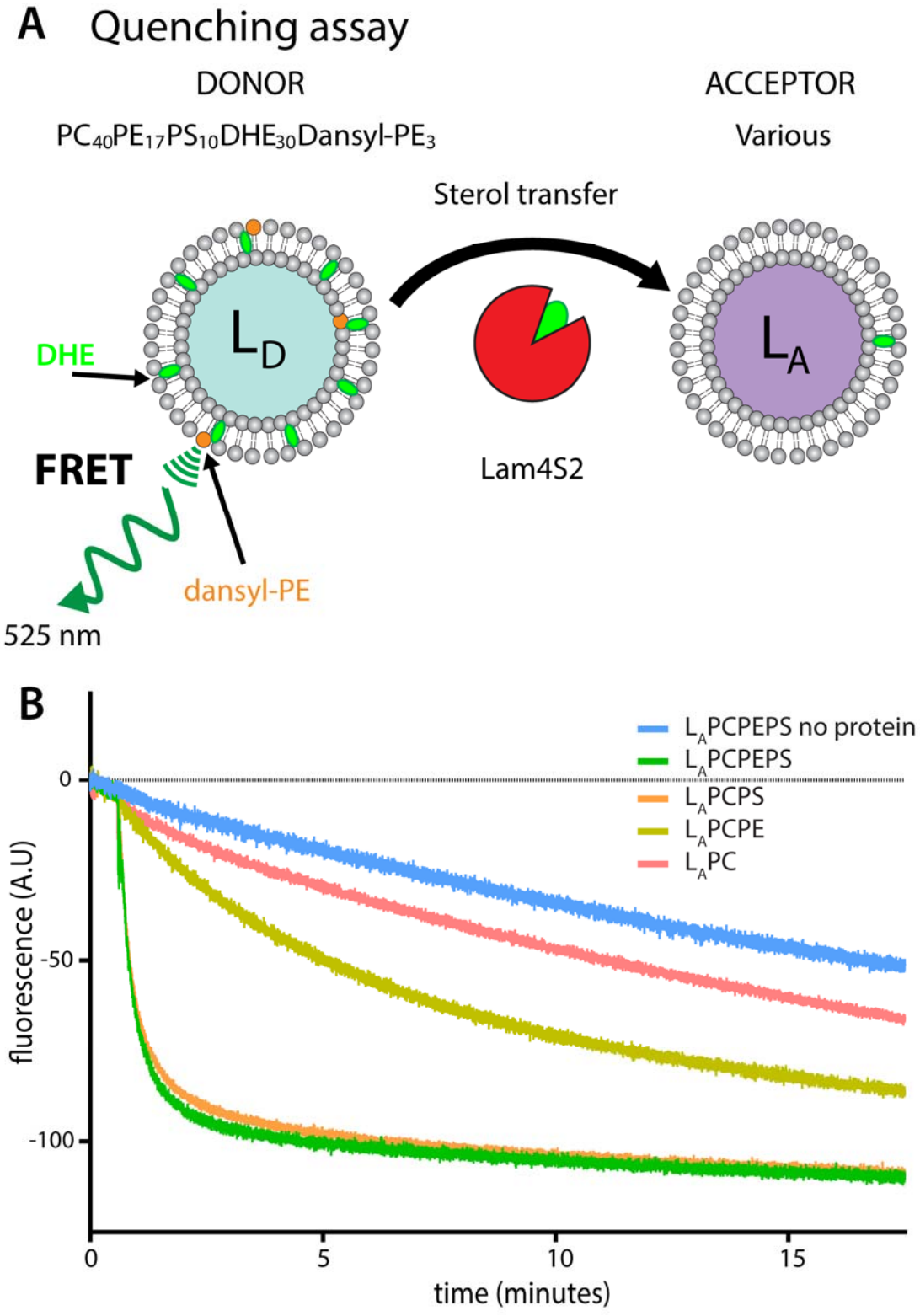

Figure 6.20 **Quenching transfer assay shows requirement of PS**
A) Schematic of a transfer assay where a positive transfer is observed as a decrease of FRET between Dansyl-PE and DHE, which are both initially in the donor liposome (L_D). DHE is transferred from the donor liposomes to the acceptor liposomes (L_A) thus reducing FRET activity in the acceptor liposomes. **B**) Time course of a quenching assay measuring FRET signal at 525 nm emission from 340 nm excitation. L_D = $PC_{40}PE_{20}PS_{10}DHE_{30}$, L_APC = PC_{100}, L_APCPE = $PC_{80}PE_{20}$, $L_APCPEPS$ = $PC_{70}PE_{20}PS_{10}$. The transfer rate significantly increases with the addition of 10% mol of PS in the acceptor liposomes and to a lesser extent, with the addition of 20% mol of PE. n=1-3

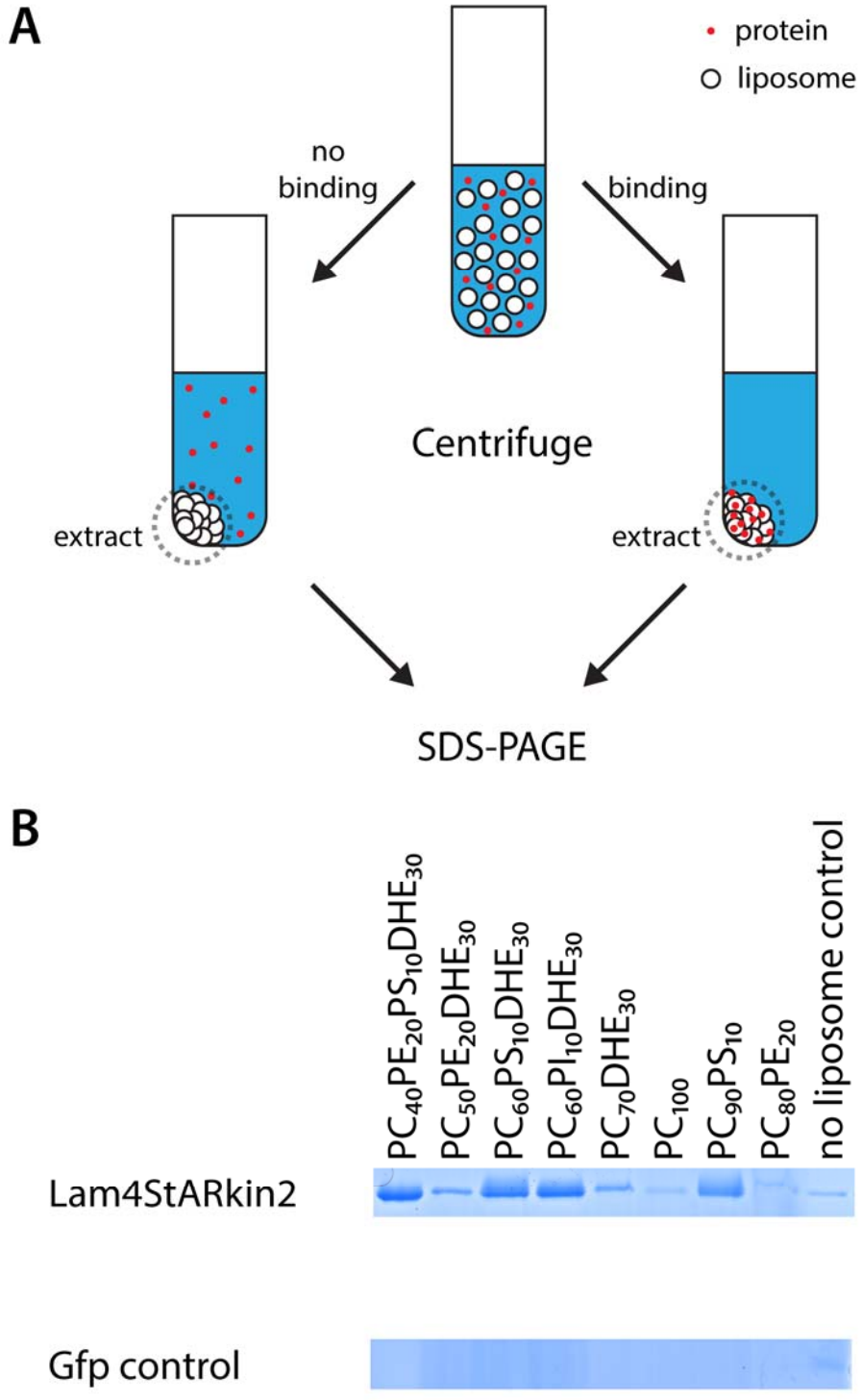

Figure 6.21 **Lam4StARkin domain associates to PS containing membranes**
A) Diagram illustrating a liposome-binding assay testing for membrane association of Lam4S2 to liposomes of various compositions containing a heavier raffinose buffer. The liposomes can be pelleted and any protein that is not associated to the liposomes can be removed. The pellet is run out on an SDS-PAGE gel to visualise the amount of protein that remained associated to the liposomes after pelleting. **B**) SDS-PAGE of liposome pellet showing association of Hisx11 Lam4S2 and Hisx11 GFP. There is no significant binding by His x11 GFP. Significantly more Lam4S2 associated to PS containing liposomes than liposomes without PS. DHE also increased protein association but to a lesser extent. This image is representative of three individual repeats.

PS bands of proteins that could be observed with Coomassie staining. Compared to the negative control where there were no added liposomes, no additional Lam4S2 bound to PC only liposomes [Figure 6.21B] which echo the slow transfer rates into PC only liposomes seen in Figure 6.20B. The addition of DHE (either to PC only or to PC and PE-containing liposomes) increased the binding slightly; it is not expected that DHE would be the major determinant of binding of LAM protein to the liposome - for a successful extraction and transfer of DHE the protein must dissociate from the liposome. However, this is an interesting phenomenon, as it may indicate that Lam4S2 dwells for an extra time on bilayers when sterol is present. It is proposed to that the lipid binding pocket opens up when protein docks with the membrane and this process may be prolonged if the high-affinity ligand can enter/exit this pocket. Alternately, there may be a second site for sterol binding on the surface of the protein (*i.e.,* not in the pocket), which increases the binding of Lam4S2. Finally, it is possible that when sterol is bound inside the pocket of Lam4S2 (sterol extraction is likely to have taken place during the time required for the pelleting assays), the protein changes its binding characteristics, even towards PC only liposomes.

The biggest effect on protein binding was seen with the addition of negatively charged lipids, PI and PS. Sterols are found buried within the membrane, and for the StARkin domain to be bound to a liposome via sterol molecules, the StARkin domain would be partially buried into the surface of the membrane. PS and PI lipids have anionic head groups that are exposed on the outer side of the bilayer. One interpretation of the increased association to PS or PI-containing liposomes is that it allows the StARkin domain to associate with the membrane without being buried in the membrane. In all cases, PE had no discernible effect.

It would be informative to test liposomes that better reflect the lipid composition in the ER or PM where the LAM proteins reside in both the transfer assays and the liposome pelleting in addition to testing Lam4S1 on its own and in tandem with StARkin 2, as it would be found in the cell.

To better understand the dependency on PS for binding to liposomes and PS for DHE transfer the sequence of the StARkin domain was investigated in more depth. Polybasic regions are short stretches of sequences with a high proportion of positively charged residues such as Arginine [Table 6-3]. The charge of an amino acid is determined by its side chain. If the pK of the side chain is above that of the solvent pH, the side chain can accept a proton (H^+) and become positively charged. Proteins such as small GTPases have a polybasic cluster that has been shown to bind negatively charged

phosphatidylserine and PI(4,5)P_2, targeting them to the PM (Heo *et al.*, 2006; Li *et al.*, 2014). The PM has more negatively charged lipids than other cellular membranes, and thus clusters of positively charged amino acids in a polybasic region would favour PM membrane targeting. STIM1 is an ER integral membrane protein and PI lipids in the PM interact with the polybasic area of STIM1 to localise it specifically to ER-PM contacts where it can bind Orai1 (Maléth *et al.*, 2014). Another example of interest is StARD4 has a patch of basic residues that is thought to encourage association to membranes containing anionic lipids (see section 1.5.4 for details on StARD4) (Iaea *et al.*, 2015).

Table 6-3 List of basic amino acids and their respective pK

Amino Acid	pK of the side chain group
Arginine	12.5
Lysine	10.5
Histidine	6.0

The sequence of the linker region between the StARkin 2 domain and the TM domain, there is a polybasic sequence composed of mainly arginine and lysine in both Lam2p and Lam4p [Figure 6.22A]. The 27 residues subsequent to the StARkin 2 of Lam2p consist of seven lysines and four arginines to total a +11 charge score [Figure 6.22B]. This score is calculated from lysines and arginines defined as +1 and glutamic acid and aspartic acid defined as -1. Histidine is neutral in this calculation due to the low pK value. For the polybasic region of Lam4, there are eight lysines and two arginines but one aspartic acid totalling a +9 charge [Figure 6.22B]. The polybasic region is conserved across most members of the LAM family – Lam1p/3p/2p/4p and all human LAMs, *Hs*LAMa/b/c (Wong and Levine, 2016). The purified StARkin 2 domain of Lam4p includes most of the polybasic region, which was kept due to the high solubility of the expressed protein. Therefore, it can be possible that this polybasic region can be responsible for the tethering to PS-containing liposomes.

6.2.23 Construct of LAM4S2 with tether

To better simulate the endogenous protein and to investigate the polybasic tethering, two new plasmid constructs were made. One construct was made to study the polybasic region of the linker between the StARkin domain and the TM domain. To do that, the plasmid construct was designed, to begin with the polybasic region followed by the rest of the linker before ending with a poly-histidine tag rather than the endogenous TM domain [Figure 6.22C]. This protein will be ‘tethered’ onto the liposomes by its

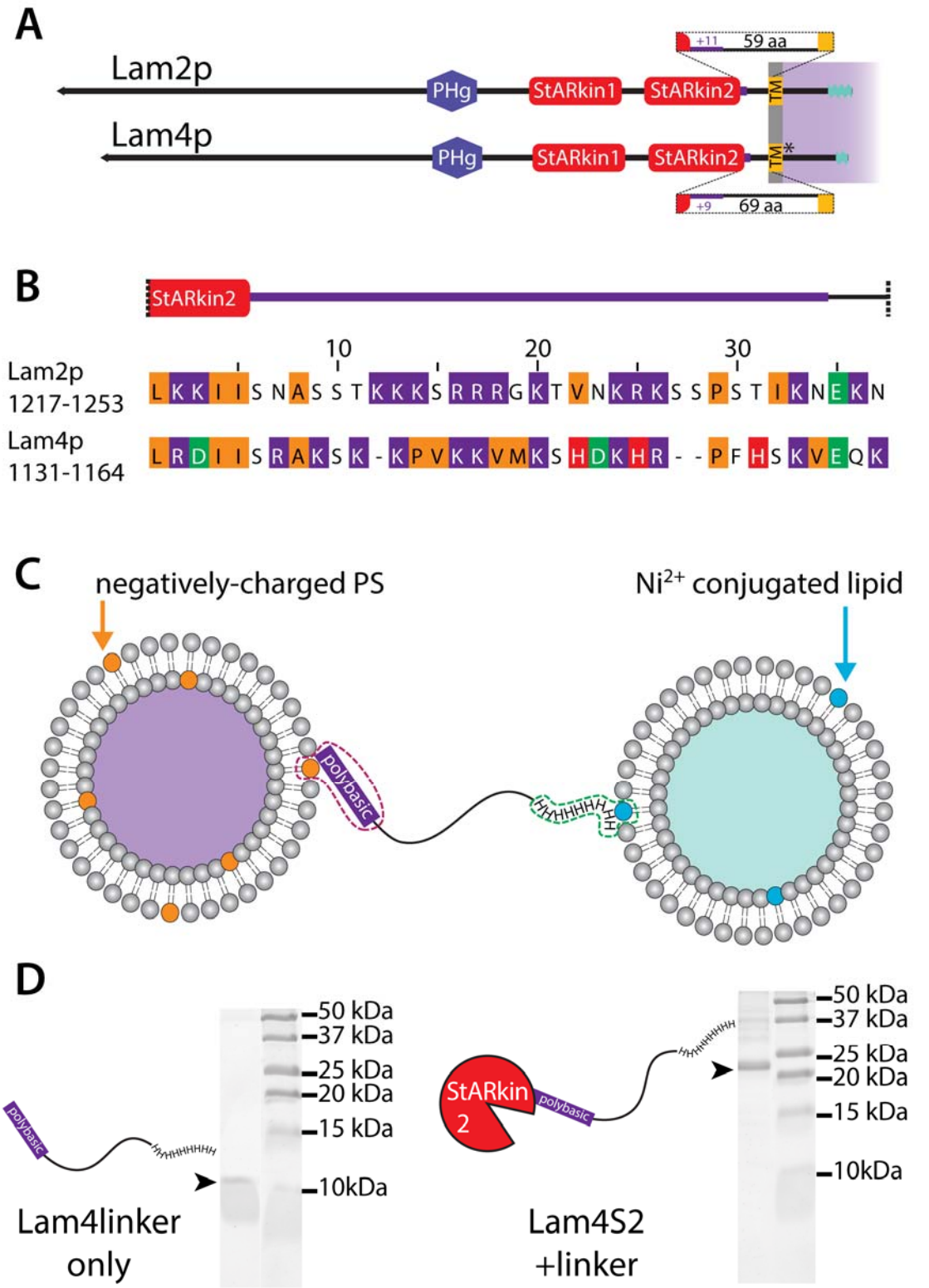

Figure 6.22 **Lam4S2 is followed by a polybasic domain**
A) Domain architecture of Lam2p and Lam4p with a magnification of the polybasic region (purple) between StARkin2 (red) and the transmembrane domain (orange). The overall charge score of the polybasic sequence is +11 for Lam2p and +9 for Lam4p where K and R = 1, D + E = -1. H = 0 due to pH neutralising its effect. **B**) Sequence of the polybasic regions of Lam2p and Lam4p. Basic residues K and R are purple, H is red, acidic residues D + E are green and hydrophobic residues are orange. C) Illustration of the tethering function of the purified linker region where the polybasic is predicted to associate with PS residues and the histidine tag is associating to the Ni^{2+} conjugated lipid. D) SDS-PAGE of the linker construct (~9 kDa) and Lam4S2-linker construct.

Histidine tag and Ni^{2+} conjugated lipid molecules in the artificial membrane. The second plasmid construct that was created was composed of the predicted Lam4S2 as used in the previous assays and the linker between the StARkin domain and the TM domain. The tethering would require the Histidine tag to be moved to the C-terminal similar to the linker only plasmid construct. The Lam4S2 linker His tag protein was purified with no problems using the same optimum conditions as the previous plasmid construct containing only Lam4S2 where the bacteria were induced with 0.2 mM IPTG at 37°C for 5 hours [Figure 6.22D]. However, the construct of just the linker region of just 9 kDa required induction for 8 hours at 30°C for protein to be soluble and visible on an SDS-PAGE gel. The linker protein was purified to approximately 0.5 $mgml^{-1}$, which equates to 0.6 μM [Figure 6.22D]. The purification protocol requires further optimisation for the production of high volumes of tethering linker proteins.

6.3 Discussion

6.3.1 Defining binding and transfer

Lipid binding protein is a loosely used term describing proteins that solubilise lipid [Figure 6.23B]. 'Lipid transfer protein' is an *in vitro* definition first applied to proteins that transfer radiolabelled lipids between donor and acceptor membranes (Wirtz, 1991). Thus all LTPs are lipid binding proteins. Assuming that no association (protein-lipid) is permanent, lipid binding proteins that can extract lipids from within a membrane can also be assumed to be able to release lipids to a membrane. Thus these lipid binding proteins that extract membrane lipids are also LTPs [Figure 6.23A]. Studying lipid transfer proteins and indeed lipid binding proteins, the *in vitro* gold standard is by exploiting artificial membranes to measure transfer. These assays, whilst necessary for membrane-to-membrane lipid transfer, do not measure protein-to-protein lipid transfer. It is possible that lipid binding proteins can bind a lipid and act as a chaperone, escorting the lipid to a second protein, hence transporting the lipid from A to B (Schaaf *et al.*, 2008). It is even a possibility that a lipid binding protein extracts and lifts a lipid from the membrane but whilst still associated with the membrane, presents the lipid to a second protein, which would otherwise not be able to extract the lipid from the membrane (Fürst and Sandhoff, 1992). A question now arises regarding whether the definition of these proteins, which transfer between membrane and protein or even protein and protein, would be an *in vivo* 'LTP'. An inefficient *in vitro* LTP could be transferring a lipid from protein to protein and thus would have very low activities for membrane association and dissociation.

Presentation or chaperoning may also be via a mechanism where the lipid binding protein exposes part of the lipid, for instance, the head group, to a second protein for modification or sensing without releasing the lipid [Figure 6.23E] (Wright *et al.*, 2005). After lipid modification or sensing by a second protein, the first protein can proceed to transfer the lipid back to the source or to another location. The second protein that carries out the modification or sensing of part of a lipid is physically interacting with the lipid. Therefore the definition of lipid binding proteins could include these partial lipid partners. In extension, proteins that interact and sense or modify lipids in a membrane without extracting the lipid can also be defined as a lipid binding protein. However, in both cases, the lipid is not solubilised by the lipid binding protein, and thus the definition of a lipid binding protein becomes contradictory.

Lipid 'solubilising' proteins can additionally act as direct sensors or direct modifiers [Figure 6.23C+D]. It can be predicted that any binding of a ligand to an

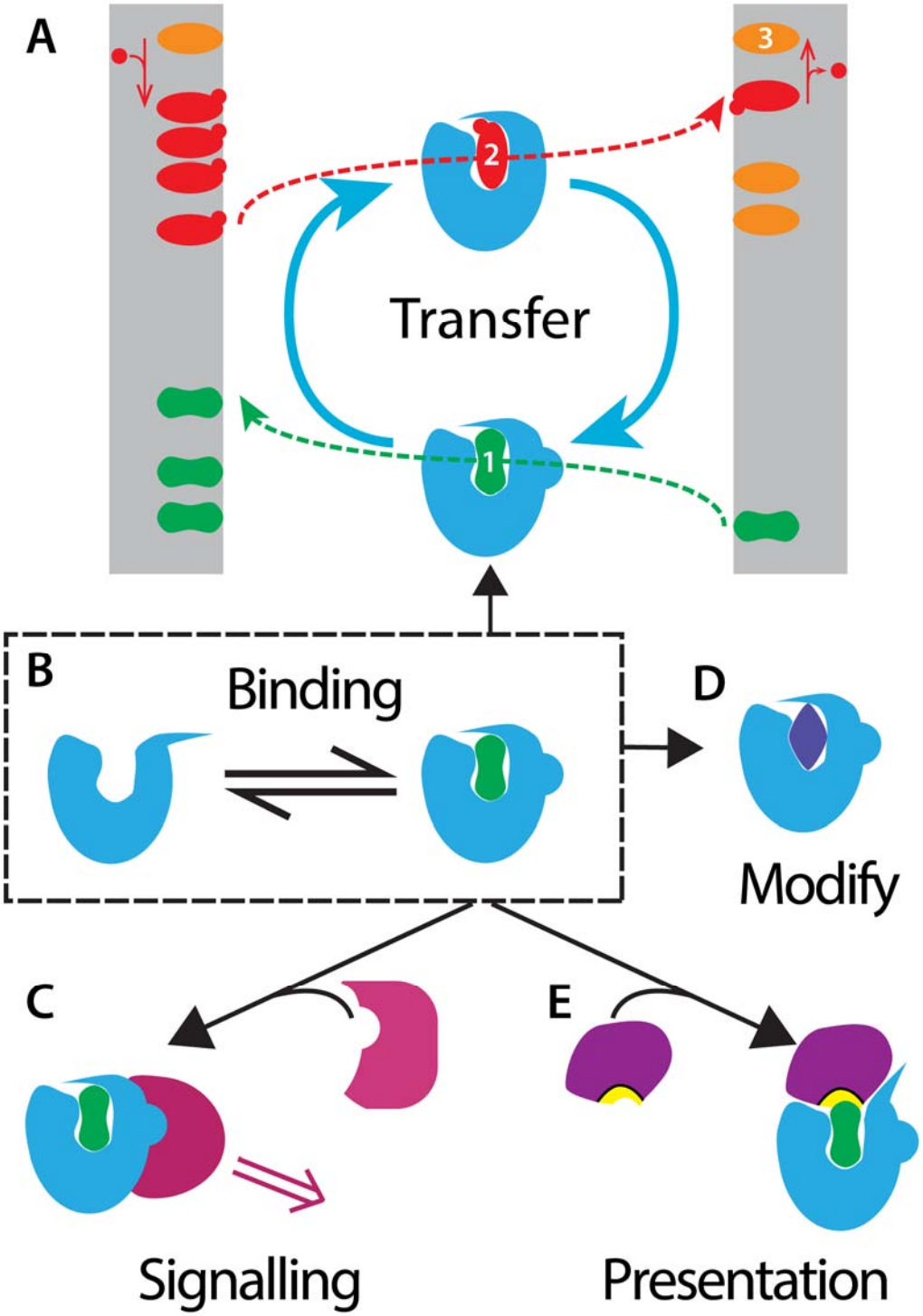

Figure 6.23 **Functions of lipid transfer proteins**
LTPs that can bind transiently to a lipid ligand (**B**) can be involved in: **A**) transfer or exchange of lipids, **C**) signalling upon lipid binding, **D**) modifying or **E**) presentation of the bound lipid. **A**) Diagram of a countercurrent model, where one LTP exchanges two lipids (#1 and 2) between membranes. In this example, a steep gradient of #2 is maintained by its synthesis from #3 on the left, and conversion back to #3 on the right. Such a gradient can drive the counter exchange of #1 up a gradient (this gradient is less steep than that of #2). **C**) An LTP directly senses a lipid if it changes conformation upon binding a lipid and passes information to a binding partner (pink) leading to lipid dependent signalling. **D**) A lipid modifying enzyme that can solubilise a lipid ligand will also have properties of a lipid transfer protein. **C**) An LTP can act as a chaperone to expose part of the lipid (typically the headgroup) to other proteins (purple). Figure published in (Wong, Čopič and Levine, 2017).

internal cavity of protein can change the protein conformation thus causing downstream signalling or modifying a ligand (Iyer, Koonin and Aravind, 2001; Wang, Zhang, *et al.*, 2005; Eberhardt *et al.*, 2013). Again, in these scenarios, the lipid, original or altered, can be returned to the source or moved on to another location. If the lipid is returned to its origin, there is no net transfer of lipid; therefore would *in vitro* assays define such a protein as an LTP? These ambiguities suggest that a stricter and more defined classification of lipid binding proteins should be described and further development *in vivo* experiments to show direct evidence of lipid transfer by lipid transfer proteins. One possibility is the greater use of pseudo-symmetrical transfer assays such as that used in this study to study which may reveal more subtleties in lipid transfer by LTPs.

6.3.2 Transfer by LAM StARkin domains

The most convincing evidence of Lam2p involvement in sterol homeostasis between the ER-PM is that the deletion of Lam2p was shown to slow sterol traffic to the ER from the PM (Gatta *et al.*, 2015). This assay was carried out by a collaborating group (Menon, Cornell University USA) by measuring DHE and cholesterol esterification, which only occurs after transport to the ER (and then to lipid droplets). The very same assay previously suggested that the OSBP proteins were not fully responsible for sterol traffic between the ER and PM as the deletion of all seven members of the OSBP family did not abolish sterol transfer. Instead, sterol transfer was only decreased by approximately 50% (Georgiev *et al.*, 2011). In contrast, a single deletion of Lam2p decreased the sterol transfer by ≥ 50% [Figure 4.23B] (Gatta *et al.*, 2015). A role in cellular sterol traffic would correspond to *in vitro* transfer activity seen with the second StARkin domain of Lam2p. As the deletion of Lam2S2 abolished the activity of Lam2p shown by a growth phenotype on ergosterol sequestering antifungals, it would be prudent to repeat the retrograde sterol transport assay with yeast expressing Lam2ΔS2 compared to WT and *Δlam2* to strengthen the hypothesis of trafficking by Lam2p via its StARkin 2 domain.

6.3.3 First StARkin domain of Lam2p

All StARkin domains of Lam2p and Lam4p have been shown to be capable of at least binding sterol. However, this leads to the question of what the first StARkin domain of Lam2p and Lam4p are doing. In contrast of the second StARkins of Lam2p/Lam4p, the first StARkins are less able to rescue delete strain growth on AmB when expressed on their own (Gatta *et al.*, 2015). Also in the context of the whole protein, Lam2S1 is inactive; yeast containing Lam2p with a deletion or mutation in S2 has the same phenotype as the absence of the full Lam2p protein yet the lack of Lam2S1

does not show a growth defect [Figure 4.11]. This suggests that the first can bind to sterol but appears not to traffic cellular sterol. Transfer assays using the first StARkin will show whether the first StARkin has the ability to transfer efficiently; however, this will not provide any specifics of its *in vivo* function. If the first StARkin is able to transfer, what role does it play in the whole protein, especially since Lam2p does not need the first StARkin to rescue the AmB phenotype? Although AmB is a sterol sequestering agent which is a useful tool to test sterol affecting proteins, it may not be revealing the specific role of the first StARkin domain. Additional retrograde transfer assays with DHE to test yeast expressing Lam2ΔS1 compared to WT and *Δlam2* would confirm if there is a role in PM to ER sterol traffic by the first StARkin domain. Nonetheless, if there is no evidence of retrograde transport, there are still possibilities that the first StARkin may be involved in forward traffic (for which there is no direct assay for) in addition to functions in conditions yet to be tested.

6.3.4 Binding and transfer by Lam4S2

The second StARkin domain from Lam4p has been studied the most in this investigation due to its ease of purification. Binding assays revealed that 1 μM Lam4S2 binds to DHE with a K_d of ~0.6 μM DHE. Competition assays showed that Lam4S2 is able to bind to cholesterol and ergosterol equally well as DHE, but there was little if any ability to bind PLs. This binding preference by Lam4S2 was corroborated by an optimised version of the radiolabelled lipid binding assay. For this assay, Alberto Gatta incubated the same purified Lam4S2 protein with radiolabelled lipids from human HL60 cells and analysed the bound lipid in re-isolated protein samples. The TLC plate showed that cholesterol was the major lipid ligand with no visible bands for sphingomyelin, PC, PI, PS, PE and cardiolipin. Using radiolabelled cellular lipids allows the considered protein to be exposed to all lipid species at cellular levels Although the limitation of this assay is that by using human cells rather than yeast cells to produce the radiolabelled membranes, more lipid species would have been exposed to the StARkin domain than artificially composed liposomes. However, the repurification step of the protein is considered a harsh process to be carried out on a protein and therefore only lipids with a strong binding affinity may be revealed. Interestingly, it was shown using the *in vitro* competition assay that human steroid hormone progesterone was able to compete for the binding site of DHE in Lam4S2. The binding affinity was similar or even slightly stronger than that of Lam4S2 to cholesterol. The ring structure of progesterone is similar to cholesterol, being a steroid product of cholesterol modification. However, the 'tail' side chain is much smaller. This raises the possibility

that the binding site of the StARkin domain recognises and interacts specifically with the ring structure.

Mutation of the G1119R was shown to abolish the cellular activity of Lam4S2 demonstrated by growth assays on AmB (see section 4.2.10 for details on the mutations). With these *in vitro* lipid binding assays, the strong DHE binding exhibited by WT Lam4S2 was abolished. The G1119 residue is situated within the binding pocket, and the replacement arginine is a much larger residue. This residue is predicted to block the binding cavity of the protein [Figure 4.14B]. The transfer assay allowed mutant Lam4S2 G1119R access to five-fold more DHE. However, the transfer activity was significantly hindered compared to the WT protein implying that there is a minute binding affinity (>18 μM) that was not revealed by the binding assay. The lack of activity of Lam4S2 G1119R *in vivo* indicates that this low binding affinity is not applicable with sterol levels in the cell [Figure 4.13].

6.3.5 Membrane association by a polybasic region

Using liposome pelleting and transfer assays, it has been shown that Lam4S2 requires PS to bind to membranes. Competition assays with sterols as well as cellular radiolabelled lipid binding assay do not show PS to be a lipid ligand of the binding pocket. This association is likely to be due to a conserved polybasic region containing clusters of positively charged arginines and lysines. PS and PI are PLs with a negatively charged head group which would attract positively charged amino groups. The StARkin domain is predicted to be a StART-like domain with one main binding pocket, and PS is unable to compete for DHE binding,

The PM has a much higher level of PS (~25 % mol) than the ER (~5 % mol) (van Meer, Voelker and Feigenson, 2008) hinting that the StARkin domain may be acting on the PM membrane. However, the whole of Lam2p is tethered between two membranes independent of the StARkin domains, which introduce the question of the purpose of PS-rich membrane association by StARkin domains. Clearly, net cellular transfer of sterol cannot occur if the StARkin domain associates solely with the PM due to the PS content. One possibility would be that the association of the domain to PS changes the structure of the StARkin domain. It is known that some StARkin domains have a lid at the opening of the hydrophobic cavity (Mesmin *et al.*, 2011). The PS interaction with a polybasic patch of residues is suggested to induce a conformation change in StARD4, allowing the Ω loop lid to swing open when close to a PS-containing membrane thereby promoting the movement of sterol in and out of the cavity via a currently unknown method (Iaea *et al.*, 2015). It is important to note that the

predicted lid of Lam4S2 contain several basic residues including a conserved lysine which could also be involved in determining the transfer activity, for example, the lid operation may be different when associated to membranes with PS compared to without (Gatta *et al.*, 2015). It has been determined for other proteins such as ion channels that a polybasic region is responsible for modulating the conformation of the channel structure (Bernier *et al.*, 2012). The cluster of positively charged residues is close to but away from the region of amino acids coding for the transmembrane channel forming domain and is suggested to open and close the channel via interaction to the negatively charged inositol triphosphate head group of PI. A similar situation could be occurring with the StARkin domain by which the lid can open or close dependent on the interaction of the polybasic region to nearby PS/PI lipids.

Alternately, a high PS concentration with significant binding may be a way to induce sufficient dwell time to allow the domain to access sterol (which is in some way hard to achieve) while the reverse reaction in the acceptor (ER) has different (perhaps much less stringent) requirements, for a reason such as the lid opening differently depending the lipid content of the domain (von Filseck, Vanni, *et al.*, 2015).

6.3.6 Future experiments for LAM transfer

As considered above, the new constructs consisting of the linker region between Lam4S2 and the TM domain with and without of the StARkin domain should be used first to test the tethering activity of the linker region which includes the identified polybasic region. If there is indeed tethering, the role of the polybasic region must be determined by mutagenesis of the positively charged residues to negatively charged or neutral amino acids and the recombinant protein should be checked *in vivo* and *in vitro*. Specific basic residues in the flexible lid can also be explored, most notably the conserved lysine residue between the third and fourth β-strand.

One key route of investigation would be to use additional domains of the LAM proteins to test the transfer. This study only tested the individual StARkin domains. However, there are other membrane-associating domains such as PH and BAR domains in the full-length endogenous protein. To obtain a more accurate representation of the LAM proteins role and conditions for transfer, the full-length protein should be purified and used for the lipid transfer assay. It is likely that there is a role for these domains that is yet to be determined. Initial steps for this further work could utilise the linker region and replicate the TM domain by a poly-histidine tag alongside Ni^{2+} conjugated lipid containing artificial membranes. It would be likely that the localising role of the TM domain would increase the speed of transfer of sterol by LAM proteins as suggested by

the requirement of overexpression of StARkin domains to rescue full-length LAM delete strains (Gatta *et al.*, 2015).

6.3.7 Role of *in vitro* assays for lipid transfer

These experiments have only begun to characterise the function of LAM proteins. The field of lipid transfer proteins has grown tremendously in the past decade. With that, new, more complex *in vitro* assays have been carried out and have revealed surprising information that has been hugely beneficial to the field including that of counter transfer of PI4P by OSH proteins to move PS and cholesterol, potentially up a concentration gradient (de Saint-Jean *et al.*, 2011; Mesmin *et al.*, 2013; Chung *et al.*, 2015; von Filseck, Čopič, *et al.*, 2015; von Filseck, Vanni, *et al.*, 2015). If LAM proteins are involved in the forward traffic between ER and the PM, there is a significant sterol concentration gradient which must be overcome. No secondary ligand has been detected for the LAM StARkin. However, a limited number of lipids were used with artificially composed liposomes, and human cells were used rather than yeast cells. In addition, a secondary lipid ligand may only have a low binding affinity that is inferior to the binding to sterols.

6.3.8 Key results

Both StARkin domains of Lam2p and Lam4p have been shown to preferentially bind sterols by FRET between an intrinsic tryptophan and DHE, a fluorescent derivative of ergosterol. The G1119R mutation of Lam4S2 which prevented the cellular function of the StARkin domain also prevented binding of sterols. Using artificial membranes in the form of liposomes, StARkin 2 from both Lam4p and Lam2p were able to show significant transfer of DHE compared to mutated Lam4S2. In addition, Lam4S2 WT was calculated to be able to transfer two molecules per second. Lam4S2 was shown to associate with PS or PI-containing liposomes, and PS levels in the membranes were shown to affect the efficiency of the transfer. There is a conserved polybasic region after the StARkin domain in LAMs that could potentially regulate association with positively charged lipids.

Discussion

CHAPTER 7

Discussion

The aim of section 7.1 is to collate and generalise beyond the data set out in the prior three chapters. In addition, Section 7.2 will set out possible lines of inquiry that can be taken beyond the work carried out in this particular study.

7.1 Final discussion

7.1.1 The StARkin superfamily

The StARkin fold is determined by a helix-grip fold consisting of seven β-strands wrapped around one long α-helix and two additional shorter α helices. Major members of this superfamily are known to bind different ligands, many of which are lipid molecules. Sequence-to-sequence searches do not link all previously classified StARkin domains, which were recognised by structural methods. Utilising HHpred, we have identified a new eukaryotic family of proteins, LAMs, containing a conserved StARkin domain. Independent bioinformatics studies simultaneously detected a subgroup of LAMs using an alternative structural predictor iTASSER (Khafif *et al.*, 2014; Murley *et al.*, 2015). The identification of LAM StARkin domains using structural bioinformatics has added to the discovery of SMP domains as being lipid transfer TULIP domains, which was also via HHpred (Kopec, Alva and Lupas, 2010). The continuing development of powerful computational tools such as HHpred and iTASSER promises further additions to LTPs, or indeed other distinctive folds, to be made by structural bioinformatics.

7.1.2 The LAM family and their domains

Further to the StARkin domain, LAM proteins contain multiple membrane targeting domains, granting them the ability to localise to more than one membrane, in other words, at membrane contact sites [Figure 7.1]. The distinct StARkin structure and localisation are ideal for a lipid transfer protein. A close proximity to both donor and acceptor membranes allows far more efficient activity than when the LTP is required to diffuse long distances in the cytosol or targeted to a single membrane. Lam1-4p localise

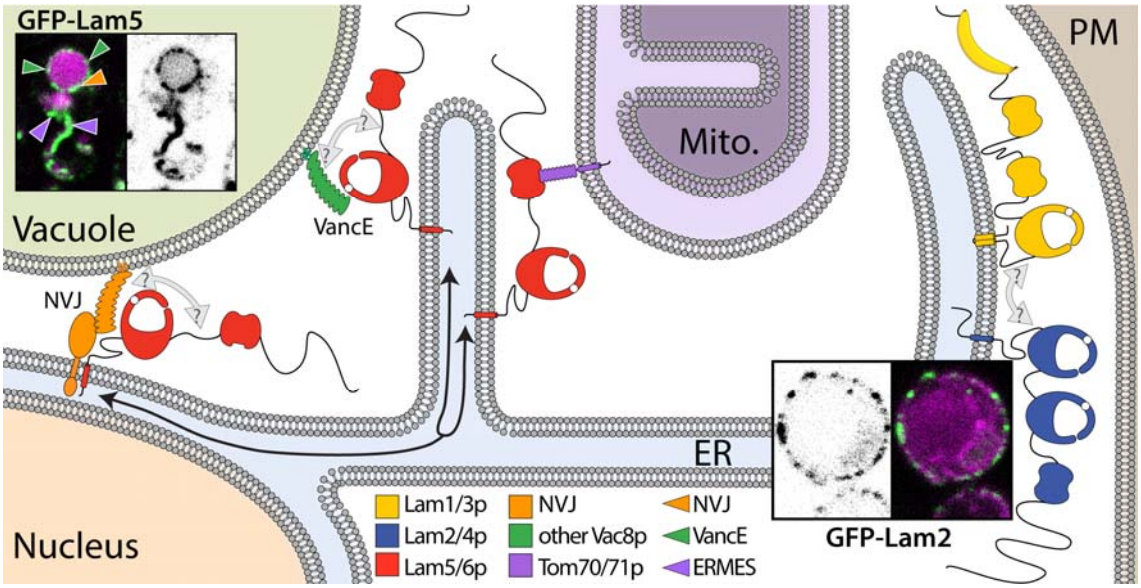

Figure 7.1 **Diagram of LAM targeting to different contacts**
LAM proteins localise to intracellular MCS while retained on the ER membrane via a TM domain. Lam6p (red) localise to NVJ and VancE contacts via interaction with Vac8p and to ER–mitochondria contacts via interaction with Tom70/71p. Lam5p has the same targeting as Lam6p when overexpressed – inset shows GFP-Lam5p colocalisation with RFP-Tom6p (magenta), an OMM protein and in the vacuolar lumen likely as a result of mitophagy, though its distribution when expressed at endogenous levels is not yet reported. Thus far, Lam1–4p are only known to localize at one contact site at ER-PM contacts. Lam2/4p (blue) consist of two StARkin domains and one PH-like domain, which are all able to reach in trans to the plasma membrane (PM) while tethered by a single transmembrane helix to the ER. Lam3p (yellow) possesses two transmembrane helix with very little ER luminal domain. Lam1/3p have a single StARkin domain, two PH-like domains and a BAR domain, which are all able to interact with the plasma membrane. Inset shows a cell expressing GFP-Lam2p at punctate ER–plasma membrane contacts and co-expressing RFP-ER (magenta). Both GFP images are also shown as black on white background. Confocal microscopy images courtesy of Alberto Gatta. Figure published in (Wong and Levine, 2016).

to ER-PM contact sites whereas Lam5p/Lam6p targets contact sites at the NVJ, mitochondrial-ER contacts and also ER-vacuole contacts [Figure 7.1] (Elbaz-Alon *et al.*, 2015; Gatta *et al.*, 2015; Murley *et al.*, 2015)

PH domains

Though Lam6p interacts with ERMES, the regulation of Lam6p localisation depends on other interactions. When Lam6p is located at ER-Vacuole contacts or the NVJ, it interacts with Vac8p and, when located at ER-mitochondrial contacts, Lam6p interacts with Tom70/71p (Murley *et al.*, 2015). The details of Vac8p recruiting of Lam6p are yet to be determined. However the Tom70/71p interaction has been pinpointed to the PH (GRAM) domain of Lam6p, as without this domain, Lam6p localise only to ER-Vacuole contacts. In normal growth conditions, Lam6p is found at these ER-mitochondria contacts, but when these contacts are disturbed with the deletion of one component of the ERMES complex or when the removal of the Tom70/71p interacting PH domain disrupts the mitochondrial targeting, Lam6p is rerouted to ER-vacuolar contacts. The crucial and important role of the PH GRAM-like domain of Lam6p in the regulation of Lam6p localisation insinuates that the domain in other LAM proteins may be of similar significance. The GRAM-like PH domain is a shared and conserved domain across the LAM family, and there is likely a common function that is retained across the LAM family but is yet to be identified (see section 7.1.5 for further discussion).

Lam1/3p have two PH domains; one is the GRAM-like PH domain that is shared with all members of LAMs whereas the other is not GRAM-like. In high throughput lipid screens the purified PH domain unique to Lam1/3p binds to PIs and phosphorylated sphingoid long-chain bases. However it was not investigated what protein partners this domain may have (Gallego *et al.*, 2010; Vonkova *et al.*, 2015).

BAR domains

The BAR domain is another Lam1/3p specific domain thought to have a role in membrane curvature. Although it was not tested with the StARkin domain of Lam3p, a Lam2p StARkin domain was able to transfer lipid more efficiently with membranes of a high curvature. Thus the BAR domains may have a role in promoting the lipid transfer activity of LAMs. BAR domains have dimerisation motifs that would promote oligomerisation of these domains. Whether Lam3p BAR would interact with another copy of Lam3p BAR or to a different protein containing a BAR domain remains to be established.

Another line of inquiry in the function of the BAR domain is the previously known investigation result regarding the transcriptional function found during overexpression of the BAR-PH C-terminal domain. Though the authors suggested a transcriptional role linked to SNF1 when overexpressed, no interaction was detected under endogenous levels (Lesage, Yang and Carlson, 1994). However, it is interesting that the strains deleted for the rest of the protein (PH (GRAM), StARkin and TM C-terminal domains) showed lowered growth and defected sporulation. This effect was not seen in the full-length delete. This reveals a strong function of the BAR-PH domain that is likely acting in the incorrect localisation away from the specific ER-PM membrane contact site, much like the detrimental effect of the expression of Lam3p StARkin alone. However, it is important to note that this line of inquiry has not been pursued since the original study in 1994.

TM and luminal domains

High expression of the short C-terminal domain after the second transmembrane domain of Lam3p, predicted to be cytosolic is detrimental to the growth of yeast (Lesage, Yang and Carlson, 1994). Likewise, the C-terminus tagged versions of Lam1/3p show mitochondrial localisation, suggesting a disruption of the normal localisation. No domain or interaction has yet been found for the C-terminus end of Lam3p, but as the last ~130 residues of Lam2p are fundamental to specific contact localisation, it is possible a similar functionality is yet to be found for that of Lam1/3p.

The evidence thus far has suggested that Lam3p interacts with the C-terminal lumen domain of Lam2p. This could be via direct interaction with Lam3p via the double TM helix and short luminal domain or via a secondary protein. Accordingly, with the evidence of dimerisation of the BAR domain, these LAMs must be able to form a complex of multiple proteins at these contact sites. Furthermore, examples of Lam1/3p homologues such as *Fo*LamB, which is C-terminally extended to also contain the DUF3074 protein, lead to speculation of links between Lam1/3p and DUF3074. Add together the possibility of PH (GRAM) domain to protein interaction being conserved from Lam6p (which binds to Tom70/71p); there becomes a large variety of protein interactions. BiFC microscopy has found interactions between Lam3p and Lam4p in addition to interactions between the two paralog Lam2p and Lam4p (carried out by Marion Weber-Boyvat, personal communication). The idea of a large complex containing a range of proteins, including Lam1p, Lam2p, Lam3p and Lam4p, is a strong hypothesis and should be investigated accordingly.

Double StARkins

Another theory relating to a Lam1/3p combination with DUF3074 is the formation of a double StARkin protein. It is possible that this combination is caused by the same evolutionary pressure, which granted the development of Lam2/4p, a LAM member with two LAM StARkin domains, in a subfamily of fungi. However, the functionality of two StARkin domains is yet unknown. Both StARkin domains from Lam2/4p display sterol binding activities and both isolated domains can substitute for the full protein when overexpressed. Yet, within the framework of the full-length protein, the removal of only the second StARkin, not the first, abolished the protein function. Thus there is significant ambiguity regarding the role of the first StARkin domain. One explanation would be that the first StARkin domain inhibited within the full-length protein or in the conditions where AmB basal resistance is assessed. Other possible functions could be a sensing or chaperone activity, both of which would require the ability to transiently bind sterol. Thus the domain would still possess transfer activity (see section 6.3.1 for a detailed discussion on functions of lipid transfer proteins).

StARkin

As the StARkin fold is a known lipid transfer domain and is the active domain of Lam2p for AmB resistance, the analysis in this work was concentrated to the Lam2/4p StARkin domains. FRET between DHE, a fluorescent analogue of sterol and an intrinsic tryptophan show that purified LAM StARkin domains are able to bind sterol with high specificity. Preliminary NMR studies carried out by Alberto Gatta have indicated that this tryptophan undergoes movement upon the addition of sterol to the pure protein, confirming that there is indeed an active binding within the cavity. These LAM StARkins are able to execute significant sterol transfer during *in vitro* lipid transfer assays. A mutation in the predicted cavity, G1119R, shown to abolish cellular function in relation to basal resistance to AmB, drastically reduced sterol binding and significantly decreased speed of *in vitro* sterol transfer. This data indicates that the cellular activity of Lam2p is related to its ability to bind and transfer sterols.

An independent study also showed that purified Lam6p without the TM domain transfers sterol, although it was not time evaluated (Murley *et al.*, 2015). Under certain stress situations such as glucose starvation, ergosterol-rich domains are formed on the vacuolar membranes. This stress response cannot occur without the presence of Lam6p. The genetic redirecting of Lam6p to ER-vacuole contacts by the removal of the PH (GRAM) domain, responsible for mitochondrial targeting, promotes the spontaneous

formation of these ergosterol-rich domains when yeast are not stressed. Together there is a strong indication that Lam6p affects ergosterol homoeostasis by its StARkin domain.

7.1.3 LAM StARkin function for sterol transfer

Although the retrograde sterol traffic of a strain deleted for the full-length Lam2p was assessed, the deletion of only the second StARkin of Lam2p was not. For direct evidence linking LAM StARkins to bulk sterol traffic between the ER-PM, the specific deletion of the StARkin domains should be investigated. However, assuming that Lam2p StARkin is indeed responsible for the sterol trafficking function of Lam2p, *in vitro* and *in vivo* sterol transfer rates can be compared.

***In vitro* transfer rates do not match *in vivo* transfer rates**

The rate of sterol traffic in and out of the PM is proposed to be approximately 10^5 molecules per second (Sullivan *et al.*, 2006). The maximum calculated rate for Lam4S2 was approximately 2 sterol molecules per second. Although the maximum transfer rate of the StARkin from Lam2p was not directly tested, an asymmetrical assay suggested K_{Fast} of Lam2p StARkin is similar to the Lam4p StARkin value. Though this is not a comparative transfer assay, a rough estimate of 2 sterol molecules per second can be obtained. *In vivo* transfer assays show a 50% reduction in retrograde sterol traffic without Lam2p (carried out by Yves Sere, Cornell University USA). Thus Lam2p is involved in 5 $x10^4$ transfers of sterol per second. Therefore taking Lam2p sterol transfer rate to be 2 s^{-1} provides an approximate number of Lam2p required to be 2.5 $x10^4$ copies per cell. However, this number is 100-fold higher than the high throughput data that suggest only 199 copies of Lam2p in the cell (Kulak *et al.*, 2014). It is important to note that microscopy of GFP-tagged Lam2p suggests that this number is incorrect and likely an underestimation. For example, the same high throughput study found Lam1p to have 537 copies per cell, yet GFP-Lam2p was consistently much brighter than Lam1p, or indeed any other LAM member. Also, it is likely that under certain conditions, LAMs are up- or down-regulated (see section 7.1.4 for speculation on expression of Lam4).

Though these numbers are based on numerous assumptions, it is certain that the measured rates *in vitro* are not as high as calculated *in vivo* values. Still, this is not unusual for *in vitro* lipid transfer assays. For comparison, the transfer rate for other sterol transfer proteins are: 0.1 sec^{-1} for StARD4 (Mesmin *et al.*, 2011; Iaea *et al.*, 2015), 0.3 sec^{-1} by Osh4p (when stimulated by a PI4P gradient generated with Sac1p (von Filseck, Vanni, *et al.*, 2015)) and 0.5 sec^{-1} for OSBP (when its PH domain and

FFAT motif tethers it to one membrane and VAP-A on a second membrane respectively) (Mesmin *et al.*, 2013).

Reasons for disagreement between *in vitro* and *in vivo* rates

The cause of the discrepancy can be due to a range of complexities surrounding *in vitro* transfer assays. A major consideration is that the optimal or cellular conditions are not precisely simulated. One aspect that has been considered is the composition of the membranes required to facilitate protein docking. As determined by studies on the OSH members, the continued presence of a co-ligand, in this case, PI4P, greatly increased transfer function even against the gradient (Mesmin *et al.*, 2013; von Filseck, Čopič, *et al.*, 2015; von Filseck, Vanni, *et al.*, 2015). A secondary ligand has yet to be identified for LAMs, however, for LAMs to be the bulk sterol mover; a tool such as a secondary ligand would also explain the counter gradient transport of sterol to the PM. However, it is important to note that Lam1-3p have only been directly proven to be involved in retrograde transfer due to experimental shortfalls in measuring forward sterol transport.

The data from this study has shown that negatively charged lipids have a role in recruiting LAM StARkin possibly due to positive residues close to or within the domain. This could be similar to the role for the polybasic region of StARD4 in membrane interaction and orientation of the protein (see section 1.5.4 and Figure 1.8) (Iaea *et al.*, 2015). Another condition for an increased rate under real conditions would be additional domains or proteins, which would facilitate the trafficking. This is emulated with OSBP liposome tethering, which uses a PH domain to associate with one membrane and a FFAT motif to interact with VAP-A, a protein on the other membrane. Based on the data currently available, it seems fair to suggest that Lam2p (and Lam4p) is only a part of a complex and other domains such as an oligomerised Lam1/3p BAR domain may accelerate transfer speed.

With Lam2p, *in vivo* sterol transfer speeds are far higher than the transfer observed *in vitro*. However, with Lam4p, the disagreement is vice versa; *in vitro* assays show that Lam4p can transfer sterol yet it has not been shown to carry out *in vivo* transport. It is possible there is an activation mechanism that regulates transfer activity of Lam4p (see section 7.1.4 for further discussion regarding Lam4p).

LAM StARkin does not share function with OSH

Any one OSH protein is able to substitute for the removal of all seven OSH proteins, indicating a shared OSH protein function. However, the overexpression of full-length LAMs or their active StARkin domains does not rescue the lethality of the

sevenfold *OSH* delete. Therefore, there is no overlap between the function of LAMs and the essential shared function of OSH proteins. Studies carried out during the course of this investigation show that the shared ligand of OSH protein is not sterol. Instead, PI4P has emerged as a common ligand. It is possible that the essential role of OSH is the maintenance of PI4P gradients between membranes. There has been no evidence for PI binding by LAM StARkin domains even when presented with all cellular lipids, and thus it is unlikely that LAM StARkin prime function is related to PI4P maintenance.

LAM StARkin shared *in vivo* function

Lam2p, Lam4p and Lam6p (and in extension Lam5p) have been shown to directly and specifically bind and transfer sterol *in vitro*. As discussed in section 6.3.1, the definition of a lipid transfer domain is solely *in vitro*. Proteins displaying lipid transfer ability may also or exclusively have functions as sensors, chaperones or enzymes in the cellular context. However, circumstantial evidence suggests that the chief function of both StARkins is due to direct transfer ability – both Lam2/4p StARkins show similar activity and MLN64, a human sterol transfer protein, show this same activity as Lam2/4p StARkins. Therefore, we hypothesise that the LAM protein family are directly involved in sterol transfer via its StARkin domain.

It is important to note that the ligands of Lam1/3p have yet to be determined. Cellular ergosterol traffic is perturbed in strains lacking these proteins. Thus there is strong evidence that Lam1/3p is involved in cellular sterol traffic. However, it is unknown whether this is a direct or indirect effect. For instance, instead of directly transferring sterol, Lam1/3p could be directly transferring sphingolipids such as sphingomyelin to which sterol has high affinity to and thus effect the homoeostasis of sterol. Indeed, lipidomics suggest that cellular sphingolipids levels are perturbed in strains lacking Lam1/3p though this is not indicative of direct sphingolipids transfer as it could be an indirect effect caused by defective sterol homoeostasis (personal communication from Alberto Gatta). Expression of isolated Lam1/3p StARkin does not rescue growth defect of delete *LAM* strains on AmB, signalling a difference in function with Lam2/4/5/6p StARkin domain. However further work by Alberto Gatta showed that the same Lam1/3p StARkin constructs were insoluble in bacteria and thus the lack of rescue may be due to an inactive StARkin domain rather than a difference in function.

Another point to consider is that Lam2/4p and Lam6p do not have specific binding to ergosterol but to sterols in general as they are shown to be able to bind cholesterol. In addition, Lam4S2 was able to bind progesterone. Since both fungi and

mammals have LAM proteins, it is likely LAM proteins evolved from an ancestor which was able to synthesise cholesterol, thus it is possible that LAM proteins developed the ability to bind ergosterol from binding cholesterol. However, this unspecific binding of sterols could allow them to transfer other types of sterols such as episterol, an ergosterol precursor. Furthermore, only ergosterol is detected in the PM which suggests that any activity involving ergosterol precursors would only occur at locations away from the ER-PM contacts (see section 7.1.5 on the discussion on Lam2/4p localisation) (Zinser, Paltauf and Daum, 1993). As Lam4S2 was able to bind to progesterone, ait is ambiguous whether human LAMs bind lipids or steroids. For human LAMs to be sterol transfer proteins, it would be logical for it not to bind other molecules such as steroids, and thus further investigation for the role of human LAMs should be carried out.

7.1.4 Why is Lam4p different?

One major unresolved issue is the difference between Lam4p to Lam1p/2p/3p. Isolated domain function does not always correlate with protein function as full-length protein could have downstream effects on protein interactions. This is shown by Lam5p/Lam6p delete strains lacking a significant phenotype on Amphotericin B even when their StARkin domains are able to rescue *Δlam1/Δlam3* phenotype on AmB (carried out by Alberto Gatta) (Gatta *et al.*, 2015). This result could be due to Lam5p/6p having localisation that is away from the ER-PM contact sites, which would affect PM sterol, and therefore would not contribute as significantly to AmB basal resistance. However, Lam4p does have an ER-PM localisation, which is shared with Lam1/2/3p, so it is unclear what differences there are between them. As with the growth assays on AmB, Lam4S2 is active and able to rescue *Δlam1/2/3,* which all have severe AmB phenotypes (carried out by Alberto Gatta + Tim Levine) (Gatta *et al.*, 2015). Lam4p StARkins clearly has a strong ability to transfer sterol, and full-length proteins localised to the exactly the same puncta (BiFC microscopy of Lam4p with Lam2p and Lam3p carried out by Marion Weber-Boyvat, personal communication). Thus it is perhaps surprising that *Δlam4* cells do not have a similar phenotype to *Δlam1/2/3* in either the AmB growth assay or the DHE retrograde traffic assay. Moreover, the *Δlam4* strain is slightly resistant to AmB. One possibility of the difference is that Lam4p affects a different pool of sterol that is sequestered by AmB or measured in the *in vivo* retrograde sterol transfer. In addition, it is possible that the phenotypical assays have not been under the correct conditions to test for the function of Lam4p. For example, there is upregulation of *LAM4* during growth on ethanol as one of 70 targets by ERT1, a

transcription factor (Gasmi *et al.*, 2014). Therefore, the importance of Lam4p for sterol transport may be revealed only in certain conditions. Another possibility is that there is regulation of Lam4p activity that is dependent on cellular stimuli. Evidence in both plants and humans regarding the effects of extracellular stimuli on LAM protein functions, along with Lam6p relocation during starvation and Lam2p implication in downstream TORC signalling points to LAM proteins being essential for cellular response to stress. Therefore, the lack of effects on cellular sterol traffic detected thus far may not be indicative of Lam4p as having no role in sterol transfer.

7.1.5 Regulation of the localisation of LAM proteins

Lam6p was identified to be involved in the dynamic regulation of contacts between the ER, vacuole and mitochondria by Schuldiner lab concurrent to this project (Elbaz-Alon *et al.*, 2015). Lipid transport is highly linked throughout the cell, and loss of one contact diverts lipid transport through upregulation of another (Elbaz-Alon *et al.*, 2014). It is possible that this dynamic regulation of localisation will also be relevant for the other LAM proteins, which have been shown to require precise regulation. However, it is important to note that Lam1-4p have only been confirmed at ER-PM contact site although the overexpression of Lam1/3p causes some to be found in other parts of the ER.

Evidence suggests that there is a protein interactor at the C-terminus, which can regulate and localise Lam2p. This could be the reason why some LAM proteins when tagged at the C-terminus primarily localise to mitochondria (Sokolov *et al.*, 2006; Koh *et al.*, 2015). Regulation of the Lam2/4p localisation could be due to disrupting the C-terminus interaction with its protein interactor in certain conditions. It is unlikely to be coincidental that Lam1/3p and Lam2/4p have been linked to mitochondria. Additional evidence such as fragmented mitochondria cables when Lam4p is removed indicates that there could be a second localisation like that of Lam5/6p regulation between ER-mitochondria and ER-vacuolar localisation (Jin *et al.*, 2015). As the PH (GRAM) domain of Lam2p does not affect its function regarding AmB basal resistance, there is a possibility that like in Lam5/6p, the domain also recruits these LAM proteins to the ER-mitochondria that is yet unseen in the conditions that were tested and therefore the PH (GRAM) domain is inactive with Lam2p is localised to ER-PM contacts. A co-purification with the PH (GRAM) domains of the LAM domains would identify any shared protein interactor. An indication that Lam2p may be phosphorylated also suggests that there may be substantial regulation of LAM proteins that may switch on or switch off activity dependent on cellular stimuli. This may be similar to the regulation

of CERT by different phosphorylation states which activates or inactivates its localisation and StART transfer activity (see section 1.5.4 for details).

There is a further consideration of multiple contact sites targeting for all LAMs. The most universal LAM form is the Lam5/6p with a PH (GRAM), a singular StARkin domain and a transmembrane domain. In some fungal species, there is only one LAM protein with the one StARkin. However, the StARkin domain itself is homologous to both *Sc*Lam5/6p and *Sc*Lam2/4p. Consequently, it is difficult to tell where fungal LAMs may localise aside from direct tagging and microscopy of the *Af*LamA or *Cn*Lam. However, human LAM proteins have been localised to multiple membrane contact sites (microscopy by Alberto Gatta and Elina Ikonen) like that of Lam6p. Therefore if Lam2/4p and Lam1/3p are evolved from the most common Lam5/6p form, they may retain the ability to localise to multiple contact sites.

7.1.6 LAM StARkin, an antifungal drug target?

A significance of the AmB growth defect of budding yeast deletion strains is the possibility that Lam1/Lam2/Lam3p singly or together could be a drug target that can be used alongside AmB. Clearly, *Af*LamA is more essential in *Aspergillus* than its individual homologs *Sc*Lam2/4/5/6p in budding yeast as growth was severely affected when removed. Due to the severe growth defect upon removal of *Af*LamA, obstruction of normal *Af*LamA cellular function is an attractive target to treat *Aspergillus* infections. It is likely that the function of *Af*LamA is the StARkin domain, indicated by the conserved function of all eukaryotic StARkins to rescue *ScLAM* deletes (including human LAM StARkins (Gatta *et al.*, 2015)). An appealing but highly optimistic translation of this research would be to use the fluorescence of the conserved tryptophans in LAM StARkin domains to screen a molecule library. Any reduction in tryptophan fluorescence from *Af*LAM StARkin would signify a binding ligand. These molecules could be adjusted for increased affinity to compete out any normal transfer function of the StARkin domain thus being potential molecules to use as an antifungal. In addition, further work on the regulation of LAM protein localisation may reveal ways to restrict the activity of *Af*LamA at ER-PM contact sites thus affecting any activity on ER-PM sterol transfer.

7.2 Future work

Although this investigation has begun to characterise a newly discovered family of proteins, it has also revealed many mysteries. The main revelation of LAM proteins is the presence of a predicted StARkin domain. Although there is strong evidence for a

folded domain with a hydrophobic cavity, it is important that this prediction is confirmed by structural studies such as NMR or crystallography, which is the gold standard. Preliminary crystallography work with the construct used for lipid binding and transfer assays was unsuccessful, likely due to the small additions either side of the domain that included the polybasic region.

One puzzle of the LAM protein family is the function of Lam4p, which does not show any function for AmB resistance. The growth of the delete strain should be tested in various stress conditions as the activity of Lam4p may be regulated possibly genetically or by its localisation. In addition, the phosphorylation of Lam4p and indeed all LAM proteins should be investigated, as this may also be a mode of regulation as is the case for CERT (Kawano *et al.*, 2006; Kumagai *et al.*, 2007; Saito *et al.*, 2008; Kumagai, Kawano-Kawada and Hanada, 2014). Especially relevant is Lam2p/4p as it has been suggested that it is involved in the TORC signalling cascade (Uetz *et al.*, 2000; Muir *et al.*, 2014). Expression levels of LAM proteins should also be confirmed by Western blotting although there are no known antibodies specific for LAMs thus the proteins would have to be tagged, ideally at the N-terminus. The expression of LAMs should also be quantified on AmB to find whether there is regulation of LAM expression when ergosterol is sequestered by the polyene.

A triple delete strain has been generated during the time of this work by the collaborating group (Menon, Cornell University USA) of *LAM1*, *LAM2* and *LAM3*. It would be informative to delete *LAM4* in this strain to find any phenotype of deleting Lam4p when other LAM proteins are absent. Further deletion can be carried out to make a six-fold delete. It would be interesting to see, if like the seven-fold *OSH* delete, the complete removal of LAMs might be lethal for the cell. The removal of *Af*LamA, homologous to all *Sc*Lam2/4/5/6p, in *Aspergillus* caused severe growth phenotype without any antifungals. It is probably that the removal of the same in budding yeast would cause significant growth defects without use of AmB.

As discussed in section [7.1.6], the discovery of LAM proteins has given an appealing target for fungal infection treatments either alone or alongside AmB. Once the growth phenotypes of *Aspergillus Aflam*Δ can be verified by LAM reconstitution, virulence assays can be carried out in model *Galleria* larvae. High throughput screening of a small molecule library to identify chemicals that can block the *Af*StARkin cavity would be highly attractive for antifungal discovery.

The PH GRAM-like domain of Lam6p is essential for targeting to ER-mitochondria contact sites, and thus this function may be conserved in other LAM

proteins. Initially, a co-immunoprecipitation with isolated LAM PH (GRAM) domains could identify whether they can all interact with mitochondrial residing Tom70/71p. However, a full screening using mass spectrometry would be much more thorough. In addition, screenings with full-length proteins or the other domains may show other interactions. The ER-PM localising LAM proteins form complexes with each other, and thus they would be expected to be positive on the screen.

The BAR domains of Lam1/3p may bind to either ER membranes, PM membranes or membranes at a yet unidentified localisation. Microscopy FRET analysis can be very sensitive to distances and thus labelling the N-terminus before the BAR domain and tethering the second fluorophore on to the PM or the ER may indicate whether the BAR domain interacts with the PM or the ER. Binding assays to liposomes with compositions that are similar to the PM or ER may also reveal this information. However, the dimerisation of BAR domains may not occur *in vitro* and more importantly, membrane curvature would be difficult to reproduce. The conundrum of the first StARkin domain could first be investigated by constructing a recombinant Lam2p where the first and second StARkin domains are swapped. As both isolated StARkin domains are active when expressed alone, it is possible that it is due to the position of the first StARkin domain where there may be physical inhibition.

The binding and transfer assays presented in this work have only just begun the characterisations of *in vitro* transfer by LAM StARkins. The specifics of membrane requirements have been started in this work but can be progressed further. Discovering the specific requirements of each StARkin may provide insights into which direction of sterol transfer the StARkin domain carries out. In addition, the StARkin domain in the whole protein is, of course, tethered to the membranes. This indicates that a more biologically relevant system where the purified StARkin domain can be tethered to the donor and acceptor membrane might profitably be used to analyse the domain. This can be carried out with the use of Nickel conjugated PLs with histidine-tagged StARkin domains. One question to be answered is whether there is a requirement of anionic in the donor or acceptor membrane when the StARkin is tethered. The polybasic region of Lam2p could be easily mutated and tested for its activity regarding the basal resistance of AmB. Transfer assays can also be carried out with the first StARkin either alone or in tandem with the second StARkin domain. There is a possibility that the first StARkin facilitates the transfer of the second thus speeding up the transfer. Further studies with StARkin domains from the other LAM proteins in *Sc* and other organisms such as *Aspergillus* and humans may yield valuable information about the function of LAM

StARkins. Especially interesting would be whether the human LAM StARkins are also able to bind steroids or if they have evolved to be more specific with their preference of ligand.

The recent discovery of some LTPs carrying out counter transport of two lipids also raises questions of a similar mechanism for LAM StARkin. As Lam2/4/5/6p StARkins bind with high affinity to sterol, a mixture of cellular lipids without sterol could be used to identify a secondary ligand that would have a lower affinity. Thus far, Lam1/3p StARkin domains have not been successfully purified and so to detect lipid ligands, the full-length protein (without the TM helices) could be purified and subjected to a binding assay. This would determine whether, like the other LAM members, Lam1/3p is able to bind ergosterol or perhaps another lipid. Further characterisation to the binding and transfer of LAM StARkin domain could yield valuable information to the lipid transfer field in general. Generating mutations in LAM StARkins to detect critical residues or flexible loops could increase knowledge of important mechanisms by which sterol-binding proteins operate.

One major issue within the field of lipid transfer by proteins is how to directly prove *in vivo* lipid transfer. Retrograde sterol transfer is dependent on Lam1-3p, yet this does not directly prove that the StARkin domains are transferring the sterol molecule themselves. However, heterologous replacement with MLN64, a mammalian sterol transfer protein only partially substitutes for LAM StARkin, suggesting that direct transfer is a function of the LAM StARkin domains of Lam2/4/5/6p. Further investigation into *in vivo* transfer could involve the use of 'clickable' sterols, a recent addition to the repertoire of lipid transfer investigators (Hulce *et al.*, 2013; Solanko *et al.*, 2015). As with DHE, there is a minimal change to the sterol structure and upon UV treatment, crosslinking to the protein is induced. The proteins can then be tested for their *in vivo* interaction with the sterol. This would also verify whether the first StARkin domain in Lam2/4p interacts with sterol as part of the whole protein *in vivo* and thus corroborate the *in vitro* transfer studies.

Summary

CHAPTER 8

Summary

This work focused on characterising the activity of the newly identified family of StARkin containing LAM proteins and implicates their involvement in cellular sterol movement between membranes.

Three questions were investigated in the above experiments:

1) What is the cellular role of LAM protein family members?
   All eukaryotes contain at least one form of LAMs yet not all organisms have either StARTs or DUF3074. LAM proteins, specifically the predicted StARkin domain, were shown to be essential for basal resistance of ergosterol sequestering polyenes. Furthermore, *Af*LamA is necessary for vigorous filamentous growth. The activity of Lam2p is dependent upon correct localisation of the protein but was pinpointed to the predicted StARkin domain. Overexpression of the active StARkin domains from *Af*LamA (homolog of *Sc*Lam2/4/5/6p) was able to rescue the growth defect in budding yeast on AmB. The *Sc*LAM family have been located to ER contact sites, and *Sc*Lam1/2/3p are essential for the efficient *in vivo* retrograde trafficking of sterol between the PM and the ER.
2) Do LAM StARkin domains have lipid transfer activity?
   It was found that the predicted StARkin domains of Lam2p and Lam4p can be easily purified and were shown to be active in *in vitro* lipid assays. All tested LAM StARkin domains bound DHE, Cholesterol and Ergosterol with similar affinities but had no visible binding to a variety of phospholipids. In addition, the StARkin domains were demonstrated to have the ability to bind and transfer sterol between different artificial membranes, establishing the classification of Lam2/4p as lipid transfer proteins.
3) What is important for the function of LAM proteins?
   Some of the overexpression of isolated LAM StARkins can compensate for the removal of the full-length protein, and these same domains are proven *in vitro* sterol

transporters. The C-terminus of the StARkin domain contains a cluster of positively charged residues, which may account for the requirement of negatively charged lipids in order for the association to membranes. This may be significant in the case of binding to the PM where there is a comparatively high composition of PS. Although the overexpression of cytosolic LAM StARkin can rescue the removal of Lam2p, endogenous levels of the full-length protein required the TM C-terminus region for activity, indicating that correct localisation at ER-PM contacts is essential for Lam2p functionality. A mutation rendering purified Lam2StARkin unable to efficiently bind and transfer sterol deactivates the activity of the full-length Lam2p *in vivo* for growth on AmB, indicating the overall role of the protein is related to sterol transfer.

Overall, the evidence demonstrates that this novel family of LAMs (Lipid transfer proteins Anchored at Membrane contact sites) have StARkin domains, with sterol transfer activity, which requires specific ER contact site localisation and that they are essential for cellular sterol homoeostasis. Prior to this investigation, the most qualified family of proteins with the potential to function as the yet unidentified machinery for cellular sterol traffic was the OSH family. However, the validity of OSH proteins being the sole master for controlling sterol transport around the cell has been questioned. The data established in this work has provided a major alternative to OSH proteins for the cellular traffic of sterol.

References

Aaltonen, M. J., Friedman, J. R., Osman, C., Salin, B., di Rago, J. P., Nunnari, J., Langer, T., and Tatsuta, T. (2016) 'MIC OS and phospholipid transfer by Ups2-Mdm35 organize membrane lipid synthesis in mitochondria', *Journal of Cell Biology*, 213(5), 525–534.

Agarwal, A. K., Rogers, P. D., Baerson, S. R., Jacob, M. R., Barker, K. S., Cleary, J. D., Walker, L. A., Nagle, D. G., and Clark, A. M. (2003) 'Genome-wide expression profiling of the response to polyene, pyrimidine, azole, and echinocandin antifungal agents in Saccharomyces cerevisiae', *Journal of Biological Chemistry*, 278(37), 34998–35015.

AhYoung, A. P., Jiang, J., Zhang, J., Khoi Dang, X., Loo, J. A., Zhou, Z. H., and Egea, P. F. (2015) 'Conserved SMP domains of the ERMES complex bind phospholipids and mediate tether assembly', *Proceedings of the National Academy of Sciences*, 112(25), E3179–E3188.

Alcazar-Fuoli, L., and Mellado, E. (2012) 'Ergosterol biosynthesis in Aspergillus fumigatus: Its relevance as an antifungal target and role in antifungal drug resistance', *Frontiers in Microbiology*, 3(439).

Allen-Baume, V., Ségui, B., and Cockcroft, S. (2002) 'Current thoughts on the phosphatidylinositol transfer protein family', *FEBS Letters*, 531(1), 74–80.

Alpy, F., and Tomasetto, C. (2005) 'Give lipids a START: the StAR-related lipid transfer (START) domain in mammals', *Journal of Cell Science*, 118(13), 2791–2801.

Alpy, F., and Tomasetto, C. (2014) 'START ships lipids across interorganelle space', *Biochimie*, 96(1), 85–95.

Alvarez, F. J., Douglas, L. M., and Konopka, J. B. (2007) 'Sterol-rich plasma membrane domains in fungi', *Eukaryotic Cell*, 6(5), 755–763.

Anderson, T. M., Clay, M. C., Cioffi, A. G., Diaz, K. A., Hisao, G. S., Tuttle, M. D., Nieuwkoop, A. J., Comellas, G., Maryum, N., Wang, S., Uno, B. E., Wildeman, E. L., Gonen, T., Rienstra, C. M., and Burke, M. D. (2014) 'Amphotericin forms an extramembranous and fungicidal sterol sponge', *Nature Chemical Biology*, 10(5), 400–406.

Aries, V. and B. H. K. (1978) 'Sterol biosynthesis by strains of Saccharomyces cerevisiae in the presence and absence of dissolved oxygen', *Journal of the Institute of Brewing*, 84(2), 118–122.

Baginski, M., Czub, J., and Sternal, K. (2006) 'Interaction of amphotericin B and its selected derivatives with membranes: Molecular modeling studies', *Chemical Record*, 6(6), 320–332.

Baginski, M., Resat, H., and Borowski, E. (2002) 'Comparative molecular dynamics simulations of amphotericin B-cholesterol/ergosterol membrane channels', *Biochimica et Biophysica Acta - Biomembranes*, 1567(SUPPL.), 63–78.

Baginski, M., Resat, H., and McCammon, J. A. (1997) 'Molecular properties of amphotericin B membrane channel: a molecular dynamics simulation.', *Molecular pharmacology*, 52(4), 560–70.

Bagiński, M., Tempczyk, A., and Borowski, E. (1989) 'Comparative conformational analysis of cholesterol and ergosterol by molecular mechanics', *European Biophysics Journal*, 17(3), 159–166.

Bagnat, M., and Simons, K. (2002) 'Cell surface polarization during yeast mating.', *Proceedings of the National Academy of Sciences of the United States of America*, 99(22), 14183–14188.

Baker, B. Y., Yaworsky, D. C., and Miller, W. L. (2005) 'A pH-dependent molten globule transition is required for activity of the steroidogenic acute regulatory protein, StAR', *Journal of Biological Chemistry*, 280(50), 41753–41760.

Baum, M., Erdel, F., Wachsmuth, M., and Rippe, K. (2014) 'Retrieving the intracellular topology from multi-scale protein mobility mapping in living cells.', *Nature Communications*, 5(4494).

Baumann, N. A., Sullivan, D. P., Ohvo-Rekilä, H., Simonot, C., Pottekat, A., Klaassen, Z., Beh, C. T., and

Menon, A. K. (2005) ‘Transport of newly synthesized sterol to the sterol-enriched plasma membrane occurs via nonvesicular equilibration’, *Biochemistry*, 44(15), 5816–5826.

Beamer, L. J., Carroll, S. F., and Eisenberg, D. (1997) ‘Crystal structure of human BPI and two bound phospholipids at 2.4 angstrom resolution.’, *Science (New York, N.Y.)*, 276(5320), 1861–4.

Beh, C. T., Alfaro, G., Duamel, G., Sullivan, D. P., Kersting, M. C., Dighe, S., Kozminski, K. G., and Menon, A. K. (2009) ‘Yeast oxysterol-binding proteins: sterol transporters or regulators of cell polarization?’, *Molecular and Cellular Biochemistry*, 326(1–2), 9–13.

Beh, C. T., Cool, L., Phillips, J., and Rine, J. (2001) ‘Overlapping functions of the yeast oxysterol-binding protein homologues’, *Genetics*, 157(3), 1117–1140.

Beh, C. T., McMaster, C. R., Kozminski, K. G., and Menon, A. K. (2012) ‘A detour for yeast oxysterol binding proteins’, *Journal of Biological Chemistry*, 287(14), 11481–11488.

Beh, C. T., and Rine, J. (2004) ‘A role for yeast oxysterol-binding protein homologs in endocytosis and in the maintenance of intracellular sterol-lipid distribution.’, *Journal of Cell Science*, 117(14), 2983–2996.

Benhard, W., and and Rouiller, C. (1956) ‘Close topographical relaionship between mitochondria and ergastoplasm of liver cells in a definite phase of cellular activity’, *The Journal of Biophysical and Biochemical Cytology*, 2(4), 73–78.

Bennett, H. J., Davenport, J. B., Collins, R. F., Trafford, A. W., Pinali, C., and Kitmitto, A. (2013) ‘Human junctophilin-2 undergoes a structural rearrangement upon binding PtdIns(3,4,5)P3 and the S101R mutation identified in hypertrophic cardiomyopathy obviates this response.’, *The Biochemical journal*, 456(2), 205–17.

Berchtold, D., Piccolis, M., Chiaruttini, N., Riezman, I., Riezman, H., Roux, A., Walther, T. C., and Loewith, R. (2012) ‘Plasma membrane stress induces relocalization of Slm proteins and activation of TORC2 to promote sphingolipid synthesis.’, *Nature Cell Biology*, 14(5), 542–7.

Di Bernardo, M. C., Crowther-Swanepoel, D., Broderick, P., Webb, E., Sellick, G., Wild, R., Sullivan, K., Vijayakrishnan, J., Wang, Y., Pittman, A. M., Sunter, N. J., Hall, A. G., Dyer, M. J. S., Matutes, E., Dearden, C., Mainou-Fowler, T., Jackson, G. H., Summerfield, G., Harris, R. J., Pettitt, A. R., Hillmen, P., Allsup, D. J., Bailey, J. R., Pratt, G., Pepper, C., Fegan, C., Allan, J. M., Catovsky, D., and Houlston, R. S. (2008) ‘A genome-wide association study identifies six susceptibility loci for chronic lymphocytic leukemia.’, *Nature Genetics*, 40(10), 1204–1210.

Bernier, L. P., Blais, D., Boué-Grabot, É., and Séguéla, P. (2012) ‘A dual polybasic motif determines phosphoinositide binding and regulation in the P2X channel family’, *PLoS ONE*, 7(7), e40595.

Bigay, J., and Antonny, B. (2012) ‘Curvature, Lipid Packing, and Electrostatics of Membrane Organelles: Defining Cellular Territories in Determining Specificity’, *Developmental Cell*, 23(5), 886–895.

Blagoveshchenskaya, A., Fei, Y. C., Rohde, H. M., Glover, G., Knödler, A., Nicolson, T., Boehmelt, G., and Mayinger, P. (2008) ‘Integration of Golgi trafficking and growth factor signaling by the lipid phosphatase SAC1’, *Journal of Cell Biology*, 180(4), 803–812.

Bose, H. S., Sugawara, T., Strauss, J. F., and Miller, W. L. (1996) ‘The pathophysiology and genetics of congenital lipoid adrenal hyperplasia.’, *The New England journal of medicine*, 335(25), 1870–1878.

Bottema, C., and Parks, L. (1980) ‘Sterol analysis of the inner and outer mitochondrial membranes in yeast’, *Lipids*, 15(12), 987–992.

Bretscher, M. (1973) ‘Membrane structure: some general principles’, *Science*, 181(4100), 622–9.

de Brito, O. M., and Scorrano, L. (2008) ‘Mitofusin 2 tethers endoplasmic reticulum to mitochondria’, *Nature*, 456(7222), 605–610.

Brown, G. D., Denning, D. W., Gow, N. A. R., Levitz, S. M., Netea, M. G., and White, T. C. (2012) ‘Hidden killers: human fungal infections.’, *Science Translational Medicine*, 4(165), 165rv13.

Bruder Nascimento, A. C. M. de O., dos Reis, T. F., de Castro, P. A., Hori, J. I., Bom, V. L. P., de Assis, L. J., Ramalho, L. N. Z., Rocha, M. C., Malavazi, I., Brown, N. A., Valiante, V., Brakhage, A. A., Hagiwara, D., and Goldman, G. H. (2016) ‘Mitogen activated protein kinases SakAHOG1 and MpkC collaborate for Aspergillus

fumigatus virulence', *Molecular Microbiology*, 100(5), 841–859.

Bühler, N., Hagiwara, D., and Takeshita, N. (2015) 'Functional analysis of sterol transporter orthologues in the filamentous fungus Aspergillus nidulans', *Eukaryotic Cell*, 14(9), 908–921.

Carrasco, S., and Meyer, T. (2011) 'STIM proteins and the endoplasmic reticulum-plasma membrane junctions.', *Annual review of biochemistry*, 80(1), 973–1000.

Champion, O. L., Wagley, S., and Titball, R. W. (2016) 'Galleria mellonella as a model host for microbiological and toxin research', *Virulence*, 7(7), 840–845.

Chandra, J., Kuhn, D. M., Mukherjee, P. K., Hoyer, L. L., McCormick, T., and Ghannoum, M. A. (2001) 'Biofilm formation by the fungal pathogen Candida albicans: Development, architecture, and drug resistance', *Journal of Bacteriology*, 183(18), 5385–5394.

Chang, C.-L., Hsieh, T.-S., Yang, T. T., Rothberg, K. G., Azizoglu, D. B., Volk, E., Liao, J.-C., and Liou, J. (2017) 'Feedback Regulation of Receptor-Induced Ca^{2+} Signaling Mediated by E-Syt1 and Nir2 at Endoplasmic Reticulum-Plasma Membrane Junctions', *Cell Reports*, 5(3), 813–825.

Chong, P. L. (1994) 'Evidence for regular distribution of sterols in liquid crystalline phosphatidylcholine bilayers.', *Proceedings of the National Academy of Sciences of the United States of America*, 91(21), 10069–73.

Christian, A. E., Haynes, M. P., Phillips, M. C., and George, H. (1997) 'Use of cyclodextrins for manipulating cellular cholesterol content', *Journal Of Lipid Research*, 38(11), 2264–2272.

Chung, J., Torta, F., Masai, K., Lucast, L., Czapla, H., Tanner, L. B., Narayanaswamy, P., Wenk, M. R., Nakatsu, F., and De Camilli, P. (2015) 'PI4P/phosphatidylserine countertransport at ORP5- and ORP8-mediated ER-plasma membrane contacts.', *Science*, 349(6246), 428–32.

Clark, B. J. (2012) 'The mammalian START domain protein family in lipid transport in health and disease', *Journal of Endocrinology*, 212(3), 257–275.

Cockcroft, S., Garner, K., Yadav, S., Gomez-Espinoza, E., and Raghu, P. (2016) 'RdgBα reciprocally transfers PA and PI at ER-PM contact sites to maintain PI(4,5)P2 homoeostasis during phospholipase C signalling in Drosophila photoreceptors.', *Biochemical Society transactions*, 44(1), 286–92.

Cohen, R., and Engelberg, D. (2007) 'Commonly used Saccharomyces cerevisiae strains (e.g. BY4741, W303) are growth sensitive on synthetic complete medium due to poor leucine uptake', *FEMS Microbiology Letters*, 273(2), 239–243.

Colotelo, N. (1978) 'Fungal exudates.', *Canadian journal of microbiology*, 24(10), 1173–81.

Conde, L., Halperin, E., Akers, N. K., Brown, K. M., Smedby, K. E., … Skibola, C. F. (2010) 'Genome-wide association study of follicular lymphoma identifies a risk locus at 6p21.32.', *Nature Genetics*, 42(8), 661–4.

Connerth, M., Tatsuta, T., Haag, M., Klecker, T., Westermann, B., and Langer, T. (2012) 'Intramitochondrial transport of phosphatidic acid in yeast by a lipid transfer protein.', *Science*, 338(6108), 815–818.

Corbalan-Garcia, S., and Gómez-Fernández, J. C. (2014) 'Signaling through C2 domains: More than one lipid target', *Biochimica et Biophysica Acta - Biomembranes*, 1838(6), 1536–1547.

Corvera, E., Mouritsen, O. G., Singer, M. A., and Zuckermann, M. J. (1992) 'The permeability and the effect of acyl-chain length for phospholipid bilayers containing cholesterol: theory and experiment', *BBA - Biomembranes*, 1107(2), 261–270.

Cyster, J. G., Dang, E. V, Reboldi, A., and Yi, T. (2014) '25-Hydroxycholesterols in innate and adaptive immunity', *Nature Reviews Immunology*, 14(11), 731–743.

D'Angelo, G., Vicinanza, M., and De Matteis, M. A. (2008) 'Lipid-transfer proteins in biosynthetic pathways', *Current Opinion in Cell Biology*, 20(4), 360–370.

Das, A., Brown, M. S., Anderson, D. D., Goldstein, J. L., and Radhakrishnan, A. (2014) 'Three pools of plasma membrane cholesterol and their relation to cholesterol homeostasis', *eLife*, 3(e02882).

Dawidowicz, E. (1987) 'Dynamics Of Membrane Lipid Metabolism And Turnover', *Annual Review of Biochemistry*, 56(1), 43–61.

Dawson, P. A., Ridgway, N. D., Slaughter, C. A., Brown, M. S., and Goldstein, J. L. (1989) 'cDNA cloning

and expression of oxysterol-binding protein, an oligomer with a potential leucine zipper', *Journal of Biological Chemistry*, 264(28), 16798–16803.

Dittman, J. S., and Menon, A. K. (2016) 'Speed Limits for Nonvesicular Intracellular Sterol Transport', *Trends in Biochemical Sciences*, 42(2), 90–97.

Eberhardt, R. Y., Chang, Y., Bateman, A., Murzin, A. G., Axelrod, H. L., Hwang, W. C., and Aravind, L. (2013) 'Filling out the structural map of the NTF2-like superfamily.', *BMC bioinformatics*, 14(327).

Elbaz-Alon, Y., Eisenberg-Bord, M., Shinder, V., Stiller, S. B., Shimoni, E., Wiedemann, N., Geiger, T., and Schuldiner, M. (2015) 'Lam6 Regulates the Extent of Contacts between Organelles', *Cell Reports*, 12(1), 7–14.

Elbaz-Alon, Y., Rosenfeld-Gur, E., Shinder, V., Futerman, A. H., Geiger, T., and Schuldiner, M. (2014) 'A dynamic interface between vacuoles and mitochondria in yeast', *Developmental Cell*, 30(1), 95–102.

Erickson, F. Les, and Hannig, E. M. (1995) 'Characterization of Schizosaccharomyces pombe his1 and his5 cDNAs', *Yeast*, 11(2), 157–167.

Fahey, P. F., Koppel, D. E., Barak, L. S., Wolf, D. E., Elson, E. L., and Webb, W. W. (1977) 'Lateral diffusion in planar lipid bilayers.', *Science*, 195(4275), 305–306.

Fahy, E., Subramaniam, S., Murphy, R. C., Nishijima, M., Raetz, C. R. H., Shimizu, T., Spener, F., van Meer, G., Wakelam, M. J. O., and Dennis, E. A. (2008) 'Update of the LIPID MAPS comprehensive classification system for lipids', *The Journal of Lipid Research*, 50(Supplement), S9–S14.

Fairn, G. D., Curwin, A. J., Stefan, C. J., and McMaster, C. R. (2007) 'The oxysterol binding protein Kes1p regulates Golgi apparatus phosphatidylinositol-4-phosphate function.', *Proceedings of the National Academy of Sciences of the United States of America*, 104(39), 15352–7.

Fantini, J., and Barrantes, F. J. (2013) 'How cholesterol interacts with membrane proteins: An exploration of cholesterol-binding sites including CRAC, CARC, and tilted domains', *Frontiers in Physiology*, 4(31).

Faulhammer, F., Kanjilal-Kolar, S., Knödler, A., Lo, J., Lee, Y., Konrad, G., and Mayinger, P. (2007) 'Growth control of golgi phosphoinositides by reciprocal localization of sac1 lipid phosphatase and pik1 4-kinase', *Traffic*, 8(11), 1554–1567.

Feigenson, G. W. (2006) 'Phase behavior of lipid mixtures.', *Nature chemical biology*, 2(11), 560–563.

Feng, B., Yao, P. M., Li, Y., Devlin, C. M., Zhang, D., Harding, H. P., Sweeney, M., Rong, J. X., Kuriakose, G., Fisher, E. a, Marks, A. R., Ron, D., and Tabas, I. (2003) 'The endoplasmic reticulum is the site of cholesterol-induced cytotoxicity in macrophages', *Nature Cell Biology*, 5(9), 781–792.

Ferdinandusse, S., and Houten, S. M. (2006) 'Peroxisomes and bile acid biosynthesis.', *Biochimica et biophysica acta*, 1763(12), 1427–40.

von Filseck, J. M., Čopič, A., Delfosse, V., Vanni, S., Jackson, C. L., Bourguet, W., and Drin, G. (2015) 'Phosphatidylserine transport by ORP/Osh proteins is driven by phosphatidylinositol 4-phosphate.', *Science*, 349(6246), 432–6.

von Filseck, J. M., Vanni, S., Mesmin, B., Antonny, B., and Drin, G. (2015) 'A phosphatidylinositol-4-phosphate powered exchange mechanism to create a lipid gradient between membranes', *Nature Communications*, 6(6671).

Frickey, T., and Lupas, A. (2004) 'CLANS: A Java application for visualizing protein families based on pairwise similarity', *Bioinformatics*, 20(18), 3702–3704.

Friedman, J. R., Dibenedetto, J. R., West, M., Rowland, A. A., and Voeltz, G. K. (2013) 'Endoplasmic reticulum-endosome contact increases as endosomes traffic and mature.', *Molecular biology of the cell*, 24(7), 1030–40.

Friedman, J. R., Lackner, L. L., West, M., DiBenedetto, J. R., Nunnari, J., and Voeltz, G. K. (2011) 'ER tubules mark sites of mitochondrial division', *Science*, 334(6054), 358–362.

Frost, A., Unger, V. M., and De Camilli, P. (2009) 'The BAR Domain Superfamily: Membrane-Molding Macromolecules', *Cell*, 137(2), 191–196.

Fu, B., Meng, W., Zhao, H., Zhang, B., Tang, H., Zou, Y., Yao, J., Li, H., and Zhang, T. (2016) 'GRAM

domain-containing protein 1A (GRAMD1A) promotes the expansion of hepatocellular carcinoma stem cell and hepatocellular carcinoma growth through STAT5', *Scientific Reports*, 6(31963).

Fugmann, T., Hausser, A., Schöffler, P., Schmid, S., Pfizenmaier, K., and Olayioye, M. A. (2007) 'Regulation of secretory transport by protein kinase D-mediated phosphorylation of the ceramide transfer protein', *Journal of Cell Biology*, 178(1), 15–22.

Fürst, W., and Sandhoff, K. (1992) 'Activator proteins and topology of lysosomal sphingolipid catabolism.', *Biochimica et biophysica acta*, 1126(1), 1–16.

Gallego, O., Betts, M. J., Gvozdenovic-Jeremic, J., Maeda, K., Matetzki, C., Aguilar-Gurrieri, C., Beltran-Alvarez, P., Bonn, S., Fernández-Tornero, C., Jensen, L. J., Kuhn, M., Trott, J., Rybin, V., Müller, C. W., Bork, P., Kaksonen, M., Russell, R. B., and Gavin, A.-C. (2010) 'A systematic screen for protein–lipid interactions in Saccharomyces cerevisiae', *Molecular Systems Biology*, 6(430).

Gallo-Ebert, C., McCourt, P. C., Donigan, M., Villasmil, M. L., Chen, W., Pandya, D., Franco, J., Romano, D., Chadwick, S. G., Gygax, S. E., and Nickels, J. T. (2012) 'Arv1 lipid transporter function is conserved between pathogenic and nonpathogenic fungi', *Fungal Genetics and Biology*, 49(2), 101–113.

Garcia-Vidal, C., Peghin, M., Cervera, C., Gudiol, C., Ruiz-Camps, I., Moreno, A., Royo-Cebrecos, C., Roselló, E., de la Bellacasa, J. P., Ayats, J., and Carratalà, J. (2015) 'Causes of death in a contemporary cohort of patients with invasive aspergillosis.', *PloS one*, 10(3), e0120370.

Gasmi, N., Jacques, P. E., Klimova, N., Guo, X., Ricciardi, A., Robert, F., and Turcotte, B. (2014) 'The switch from fermentation to respiration in Saccharomyces cerevisiae is regulated by the Ert1 transcriptional activator/repressor', *Genetics*, 198(2), 547–560.

Gatta, A. T., Wong, L. H., Sere, Y. Y., Calderón-Noreña, D. M., Cockcroft, S., Menon, A. K., and Levine, T. P. (2015) 'A new family of StART domain proteins at membrane contact sites has a role in ER-PM sterol transport', *eLife*, 4(e07253).

Georgiev, A. G., Johansen, J., Ramanathan, V. D., Sere, Y. Y., Beh, C. T., and Menon, A. K. (2013) 'Arv1 regulates PM and ER membrane structure and homeostasis but is dispensable for intracellular sterol transport', *Traffic*, 14(8), 912–921.

Georgiev, A. G., Sullivan, D. P., Kersting, M. C., Dittman, J. S., Beh, C. T., and Menon, A. K. (2011) 'Osh proteins regulate membrane sterol organization but are not required for sterol movement between the ER and PM', *Traffic*, 12(10), 1341–1355.

Ghannoum, M. A., and Rice, L. B. (1999) 'Antifungal agents: Mode of action, mechanisms of resistance, and correlation of these mechanisms with bacterial resistance', *Clinical Microbiology Reviews*, 12(4), 501–517.

Ghisaidoobe, A. B. T., and Chung, S. J. (2014) 'Intrinsic tryptophan fluorescence in the detection and analysis of proteins: A focus on förster resonance energy transfer techniques', *International Journal of Molecular Sciences*, 15(12), 22518–22538.

Giaever, G., Chu, A. M., Ni, L., Connelly, C., Riles, L., … Johnston, M. (2002) 'Functional profiling of the Saccharomyces cerevisiae genome.', *Nature*, 418(6896), 387–391.

Giordano, F., Saheki, Y., Idevall-Hagren, O., Colombo, S. F., Pirruccello, M., Milosevic, I., Gracheva, E. O., Bagriantsev, S. N., Borgese, N., and De Camilli, P. (2013) 'PI(4,5)P2-Dependent and Ca2+-Regulated ER-PM interactions mediated by the extended synaptotagmins', *Cell*, 153(7), 1494–509.

Goldstein, J. L., and Brown, M. S. (1990) 'Regulation of the mevalonate pathway', *Nature*, 343(6257), 425–430.

Gray, K. C., Palacios, D. S., Dailey, I., Endo, M. M., Uno, B. E., Wilcock, B. C., and Burke, M. D. (2012) 'Amphotericin primarily kills yeast by simply binding ergosterol', *Proceedings of the National Academy of Sciences of the United States of America*, 109(7), 2234–2239.

Grove, S. N., and Bracker, C. E. (1970) 'Protoplasmic organization of hyphal tips among fungi: vesicles and Spitzenkörper.', *Journal of Bacteriology*, 104(2), 989–1009.

Haberland, M. E., and Reynolds, J. A. (1973) 'Self-association of cholesterol in aqueous solution.',

Proceedings of the National Academy of Sciences of the United States of America, 70(8), 2313–6.

Hanada, K., Kumagai, K., Yasuda, S., Miura, Y., Kawano, M., Fukasawa, M., and Nishijima, M. (2003) 'Molecular machinery for non-vesicular trafficking of ceramide.', *Nature*, 426(6968), 803–809.

Harlan, J. E., Hajduk, P. J., Yoon, H. S., and Fesik, S. W. (1994) 'Pleckstrin homology domains bind to phosphatidylinositol-4,5-bisphosphate.', *Nature*, 371(6493), 168–70.

Harris, S. D., Read, N. D., Roberson, R. W., Shaw, B., Seiler, S., Plamann, M., and Momany, M. (2005) 'Polarisome meets Spitzenkörper: Microscopy, genetics, and genomics converge', *Eukaryotic Cell*, 4(2), 225–229.

Heino, S., Lusa, S., Somerharju, P., Ehnholm, C., Olkkonen, V. M., and Ikonen, E. (2000) 'Dissecting the role of the golgi complex and lipid rafts in biosynthetic transport of cholesterol to the cell surface.', *Proceedings of the National Academy of Sciences of the United States of America*, 97(15), 8375–80.

Helmkamp, G. M., Harvey, M. S., Wirtz, K. W. A., and Van Deenen, L. L. M. (1974) 'Phospholipid exchange between membranes. Purification of bovine brain proteins that preferentially catalyze the transfer of phosphatidylinositol', *Journal of Biological Chemistry*, 249(20), 6382–6389.

Henne, W. M., Zhu, L., Balogi, Z., Stefan, C., Pleiss, J. A., and Emr, S. D. (2015) 'Mdm1/Snx13 is a novel ER-endolysosomal interorganelle tethering protein', *Journal of Cell Biology*, 210(4), 541–551.

Heo, W. Do, Inoue, T., Park, W. S., Kim, M. L., Park, B. O., Wandless, T. J., and Meyer, T. (2006) 'PI(3,4,5)P3 and PI(4,5)P2 Lipids Target Proteins with Polybasic Clusters to the Plasma Membrane', *Science*, 314(5804), 1458–1461.

Hillenmeyer, M. E., Fung, E., Wildenhain, J., Pierce, S. E., Hoon, S., Lee, W., Proctor, M., St Onge, R. P., Tyers, M., Koller, D., Altman, R. B., Davis, R. W., Nislow, C., and Giaever, G. (2008) 'The chemical genomic portrait of yeast: uncovering a phenotype for all genes.', *Science*, 320(5874), 362–365.

Holthuis, J. C. M., and Levine, T. P. (2005) 'Lipid traffic: floppy drives and a superhighway', *Nature Reviews Molecular Cell Biology*, 6(3), 209–220.

Hönscher, C., Mari, M., Auffarth, K., Bohnert, M., Griffith, J., Geerts, W., van der Laan, M., Cabrera, M., Reggiori, F., and Ungermann, C. (2014) 'Cellular metabolism regulates contact sites between vacuoles and mitochondria', *Developmental Cell*, 30(1), 86–94.

Howard, R. J. (1981) 'Ultrastructural analysis of hyphal tip cell growth in fungi: Spitzenkörper, cytoskeleton and endomembranes after freeze-substitution.', *Journal of cell science*, 48, 89–103.

Huang, J., Buboltz, J. T., and Feigenson, G. W. (1999) 'Maximum solubility of cholesterol in phosphatidylcholine and phosphatidylethanolamine bilayers', *Biochimica et Biophysica Acta - Biomembranes*, 1417(1), 89–100.

Huang, J., and Feigenson, G. W. (1999) 'A microscopic interaction model of maximum solubility of cholesterol in lipid bilayers.', *Biophysical journal*, 76(4), 2142–57.

Huh, W. K., Falvo, J. V., Gerke, L. C., Carroll, a. S., Howson, R. W., Weissman, J. S., and O'Shea, E. K. (2003) 'Global analysis of protein localization in budding yeast', *Nature*, 425(6959), 686–691.

Hulce, J. J., Cognetta, A. B., Niphakis, M. J., Tully, S. E., and Cravatt, B. F. (2013) 'Proteome-wide mapping of cholesterol-interacting proteins in mammalian cells.', *Nature methods*, 10(3), 259–64.

Iaea, D. B., Dikiy, I., Kiburu, I., Eliezer, D., and Maxfield, F. R. (2015) 'STARD4 Membrane Interactions and Sterol Binding', *Biochemistry*, 54(30), 4623–4636.

Iaea, D. B., and Maxfield, F. R. (2015) 'Cholesterol trafficking and distribution', *Essays In Biochemistry*, 57, 43–55.

Ikonen, E. (2006) 'Mechanisms for Cellular Cholesterol Transport : Defects and Human Disease', *Physiological reviews*, 86(4), 1237–1261.

Im, Y. J., Raychaudhuri, S., Prinz, W. a, and Hurley, J. H. (2005) 'Structural mechanism for sterol sensing and transport by OSBP-related proteins.', *Nature*, 437(7055), 154–158.

Iyer, L. M., Koonin, E. V., and Aravind, L. (2001) 'Adaptations of the helix-grip fold for ligand binding and catalysis in the START domain superfamily', *Proteins: Structure, Function and Genetics*, 43(2), 134–144.

Jacquier, N., and Schneiter, R. (2012) 'Mechanisms of sterol uptake and transport in yeast.', *The Journal of steroid biochemistry and molecular biology*, 129(1–2), 70–8.

Jeong, H., Park, J., and Lee, C. (2016) 'Crystal structure of Mdm12 reveals the architecture and dynamic organization of the ERMES complex', *EMBO Reports*, 17(12), 1857–1871.

Jiang, B., Brown, J. L., Sheraton, J., Fortin, N., and Bussey, H. (1994) 'A new family of yeast genes implicated in ergosterol synthesis is related to the human oxysterol binding protein', *Yeast*, 10(3), 341–353.

Jiang, S. Y., Ramamoorthy, R., and Ramachandran, S. (2008) 'Comparative transcriptional profiling and evolutionary analysis of the GRAM domain family in eukaryotes', *Developmental Biology*, 314(2), 418–432.

Jin, K., Musso, G., Vlasblom, J., Jessulat, M., Deineko, V., Negroni, J., Mosca, R., Malty, R., Nguyen-Tran, D. H., Aoki, H., Minic, Z., Freywald, T., Phanse, S., Xiang, Q., Freywald, A., Aloy, P., Zhang, Z., and Babu, M. (2015) 'Yeast mitochondrial protein-protein interactions reveal diverse complexes and disease-relevant functional relationships', *Journal of Proteome Research*, 14(2), 1220–1237.

John, K., Kubelt, J., Müller, P., Wüstner, D., and Herrmann, A. (2002) 'Rapid transbilayer movement of the fluorescent sterol dehydroergosterol in lipid membranes', *Biophysical Journal*, 83(3), 1525–1534.

Jorgensen, P., Edgington, N. P., Schneider, B. L., Rupes, I., Tyers, M., and Futcher, B. (2007) 'The Size of the Nucleus Increases as Yeast Cells Grow', *Molecular Biology of the Cell*, 18(9), 3523–3532.

Kagiwada, S., and Hashimoto, M. (2007) 'The yeast VAP homolog Scs2p has a phosphoinositide-binding ability that is correlated with its activity', *Biochemical and Biophysical Research Communications*, 364(4), 870–876.

Kamiński, D. M. (2014) 'Recent progress in the study of the interactions of amphotericin B with cholesterol and ergosterol in lipid environments', *European Biophysics Journal*, 43(10–11), 453–467.

Kaplan, M. R., and Simoni, R. D. (1985a) 'Intracellular transport of phosphatidylcholine to the plasma membrane', *Journal of Cell Biology*, 101(2), 441–445.

Kaplan, M. R., and Simoni, R. D. (1985b) 'Transport of cholesterol from the endoplasmic reticulum to the plasma membrane', *Journal of Cell Biology*, 101(2), 446–453.

Kawano, M., Kumagai, K., Nishijima, M., and Hanada, K. (2006) 'Efficient trafficking of ceramide from the endoplasmic reticulum to the golgi apparatus requires a VAMP-associated protein-interacting FFAT motif of CERT', *Journal of Biological Chemistry*, 281(40), 30279–30288.

Kellis, M., Birren, B. W., and Lander, E. S. (2004) 'Proof and evolutionary analysis of ancient genome duplication in the yeast Saccharomyces cerevisiae', *Nature*, 428(6983), 617–624.

Khafif, M., Cottret, L., Balagué, C., and Raffaele, S. (2014) 'Identification and phylogenetic analyses of VASt, an uncharacterized protein domain associated with lipid-binding domains in Eukaryotes', *BMC Bioinformatics*, 15(1), 222.

Kim, S., Kedan, A., Marom, M., Gavert, N., Keinan, O., Selitrennik, M., Laufman, O., and Lev, S. (2013) 'The phosphatidylinositol-transfer protein Nir2 binds phosphatidic acid and positively regulates phosphoinositide signalling', *EMBO reports*, 14(10), 891–899.

Klecker, T., and Westermann, B. (2014) 'Mitochondria are clamped to vacuoles for lipid transport.', *Developmental Cellell*, 30(1), 1–2.

Klemm, R. W., Ejsing, C. S., Surma, M. A., Kaiser, H. J., Gerl, M. J., Sampaio, J. L., De Robillard, Q., Ferguson, C., Proszynski, T. J., Shevchenko, A., and Simons, K. (2009) 'Segregation of sphingolipids and sterols during formation of secretory vesicles at the trans-Golgi network', *Journal of Cell Biology*, 185(4), 601–612.

Koh, J. L. Y., Chong, Y. T., Friesen, H., Moses, A., Boone, C., Andrews, B. J., and Moffat, J. (2015) 'CYCLoPs: A Comprehensive Database Constructed from Automated Analysis of Protein Abundance and Subcellular Localization Patterns in Saccharomyces cerevisiae.', *G3 (Bethesda,)*, 5(6), 1223–32.

Koide, T., Tsunasawa, S., and Ikenaka, T. (1972) 'The Amino Acid Sequence of Soybean Trypsin Inhibitor (Kunitz)*', *Biochemistry*, 167(1), 165–167.

Kojima, R., Endo, T., and Tamura, Y. (2016) 'A phospholipid transfer function of ER-mitochondria encounter structure revealed in vitro.', *Scientific reports*, 6, 30777.

Kontoyiannis, D. P. (2000) ‘Fluconazole inhibits pseudohyphal growth in Saccharomyces cerevisiae.’, *Chemotherapy*, 46(2), 100–103.

Kopec, K. O., Alva, V., and Lupas, A. N. (2010) ‘Homology of SMP domains to the TULIP superfamily of lipid-binding proteins provides a structural basis for lipid exchange between ER and mitochondria’, *Bioinformatics*, 26(16), 1927–1931.

Kornmann, B., Currie, E., Collins, S. R., Schuldiner, M., Nunnari, J., Weissman, J. S., and Walter, P. (2009) ‘An ER-Mitochondria Tethering Complex Revealed by a Synthetic Biology Screen’, *Science*, 325(5939).

Kornmann, B., and Walter, P. (2010) ‘ERMES-mediated ER-mitochondria contacts: molecular hubs for the regulation of mitochondrial biology.’, *Journal of cell science*, 123(Pt 9), 1389–93.

Krappmann, S. (2006) ‘Tools to study molecular mechanisms of Aspergillus pathogenicity’, *Trends in Microbiology*, 14(8), 356–364.

Krappmann, S., Sasse, C., and Braus, G. H. (2006) ‘Gene targeting in Aspergillus fumigatus by homologous recombination is facilitated in a nonhomologous end-joining-deficient genetic background’, *Eukaryotic Cell*, 5(1), 212–215.

Kulak, N. A., Pichler, G., Paron, I., Nagaraj, N., and Mann, M. (2014) ‘Minimal, encapsulated proteomic-sample processing applied to copy-number estimation in eukaryotic cells’, *Nature Methods*, 11(3), 319–324.

Kumagai, K., Kawano-Kawada, M., and Hanada, K. (2014) ‘Phosphoregulation of the ceramide transport protein CERT at serine 315 in the interaction with VAMP-associated protein (VAP) for inter-organelle trafficking of ceramide in mammalian cells’, *Journal of Biological Chemistry*, 289(15), 10748–10760.

Kumagai, K., Kawano, M., Shinkai-Ouchi, F., Nishijima, M., and Hanada, K. (2007) ‘Interorganelle trafficking of ceramide is regulated by phosphorylation- dependent cooperativity between the PH and START domains of CERT’, *Journal of Biological Chemistry*, 282(24), 17758–17766.

Lahiri, S., Chao, J. T., Tavassoli, S., Wong, A. K. O., Choudhary, V., Young, B. P., Loewen, C. J. R., and Prinz, W. A. (2014) ‘A Conserved Endoplasmic Reticulum Membrane Protein Complex (EMC) Facilitates Phospholipid Transfer from the ER to Mitochondria’, *PLoS Biology*, 12(10), e1001969.

Lang, A. B., John Peter, A. T. A. T., Walter, P., and Kornmann, B. (2015) ‘ER-mitochondrial junctions can be bypassed by dominant mutations in the endosomal protein Vps13’, *Journal of Cell Biology*, 210(6), 883–890.

Lange, Y., and Steck, T. L. (1997) ‘Quantitation of the pool of cholesterol associated with Acyl-CoA. Cholesterol acyltransferase in human fibroblasts’, *Journal of Biological Chemistry*, 272(20), 13103–13108.

Lange, Y., Strebel, F., and Steck, T. L. (1993) ‘Role of the plasma membrane in cholesterol esterification in rat hepatoma cells’, *Journal of Biological Chemistry*, 268(19), 13838–13843.

Lange, Y., Ye, J., Rigney, M., and Steck, T. L. (1999) ‘Regulation of endoplasmic reticulum cholesterol by plasma membrane cholesterol’, *Journal of Lipid Research*, 40(12), 2264–2270.

LeBlanc, M. A., and McMaster, C. R. (2010) ‘Lipid binding requirements for oxysterol-binding protein Kes1 inhibition of autophagy and endosome-trans-Golgi trafficking pathways’, *Journal of Biological Chemistry*, 285(44), 33875–33884.

Lee, J.-Y., Kinch, L. N., Borek, D. M., Wang, J., Wang, J., Urbatsch, I. L., Xie, X.-S., Grishin, N. V., Cohen, J. C., Otwinowski, Z., Hobbs, H. H., and Rosenbaum, D. M. (2016) ‘Crystal structure of the human sterol transporter ABCG5/ABCG8’, *Nature*, 533(7604), 561–564.

Van Leeuwen, M. R., Golovina, E. A., and Dijksterhuis, J. (2009) ‘The polyene antimycotics nystatin and filipin disrupt the plasma membrane, whereas natamycin inhibits endocytosis in germinating conidia of Penicillium discolor’, *Journal of Applied Microbiology*, 106(6), 1908–1918.

Van Leeuwen, M. R., Smant, W., de Boer, W., and Dijksterhuis, J. (2008) ‘Filipin is a reliable in situ marker of ergosterol in the plasma membrane of germinating conidia (spores) of Penicillium discolor and stains intensively at the site of germ tube formation’, *Journal of Microbiological Methods*, 74(2–3), 64–73.

Lemmon, M. A. (2007) ‘Pleckstrin homology (PH) domains and phosphoinositides.’, *Biochemical Society symposium*, (74), 81–93.

Lesage, P., Yang, X., and Carlson, M. (1994) 'Analysis of the SIP3 protein identified in a two-hybrid screen for interaction with the SNF1 protein kinase', *Nucleic Acids Research*, 22(4), 597–603.

Lev, S., Halevy, D. Ben, Peretti, D., and Dahan, N. (2008) 'The VAP protein family: from cellular functions to motor neuron disease', *Trends in Cell Biology*, 18(6), 282–290.

Levine, T. (2004) 'Short-range intracellular trafficking of small molecules across endoplasmic reticulum junctions', *Trends in Cell Biology*, 14(9), 483–490.

Levine, T. P., and Munro, S. (2001) 'Dual targeting of Osh1p, a yeast homologue of oxysterol-binding protein, to both the Golgi and the nucleus-vacuole junction.', *Molecular biology of the cell*, 12(6), 1633–44.

Levine, T. P., and Munro, S. (2002) 'Targeting of Golgi-specific pleckstrin homology domains involves both Ptdlns 4-kinase-dependent and -independent components', *Current Biology*, 12(9), 695–704.

Li, L., Shi, X., Guo, X., Li, H., and Xu, C. (2014) 'Ionic protein-lipid interaction at the plasma membrane: What can the charge do?', *Trends in Biochemical Sciences*, 39(3), 130–140.

Li, S. (2005) 'Distinct Ceramide Synthases Regulate Polarized Growth in the Filamentous Fungus Aspergillus nidulans', *Molecular Biology of the Cell*, 17(3), 1218–1227.

Li, X., Rivas, M. P., Fang, M., Marchena, J., Mehrotra, B., Chaudhary, A., Li, F., Prestwich, G. D., and Bankaitis, V. A. (2002) 'Analysis of oxysterol binding protein homologue Kes1p function in regulation of Sec14p-dependent protein transport from the yeast Golgi complex', *Journal of Cell Biology*, 157(1), 63–77.

Li, Y., Kabbage, M., Liu, W., and Dickman, M. B. (2016) 'Aspartyl Protease-Mediated Cleavage of BAG6 Is Necessary for Autophagy and Fungal Resistance in Plants.', *The Plant cell*, 28(1), 233–47.

Li, Y., and Prinz, W. A. (2004) 'ATP-binding cassette (ABC) transporters mediate nonvesicular, raft-modulated sterol movement from the plasma membrane to the endoplasmic reticulum', *Journal of Biological Chemistry*, 279(43), 45226–45234.

Ling, Y., Hayano, S., and Novick, P. (2014) 'Osh4p is needed to reduce the level of phosphatidylinositol-4-phosphate on secretory vesicles as they mature', *Molecular Biology of the Cell*, 25(21), 3389–3400.

Liou, J., Kim, M. L., Won, D. H., Jones, J. T., Myers, J. W., Ferrell, J. E., and Meyer, T. (2005) 'STIM is a Ca2+ sensor essential for Ca2+-store- depletion-triggered Ca2+ influx', *Current Biology*, 15(13), 1235–1241.

Litvak, V., Dahan, N., Ramachandran, S., Sabanay, H., and Lev, S. (2005) 'Maintenance of the diacylglycerol level in the Golgi apparatus by the Nir2 protein is critical for Golgi secretory function.', *Nature cell biology*, 7(3), 225–234.

Liu, B. (2012) 'Therapeutic potential of cyclodextrins in the treatment of Niemann–Pick type C disease', *Clinical Lipidology*, 7(3), 289–301.

Liu, G., Vellucci, V. F., Kyc, S., and Hostetter, M. K. (2009) 'Simvastatin inhibits candida albicans biofilm in vitro', *Pediatric Research*, 66(6), 600–604.

Liu, L.-K., Choudhary, V., Toulmay, A., and Prinz, W. A. (2016) 'An inducible ER-Golgi tether facilitates ceramide transport to alleviate lipotoxicity.', *The Journal of cell biology*, 216(1), 131–147.

Liu, X., Jiang, J., Yin, Y., and Ma, Z. (2013) 'Involvement of FgERG4 in ergosterol biosynthesis, vegetative differentiation and virulence in Fusarium graminearum', *Molecular Plant Pathology*, 14(1), 71–83.

Lodowski, D. T., Pitcher, J. A., Capel, W. D., Lefkowitz, R. J., and Tesmer, J. J. G. (2003) 'Keeping G Proteins at Bay: A Complex Between G Protein-Coupled Receptor Kinase 2 and Gbetagamma', *Science*, 300(5623), 1256–1262.

Loeb, J. D. J., Kerentseva, T. A., Pan, T., Sepulveda-becerra, M., and Liu, H. (1999) 'Saccharomyces cerevisiae G1 Cyclins Are Differentially Involved in Invasive and Protein Kinase Pathway', *Genetics*, 153(4).

Loewen, C. J. R., Roy, A., and Levine, T. P. (2003) 'A conserved ER targeting motif in three families of lipid binding proteins and in Opi1p binds VAP', *EMBO Journal*, 22(9), 2025–2035.

Long, N., Xu, X., Zeng, Q., Sang, H., and Lu, L. (2017) 'Erg4A and Erg4B Are Required for Conidiation and Azole Resistance via Regulation of Ergosterol Biosynthesis in Aspergillus fumigatus', *Applied and Environmental Microbiology*, 83(4), e02924-16.

Lorent, J., Le Duff, C. S., Quetin-Leclercq, J., and Mingeot-Leclercq, M.-P. (2013) 'Induction of highly curved structures in relation to membrane permeabilization and budding by the triterpenoid saponins, α- and δ-Hederin.', *The Journal of biological chemistry*, 288(20), 14000–17.

Loura, L. M. S., Fedorov, A., and Prieto, M. (2001) 'Exclusion of a cholesterol analog from the cholesterol-rich phase in model membranes', *Biochimica et Biophysica Acta - Biomembranes*, 1511(2), 236–243.

Lupetti, A., Danesi, R., Campa, M., Tacca, M. Del, and Kelly, S. (2002) 'Molecular basis of resistance to azole antifungals', *Trends in Molecular Medicine*, 8(2), 76–81.

Maeda, K., Anand, K., Chiapparino, A., Kumar, A., Poletto, M., Kaksonen, M., and Gavin, A.-C. C. (2013) 'Interactome map uncovers phosphatidylserine transport by oxysterol-binding proteins.', *Nature*, 501(7466), 257–261.

Maléth, J., Choi, S., Muallem, S., and Ahuja, M. (2014) 'Translocation between PI(4,5)P2-poor and PI(4,5)P2-rich microdomains during store depletion determines STIM1 conformation and Orai1 gating', *Nature Communications*, 5(5843).

Manford, A. G., Stefan, C. J., Yuan, H. L., MacGurn, J. A., and Emr, S. D. (2012) 'ER-to-Plasma Membrane Tethering Proteins Regulate Cell Signaling and ER Morphology', *Developmental Cell*, 23(6), 1129–1140.

Mania, D., Hilpert, K., Ruden, S., Fischer, R., and Takeshita, N. (2010) 'Screening for antifungal peptides and their modes of action in Aspergillus nidulans', *Applied and Environmental Microbiology*, 76(21), 7102–7108.

Marty, A., and Finkelstein, A. (1975) 'Pores formed in lipid bilayer membranes by nystatin, Differences in its one-sided and two-sided action', *The Journal of General Physiology*, 65(4), 515–526.

Maruyama, J. ichi, Kikuchi, S., and Kitamoto, K. (2006) 'Differential distribution of the endoplasmic reticulum network as visualized by the BipA-EGFP fusion protein in hyphal compartments across the septum of the filamentous fungus, Aspergillus oryzae', *Fungal Genetics and Biology*, 43(9), 642–654.

Mattjus, P., Bittman, R., Vilchèze, C., and Slotte, J. P. (1995) 'Lateral domain formation in cholesterol/phospholipid monolayers as affected by the sterol side chain conformation.', *Biochimica et biophysica acta*, 1240(2), 237–47.

Mauch, D. H., Nägler, K., Schumacher, S., Göritz, C., Müller, E.-C., Otto, A., and Pfrieger, F. W. (2001) 'CNS Synaptogenesis Promoted by Glia-Derived Cholesterol', *Science*, 294(5545), 1354–7.

Maxfield, F. R., and Wüstner, D. (2012) 'Analysis of Cholesterol Trafficking with Fluorescent Probes', *Methods in Cell Biology*, 108(1), 367–393.

McConnell, H. M., and Radhakrishnan, A. (2003) 'Condensed complexes of cholesterol and phospholipids', *Biochimica et Biophysica Acta - Biomembranes*, 159–173.

McCourt, P., Liu, H.-Y., Parker, J. E., Gallo-Ebert, C., Donigan, M., Bata, A., Giordano, C., Kelly, S. L., and Nickels, J. T. (2016) 'Proper Sterol Distribution Is Required for Candida albicans Hyphal Formation and Virulence.', *G3 (Bethesda)*, 6(11), 3455–3465.

McIntosh, A. L., Atshaves, B. P., Huang, H., Gallegos, A. M., Kier, A. B., and Schroeder, F. (2008) 'Fluorescence techniques using dehydroergosterol to study cholesterol trafficking', *Lipids*, 43(12), 1185–1208.

McLean, L. R., and Phillips, M. C. (1984) 'Kinetics of phosphatidylcholine and lysophosphatidylcholine exchange between unilamellar vesicles', *Biochemistry*, 23(20), 4624–4630.

van Meer, G., Voelker, D. R., and Feigenson, G. W. (2008) 'Membrane lipids: where they are and how they behave', *Nature Reviews Molecular Cell Biology*, 9(2), 112–124.

Mesmin, B., Antonny, B., and Drin, G. (2013) 'Insights into the mechanisms of sterol transport between organelles', *Cellular and Molecular Life Sciences*, 70(18), 3405–3421.

Mesmin, B., Bigay, J., Moser Von Filseck, J., Lacas-Gervais, S., Drin, G., and Antonny, B. (2013) 'XA four-step cycle driven by PI(4)P hydrolysis directs sterol/PI(4)P exchange by the ER-Golgi Tether OSBP', *Cell*, 155(4), 830–43.

Mesmin, B., and Maxfield, F. R. (2009) 'Intracellular sterol dynamics', *Biochimica et Biophysica Acta - Molecular and Cell Biology of Lipids*, 636–645.

Mesmin, B., Pipalia, N. H., Lund, F. W., Ramlall, T. F., Sokolov, A., Eliezer, D., and Maxfield, F. R. (2011) 'STARD4 abundance regulates sterol transport and sensing.', *Molecular biology of the cell*, 22(21), 4004–15.

Mikitova, V., and Levine, T. P. (2012) 'Analysis of the key elements of FFAT-like motifs identifies new proteins that potentially bind VAP on the ER, including two AKAPs and FAPP2', *PLoS ONE*, 7(1).

Miliara, X., Garnett, J. A., Tatsuta, T., Abid Ali, F., Baldie, H., Pérez-Dorado, I., Simpson, P., Yague, E., Langer, T., and Matthews, S. (2015) 'Structural insight into the TRIAP1/PRELI-like domain family of mitochondrial phospholipid transfer complexes.', *EMBO reports*, 16(7), 824–35.

Millen, J. I., Krick, R., Prick, T., Thumm, M., and Goldfarb, D. S. (2009) 'Measuring piecemeal microautophagy of the nucleus in Saccharomyces cerevisiae', *Autophagy*, 5(1), 75–81.

Miller, W. L. (2007) 'Mechanism of StAR's regulation of mitochondrial cholesterol import', *Molecular and Cellular Endocrinology*, 265–266(SUPPL.), 46–50.

Min, S.-W., Chang, W.-P., and Sudhof, T. C. (2007) 'E-Syts, a family of membranous Ca2+-sensor proteins with multiple C2 domains', *Proceedings of the National Academy of Sciences*, 104(10), 3823–3828.

Miyata, N., Watanabe, Y., Tamura, Y., Endo, T., and Kuge, O. (2016) 'Phosphatidylserine transport by Ups2-Mdm35 in respiration-active mitochondria', *Journal of Cell Biology*, 214(1), 77–88.

Moog-Lutz, C., Tomasetto, C., Régnier, C. H., Wendling, C., Lutz, Y., Muller, D., Chenard, M. P., Basset, P., and Rio, M. C. (1997) 'MLN64 exhibits homology with the steroidogenic acute regulatory protein (STAR) and is over-expressed in human breast carcinomas', *International Journal of Cancer*, 71(2), 183–191.

Mouri, R., Konoki, K., Matsumori, N., Oishi, T., and Murata, M. (2008) 'Complex formation of amphotericin B in sterol-containing membranes as evidenced by surface plasmon resonance', *Biochemistry*, 47(30), 7807–7815.

Muir, A., Ramachandran, S., Roelants, F. M., Timmons, G., and Thorner, J. (2014) 'TORC2-dependent protein kinase Ypk1 phosphorylates ceramide synthase to stimulate synthesis of complex sphingolipids.', *eLife*, 3, 1–34.

Mukherjee, P. K., Chandra, J., Kuhn, D. M., and Ghannoum, M. A. (2003) 'Mechanism of fluconazole resistance in Candida albicans biofilms: Phase-specific role of efflux pumps and membrane sterols', *Infection and Immunity*, 71(8), 4333–4340.

Mukherjee, S., and Maxfield, F. R. (2004) 'Lipid and cholesterol trafficking in NPC', *Biochimica et Biophysica Acta - Molecular and Cell Biology of Lipids*, 1685(1–3), 28–37.

Mukherjee, S., Zha, X., Tabas, I., and Maxfield, F. R. (1998) 'Cholesterol distribution in living cells: fluorescence imaging using dehydroergosterol as a fluorescent cholesterol analog', *Biophysical Journal*, 75(4), 1915–1925.

Munn, A. L., Heese-Peck, A., Stevenson, B. J., Pichler, H., and Riezman, H. (1999) 'Specific Sterols Required for the Internalization Step of Endocytosis in Yeast', *Molecular Biology of the Cell*, 10(11), 3943–3957.

Murcia, M., Faráldo-Gómez, J. D., Maxfield, F. R., and Roux, B. (2006) 'Modeling the structure of the StART domains of MLN64 and StAR proteins in complex with cholesterol.', *Journal of lipid research*, 47(12), 2614–2630.

Murley, A., Lackner, L. L., Osman, C., West, M., Voeltz, G. K., Walter, P., and Nunnari, J. (2013) 'ER-associated mitochondrial division links the distribution of mitochondria and mitochondrial DNA in yeast', *eLife*, 2(e00422).

Murley, A., Sarsam, R. D., Toulmay, A., Yamada, J., Prinz, W. A., and Nunnari, J. (2015) 'Ltc1 is an ER-localized sterol transporter and a component of ER-mitochondria and ER-vacuole contacts', *Journal of Cell Biology*, 209(4), 539–548.

Murphy, S. E., and Levine, T. P. (2016) 'VAP, a Versatile Access Point for the Endoplasmic Reticulum: Review and analysis of FFAT-like motifs in the VAPome', *Biochimica et Biophysica Acta - Molecular and Cell Biology of Lipids*, 952–961.

Naon, D., Zaninello, M., Giacomello, M., Varanita, T., Grespi, F., Lakshminaranayan, S., Serafini, A.,

Semenzato, M., Herkenne, S., Hernández-Alvarez, M. I., Zorzano, A., De Stefani, D., Dorn Ii, G. W., and Scorrano, L. (2016) 'Critical reappraisal confirms that Mitofusin 2 is an endoplasmic reticulum–mitochondria tether', *Proceedings of the National Academy of Sciences of the United States of America*, 113(40), 11249–11254.

Nguyen, T. T., Lewandowska, A., Choi, J. Y., Markgraf, D. F., Junker, M., Bilgin, M., Ejsing, C. S., Voelker, D. R., Rapoport, T. A., and Shaw, J. M. (2012) 'Gem1 and ERMES Do Not Directly Affect Phosphatidylserine Transport from ER to Mitochondria or Mitochondrial Inheritance', *Traffic*, 13(6), 880–890.

Nielsen, M. L., Albertsen, L., Lettier, G., Nielsen, J. B., and Mortensen, U. H. (2006) 'Efficient PCR-based gene targeting with a recyclable marker for Aspergillus nidulans', *Fungal Genetics and Biology*, 43(1), 54–64.

Nilsson, I. . c, Ohvo-Rekilä, H. ., Slotte, J. P. ., Johnson, A. E. ., and Von Heijne, G. . (2001) 'Inhibition of Protein Translocation across the Endoplasmic Reticulum Membrane by Sterols', *Journal of Biological Chemistry*, 276(45), 41748–41754.

Novotny, C., Behalova, B., Dolezalova, L., and Zajicek, J. (1987) 'Regulation of sterol synthesis by glucose in baker's yeast', *Acta Biotechnologica*, 7(4), 347–351.

Ohtani, Y., Irie, T., Uekama, K., Fukunaga, K., and Pitha, J. (1989) 'Differential effects of alpha-, beta- and gamma-cyclodextrins on human erythrocytes', *European Journal of Biochemistry*, 186(1–2), 17–22.

Ohvo, H., and Slotte, J. P. (1996) 'Cyclodextrin-mediated removal of sterols from monolayers: Effects of sterol structure and phospholipids on desorption rate', *Biochemistry*, 35(24), 8018–8024.

Opekarová, M., and Tanner, W. (1994) 'Nystatin changes the properties of transporters for arginine and sugars An in vitro study', *FEBS Letters*, 350(1), 46–50.

Osman, C., Haag, M., Potting, C., Rodenfels, J., Dip, P. V., Wieland, F. T., Brügger, B., Westermann, B., and Langer, T. (2009) 'The genetic interactome of prohibitins: Coordinated control of cardiolipin and phosphatidylethanolamine by conserved regulators in mitochondria', *Journal of Cell Biology*, 184(4), 583–596.

Oura, M., Sternberg, T. H., and Wright, E. T. (1955) 'A new antifungal antibiotic, amphotericin B.', *Antibiotics annual*, 3, 566–573.

Palacios, D. S., Anderson, T. M., and Burke, M. D. (2007) 'A post-PKS oxidation of the amphotericin B skeleton predicted to be critical for channel formation is not required for potent antifungal activity', *Journal of the American Chemical Society*, 129(45), 13804–13805.

Palacios, D. S., Dailey, I., Siebert, D. M., Wilcock, B. C., and Burke, M. D. (2011) 'Synthesis-enabled functional group deletions reveal key underpinnings of amphotericin B ion channel and antifungal activities', *Proceedings of the National Academy of Sciences of the United States of America*, 108(17), 6733–6738.

Pan, X., Roberts, P., Chen, Y., Kvam, E., Shulga, N., Huang, K., Lemmon, S., and Goldfarb, D. S. (2000) 'Nucleus-vacuole junctions in Saccharomyces cerevisiae are formed through the direct interaction of Vac8p with Nvj1p.', *Molecular biology of the cell*, 11(7), 2445–57.

Papahadjopoulos, D., Jacobson, K., Nir, S., and Isac, T. (1973) 'Phase transitions in phospholipid vesicles. Fluorescence polarization and permeability measurements concerning the effect of temperature and cholesterol.', *Biochimica et biophysica acta*, 311(3), 330–48.

Park, J.-S., Thorsness, M. K., Policastro, R., McGoldrick, L. L., Hollingsworth, N. M., Thorsness, P. E., and Neiman, A. M. (2016) 'Yeast Vps13 promotes mitochondrial function and is localized at membrane contact sites', *Molecular Biology of the Cell*, 27(15), 2435–2449.

Paul, S., Diekema, D., and Moye-Rowley, W. S. (2013) 'Contributions of Aspergillus fumigatus ATP-binding cassette transporter proteins to drug resistance and virulence', *Eukaryotic Cell*, 12(12), 1619–1628.

Peretti, D., Dahan, N., Shimoni, E., Hirschberg, K., and Lev, S. (2008) 'Coordinated Lipid Transfer between the Endoplasmic Reticulum and the Golgi Complex Requires the VAP Proteins and Is Essential for Golgi-mediated Transport', *Molecular Biology of the Cell*, 19(9), 3871–3884.

Perry, R. J., and Ridgway, N. D. (2006) 'Oxysterol-binding protein and vesicle-associated membrane protein-associated protein are required for sterol-dependent activation of the ceramide transport protein.', *Molecular biology of the cell*, 17(6), 2604–16.

Pettersen, E. F., Goddard, T. D., Huang, C. C., Couch, G. S., Greenblatt, D. M., Meng, E. C., and Ferrin, T. E. (2004) 'UCSF Chimera--a visualization system for exploratory research and analysis.', *Journal of Computational Chemistry*, 25(13), 1605–12.

Phillips, M. C., McLean, L. R., Stoudt, G. W., and Rothblat, G. H. (1980) 'Mechanism of cholesterol efflux from cells', *Atherosclerosis*, 36(3), 409–422.

Phillips, M. J., and Voeltz, G. K. (2015) 'Structure and function of ER membrane contact sites with other organelles', *Nature Reviews Molecular Cell Biology*, 17(2), 69–82.

Pichler, H., Gaigg, B., Hrastnik, C., Achleitner, G., Kohlwein, S. D., Zellnig, G., Perktold, A., and Daum, G. (2001) 'A subfraction of the yeast endoplasmic reticulum associates with the plasma membrane and has a high capacity to synthesize lipids', *European Journal of Biochemistry*, 268(8), 2351–2361.

Pozniakovsky, A. I., Knorre, D. A., Markova, O. V., Hyman, A. A., Skulachev, V. P., and Severin, F. F. (2005) 'Role of mitochondria in the pheromone- and amiodarone-induced programmed death of yeast', *Journal of Cell Biology*, 168(2), 257–269.

Proszynski, T. J., Klemm, R., Bagnat, M., Gaus, K., and Simons, K. (2006) 'Plasma membrane polarization during mating in yeast cells', *Journal of Cell Biology*, 173(6), 861–866.

Proszynski, T. J., Klemm, R. W., Gravert, M., Hsu, P. P., Gloor, Y., Wagner, J., Kozak, K., Grabner, H., Walzer, K., Bagnat, M., Simons, K., and Walch-Solimena, C. (2005) 'A genome-wide visual screen reveals a role for sphingolipids and ergosterol in cell surface delivery in yeast.', *Proceedings of the National Academy of Sciences of the United States of America*, 102(50), 17981–6.

Qiu, X., Mistry, A., Ammirati, M. J., Chrunyk, B. A., Clark, R. W., Cong, Y., Culp, J. S., Danley, D. E., Freeman, T. B., Geoghegan, K. F., Griffor, M. C., Hawrylik, S. J., Hayward, C. M., Hensley, P., Hoth, L. R., Karam, G. A., Lira, M. E., Lloyd, D. B., McGrath, K. M., Stutzman-Engwall, K. J., Subashi, A. K., Subashi, T. A., Thompson, J. F., Wang, I.-K., Zhao, H., and Seddon, A. P. (2007) 'Crystal structure of cholesteryl ester transfer protein reveals a long tunnel and four bound lipid molecules', *Nature Structural & Molecular Biology*, 14(2), 106–113.

Radhakrishnan, A., Goldstein, J. L., McDonald, J. G., and Brown, M. S. (2008) 'Switch-like Control of SREBP-2 Transport Triggered by Small Changes in ER Cholesterol: A Delicate Balance', *Cell Metabolism*, 8(6), 512–521.

Raghuraman, H., and Chattopadhyay, A. (2004) 'Interaction of melittin with membrane cholesterol: a fluorescence approach.', *Biophysical journal*, 87(4), 2419–32.

Ramage, G., Rajendran, R., Sherry, L., and Williams, C. (2012) 'Fungal biofilm resistance', *International Journal of Microbiology*, 2012(528521).

Ramstedt, B., and Slotte, J. P. (2002) 'Membrane properties of sphingomyelins', *FEBS Letters*, 33–37.

Raychaudhuri, S., Im, Y. J., Hurley, J. H., and Prinz, W. A. (2006) 'Nonvesicular sterol movement from plasma membrane to ER requires oxysterol-binding protein-related proteins and phosphoinositides', *Journal of Cell Biology*, 173(1), 107–119.

Reitz, J., Gehrig-Burger, K., Strauss, J. F., and Gimpl, G. (2008) 'Cholesterol interaction with the related steroidogenic acute regulatory lipid-transfer (START) domains of StAR (STARD1) and MLN64 (STARD3)', *FEBS Journal*, 275(8), 1790–1802.

Rodriguez-Agudo, D., Calderon-Dominguez, M., Ren, S., Marques, D., Redford, K., Medina-Torres, M. A., Hylemon, P., Gil, G., and Pandak, W. M. (2011) 'Subcellular localization and regulation of StarD4 protein in macrophages and fibroblasts', *Biochimica et Biophysica Acta - Molecular and Cell Biology of Lipids*, 1811(10), 597–606.

Roostaee, A., Barbar, E., Lavigne, P., and LeHoux, J.-G. (2009) 'The mechanism of specific binding of free cholesterol by the steroidogenic acute regulatory protein: evidence for a role of the C-terminal alpha-helix in the gating of the binding site.', *Bioscience reports*, 29(2), 89–101.

Rowland, A. A., Chitwood, P. J., Phillips, M. J., and Voeltz, G. K. (2014) 'ER contact sites define the

position and timing of endosome fission', *Cell*, 159(5), 1027–1041.

Royer, C. A. (2006) 'Probing protein folding and conformational transitions with fluorescence', *Chemical Reviews*, 106(5), 1769–1784.

Saad, H. Y., and Higuchi, W. I. (1965) 'Water solubility of cholesterol', *Journal of Pharmaceutical Sciences*, 54(8), 1205–1206.

Saheki, Y., Bian, X., Schauder, C. M., Sawaki, Y., Surma, M. A., Klose, C., Pincet, F., Reinisch, K. M., and De Camilli, P. (2016) 'Control of plasma membrane lipid homeostasis by the extended synaptotagmins.', *Nature cell biology*, 18(5), 504–15.

de Saint-Jean, M., Delfosse, V., Douguet, D., Chicanne, G., Payrastre, B., Bourguet, W., Antonny, B., and Drin, G. (2011) 'Osh4p exchanges sterols for phosphatidylinositol 4-phosphate between lipid bilayers', *Journal of Cell Biology*, 195(6), 965–978.

Saito, S., Matsui, H., Kawano, M., Kumagai, K., Tomishige, N., Hanada, K., Echigo, S., Tamura, S., and Kobayashi, T. (2008) 'Protein phosphatase 2Cepsilon is an endoplasmic reticulum integral membrane protein that dephosphorylates the ceramide transport protein CERT to enhance its association with organelle membranes', *Journal of Biological Chemistry*, 283(10), 6584–6593.

Schaaf, G., Ortlund, E. A., Tyeryar, K. R., Mousley, C. J., Ile, K. E., Garrett, T. A., Ren, J., Woolls, M. J., Raetz, C. R. H., Redinbo, M. R., and Bankaitis, V. A. (2008) 'Functional Anatomy of Phospholipid Binding and Regulation of Phosphoinositide Homeostasis by Proteins of the Sec14 Superfamily', *Molecular Cell*, 29(2), 191–206.

Schauder, C. M., Wu, X., Saheki, Y., Narayanaswamy, P., Torta, F., Wenk, M. R., De Camilli, P., and Reinisch, K. M. (2014) 'Structure of a lipid-bound extended synaptotagmin indicates a role in lipid transfer.', *Nature*, 510(7506), 552–5.

Scheek, S., Brown, M. S., and Goldstein, J. L. (1997) 'Sphingomyelin depletion in cultured cells blocks proteolysis of sterol regulatory element binding proteins at site 1', *Proceedings of the National Academy of Sciences of the United States of America*, 94(21), 11179–11183.

Scheffzek, K., and Welti, S. (2012) 'Pleckstrin homology (PH) like domains - Versatile modules in protein-protein interaction platforms', *FEBS Letters*, 586(17), 2662–2673.

Scheidt, H. A., Muller, P., Herrmann, A., and Huster, D. (2003) 'The Potential of Fluorescent and Spin-labeled Steroid Analogs to Mimic Natural Cholesterol', *Journal of Biological Chemistry*, 278(46), 45563–45569.

Schneiter, R., Brügger, B., Sandhoff, R., Zellnig, G., Leber, A., Lampl, M., Athenstaedt, K., Hrastnik, C., Eder, S., Daum, G., Paltauf, F., Wieland, F. T., and Kohlwein, S. D. (1999) 'Analysis of the Lipid Molecular Species Composition of Yeast Subcellular Membranes Reveals Acyl Chain-based Sorting / Remodeling of Distinct Molecular Species En Route to the Plasma Membrane', *Cell*, 146(4), 741–754.

Schouten, A., Agianian, B., Westerman, J., Kroon, J., Wirtz, K. W. A., and Gros, P. (2002) 'Structure of apo-phosphatidylinositol transfer protein alpha provides insight into membrane association.', *The EMBO journal*, 21(9), 2117–21.

Schrick, K., Nguyen, D., Karlowski, W. M., and Mayer, K. F. X. (2004) 'START lipid/sterol-binding domains are amplified in plants and are predominantly associated with homeodomain transcription factors.', *Genome biology*, 5(6), R41.

Schroeder, F., Butko, P., Nemecz, G., and Scallen, T. J. (1990) 'Interaction of fluorescent delta 5,7,9(11),22-ergostatetraen-3 beta-ol with sterol carrier protein-2', *Journal of Biological Chemistry*, 265(1), 151–7.

Schulz, T. A., Choi, M.-G. G., Raychaudhuri, S., Mears, J. A., Ghirlando, R., Hinshaw, J. E., and Prinz, W. A. (2009) 'Lipid-regulated sterol transfer between closely apposed membranes by oxysterol-binding protein homologues', *Journal of Cell Biology*, 187(6), 889–903.

Schulz, T. A., and Prinz, W. A. (2007) 'Sterol transport in yeast and the oxysterol binding protein homologue (OSH) family', *Biochimica et Biophysica Acta - Molecular and Cell Biology of Lipids*, 1771(6), 769–780.

Segal, B. H. (2009) 'Aspergillosis', *New England Journal of Medicine*, 360(18), 1870–1884.

Siafakas, A. R., Wright, L. C., Sorrell, T. C., and Djordjevic, J. T. (2006) 'Lipid rafts in Cryptococcus neoformans concentrate the virulence determinants phospholipase B1 and Cu/Zn superoxide dismutase', *Eukaryotic Cell*, 5(3), 488–498.

Sikorski, R. S., and Hieter, P. (1989) 'A system of shuttle vectors and yeast host strains designed for efficient manipulation of DNA in Saccharomyces cerevisiae.', *Genetics*, 122(1), 19–27.

da Silva Ferreira, M. E., Kress, M. R. V. Z., Savoldi, M., Goldman, M. H. S., Härtl, A., Heinekamp, T., Brakhage, A. A., and Goldman, G. H. (2006) 'The akuBKU80 mutant deficient for nonhomologous end joining is a powerful tool for analyzing pathogenicity in Aspergillus fumigatus', *Eukaryotic Cell*, 5(1), 207–211.

Sleight, R. G., and Pagano, R. E. (1983) 'Rapid appearance of newly synthesized phosphatidylethanolamine at the plasma membrane.', *Journal of Biological Chemistry*, 258(15), 9050–9058.

Slotte, J. P., and Bierman, E. L. (1988) 'Depletion of plasma-membrane sphingomyelin rapidly alters the distribution of cholesterol between plasma membranes and intracellular cholesterol pools in cultured fibroblasts.', *The Biochemical journal*, 250(3), 653–658.

Soccio, R. E., Adams, R. M., Maxwell, K. N., and Breslow, J. L. (2005) 'Differential gene regulation of StarD4 and StarD5 cholesterol transfer proteins: Activation of StarD4 by sterol regulatory element-binding protein-2 and StarD5 by endoplasmic reticulum stress', *Journal of Biological Chemistry*, 280(19), 19410–19418.

Söding, J., Biegert, A., and Lupas, A. N. (2005) 'The HHpred interactive server for protein homology detection and structure prediction', *Nucleic Acids Research*, 33(SUPPL. 2), W244-8.

Sokolov, S., Knorre, D., Smirnova, E., Markova, O., Pozniakovsky, A., Skulachev, V., and Severin, F. (2006) 'Ysp2 mediates death of yeast induced by amiodarone or intracellular acidification', *Biochimica et Biophysica Acta - Bioenergetics*, 1757(9–10), 1366–1370.

Solanko, K. A., Modzel, M., Solanko, L. M., and Wüstner, D. (2015) 'Fluorescent Sterols and Cholesteryl Esters as Probes for Intracellular Cholesterol Transport.', *Lipid insights*, 8(Suppl 1), 95–114.

Stefan, C. J., Manford, A. G., Baird, D., Yamada-Hanff, J., Mao, Y., and Emr, S. D. (2011) 'Osh proteins regulate phosphoinositide metabolism at ER-plasma membrane contact sites', *Cell*, 144(3), 389–401.

Stefan, C. J., Manford, A. G., and Emr, S. D. (2013) 'ER-PM connections: Sites of information transfer and inter-organelle communication', *Current Opinion in Cell Biology*, 25(4), 434–442.

Steichen, J. M., Iyer, G. H., Li, S., Saldanha, A., Deal, M. S., Woods, V. L., and Taylor, S. S. (2010) 'Global consequences of activation loop phosphorylation on protein kinase A', *Journal of Biological Chemistry*, 285(6), 3825–3832.

Steiner, S., and Philippsen, P. (1994) 'Sequence and promoter analysis of the highly expressed TEF gene of the filamentous fungus Ashbya gossypii', *MGG Molecular & General Genetics*, 242(3), 263–271.

Stocco, D. M., and Clark, B. J. (1996) 'Role of the steroidogenic acute regulatory protein (StAR) in steroidogenesis', *Biochemical Pharmacology*, 51(3), 197–205.

Stockton, G. W., and C.P. Smith, I. (1976) 'A deuterium nuclear magnetic resonance study of the condensing effect of cholesterol on egg phosphatidylcholine bilayer membranes. I. Perdeuterated fatty acid probes', *Chemistry and Physics of Lipids*, 17(2–3), 251–263.

Stone, S. J., and Vance, J. E. (2000) 'Phosphatidylserine synthase-1 and -2 are localized to mitochondria-associated membranes', *Journal of Biological Chemistry*, 275(44), 34534–34540.

Sullivan, D. P., Georgiev, A., and Menon, A. K. (2009) 'Tritium suicide selection identifies proteins involved in the uptake and intracellular transport of sterols in Saccharomyces cerevisiae', *Eukaryotic Cell*, 8(2), 161–169.

Sullivan, D. P., Ohvo-Rekilä, H., Baumann, N. A., Beh, C. T., and Menon, A. K. (2006) 'Sterol trafficking between the endoplasmic reticulum and plasma membrane in yeast', *Biochemical Society Transactions*, 34(3), 356–358.

Szabadkai, G., Bianchi, K., Várnai, P., De Stefani, D., Wieckowski, M. R., Cavagna, D., Nagy, A. I., Balla, T., and Rizzuto, R. (2006) 'Chaperone-mediated coupling of endoplasmic reticulum and mitochondrial Ca2+

channels', *Journal of Cell Biology*, 175(6), 901–911.

Tagliari, L., Toledo, M. S., Lacerda, T. G., Suzuki, E., Straus, A. H., and Takahashi, H. K. (2012) 'Membrane microdomain components of Histoplasma capsulatum yeast forms, and their role in alveolar macrophage infectivity', *Biochimica et Biophysica Acta - Biomembranes*, 1818(3), 458–466.

Takeshima, H., Komazaki, S., Nishi, M., Iino, M., and Kangawa, K. (2000) 'Junctophilins: A Novel Family of Junctional Membrane Complex Proteins', *Molecular Cell*, 6(1), 11–22.

Tamura, Y., Endo, T., Iijima, M., and Sesaki, H. (2009) 'Ups1p and Ups2p antagonistically regulate cardiolipin metabolism in mitochondria', *Journal of Cell Biology*, 185(6), 1029–1045.

Tamura, Y., Iijima, M., and Sesaki, H. (2010) 'Mdm35p imports Ups proteins into the mitochondrial intermembrane space by functional complex formation', *The EMBO Journal*, 29(17), 2875–2887.

Taylor-Smith, L. M., and May, R. C. (2016) 'New weapons in the Cryptococcus infection toolkit', *Current Opinion in Microbiology*, 34, 67–74.

Teale, F. W., and Weber, G. (1957) 'Ultraviolet fluorescence of the aromatic amino acids.', *The Biochemical journal*, 65(3), 476–482.

Tilley, S. J., Skippen, A., Murray-Rust, J., Swigart, P. M., Stewart, A., Morgan, C. P., Cockcroft, S., and McDonald, N. Q. (2004) 'Structure-Function Analysis of Phosphatidylinositol Transfer Protein Alpha Bound to Human Phosphatidylinositol', *Structure*, 12(2), 317–326.

Tollefson, J. H., Ravnik, S., and Albers, J. J. (1988) 'Isolation and characterization of a phospholipid transfer protein (LTP-II) from human plasma.', *Journal of lipid research*, 29(12), 1593–602.

Tomishige, N., Kumagai, K., Kusuda, J., Nishijima, M., and Hanada, K. (2009) 'Casein kinase Igamma2 down-regulates trafficking of ceramide in the synthesis of sphingomyelin', *Molecular biology of the cell*, 20(1), 348–357.

Tong, J., Yang, H., Yang, H., Eom, S. H., and Im, Y. J. (2013) 'Structure of Osh3 reveals a conserved mode of phosphoinositide binding in oxysterol-binding proteins', *Structure*, 21(7), 1203–1213.

Toulmay, A., and Prinz, W. A. (2012) 'A conserved membrane-binding domain targets proteins to organelle contact sites', *Journal of Cell Science*, 125(1), 49–58.

Tremblay, J. M., Voziyan, P. A., Helmkamp, G. M., and Yarbrough, L. R. (1998) 'The C-terminus of phosphatidylinositol transfer protein modulates membrane interactions and transfer activity but not phospholipid binding', *Biochimica et Biophysica Acta - Lipids and Lipid Metabolism*, 1389(2), 91–100.

Tsujishita, Y., and Hurley, J. H. (2000) 'Structure and lipid transport mechanism of a StAR-related domain.', *Nature structural biology*, 7(5), 408–14.

Uetz, P., Giot, L., Cagney, G., Mansfield, T. a, Judson, R. S., Knight, J. R., Lockshon, D., Narayan, V., Srinivasan, M., Pochart, P., Qureshi-Emili, a, Li, Y., Godwin, B., Conover, D., Kalbfleisch, T., Vijayadamodar, G., Yang, M., Johnston, M., Fields, S., and Rothberg, J. M. (2000) 'A comprehensive analysis of protein-protein interactions in Saccharomyces cerevisiae.', *Nature*, 403(6770), 623–627.

Umegawa, Y., Nakagawa, Y., Tahara, K., Tsuchikawa, H., Matsumori, N., Oishi, T., and Murata, M. (2012) 'Head-to-tail interaction between amphotericin b and ergosterol occurs in hydrated phospholipid membrane', *Biochemistry*, 51(1), 83–89.

Uppuluri, P., Chaturvedi, A. K., Srinivasan, A., Banerjee, M., Ramasubramaniam, A. K., Köhler, J. R., Kadosh, D., and Lopez-Ribot, J. L. (2010) 'Dispersion as an important step in the Candida albicans biofilm developmental cycle', *PLoS Pathogens*, 6(3), e1000828.

Urbani, L., and Simoni, R. D. (1990) 'Cholesterol and vesicular stomatitis virus G protein take separate routes from the endoplasmic reticulum to the plasma membrane', *Journal of Biological Chemistry*, 265(4), 1919–1923.

Valdez-Taubas, J., and Pelham, H. R. B. (2003) 'Slow diffusion of proteins in the yeast plasma membrane allows polarity to be maintained by endocytic cycling', *Current Biology*, 13(18), 1636–1640.

Vance, J. E., Aasman, E. J., and Szarka, R. (1991) 'Brefeldin a does not inhibit the movement of

phosphatidylethanolamine from its sites of synthesis to the cell surface', *Journal of Biological Chemistry*, 266(13), 8241–8247.

Velamakanni, S., Wei, S. L., Janvilisri, T., and Van Veen, H. W. (2007) 'ABCG transporters: Structure, substrate specificities and physiological roles - A brief overview', *Journal of Bioenergetics and Biomembranes*, 39(5–6), 465–471.

Verweij, P. E., Zhang, J., Debets, A. J. M., Meis, J. F., van de Veerdonk, F. L., Schoustra, S. E., Zwaan, B. J., and Melchers, W. J. G. (2016) 'In-host adaptation and acquired triazole resistance in Aspergillus fumigatus: a dilemma for clinical management', *The Lancet Infectious Diseases*, 16(11), e251–e260.

Vincent, B. M., Lancaster, A. K., Scherz-Shouval, R., Whitesell, L., and Lindquist, S. (2013) 'Fitness trade-offs restrict the evolution of resistance to amphotericin B.', *PLoS biology*. Edited by A. P. Mitchell, 11(10), e1001692.

Vonkova, I., Saliba, A. E., Deghou, S., Anand, K., Ceschia, S., Doerks, T., Galih, A., Kugler, K. G., Maeda, K., Rybin, V., van Noort, V., Ellenberg, J., Bork, P., and Gavin, A. C. (2015) 'Lipid Cooperativity as a General Membrane-Recruitment Principle for PH Domains', *Cell Reports*, 12(9), 1519–1530.

Wach, A., Brachat, A., Alberti-Segui, C., Rebischung, C., and Philippsen, P. (1997) 'Heterologous HIS3 marker and GFP reporter modules for PCR-targeting in Saccharomyces cerevisiae', *Yeast*, 13(11), 1065–1075.

Wach, A., Brachat, A., Pohlmann, R., and Philippsen, P. (1994) 'New heterologous modules for classical or PCR-based gene disruptions in Saccharomyces cerevisiae', *Yeast*, 10(13), 1793–1808.

Waheed, A. A., Ablan, S. D., Soheilian, F., Nagashima, K., Ono, A., Schaffner, C. P., and Freed, E. O. (2008) 'Inhibition of human immunodeficiency virus type 1 assembly and release by the cholesterol-binding compound amphotericin B methyl ester: evidence for Vpu dependence.', *Journal of virology*, 82(19), 9776–81.

Wang, P. (2009) 'OSBP Is a Cholesterol-Regulated Scaffolding Protein in Control of ERK1 / 2 Activation', *Science*, 1472(2005), 1472–1476.

Wang, P., Duan, W., Munn, A. L., and Yang, H. (2005) 'Molecular characterization of Osh6p, an oxysterol binding protein homolog in the yeast Saccharomyces cerevisiae', *FEBS Journal*, 272(18), 4703–4715.

Wang, P. Y., Weng, J., Lee, S., and Anderson, R. G. W. (2008) 'The N terminus controls sterol binding while the C terminus regulates the scaffolding function of OSBP', *Journal of Biological Chemistry*, 283(12), 8034–8045.

Wang, P., Zhang, Y., Li, H., Chieu, H. K., Munn, A. L., and Yang, H. (2005) 'AAA ATPases regulate membrane association of yeast oxysterol binding proteins and sterol metabolism', *The EMBO Journal*, 24(17), 2989–2999.

Watanabe, Y., Tamura, Y., Kawano, S., and Endo, T. (2015) 'Structural and mechanistic insights into phospholipid transfer by Ups1–Mdm35 in mitochondria', *Nature Communications*, 6(28), 7922.

Watari, H., Arakane, F., Moog-Lutz, C., Kallen, C. B., Tomasetto, C., Gerton, G. L., Rio, M. C., Baker, M. E., and Strauss, J. F. (1997) 'MLN64 contains a domain with homology to the steroidogenic acute regulatory protein (StAR) that stimulates steroidogenesis.', *Proceedings of the National Academy of Sciences of the United States of America*, 94(16), 8462–8467.

Weete, J. D., Abril, M., and Blackwell, M. (2010) 'Phylogenetic distribution of fungal sterols', *PLoS ONE*, 5(5), e10899.

Te Welscher, Y. M., Jones, L., Van Leeuwen, M. R., Dijksterhuis, J., De Kruijff, B., Eitzen, G., and Breukink, E. (2010) 'Natamycin inhibits vacuole fusion at the priming phase via a specific interaction with ergosterol', *Antimicrobial Agents and Chemotherapy*, 54(6), 2618–2625.

te Welscher, Y. M., van Leeuwen, M. R., de Kruijff, B., Dijksterhuis, J., and Breukink, E. (2012) 'Polyene antibiotic that inhibits membrane transport proteins.', *Proceedings of the National Academy of Sciences U. S. A.*, 109(28), 11156–11159.

te Welscher, Y. M., Ten Napel, H. H., Balagué, M. M., Souza, C. M., Riezman, H., De Kruijff, B., and Breukink, E. (2008) 'Natamycin blocks fungal growth by binding specifically to ergosterol without permeabilizing

the membrane', *Journal of Biological Chemistry*, 283(10), 6393–6401.

West, M., Zurek, N., Hoenger, A., and Voeltz, G. K. (2011) 'A 3D analysis of yeast ER structure reveals how ER domains are organized by membrane curvature', *Journal of Cell Biology*, 193(2), 333–346.

Westermeyer, C., and Macreadie, I. G. (2007) 'Simvastatin reduces ergosterol levels, inhibits growth and causes loss of mtDNA in Candida glabrata', *FEMS Yeast Research*, 7(3), 436–441.

Wilcox, L. J., Balderes, D. A., Wharton, B., Tinkelenberg, A. H., Rao, G., and Sturley, S. L. (2002) 'Transcriptional profiling identifies two members of the ATP-binding cassette transporter superfamily required for sterol uptake in yeast', *Journal of Biological Chemistry*, 277(36), 32466–32472.

Winzeler, E. A., Shoemaker, D. D., Astromoff, A., Liang, H., Anderson, K., … Davis, R. W. (1999) 'Functional characterization of the S. cerevisiae genome by gene deletion and parallel analysis.', *Science*, 285(5429), 901–906.

Wirtz, K. W. A. (1991) 'Phospholipid Transfer Proteins', *Annual Review of Biochemistry*, 60(1), 73–99.

Wong, L. H., Čopič, A., and Levine, T. P. (2017) 'Advances on the Transfer of Lipids by Lipid Transfer Proteins.', *Trends in Biochemical Sciencesi*, 42(7), 516–530.

Wong, L. H., and Levine, T. P. (2016) 'Lipid transfer proteins do their thing anchored at membrane contact sites… but what is their thing?', *Biochemical Society Transactions*, 44(2), 517–527.

Wright, C. S., Mi, L.-Z., Lee, S., and Rastinejad, F. (2005) 'Crystal Structure Analysis of Phosphatidylcholine−GM2-Activator Product Complexes: Evidence for Hydrolase Activity', *Biochemistry*, 44(41), 13510–13521.

Wu, S. Y., Yang, X., Gharpure, K. M., Hatakeyama, H., Egli, M., McGuire, M. H., Nagaraja, A. S., Miyake, T. M., Rupaimoole, R., Pecot, C. V., Taylor, M., Pradeep, S., Sierant, M., Rodriguez-Aguayo, C., Choi, H. J., Previs, R. A., Armaiz-Pena, G. N., Huang, L., Martinez, C., Hassell, T., Ivan, C., Sehgal, V., Singhania, R., Han, H.-D., Su, C., Kim, J. H., Dalton, H. J., Kovvali, C., Keyomarsi, K., McMillan, N. A. J., Overwijk, W. W., Liu, J., Lee, J.-S., Baggerly, K. A., Lopez-Berestein, G., Ram, P. T., Nawrot, B., and Sood, A. K. (2014) '2'-OMe-phosphorodithioate-modified siRNAs show increased loading into the RISC complex and enhanced anti-tumour activity.', *Nature communications*, 5(3459).

Wüstner, D. (2009) 'Intracellular cholesterol transport', *Cellular Lipid Metabolism*, 1438(1), 157–190.

Yang, H., Tong, J., Lee, C. W., Ha, S., Eom, S. H., and Im, Y. J. (2015) 'Structural mechanism of ergosterol regulation by fungal sterol transcription factor Upc2', *Nature Communications*, 6(6129).

Yaworsky, D. C., Baker, B. Y., Bose, H. S., Best, K. B., Jensen, L. B., Bell, J. D., Baldwin, M. A., and Miller, W. L. (2005) 'pH-dependent interactions of the carboxyl-terminal helix of steroidogenic acute regulatory protein with synthetic membranes', *Journal of Biological Chemistry*, 280(3), 2045–2054.

Yoder, M. D., Thomas, L. M., Tremblay, J. M., Oliver, R. L., Yarbrough, L. R., and Helmkamp, G. M. (2001) 'Structure of a multifunctional protein: Mammalian phosphatidylinositol transfer protein complexed with phosphatidylcholine', *Journal of Biological Chemistry*, 276(12), 9246–9252.

Young, L. Y., Hull, C. M., and Heitman, J. (2003) 'Disruption of ergosterol biosynthesis confers resistance to amphotericin B in Candida lusitaniae', *Antimicrobial Agents and Chemotherapy*, 47(9), 2717–2724.

Yu, F., He, F., Yao, H., Wang, C., Wang, J., Li, J., Qi, X., Xue, H., Ding, J., and Zhang, P. (2015) 'Structural basis of intramitochondrial phosphatidic acid transport mediated by Ups1-Mdm35 complex', *EMBO reports*, 16(7), 813–823.

Yu, J. W., Mendrola, J. M., Audhya, A., Singh, S., Keleti, D., DeWald, D. B., Murray, D., Emr, S. D., and Lemmon, M. A. (2004) 'Genome-wide analysis of membrane targeting by S. cerevisiae pleckstrin homology domains', *Molecular Cell*, 13(5), 677–688.

Zaragoza, O., and Gancedo, J. M. (2000) 'Pseudohyphal growth is induced in Saccharomyces cerevisiae by a combination of stress and cAMP signalling', *Antonie van Leeuwenhoek, International Journal of General and Molecular Microbiology*, 78(2), 187–194.

Zhang, J., Olsson, L., and Nielsen, J. (2010) 'The beta-subunits of the Snf1 kinase in Saccharomyces

cerevisiae, Gal83 and Sip2, but not Sip1, are redundant in glucose derepression and regulation of sterol biosynthesis', *Molecular Microbiology*, 77(2), 371–383.

Zhang, L., Zhang, Y., Zhou, Y. M., An, S., Zhou, Y. X., and Cheng, J. (2002) 'Response of gene expression in Saccharomyces cerevisiae to amphotericin B and nystatin measured by microarrays', *Journal of Antimicrobial Chemotherapy*, 49(6), 905–915.

Zhang, M., Liu, P., Dwyer, N. K., Christenson, L. K., Fujimoto, T., Martinez, F., Comly, M., Hanover, J. A., Joan Blanchette-Mackie, E., and Strauss, J. F. (2002) 'MLN64 mediates mobilization of lysosomal cholesterol to steroidogenic mitochondria', *Journal of Biological Chemistry*, 277(36), 33300–33310.

Zhao, H., Michelot, A., Koskela, E. V., Tkach, V., Stamou, D., Drubin, D. G., and Lappalainen, P. (2013) 'Membrane-Sculpting BAR Domains Generate Stable Lipid Microdomains', *Cell Reports*, 4(6), 1213–1223.

Zhou, Y., Meraner, P., Kwon, H. T., Machnes, D., Oh-hora, M., Zimmer, J., Huang, Y., Stura, A., Rao, A., and Hogan, P. G. (2010) 'STIM1 gates the store-operated calcium channel ORAI1 in vitro', *Nature structural & molecular biology*, 17(1), 112–116.

Zilversmit, D. B., Hughes, L. B., and Balmer, J. (1975) 'Stimulation of cholesterol ester exchange by lipo-protein-free rabbit plasma', *Biochimica et Biophysica Acta (BBA) - Lipids and Lipid Metabolism*, 409(3), 393–398.

Zinser, E., Paltauf, F., and Daum, G. (1993) 'Sterol composition of yeast organelle membranes and subcellular distribution of enzymes involved in sterol metabolism', *Journal of Bacteriology*, 175(10), 2853–2858.